

Pro- and antidegenerative effects of JNK stresskinases
in neuronal cells

Dissertation
zur Erlangung des Doktorgrades
der Mathematisch-Naturwissenschaftlichen Fakultät
der Christian-Albrechts-Universität
zu Kiel

vorgelegt von
Lutz Römer

Kiel, 2008

Deutscher Titel:

Pro- und antidegenerative Wirkungen der
JNK Stresskinasen in neuronalen Zellen

Referent:

Prof. Dr. Thomas Herdegen

Koreferent:

Prof. Dr. Eric Beitz

Tag der mündlichen Prüfung:

04.06.2008

Zum Druck genehmigt:

04.06.2008

“I believe that unarmed truth and unconditional love will have the final word in reality. This is why right, temporarily defeated, is stronger than evil triumphant.”

Martin Luther King, Jr.

TABLE OF CONTENTS

1.	INTRODUCTION	9
1.1	Parkinson's disease (PD)	9
1.1.1	Current treatment of PD	9
1.1.2	PD in clinical research	10
1.1.3	Experimental models of PD	10
1.1.3.1	<i>6-hydroxydopamine</i>	11
1.1.3.2	<i>MPTP</i>	12
1.1.4	Genetic factors and implications for idiopathic PD	13
1.2	Oxidative stress	13
1.2.1	Antioxidant defense	16
1.2.2	Role of ROS and ROS products in cell death	18
1.3	Hallmarks of apoptosis	20
1.4	Mitochondria in neuronal cell death	20
1.5	MAPK cascades	23
1.5.1	JNK	24
2.	AIMS OF THE THESIS	27
3.	MATERIALS AND METHODS	28
3.1	Materials	28
3.2	Laboratory Equipment	32
3.3	Methods	33
3.3.1	PC12 cell culture	33
3.3.1.1	<i>Splitting</i>	34
3.3.1.2	<i>Freezing and thawing</i>	34
3.3.2	Applied stimuli	35
3.3.2.1	<i>6-hydroxydopamine (6-OHDA)</i>	35
3.3.2.2	<i>1-Methyl-4-phenylpyridinium ion (MPP⁺)</i>	35
3.3.2.3	<i>Staurosporine (STS)</i>	36
3.3.2.4	<i>Valinomycin</i>	37
3.3.3	Protection of PC12 cells	37
3.3.3.1	<i>The JNK inhibitor SP600125</i>	37

TABLE OF CONTENTS

3.3.3.2	<i>Methysticin</i>	37
3.3.3.3	<i>Luteolin</i>	39
3.3.3.4	<i>Resveratrol</i>	39
3.3.3.5	<i>tert-butylhydroquinone</i>	40
3.3.4	Trypan blue viability assay	40
3.3.5	Preparation of mitochondria	40
3.3.6	Protein identification by Western blot	42
3.3.6.1	<i>Denaturing protein extraction</i>	42
3.3.6.2	<i>SDS-PAGE</i>	42
3.3.6.3	<i>Preparation of polyacrylamide gels</i>	43
3.3.6.4	<i>Preparation of protein samples</i>	45
3.3.6.5	<i>Electrophoresis</i>	45
3.3.6.6	<i>Immunoblotting</i>	45
3.3.6.7	<i>ECL-reaction</i>	47
3.3.6.8	<i>Stripping of Western blot membranes</i>	47
3.3.6.9	<i>Ponceau S staining of Western blot membranes</i>	48
3.3.7	Basic principles of flow cytometry	48
3.3.7.1	<i>Flow cytometrical data analysis</i>	49
3.3.7.2	<i>Staining of PC12 cells with ROS-sensitive fluorescent dyes</i>	50
3.3.7.2.1	<i>2',7'-Dichlorofluorescein (DCF)</i>	50
3.3.7.2.2	<i>Dihydrorhodamine (DHR)</i>	51
3.3.7.3	<i>Assessment of the mitochondrial membrane potential with JC-1</i>	51
3.3.7.4	<i>Detection of apoptosis and necrosis in the flow cytometer</i>	54
3.3.8	Experiments using the fluorescence microplate reader	56
3.3.9	Experiments using the spectrofluorometer	58
3.3.10	Fluorescence microscopy	59
3.3.10.1	<i>Principle of confocal laser scanning microscopy</i>	59
3.3.10.2	<i>Experimental setup</i>	60
3.3.11	Breeding of mice	61
3.3.12	Genetic characterization of JNK knock-out mice strains	61
3.3.12.1	<i>Polymerase chain reaction (PCR)</i>	62
3.3.12.2	<i>Detection and analysis of the PCR reaction product</i>	64
3.3.13	Isolation of mitochondria from mice brain	65
3.3.13.1	<i>Determination of mitochondrial proteins</i>	66

3.3.13.2	<i>Estimation of the quality of isolated mitochondria measuring the respiratory control ratio (RCR)</i>	67
3.3.13.3	<i>Purity of mitochondrial preparations</i>	69
3.3.14	Primary cells	69
3.3.14.1	<i>Coating of the plates</i>	70
3.3.14.2	<i>Obtaining and cultivating primary murine neurons</i>	70
3.3.14.3	<i>Treatment of primary cells</i>	71
3.3.14.4	<i>Immunocytochemistry</i>	71
3.3.15	Statistical analysis	72
<hr/>		
4.	RESULTS	73
<hr/>		
4.1	Mechanisms of 6-hydroxydopamine mediated cell death	74
4.1.1	6-hydroxydopamine induces cell death in PC12 cells	74
4.1.2	6-hydroxydopamine generates reactive oxygen species in PC12 cells	74
4.1.3	The mitochondrial membrane potential collapses after 6-hydroxydopamine treatment	80
4.1.4	6-hydroxydopamine induces cytochrome c release	89
4.2	Responsiveness of isolated mitochondria to 6-hydroxydopamine	90
4.2.1	Analyses with isolated mitochondria	90
4.2.2	Quality of isolated mitochondria	90
4.2.3	Purity of mitochondrial fractions	91
4.2.4	ROS levels in isolated mitochondria following 6-hydroxydopamine	91
4.2.5	The mitochondrial membrane potential of isolated mitochondria following 6-OHDA	92
4.3	The mitochondrial death pathway and c-Jun N-terminal kinase (JNK) signaling	97
4.3.1	Purification of PC12 cell mitochondrial fractions	97
4.3.2	Activation of the mitochondrial pool of JNK following 6-OHDA	98
4.3.3	Translocation of c-Jun N-terminal kinase 2 (JNK2) to mitochondria	98
4.3.4	Upstream kinases and JNK scaffolds in mitochondrial fractions	102
4.4	Inhibition of JNK and ROS production	104
4.4.1	JNK inhibition does not prevent from oxidative stress	104
4.4.2	Anti-oxidant mediated neuroprotection against ROS generation	105
4.5	Involvement of JNK isoforms in neurite outgrowth	107

5.	DISCUSSION	110
5.1	6-OHDA-induced cell death	110
5.2	6-OHDA toxicity to mitochondria	112
5.3	Profound and early oxidative stress in PC12 cells, but not isolated mitochondria following 6-OHDA	114
5.4	6-OHDA-induced JNK2 activation and translocation to mitochondria	116
5.5	Intracellular JNK pools	118
5.6	Upstream and downstream effectors of JNK signaling at the mitochondria	119
5.7	Time course of pathological events mediated by 6-OHDA	121
5.8	JNK inhibition and protection from oxidative stress	122
5.9	JNK in neuronal death and survival	123
5.10	Technical considerations	125
5.10.1	The PC12 cell model	125
5.10.2	Preparation of isolated mitochondria	125
6.	REFERENCES	127
7.	ABBREVIATIONS	158
8.	DANKSAGUNG	162
9.	LEBENS LAUF	163
10.	ERKLÄRUNG ZU §10 ABS. 2 NR. 2 DER PROMOTIONS- ORDNUNG	165
11.	SUMMARY	166
12.	KURZFASSUNG	167

1. INTRODUCTION

1.1 Parkinson's disease (PD)

Parkinson's disease (PD), first described by James Parkinson in 1817 (Parkinson, 1817), is a progressive neurodegenerative disorder characterized by a preferential loss of dopaminergic neurons in the substantia nigra pars compacta (Tretiakoff, 1919, for review see Beal, 1995). This brain structure is essential for the initiation of movement. Consequently, the diagnosis of PD is usually given by the clinician from the cardinal features of bradykinesia with at least one or more of the following: resting tremor, gait difficulties, postural instability, and/or rigidity. Responsiveness to dopamine (DA) replacement treatments is taken as supportive evidence for the diagnosis. The London Brain Bank criteria for the diagnosis of PD include neuronal loss in the substantia nigra and presence of Lewy bodies, deposits formed from fibrillary α -synuclein and hyper-phosphorylated neurofilament protein (Hughes *et al.*, 1992). More than 90% of PD patients are likely to have Lewy bodies in the substantia nigra in the end stage of the disease (Hughes *et al.*, 2001). However, there is no evidence that Lewy bodies would be specific for PD since they are found in a variety of other age-related disorders, and even in aging brains of people without any signs of locomotor impairment or dementia (Arai *et al.*, 1992; Forno, 1986). Today, PD is the second most prevalent neurodegenerative disease. Its occurrence increases with age and is considered to affect more than 2% of the population beyond 65 years. Less frequently, PD may have an onset below 40 years. This early onset usually coincides with familial genetic defects (Blum *et al.* 2001; Golbe *et al.*, 1991; Hardy *et al.*, 2006).

1.1.1 Current treatment of PD

Current conventional treatment is directed to restore voluntary movement by substitution of dopamine input to the caudate nucleus/putamen and subsequently the motor cortex. The prodrug levodopa (the natural precursor in dopamine synthesis L-DOPA) is converted to dopamine by the aromatic L-amino acid decarboxylase (DOPA decarboxylase, DDC). DDC inhibitors (Carbidopa, Benserazid) do not pass the blood brain barrier, consequently they reduce peripheral side effects and enhance levodopa efficacy. Inhibitors of the monoamine oxidase B (MAO-B) – selegiline or rasagiline – raise dopamine levels by blocking its degradation. A direct effect on dopamine D1 and D2 receptors in the putamen is provided by

dopamine agonists such as bromocriptine, pergolide or cabergoline. Initially, patients respond well to this dopamine replacement therapy but treatment is effective for only a limited period and fails to halt disease progression (Rang *et al.*, 2003).

1.1.2 PD in clinical research

Even though the neurochemical defects and the neuropathological characteristics of PD are well defined, the etiology of the disease is still unclear. The first clinical signs of PD can only be observed when the loss of dopaminergic neurons is already strongly advanced (typically more than 80%), which increases the difficulty to determine the real onset of neurodegenerative processes and to identify early changes in the brain. Another drawback are technical problems, a limited number of reliable, non-invasive imaging techniques and early disease markers (Bostantjopoulou *et al.*, 1997; Younes-Mhenni *et al.*, 2007). Additionally, the progressive mode hardly allows follow-up studies, with only a few neurons dying everyday (Mochizuki *et al.*, 1996). Data that are obtained from autopsy brains or patients diagnosed with PD may not at all or not sufficiently reflect events the disease originated from (Hirsch *et al.*, 1998; Hunot *et al.*, 1997; Tatton *et al.*, 1998).

Smoking, higher coffee and caffeine intake are associated with a significantly lower risk of PD (Logroscino, 2005; Ross *et al.*, 2000). Infections in early life increase the risk of progressive dopaminergic cell death. Anti-inflammatory drugs can reduce incidence of PD in clinical studies, but do not stop the disease progression in patients already diagnosed with PD (Logroscino *et al.*, 2005). Furthermore, the exposure to pesticides strongly contributes to the progressive degeneration of dopaminergic neurons (Langston, 1998; Tanner *et al.*, 1999). This has led to the development of several experimental models reproducing the human disease, mostly based on the administration of a single neurotoxic compound *in vivo* or *in vitro*.

1.1.3 Experimental PD models

Environmental toxins modelling PD include 6-hydroxydopamine (6-OHDA), 1-methyl-4-phenyl-1,2,3,6-tetrahydropyridine (MPTP) or the metabolite 1-methyl-4-phenyl-1,2,3,6-tetrahydropyridinium ion (MPP⁺), rotenone, maneb, and paraquat (Betarbet *et al.* 2000; Manning-Bog *et al.* 2002; McCormack *et al.* 2002; Sherer *et al.* 2003; Thiruchelvam *et al.* 2000). The amount of model toxins gives rise to the crucial involvement of environmental factors in the pathogenesis of PD (Blum *et al.*, 2001a; Grünblatt *et al.*, 2000; Meco *et al.*,

1994; Snyder and D'Amato, 1985). Despite a number of differences between the pathological symptoms induced by these substances, common mechanisms include mitochondrial impairment, with great evidence for the inhibition of complex I from the electron transport chain, and reactive oxygen species (ROS) generation (Ikebe *et al.*, 1995; Kapsa *et al.*, 1996; Mizuno *et al.*, 1989; Schapira, 1994; Sherer *et al.* 2002). Environmental PD models are often not able to reflect relevant features of the disease; *e.g.* the progressive dopaminergic cell death is only characteristic following 6-OHDA, and Lewy bodies are only found after rotenone treatment (Betarbet *et al.*, 2000; Jeon *et al.*, 1995). In this study, 6-OHDA and MPP⁺ were used.

1.1.3.1 6-Hydroxydopamine (6-OHDA)

6-Hydroxydopamine (6-OHDA) was the first agent used to produce an animal model of PD (Ungerstedt, 1971). The toxin is the hydroxylated analogue of the natural neurotransmitter dopamine. Like dopamine, it is not able to pass the blood brain barrier, so 6-OHDA has been studied via direct administration to the nigra, the striatum or the medial forebrain bundle (MFB) of rodent brains or in cell culture models. The bilateral 6-OHDA lesion of the striatum stands the advantage of being the best suitable model, mimicking closely the human disease (Deumens, 2002). In low concentrations ($\leq 50 \mu\text{M}$) 6-OHDA promotes apoptotic cell death, higher concentrations induce necrotic features as well (Dodel *et al.*, 1999; Walkinshaw and Waters, 1994).

Biochemical hallmarks of 6-OHDA-mediated cell death are oxidative stress, mitochondrial dysfunction and activation of intracellular “stress pathways”, namely c-Jun N-terminal/stress-activated kinases (JNK) and NF κ B-signaling (Blum *et al.*, 2001b; Choi *et al.*, 1999). Yet the mechanisms, especially the interconnection between these means of action, remain controversial and poorly understood (Blum *et al.*, 2001a; Jenner, 2003; Walkinshaw and Waters, 1994).

Oxidative stress is the imbalance between ROS (in particular hydrogen peroxide), generated by 6-OHDA and dopamine metabolism, and intra- or extracellular autoxidation of 6-OHDA (Blum *et al.*, 2000; Cohen and Heikkila, 1974; Saner and Thoenen, 1971; Slivka and Cohen, 1985). Autoxidation of 6-OHDA generates *p*-quinones, toxic intermediates that target mitochondria and that are eliminated by the conversion to melanine (Arriagada *et al.*, 2004; Asanuma *et al.*, 2004). During the quinone detoxification process an array of other free

radical species, such as hydrogen peroxide, superoxide anions, and hydroxyl radicals, are generated (Blum *et al.*, 2001a). The major source of reactive oxygen species (ROS) are mitochondria. Oxidation events can be amplified by cytoplasmic free calcium and/or ferrous iron (Youdim *et al.*, 1990). Increased levels of ROS lead to the damage of cellular macromolecules and their subsequent peroxidation (Dexter *et al.*, 1989). The importance of ROS in this model of Parkinson's disease is fortified by findings that support of the cell-own antioxidant defense system is highly protective, including administration of glutathione, and, most effectively, catalase, which scavenges a cell from hydrogen peroxide by decomposition to water and oxygen (Blum *et al.*, 2000; Hanrott *et al.*, 2006).

6-OHDA impairs the activity of the mitochondrial complex I of the mitochondrial respiratory chain, thereby reducing oxidative phosphorylation/ATP production and promoting the generation of reactive oxygen species (Glinka *et al.*, 1996), yet the effect has not been demonstrated so clearly as for the other model toxins and remains controversial (Wu *et al.*, 1996). However, 6-OHDA induces a ROS-related collapse in mitochondrial membrane potential (Lotharius *et al.*, 1999) and is a strong uncoupler of oxidative phosphorylation leading to cytochrome c release and further caspase activation (Ochu *et al.*, 1998). 6-OHDA activates JNK and mediates neuronal cell death (Blum *et al.*, 2001a; Hara *et al.*, 2003). However, the mechanism of this action is not yet understood.

1.1.3.2 MPTP

In 1982, the neurotoxin MPTP (an analogue of the narcotic meperidine) was discovered accidentally (Langston *et al.*, 1983). Young drug addicts developed a parkinsonian syndrome after self-administration of a "synthetic heroin" (MPPP, 1-methyl-4-phenyl-propion-oxypiperidine). MPTP was identified as the neurotoxic contaminant responsible for this effect (Ballard *et al.*, 1985; Langston *et al.*, 1983; Langston and Ballard, 1983). MPTP is highly lipophilic and crosses the blood brain barrier easily. Mono-amine oxidase B (MAO-B) in astrocytes converts MPTP to the active metabolite MPP⁺, which is a substrate for the dopamine transporter (DAT) and accumulates in DA neurons (Javitch *et al.*, 1985). MPP⁺ inhibits mitochondrial complex I and ultimately leads to cell death (Gluck *et al.*, 1994; Markey *et al.*, 1984; Tipton *et al.*, 1993). Oxidative stress and the accumulation of free radicals cause cell death in this model, but ROS are elevated only at very high concentrations of MPP⁺ (Chen *et al.*, 2006; Shoffner *et al.*, 1991). However, antioxidant strategies increase survival also of MPP⁺-intoxicated neurons (Hantraye *et al.*, 1996; Kitamura *et al.*, 1998; Park

et al., 2004; Przedborski *et al.*, 1992; Przedborski *et al.*, 1996; Sawada *et al.*, 1996). There is evidence that the toxicity of MPP⁺ is mediated via JNK stress kinase signaling (Hunot *et al.*, 2004; Wang *et al.*; 2004).

1.3.4 Genetic factors and implications for idiopathic PD

Recently, a number of genes with implications in PD have been discovered (*PARK* family, for review see Thomas and Beal., 2007). Mutations in the *parkin* gene (*PARK-2*), the *PINK1* [phosphatase and tensin (PTEN) homolog-induced putative kinase 1] gene (*PARK6*), and the *DJ-1* gene (*PARK7*) lead to a juvenile onset of PD, marked by nigral cell death without Lewy bodies (Farrer *et al.*, 2001; Miller *et al.*, 2003; Valente *et al.*, 2004). Mutations in the *LRRK2* gene (*PARK8*) lead to classical PD pathology, but the appearance of Lewy bodies is not a necessary event in the toxicity of the model (Singleton *et al.*, 2005). Mutations in the *SNCA* gene (*PARK1/4*), which encodes for α -synuclein, were associated with a variable onset age of the locomotor disease (Polymeropoulos *et al.*, 1996).

Gene mutations account only for a minor number of PD cases (about 5%). Some changes do not result in locomotor impairment, but it has been demonstrated that the genetic background can enhance toxicity of environmental factors (Zimprich *et al.*, 2004). Genetic models of PD have shed a new light on mechanisms that could explain the etiology of the disease. Interestingly, those very recent discoveries about proteins encoded by the *PARK* gene family have strengthened again the importance of oxidative stress (DJ-1 as a ROS sensor; Kim *et al.*, 2005; Park *et al.*, 2005), mitochondrial dysfunction (α -synuclein; Klivenyi *et al.*, 2006; Song *et al.*, 2004) and stress kinase signaling pathways in PD (*parkin*, *LRRK2*, *PINK1*; Beilina *et al.*, 2005; Cha *et al.*, 2005; Leutenecker *et al.*, 2006; Li and Beal, 2005).

1.2 Oxidative stress

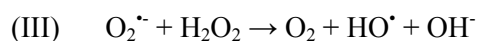
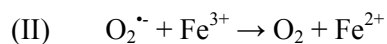
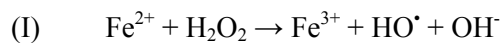
Molecular oxygen O₂ contains two unpaired electrons in its outer orbital and is therefore a bi-radical. Though relatively unreactive this triplet oxygen can be activated, e.g. by light, to singlet oxygen with antiparallel electrons and a free π orbital that readily accepts paired electrons. These molecular forms of oxygen, radicals and other non-radical derivatives of oxygen can be formed in aerobic organisms, that are equipped with the systems to exploit

INTRODUCTION

oxygen to their advantage (energy production, cellular defense, enzyme activity, metabolism), and mechanisms to detoxify the components.

Under physiological conditions the main source for intracellular oxygen radicals is the electron transport chain of mitochondria (Boveris *et al.* 1972; Boveris and Chance, 1973; Loschen *et al.* 1971). During the flow of electrons along the complexes of the respiratory chain, leakage of electrons can occur. Those are then transferred directly to molecular oxygen under formation of the superoxide radical anion $O_2^{\cdot-}$. It is estimated that about 1-3 % of oxygen consumed in mitochondria are transformed to superoxide under physiological conditions (Boveris and Chance, 1973). Superoxide anions are highly reactive, but their damaging effect in cells is limited since diffusion across biological membranes is minimal due to the negative charge. However, superoxide can be converted to other ROS, among these are hydrogen peroxide derived from further reduction as well as peroxynitrite formed in a reaction of superoxide with nitric oxide. Hydrogen peroxide shows limited reactivity but can readily diffuse across membranes (Loschen *et al.* 1973). It can be activated by transition metal ions like ferrous iron to form the highly reactive hydroxyl radical in the Fenton reaction (*Figure 1*):

A



B

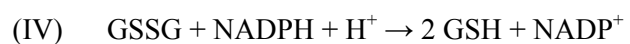
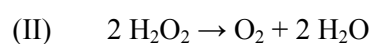
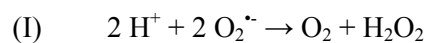


Figure 1. ROS generation and scavenging

Chemical reactions facilitating oxygen radical generation (A) and scavenging (B). (AI) Fenton reaction. (AI+II) = (AIII) Haber-Weiss reaction. (BI) Dismutation that can be accelerated by SOD. (BII) Catalase reaction. (BIII) GPx reaction. (BIV) GSH reductase reaction.

Abbreviations: GSH (glutathion), GPx (GSH peroxidases), ROS (reactive oxygen species), SOD (superoxide dismutase)

Superoxide radicals can participate in Fenton reactions by reducing Fe^{3+} to Fe^{2+} and can thus propagate reaction (*Figure 1*, AI) by providing reduced transition metal ions (AII). The net reaction of (AI) and (AII) is the so-called Haber-Weiss reaction (AIII). Apart from iron, other transition metal ions, especially copper ions, can participate in the above reactions.

In general, oxidative stress describes a state of imbalance between the production and detoxification of reactive oxygen species (Sies, 1991). Therefore, increased production of ROS as well as impaired antioxidant defense can both contribute to increased accumulation of ROS. Oxygen radicals can be detrimental to almost any component of cells, including DNA, proteins and lipids. Cells react upon oxidative stress either by adaptive responses leading to activation of repair mechanisms or – if the damage is severe – by induction of cell death. Damage to the electron transport chain or the mitochondrial membrane results in burst of superoxide production and, consequently, the conversion to hydrogen peroxide and the hydroxyl radical (Lenaz, 2001; Ueda *et al.*, 2002). The mitochondrial complexes I and III of the respiratory chain are the most important sites of ROS formation (Boveris *et al.* 1972; Turrens and Boveris 1980; Votyakova and Reynolds 2001), complex I being the major and relevant site of superoxide generation (Liu *et al.* 2002). ROS themselves can inhibit the respiratory chain. Hydroxyl radical derived from hydrogen peroxide is the most efficient inhibitor of complex I among the ROS tested (Zhang *et al.* 1990).

Although the majority of ROS derives from mitochondrial sources there are numerous other production sites as well. The enzymes cyclo-oxygenase (COX) and lipoxygenase, involved in inflammation processes, generate lipid peroxides and oxygen radicals. The lysosomal enzyme myeloperoxidase catalyzes the production of bacteriocidal hypochlorite from hydrogen peroxide and chloride. Xanthine oxidase and aldehyde oxidase convert oxygen to superoxide in the cytosol of endothelial cells. These other sources are important in inflammation and ischemia/reperfusion injuries (Ferrari *et al.*, 2004; McCord, 1985). Enzymatic oxidation is the main detoxifying method in the metabolism of xenobiotics, and largely localized to microsomes. The main component is the monooxygenase cytochrome P450, which is not only expressed in the liver, but also in catecholaminergic neurons of *e.g.* the substantia nigra (Bernhardt *et al.*, 1996). The superoxide radical anion can be generated both from dissociation of the oxygenated complex or the autoxidation of cytochrome P450 reductase (Denisov *et al.*, 2007).

The brain is metabolically one of the most active organs. 2% of the total body weight accounts for 20% of total O₂ consumption. Accompanied by that, the human brain faces a high oxidative burden that can only be alleviated by strong defense mechanisms. Dopaminergic neurons are even more susceptible, because already the enzymatic (*e.g.* MAO-B) and non-enzymatic metabolism of dopamine generates reactive oxygen species.

Along with the ROS come highly reactive intermediate metabolites. The leucoaminochrome o-semiquinone radical that leads to the disruption of the mitochondrial membrane potential ($\Delta\Psi_M$) and cell death (Arriagada *et al.*, 2004; Asanuma *et al.*, 2004; Izumi *et al.*, 2005).

1.2.1 Antioxidant defense

Superoxide anions are first in line in ROS generation, and most other ROS arise directly or indirectly from superoxide. Therefore, superoxide-detoxifying enzymes act at this early stage of enzymatic ROS defense (Forman and Azzi, 1997). Superoxide itself can undergo a dismutation reaction where two molecules of superoxide react to form molecular oxygen and hydrogen peroxide. This reaction is accelerated by superoxide dismutase (SOD) enzymes (*Figure 1*, BI). Two superoxide dismutases have been identified: copper-zinc-dependent Cu/Zn-SOD (SOD-1) and manganese-dependent Mn-SOD (SOD-2). While Mn-SOD is mainly localized to mitochondria, Cu/Zn-SOD has been found at high levels in cytosol, but also in the intermembrane space between the inner and outer mitochondrial membrane (Okado-Matsumoto and Fridovich, 2001).

Superoxide dismutase reactions result in formation of hydrogen peroxide which has to be decomposed further. This can be achieved by the reactions of catalase or glutathione peroxidases (GPx). While catalase activity directly inactivates hydrogen peroxide yielding water and molecular oxygen (*Figure 1*, BII), glutathione peroxidases need reduced glutathione (GSH) as a cosubstrate, oxidizing two molecules to the glutathione disulfide (GSSG) (*Figure 1*, BIII). Glutathione peroxidases seem to be in large part responsible for removal of physiological hydrogen peroxide levels, whereas catalase activity with its high K_m becomes important at abnormally high hydrogen peroxide concentrations (Makino *et al.*, 1994). However, catalase activity is low in the brain (Marklund *et al.*, 1982). GPx are distributed in the cytosol as well as the mitochondrial matrix (Vitorica *et al.*, 1984), where they may act in concert with SODs to decompose mitochondria-derived ROS. In brain tissue, GPx activity is mainly localized to astroglia (Damier *et al.*, 1993; Takizawa *et al.*, 1994). The reduced glutathione consumed by GPx reactions is restored from oxidized GSSG by the glutathione reductase reaction (*Figure 1*, BIV). Glutathione S-transferases (GST) are important phase II enzymes in xenobiotic metabolism and conjugate highly reactive intermediates, drug metabolites or lipid peroxides to GSH (Goon *et al.*, 1993; Hartley *et al.*, 1995). Another important enzymatic system contributing to antioxidant defense is the thioredoxin/thioredoxin reductase system. Thioredoxin (Trx) is a polypeptide containing two

adjacent thiol groups that can regenerate protein disulfide bonds formed under oxidative conditions. Trx is then regenerated by thioredoxin reductases (Chae *et al.*, 1999).

Low-molecular-mass antioxidants are either produced endogenously, for example glutathione, uric acid, coenzyme Q, lipoic acid and bilirubin, or they are taken up by the diet. The most important endogenous antioxidant is the tripeptide glutathione. Glutathione is composed of the amino acids γ -glutamate, cysteine and glycine. The antioxidant properties of glutathione are due to the thiol residue in cysteine. Glutathione is found in millimolar concentrations in most mammalian cells (Cooper and Kristal, 1997). It can react either directly with ROS like superoxide, nitric oxide or the hydroxyl radical (Winterbourn and Metodiewa, 1994) or act as cofactor for the enzymatic antioxidant defense by glutathione peroxidases. In brain, glutathione metabolism seems to be a complex interplay between astrocytes and neurons, where astrocytes have an essential function in providing neurons with glutathione precursors (Dringen, 2000).

The most prominent dietary anti-oxidants are vitamin C (ascorbic acid) and vitamin E (tocopherols). Vitamin C can donate one electron to free radicals under formation of the ascorbyl radical. Due to mesomeric stabilization of the free electron in the ascorbyl radical, this component is very stable. Lipid-soluble tocopherols are more effective against radicals generated in membranes (*e.g.* mitochondria). However, to date there is no evidence that levels of vitamins are altered in PD patients.

There are many phytochemicals that exhibit antioxidant properties, including carotenoids, flavonoids and anthocyanidines. Their efficacy might be particularly higher than classical antioxidants. Their lipophilic character may allow easy penetration of the blood brain barrier. Furthermore, several compounds were found to activate transcription factors for cytoprotective genes, *e.g.* NF-E2-related factor-2 (Nrf-2). Among those substances are the phytoalexin resveratrol (Hsieh *et al.*, 1999; Manna *et al.*, 2000), and flavonoids, *e.g.* quercetin (Hanneken *et al.*, 2006). Flavanols are therefore highly potential antioxidants (*Figure 2*).

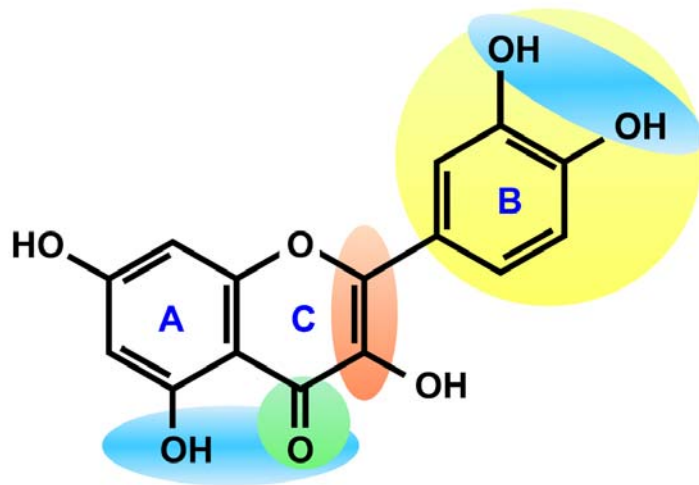


Figure 2. Antioxidant potential of flavonoids

Structure of the flavonol quercetin showing features important in defining the classical antioxidant potential of flavonoids. The most important of these is the catechol or dihydroxylated B-ring (shaded yellow) that easily donates a proton to stabilise a radical species. Other important features include the presence of unsaturation in the C-ring (shaded red) and the presence of a 4-oxo function in the C-ring (shaded green), increasing the potential to delocalize one electron. The catechol group and other functions may also ascribe an ability to chelate transition metal ions such as copper and iron (shaded blue).

Adapted from Spencer *et al.* (2003), *Biochemical Journal*, 372, 173–181.

1.2.2 Role of ROS and ROS products in cell death

Excessively elevated intracellular ROS levels lead to lipid peroxidation, oxidation of proteins, and DNA damage. Unsaturated fatty acids are an easy target for ROS. Oxidated lipids lead to membrane dysfunction, while the products of lipid decomposition, malondialdehyde and 4-hydroxynonenal, can exert cytotoxic actions, including DNA and mitochondrial damage (Eckl *et al.*, 1993; Benamira *et al.*, 1995; Keller and Mattson, 1998, Siems *et al.*, 1996; Lu *et al.*, 2002).

Oxidative protein modifications include a wide variety of reactions depending on the type of amino acids that are affected: sulfur-containing moieties in cysteine and methionine are easily oxidized to disulfides or sulfoxides, respectively, basic amino acids arginine and lysine can be oxidized to aldehydes, aromatic rings in amino acids can be oxidized or nitrated and aliphatic carbon atoms can be oxidized to alcohols. Apart from direct attack of ROS, proteins can also be oxidatively modified by lipid peroxidation products or by sugars and aldehydes that lead to

formation of advanced glycation end products (Münch *et al.*, 1997). Repair mechanisms include restoration of cysteine thiol groups from disulfides, *e.g.* by thioredoxin, and restoration of methionine from sulfoxides by methionine sulfoxide reductase (Stadtman, 2004). However, oxidized proteins can be removed by proteolysis via the proteasome complex.

Increased levels of ROS can either induce adaptive responses or elicit cell death. Often, mild oxidative stress leads to activation of antioxidant responses and resistance to higher ROS levels. Intracellular signaling triggered by ROS is very complex (reviewed in Finkel, 1998; Dalton *et al.*, 1999; Allen and Tresini, 2000). As a result, several transcription factors can be affected by ROS (reviewed in Sun and Oberley, 1996; Sen and Packer, 1996; Dalton *et al.*, 1999). One of these signaling cascades is the mitogen-activated protein kinase (MAPK) pathway (see section 1.5), which activates the transcription factor AP-1. AP-1 is a dimer of two proteins, c-Fos and c-Jun, existing either as an inactive homodimer of phosphorylated c-Jun or an active heterodimer of c-Jun and c-Fos. A consensus sequence for AP-1 binding has been found in the antioxidant response element (ARE). Among the genes with ARE sequences are glutathione-S-transferase and glutathione synthesizing enzymes, NAD(P)H quinone oxidoreductase-1, ferritin, heme oxygenase-1 and phase II detoxification enzymes (La Fauci *et al.*, 1989; Trejo *et al.*, 1994). The primary transcription factor controlling ARE is Nrf-2 (Chen *et al.*, 2004). Nrf-2 binds to ARE by homo- or heterodimerization with other leucine-zipper transcription factors, *e.g.* c-Jun (McMahon *et al.*, 2001; Venugopal and Jaiswal, 1998; Xu *et al.*, 2006). Thereby, Nrf-2 can protect from mitochondrial toxins used as models for PD (Lee *et al.*, 2003).

Damage of cellular components by ROS and insufficient repair mechanisms usually lead to a cell death. Whether cells die by apoptosis or necrosis is largely dependent on the severity of the insult: apoptosis, which is an energy-consuming process, requires some residual functionality of cellular proteins and ATP (Richter *et al.*, 1996), whereas severe oxidative damage with destruction of cellular integrity and dissipation of ATP levels usually elicits necrotic cell death (Leist *et al.*, 1997; Eguchi *et al.*, 1997).

1.3 Hallmarks of apoptosis

Apoptotic cell death can be initiated by various other (external and internal) signals apart from ROS and executed by several interrelated pathways. Cells remain intact and do not cause an inflammatory response in situ. However, there are clear and specific signs for apoptotic events: cell shrinkage, membrane budding, chromatin aggregation, margination of condensed chromatin at nuclear membrane, DNA-laddering in agarose gel, and the formation of apoptotic bodies (fragments of condensed nucleus surrounded by small rim cytoplasm). The process is energy-dependent and well-controlled, apoptotic cells and bodies are cleared promptly from the tissue by phagocytosis (macrophages or glial cells).

At the molecular level, the apoptotic cell death machinery forms a complex cascade of ordered events, controlled by the regulated expression of apoptosis-associated genes and proteins. The apoptotic pathways have been investigated intensely, with the attempt to categorize them. As the number of stimuli and pathways is great so are the categories of programmed cell death by now: intrinsic and extrinsic, mitochondrial and death receptor, p53-dependent and -independent, caspase-dependent and -independent. It is apparent that apoptosis is not a series of clearly defined pathways but a complex network of signaling systems, that, if certain mechanisms fail, can also escape to other forms of cell death, autophagy or necrosis (Lockshin and Zakeri, 2007). Complicating the attempt of pharmacological intervention of these pathways, apoptosis is an essential component of neuronal plasticity (Yousefi *et al.*, 2003). Cell death in animals is normally classified as type I (apoptotic), type II (autophagic) or type III/necrotic (Penaloza *et al.*, 2006). Signaling networks converge at the level of caspase cascades. Caspases, a family of cysteine proteases, are central mediators of apoptosis. Executioner caspases cleave essential cellular proteins. Their activation in 6-OHDA toxicity has been described previously (Ochu *et al.*, 1998; Woodgate *et al.*, 1999).

1.4 Mitochondria in neuronal cell death

Mitochondria make up to 40% of the cell volume in cells that are most metabolically active: muscle cells and neurons. A mitochondrion has two membranes: The outer mitochondrial membrane (OMM) contains small pores, freely permeable to ions and other small molecules.

The inner membrane is highly impermeable, even to protons. The proton gradient across the inner membrane creates an electric potential and is used to generate ATP molecules. This is preceded by the consecutive transfer of electrons on molecular oxygen by four protein complexes attached to the inner wall of the inner mitochondrial membrane (IMM). These protein complexes are identified as Complex I, II, III and IV and comprise the respiratory chain ("electron transport chain") (for review see Gray *et al.*, 1999). High mitochondrial activity entails a low percentage of an incomplete transfer of electrons on molecular oxygen resulting in ROS (Boveris *et al.*, 1976; Turrens and Boveris, 1980). During apoptosis mitochondria are a target of signaling molecules that alter the permeability of the mitochondrial membranes. This can lead to disturbance in mitochondrial energy production and to an increase in ROS, as well as to the disruption of the mitochondrial membrane integrity, loss of the mitochondrial membrane potential ($\Delta\Psi_M$), swelling and release of pro-apoptotic molecules (Bernardi *et al.*, 1998; Halestrap *et al.*, 1998; Kroemer *et al.*, 1998; Crompton, 1999). Therefore, mitochondria play a central role in cell death signaling pathways (for reviews see Desagher and Martinou, 2000; Green and Reed, 1998; Kroemer *et al.*, 1998; Susin *et al.*, 1998).

Among the molecules that are released from the compartment between the IMM and the OMM, the intermembrane space (IMS), during apoptosis are apoptosis-inducing factor (AIF), endonuclease g (EndoG), second mitochondria-derived activator of caspases/direct IAP-binding protein of low isoelectric point (smac/DIABLO), HtrA2/Omi, and cytochrome c (cyt c). AIF and EndoG translocate to the nucleus and induce large-scale DNA fragmentation, thus leading to chromatin condensation (Daugas *et al.*, 2000). Smac/DIABLO and HtrA2/Omi potentiate caspase-dependent cell death by neutralizing the effect of proteins that function as inhibitors of apoptosis (Rehm *et al.*, 2003; Verhagen *et al.*, 2000). Their involvement in the apoptotic machinery is preceded by the release of cyt c, which is a key molecule in the activation of caspases (Liu *et al.*, 1996; Andreyev *et al.*, 1998; Kantrow and Piantadosi, 1997; Susin *et al.*, 1999; Zamzami *et al.*, 1997; Kluck *et al.*, 1997; for review see Kroemer and Reed, 2000; Polster and Fiskum, 2004).

Cyt c participates in the electron transport chain by passing electrons from complex III to complex IV. The IMS contains 15% free cyt c while the rest is situated in the cristae to exert the function described above (Bernardi and Azzone, 1981). In the IMS cyt c can act as an antioxidant, accepting an electron from the superoxide anion (Skulachev, 1998). In apoptotic conditions the OMM becomes permeable for larger molecules, resulting in a release of cyt c

INTRODUCTION

into the cytosol. Cyt c forms a complex with apoptosis protease activating factor 1 (APAF-1), pro-caspase 9 and ATP, which in turn activates caspases 3/7 (Li *et al.*, 1997; Zou *et al.*, 1999). These executioners of apoptosis cleave a variety of essential proteins and activate other proteases and DNAses resulting in cell death (Leist and Jäätelä, 2001).

Transport of larger substances across mitochondrial membranes requires the opening of transition pores (Zamzami *et al.*, 1996, Scarlett and Murphy, 1997). The mitochondrial permeability transition pore (mPTP) is a complex of the voltage dependent anion channel (VDAC) and bax protein (Shimizu, 1999; Blatt and Glick, 2001). It is a water-filled pore, through which molecules up to 1500 D (IMM) or even higher (OMM) can leak in or out (*e.g.* cytochrome c). At low-level conductance the PTP opening is reversible, causing a collapse of the mitochondrial membrane potential (Ichas and Mazat, 1998). ATP can still be generated due to the activity of an external respiratory chain, a complex in the OMM (Skulachev, 1998). At high-level conductance the PTP opening is irreversible and leads to swelling of the mitochondrial matrix and the loss of pyridine nucleotides and substrates for the citric acid cycle in the mitochondrial matrix (Kantrow and Piantadosi, 1997; Susin *et al.*, 1998; Zamzami *et al.* 1997; Kluck *et al.*, 1997). Upon a stimulus mitochondria react individually within a cell, so that, to a certain extent, impaired mitochondrial function can be compensated (Collins *et al.*, 2002).

The mechanism of pore formation/opening is regulated by members of the Bcl-2 family. These include the anti-apoptotic Bcl-2 and Bcl-X_L, which reside on the OMM, and the proapoptotic Bax and Bak, which are predominantly cytosolic while they can also be found connected to the surface of the OMM (Zimmermann *et al.*, 2001). During apoptosis, Bax is activated, translocates to mitochondria forming pores of various diameters in the OMM that can be large enough to release cyt c. On the other hand, anti-apoptotic Bcl-2 can inhibit cyt c release to the cytosol, and prevent Bax activation, thereby protecting cells from death (Kluck *et al.*, 1997; Yang *et al.*, 1997). BH3 domain-only Bcl-2 family members (*e.g.* Bid, Bim, Bad) promote pro-apoptotic effects indirectly by inhibiting binding of Bcl-2 to Bax, thus freeing Bax to be incorporated into the mitochondrial membrane (Gross *et al.*, 1999; Zong *et al.*, 2001). The JNK stress kinases can activate bax proteins, targeting bax to the OMM (Tsuruta *et al.*, 2004).

Increased ROS, in particular superoxide, can induce the formation of the mPTP due to disulfide cross-linking (Kowaltowski *et al.*, 1998; Zamzami *et al.*, 1998). However, it is not clear whether an increased ROS production precedes the mPTP opening or if the rise in ROS production is the result of the permeability change of the mitochondrial membranes.

Oxidative stress and mitochondrial dysfunction are implicated to play a major role in PD-related neurodegeneration (Greenamyre *et al.*, 1999; Jenner and Olanow, 1998; Schapira, 2008). A significant and specific reduction in the activity and amount of complex I was found in PD patients (Ramsay *et al.*, 1989; Schapira *et al.*, 1990; Parker *et al.*, 1989; Mizuno *et al.*, 1989). The inhibition of complex I results in ROS formation, in a mechanism independent of the $\Delta\Psi_M$ (Sipos *et al.*, 2003). Additionally, complex I is highly susceptible to an oxidative attack itself (Zhang *et al.* 1990). Environmental toxins relevant in PD target complex I to various extents (see section 1.1.3.1). However, a combined action of respiratory chain inhibition and additional oxidative stress is needed to induce apoptosis (Chinopoulos and Adam-Vizi, 2001). Even up to date there is a controversy as to the point at which oxidative stress and mitochondrial dysfunction in PD first occur (Jenner and Olanow, 2006). Is there a common signaling pathway that would control both, mediate signals from ROS to mitochondria or the other way around?

1.5 MAPK cascades

The mitogen-activated protein kinase (MAPK) pathways execute signal transduction from the cell surface into the nucleus to control gene expression by means of activating transcription factors. These pathways produce a wide range of cell responses, including cell proliferation, differentiation and apoptosis (Bonni *et al.*, 1999; Chang and Karin, 2001; Pearson *et al.*, 2001; Yang *et al.*, 2005).

MAP kinase subfamilies are currently classified in 6 groups: ERK1/2, JNK, p38 MAPK, ERK5, and the atypical classes ERK3/4 and ERK7/8. The ERKs (the classical ERK1/2, extracellular signal-regulated kinases) are preferentially activated in response to growth factors, and regulate cell proliferation and cell differentiation. JNKs (c-Jun N-terminal kinases, also known as stress-activated protein kinases) and p38 isoforms are responsive to stress stimuli, such as cytokines, ultraviolet irradiation, heat shock, and osmotic shock, and

are involved in cell differentiation and apoptosis. All these pathways contain redox-sensitive sites (Sen and Packer, 1996). Although exceptions are known, antioxidant compounds inducing ERK isoforms often elicit cytoprotective signaling, whereas oxidative stress activates JNK and p38 pathways that mostly result in cell death signaling (Kamata and Hirata, 1999; Poli *et al.*, 2004; Torres, 2003). MAP kinase pathways lead to phosphorylation of AP-1, c-Jun and c-Fos, thereby affecting gene transcription.

1.5.1 c-Jun N-terminal kinases (JNK)

Three genes, *jnk 1-3*, encode the JNK family with multiple splice variants (Barr and Bogoyevitch, 2001). Each of the three JNK isoforms resolves on a SDS-PAGE gel as either an approximate 46 or 55 kDa protein. JNKs are phosphorylated and activated by the dual specificity MAPKKs, MKK4 and MKK7 (*Figure 3*), which phosphorylate JNKs on Thr183 and Tyr185 residues (Kyriakis and Avruch, 2001; Paul *et al.*, 1997). The MAPKKs, which in turn activate these two MAPKKs, include ASK1, MEKKs and MLKs (Kyriakis and Avruch, 2001).

In addition to upstream kinases, scaffold proteins from the JIP family modulate JNK signaling (*Figure 3*). They form complexes with JNKs and selected members of the upstream phosphorylating kinases (Dickens *et al.*, 1997; Whitmarsh *et al.*, 1998). JIPs also likely play a role to direct JNK and their upstream kinases to different compartments of the cell by associating to microtubules (Goldstein, 2001; Verhey *et al.*, 2001).

The best analyzed target of JNKs is the transcription factor c-Jun. The activation of c-Jun requires translocation of activated JNK to the nucleus, and subsequent phosphorylation of two sites, serine 63 and 73. Then, c-Jun becomes competent to form homo- or heterodimers, or to act as an AP-1 transcription factor component (Behrens *et al.*, 1999; Hibi *et al.*, 1993; Dérillard *et al.*, 1994; Kyriakis *et al.*, 1994). Via the pathway JNK – c-Jun apoptotic processes are regulated (Xia *et al.*, 1995; Kang *et al.*, 1998; Maroney *et al.*, 1998; Le-Niculescu *et al.*, 1999; Troy *et al.*, 2001; Schlingensiepen *et al.*, 1994). Beyond c-Jun, JNKs also phosphorylate other transcription factors, including ATF-2 (Gupta *et al.*, 1995), Elk-1 (Yang *et al.*, 1998) and NFAT (Chow *et al.*, 1997). The three JNK isoforms display differing affinities and specificity for target transcription factors. JNK2 has a 25-fold greater binding affinity for the transcription factor c-Jun, which correlates to a 10-fold increase of phosphorylated c-Jun relative to JNK1 (Kallunki *et al.*, 1994, Sluss *et al.*, 1994). JNK3

demonstrates weakest binding to c-Jun (Gupta *et al.*, 1996). There are several other contrasts between the isoforms. JNK1 and 2 exhibit a broad tissue distribution whereas JNK3 is restricted to brain and testes (Carboni *et al.*, 1997). In the adult rodent brain, JNK2 and JNK3 are widely expressed, while JNK1 is localized only to some specific regions like hippocampus (Carboni *et al.*, 1998). Moreover, not only the induction of JNK activity in these tissues per se but the subcellular localization and access to different substrates is important for specific JNK functions (Coffey *et al.*, 2000). This is still a matter of intense research. Knock-out mice that individually lack *jnk1*, *jnk2* or *jnk3* genes develop normally (Kuan *et al.*, 1999; Yang *et al.*, 1997). However, mice deficient in both JNK1 and 2 die prematurely and display brain abnormalities that are attributable to a dysregulation of apoptosis (Kuan *et al.*, 1999). This indicates overlapping regulating and/or compensating abilities of the isoforms.

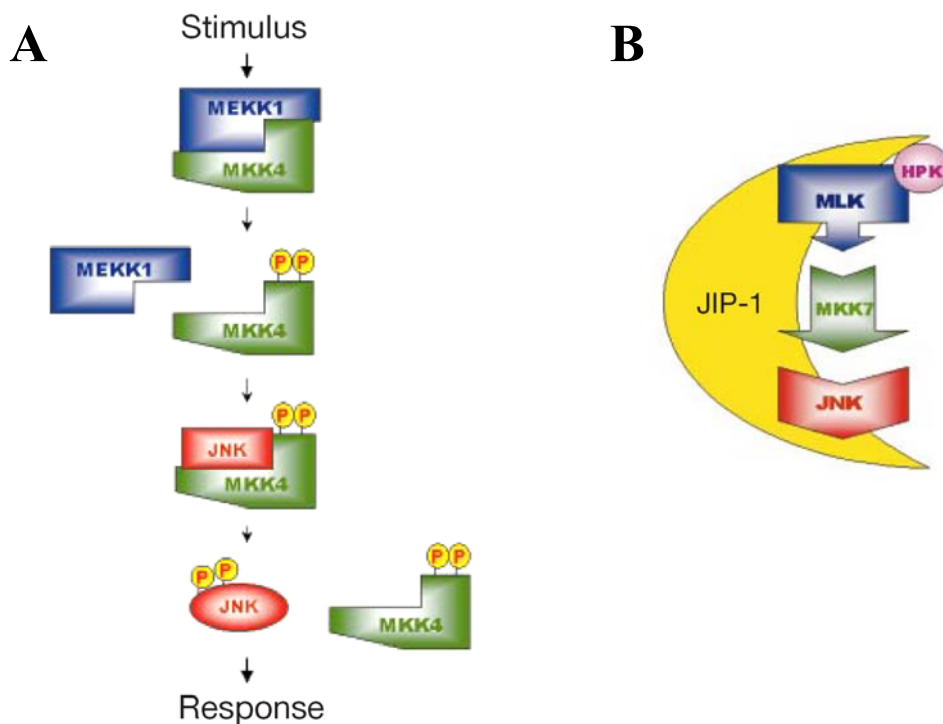


Figure 3. JNK signaling pathway

Mechanism of c-Jun N-terminal kinase (JNK) signaling by step-wise phosphorylation via upstream kinases. A stimulus mediates activation of members of the MAP3K family (MEKK1 or MLKs), which phosphorylate MAP2K (MKK4 or MKK7). In turn, MAP2Ks activate JNK (A). For activation of a downstream kinase all partners need to be in close proximity which is guaranteed by the scaffold protein JIP (B).

Adapted from Chang and Karin (2001), *Nature*, 410, 37–40.

Abbreviations: HPK (hematopoietic protein kinase), JIP-1 (JNK interacting protein-1), JNK (c-Jun N-terminal kinase), MAP2K or 3K (mitogen-activated protein 2 or 3-kinase), MEKK-1 (mitogen-activated protein 3 kinase-1), MKK-4/7 (mitogen-activated protein 2 kinase-4/7), MLK (mixed lineage kinase), P (active phosphate).

INTRODUCTION

JNKs are responsive to stress stimuli, such as cytokines, environmental toxins, oxidative stress, ultraviolet irradiation, heat shock, and osmotic shock. In certain conditions, JNKs mediate cell differentiation, but upon a strong stimulus the cell usually undergoes apoptosis that can be prevented by JNK inhibition (Waetzig and Herdegen, 2004). The endogenous level of JNK activity, at least in the rodent brain and in some cultured neuron populations, has been noted to be high (Coffey et al, 2000; Xu *et al.*, 1997). This basal tone of JNK activity is required for physiological events that sustain normal brain function (Waetzig and Herdegen, 2004).

JNKs play an important role in PD models. 6-OHDA and MPTP (MPP⁺) are strong activators of JNK and mediate neuronal cell death (Blum *et al.*, 2001a; Saporito *et al.*, 2000; Bozyczko-Coyne *et al.*, 2002 Hara *et al.*, 2003; Pan *et al.*, 2007). Consequently, JNK inhibition can rescue dopaminergic neurons from apoptosis (Saporito *et al.*, 1999; Wang *et al.*, 2004; Cha *et al.*, 2005; Pan *et al.*, 2007; Chen *et al.*, 2008). Moreover, the brains of PD patients display decreased levels of glutathione, an endogenous suppressor of JNK activity (Wilhelm *et al.*, 1997; Adler *et al.*, 1999).

JNKs are able to phosphorylate other proteins distant from the common MAPK pathway. Among such substrates have been identified tumor suppressor p53 (Buschmann *et al.*, 2001), tau protein (Goedert *et al.*, 1997) and amyloid precursor protein (Standen *et al.*, 2001). JNKs also interact with the proteins of the bcl-2 family, such as Bcl-2, Bcl-X_L, Bad, Bax or Bim, thereby regulating the mitochondrial death pathway (Park *et al.*, 1997; Kharbanda *et al.*, 2000; Donovan *et al.*, 2002; Schroeter *et al.*, 2003; Putcha *et al.*, 2003; Tsuruta *et al.*, 2004). Due to the localization of most BH3-proteins, the authors have pointed out, that JNK must be in the vicinity of mitochondria (Lei *et al.*, 2002; Aoki *et al.*, 2002). The crucial involvement of JNKs in the mitochondrial death signaling is supported by the fact that cytochrome c release into the cytosol can be prevented by JNK inhibition (Tournier *et al.*, 2000; Hatai *et al.*, 2000; Ichijo *et al.*, 1997). Moreover, JNKs release inhibitors of anti-apoptotic proteins, such as Smac/DIABLO from the mitochondria (Chauhan *et al.*, 2003).

There are several hints that JNK stresskinases are involved in the mitochondrial pathology and in ROS generation following 6-OHDA. How these events are connected has not yet been identified. And would JNKs exert any isoform specificity in compartmental signaling, *e.g.* at mitochondria?

2. AIMS OF THE THESIS

Parkinson's disease (PD) is a progressive neurodegenerative disorder of less defined etiology and limited treatment options. An important role in the development of the disease has been addressed to oxidative stress, mitochondrial impairment and stress kinase signaling. How these key events are initiated and interact with each other, remains unclear. In this thesis, the well-established 6-OHDA administration to PC12 cells was used as a model of PD. PC12 cells origin from the catecholaminergic rat pheochromocytoma. The present experiments addressed the following issues:

- The establishment of a flow cytometrical detection method for quantification of apoptosis and necrosis and analysis of PC12 cell death induced by 6-OHDA.
- The measurement of reactive oxygen species (ROS) over time to detect onset of and changes in oxidative stress following 6-OHDA. Determination of the source of ROS.
- The setup of a flow cytometrical assay and spectrofluorometrical analyses to follow-up the mitochondrial membrane potential during 6-OHDA treatment to denote any disturbances and the final disruption of $\Delta\Psi_M$.
- The analysis of the above mentioned parameters in isolated mice brain mitochondria to detect similarities and differences in the sequence of pathological events.
- The JNK isoform-specific investigation of PC12 mitochondrial fractions, the amount as well as activation status, and upstream and downstream signaling following 6-OHDA.
- The microscopical characterization of the intracellular distribution of JNK isoforms.
- The effects of JNK inhibition by SP600125 and the antioxidants methysticin, luteolin, resveratrol and *tert*-butylhydroquinone on 6-OHDA-induced oxidative stress.
- The involvement of JNK in a model of neurite outgrowth.

3. MATERIALS AND METHODS

3.1 Materials

Unless otherwise indicated, all solutions and dilutions were prepared in double-distilled water (DDW). All chemicals were *pro analysis* (*p.a.*). Apart from antibodies *Table 1* gives all materials used in this study.

Table 1. Materials

Material	Manufacturer / Supplier
Acrylamide / bis-acrylamide solution 29:1	Bio-Rad Laboratories, München, Germany
Adenosin-diphosphate	Sigma-Aldrich, München, Germany
Agarose SeaKem LE	Biozym, Oldendorf, Germany
Albumin, bovine fraction	Sigma-Aldrich, München, Germany
6-Aminocaproic acid	Merck-Schuchardt, Hohenbrunn, Germany
Ammonium persulphate	Merck, Darmstadt, Germany
Annexin V-FITC	Sigma-Aldrich, München, Germany
B-27 Supplement	Invitrogen, Karlsruhe, Germany
Boric acid	Sigma-Aldrich, München, Germany
Bromophenol blue	Merck, Darmstadt, Germany
<i>t</i> -Butylhydroquinone	Axxora, Lörrach, Germany
Calcium chloride	Merck, Darmstadt, Germany
Cell culture dishes (35 mm)	Sarstedt, Nümbrecht, Germany
Cell culture plates (10 cm, 6 wells, 24 wells)	Nunc, Wiesbaden, Germany
Chamber slides (2 wells)	Nunc, Wiesbaden, Germany
Cover glasses	Nunc, Wiesbaden, Germany
Cryotubes (2 ml)	Greiner Bio-One, Frickenhausen, Germany
Cytosine- β -D-Arabinofuranoside	Sigma-Aldrich, München, Germany
DAB tablets	Sigma-Aldrich, München, Germany
2',7'-Dichloro-dihydrofluorescein	Sigma-Aldrich, München, Germany

2',7'-Dichloro-dihydrofluorescein-diacetate	Sigma-Aldrich, München, Germany
Dihydrorhodamine 123	Sigma-Aldrich, München, Germany
Dimethylsulfoxide (DMSO)	Merck, Darmstadt, Germany
Dinitrophenol	Merck, Darmstadt, Germany
dNTP set (10 mM solutions)	Invitrogen, Karlsruhe, Germany
DTT	Invitrogen, Karlsruhe, Germany
Dye Reagent	Bio-Rad Laboratories, München, Germany
ECL Plus	GE Healthcare, Munich, Germany
EDTA	Merck, Darmstadt, Germany
EGTA	Merck, Darmstadt, Germany
Ethanol <i>p. a.</i>	Merck, Darmstadt, Germany
Ethanol, technical (denatured)	Bundesmonopol für Branntwein (BfB), Offenbach, Germany
Ethidium bromide solution (10 mg/ml)	Invitrogen, Karlsruhe, Germany
Fetal calf serum (FCS)	Bio Whittaker, Verviers, Belgium
Ficoll	Miltenyi Biotec, Bergisch-Gladbach, Germany
Filter paper	Whatman, Maidstone, UK
Filter unit 0.22 µm, syringe-driven	Qualilab, Bruchsal, Germany
Gentamycin	Invitrogen, Karlsruhe, Germany
G 418, sulfate (solution)	Stratagene, Amsterdam, The Netherlands
D-Glucose	Merck, Darmstadt, Germany
Glutamax	Invitrogen, Karlsruhe, Germany
Glycerol	Merck, Darmstadt, Germany
Glycine	Merck, Darmstadt, Germany
HEPES	Merck, Darmstadt, Germany
Hoechst 33258	Sigma-Aldrich, München, Germany
Horse serum	Invitrogen, Karlsruhe, Germany
6-hydroxydopamine hydrochloride	Sigma-Aldrich, München, Germany
Hyperfilm ECL	GE Healthcare, Munich, Germany
Immobilon P 1500	Millipore, Schwalbach, Germany

MATERIALS AND METHODS

Insulin	Sigma-Aldrich, München, Germany
JC-1	Sigma-Aldrich, München, Germany
Kaiser's glycerol gelatine	Merck, Darmstadt, Germany
Luteolin	Axxora, Lörrach, Germany
Magnesium chloride (PCR)	Invitrogen, Karlsruhe, Germany
Magnesium chloride	Merck, Darmstadt, Germany
Magnesium sulfate	Sigma-Aldrich, München, Germany
Mannitol	Merck, Darmstadt, Germany
2-Mercaptoethanol	Sigma-Aldrich, München, Germany
Methanol	Merck, Darmstadt, Germany
1-Methyl-4-phenylpyridinium iodide	Sigma-Aldrich, München, Germany
Methysticin	Axxora, Lörrach, Germany
Minimum essential medium (MEM)	Sigma-Aldrich, München, Germany
Mitotracker Red CM-H2Xros	Invitrogen, Karlsruhe, Germany
Non-fat dry milk	Uelzena, Uelzen, Germany
Paraformaldehyde	Merck, Darmstadt, Germany
PBS (w/o Ca ²⁺ and Mg ²⁺)	Invitrogen, Karlsruhe, Germany
PCR buffer (10 x)	Invitrogen, Karlsruhe, Germany
Penicillin/Streptomycin solution (10,000 IU / 10,000 µg/ml)	Invitrogen, Karlsruhe, Germany
Phenylmethylsulfonylfluorid	Sigma-Aldrich, München, Germany
Phosphatase Inhibitor Cocktail II	Sigma-Aldrich, München, Germany
Pipettes (serological, sterile; 5 / 10 / 25 ml)	Sarstedt, Nümbrecht, Germany
Pipette tips (10 / 200 / 1,000 µl)	Sarstedt, Nümbrecht, Germany
Poly-l-Lysine	Sigma-Aldrich, München, Germany
Ponceau S	Sigma-Aldrich, München, Germany
Potassium chloride	Merck, Darmstadt, Germany
Potassium dihydrogen phosphate	Merck, Darmstadt, Germany
Propidium iodide	Sigma-Aldrich, München, Germany
Protease Inhibitor (Complete)	Roche Diagnostics, Mannheim, Germany
Protein marker, prestained, broad range	New England Biolabs, Frankfurt, Germany

Proteinase K	Sigma-Aldrich, München, Germany
QIAamp DNA mini kit	Qiagen, Hilden, Germany
RPMI-1640 medium	Invitrogen, Karlsruhe, Germany
Rotenone	Sigma-Aldrich, München, Germany
SlowFade light antifade kit	Invitrogen, Karlsruhe, Germany
Sodium bicarbonate	Sigma-Aldrich, München, Germany
Sodium carbonate	Sigma-Aldrich, München, Germany
Sodium chloride	Merck, Darmstadt, Germany
Sodium dodecyl sulfate	Merck, Darmstadt, Germany
Sodium hydroxide	Merck, Darmstadt, Germany
Sodium pyruvate	Sigma-Aldrich, München, Germany
Sodium succinate	Sigma-Aldrich, München, Germany
SP600125	Axxora, Lörrach, Germany
Staurosporine	Axxora, Lörrach, Germany
Taq DNA polymerase	Invitrogen, Karlsruhe, Germany
TEMED	Carl Roth, Karlsruhe, Germany
Thermanox coverslips	Nunc, Wiesbaden, Germany
Transferrin	Merck, Darmstadt, Germany
Tris	Merck, Darmstadt, Germany
Triton X-100	Merck, Darmstadt, Germany
Trypan blue solution, cell culture tested	Sigma-Aldrich, München, Germany
Trypsin	Sigma-Aldrich, München, Germany
Trypsin inhibitor	Sigma-Aldrich, München, Germany
Tubes (0.5 / 1.5 / 2.0 ml)	Sarstedt, Nümbrecht, Germany
Tubes for PCR	Sarstedt, Nümbrecht, Germany
Tubes, sterile (15 / 50ml)	Sarstedt, Nümbrecht, Germany
Tween-20	Merck, Darmstadt, Germany
Ultrapure water	Biochrom, Berlin, Germany
Valinomycin	Sigma-Aldrich, München, Germany
Vectastain Elite ABC	Vector Labs, Burlingame, USA

3.2 Laboratory Equipment

Table 2. Equipment

Equipment	Manufacturer / Supplier
Agarose gel electrophoresis	Bio-Rad Laboratories, München, Germany
AnalySIS software	Soft Imaging System, Münster, Germany
Autoclave DS 202	Webeco, Bad Schwartau, Germany
Cell Quest Pro software	BD, Franklin Lakes, USA
Centrifuge; Biofuge fresco, Labofuge GL	Heraeus, Osterode, Germany
Centrifuge; Mikrofuge	Neolab, Heidelberg, Germany
Cell incubator	Heraeus, Osterode, Germany
DMR microscope	Leica Microsystems, Wetzlar, Germany
Electrophoresis power supply	Invitrogen, Karlsruhe, Germany
FACSCalibur flow cytometer	BD, Franklin Lakes, USA
Film processor	AGFA, Mortsel, Belgium
Fluoroskan Ascent FL microplate reader	Thermo Electron Corporation, Dreieich, Germany
GraphPad Prism Software	GraphPad Software, San Diego, USA
Hamilton syringes (10- and 50- μ l)	Hamilton, Bonaduz, Switzerland
Heating block (Thermomixer 543)	Eppendorf, Hamburg, Germany
Incubator (Innova 4000)	New Brunswick Scientific, Amsterdam, The Netherlands
Laminar flow unit	Heraeus, Osterode, Germany
Leica Qwin software	Leica Microsystems, Wetzlar, Germany
Leica DM L microscope with a fluorescence unit (100 W Hg + filter cubes)	Leica Microsystems, Wetzlar, Germany
Microplate reader 680	Bio-Rad Laboratories, München, Germany
MiniProtean II Vertical PAGE chamber	Bio-Rad Laboratories, München, Germany
Olympus CK 2 microscope	Olympus, Hamburg, Germany
Oxygraph	Hansatech Instruments, Norfolk, UK
pH meter	WTW, Weilheim, Germany
Rotator (Polymax 2040)	Heidolph, Kehlheim, Germany

Semi-dry transfer unit (Pegasus)	Phase, Lübeck, Germany
Sonicator (Sonopuls GM 70)	Bandelin, Berlin, Germany
Spectrophotometer (U-2000)	Hitachi, Wiesbaden, Germany
SPSS 14 for Windows	SPSS Inc., Chicago, USA
Thermocycler (Personal Cycler)	Biometra, Göttingen, Germany
UV light (Image Master VDS)	Bio-Rad Laboratories, München, Germany
Water bath	Heraeus, Osterode, Germany
WinMDI Software (Ver. 2.8 #13)	Freeware, Author: Joe Trotter
Zeiss LSM 5 image browser	Carl Zeiss Jena, Jena, Germany
Zeiss LSM 510 laser scanning microscope	Carl Zeiss Jena, Jena, Germany

3.3 Methods

3.3.1 PC12 cell culture

The rat pheochromocytoma cell line PC12 was purchased from the German Collection of Microorganisms and Cell Cultures (Deutsche Sammlung von Mikroorganismen und Zellkulturen GmbH; ACC159). The cells were grown in RPMI 1640 medium, supplemented as described in *Table 3*. The penicillin/streptomycin solution, horse serum and FCS were stored at -20° C, and the RPMI-1640 medium was stored in a cooling chamber (4° C). For maintenance and most experiments PC12 cells were grown in 10 cm culture dishes, for mitochondrial isolation 20 cm plates were used for better handling of the greater amount of cells, that were needed to obtain a sufficient yield of isolated mitochondria. The culture medium was stored at 4° C, and prewarmed to 37° C before giving to the cells. The volume for 10 cm plates was 7 ml, and 20 ml for 20 cm dishes. At least two times a week about 80% of the volume was replaced by fresh medium.

PC12 cells are poorly adherent, therefore all plates have to be coated with collagen (0.1 mg/ml in PBS) in advance. The bottom of the cell culture plates was covered with a thin layer of collagen solution, placed in the incubator for a minimum of 1 h and then washed with PBS to remove collagen that had not adhered to the surface. Air-dried plates were stored under sterile conditions.

Table 3. Composition of the PC12 cell culture medium

Cell culture medium	
RPMI-1640 medium	
Horse serum (HS, inactivated at 56° C for 30 min)	10%
Fetal calf serum (FCS, inactivated at 56° C for 30 min)	5%
HEPES	1%
Sodium pyruvate	1%
Penicillin/Streptomycin	1%
Adjusted with sterile 2 M glucose solution to 4,5 g/l glucose in the culture medium	

3.3.1.1 Splitting

The doubling time for PC12 cells is about 50 - 60 h. After approximately one week incubation cells reached 70 - 80% confluence and were seeded onto new plates (division of 1:3 - 1:6). For splitting, PC12 cells were pretreated with 0.5 mM EDTA in PBS to reduce cell adhesion. The following procedure was applied:

1. Cells were washed with PBS (37° C)
2. Cells were rinsed with 2 ml 0.5 mM EDTA in PBS (37° C) and placed for 2 min in the incubator (37° C, 5% CO₂)
3. 5 ml of medium was added (37° C)
4. Cells were scraped off the cell culture plate and transferred into a 15 ml tube and centrifuged for 10 min; (1000 x g; RT)
5. Pellets were first resuspended in 2 - 3 ml medium, sheared 3x through a 21 G needle/ 5 ml syringe, and culture medium was added ad 7 ml.
6. This cell suspension was usually divided 1:3 - 1:6 onto new plates so that approximately 1 - 2 million cells per plate were seeded.

3.3.1.2 Freezing and thawing

For production of PC12 stock aliquots, cells were harvested, pelleted and resuspended in 1 ml freezing medium (about two million cells per ml). Freezing medium consisted of cell culture medium adjusted to 10% FCS and supplemented with 10% DMSO. The cell solution was

aliquoted in 2 ml cryotubes, transferred to ice for 35 min, incubated at -20° C for 45 min and finally stored at -80° C.

PC12 cells were stored in aliquots at -80°C. When the cells had been passaged 20 times, they were discarded and a stock aliquot was quickly thawed in a 37° C water bath. The cell solution was pipetted slowly into 10 ml of FCS and centrifuged briefly at 1000 x g. The pellet was resuspended in cell culture medium containing twice the amount of serum than usual, and divided onto two 10 cm plates. Since DMSO is toxic for the cells, the nutrient solution was replaced by normal cell culture medium after 24 h. PC12 cells from no earlier passage than P6 were used for experiments.

3.3.2 Applied stimuli

For experiments, PC12 cells were seeded on new plates: 20 cm collagen-coated plates for mitochondrial isolations, 6 well plates for FACS analyses, 24 well plates for ROS experiments in the Fluoroskan Ascent[®] plate reader, and 10 cm plates for all other studies. Incubation time in the new plates was 2 – 3 days, since this time is needed for PC12 cells to express all relevant channels, transporters etc. (Shafer *et al.*, 1991). When splitting cells for experiments medium with reduced serum content (5% FCS) was used.

3.3.2.1 6-hydroxydopamine (6-OHDA)

Stock solutions of 10 mM and 50 mM 6-hydroxydopamine were freshly prepared in an aqueous solution of 0.02% ascorbic acid to prevent immediate autoxidation (Hayakawa, 1999). Working concentrations of 10 μM, 25 μM, 50 μM, 100 μM and 200 μM were obtained by adding the appropriate volume of stock solution to the medium at the desired time prior to harvesting the cells for analysis.

3.3.2.2 1-Methyl-4-phenylpyridinium ion (MPP⁺)

1-Methyl-4-phenylpyridinium (MPP⁺) iodide was chosen to compare antioxidant effects of methysticin, luteolin, resveratrol and tBHQ to the 6-OHDA neurodegenerative PD model. MPP⁺ is the metabolite that is generated from 1-methyl 4-phenyl 1,2,3,6-tetrahydropyridine (MPTP) by monoamine oxidases (MAO-B) in the central nervous system (Heikkila *et al.*, 1984). MPTP has been found to induce Parkinsonian-like symptoms (Langston *et al.*, 1984a; Langston *et al.* 1984b) and hence, MPTP and MPP⁺ have been used as classical agents to investigate the etiology of the disease in *in vitro* models (D'Amato *et al.*, 1986). MPP⁺ stock

solution was composed of 50 mM MPP⁺ in DDW, freshly prepared, and diluted to 50 μM, 100 μM or 200 μM.

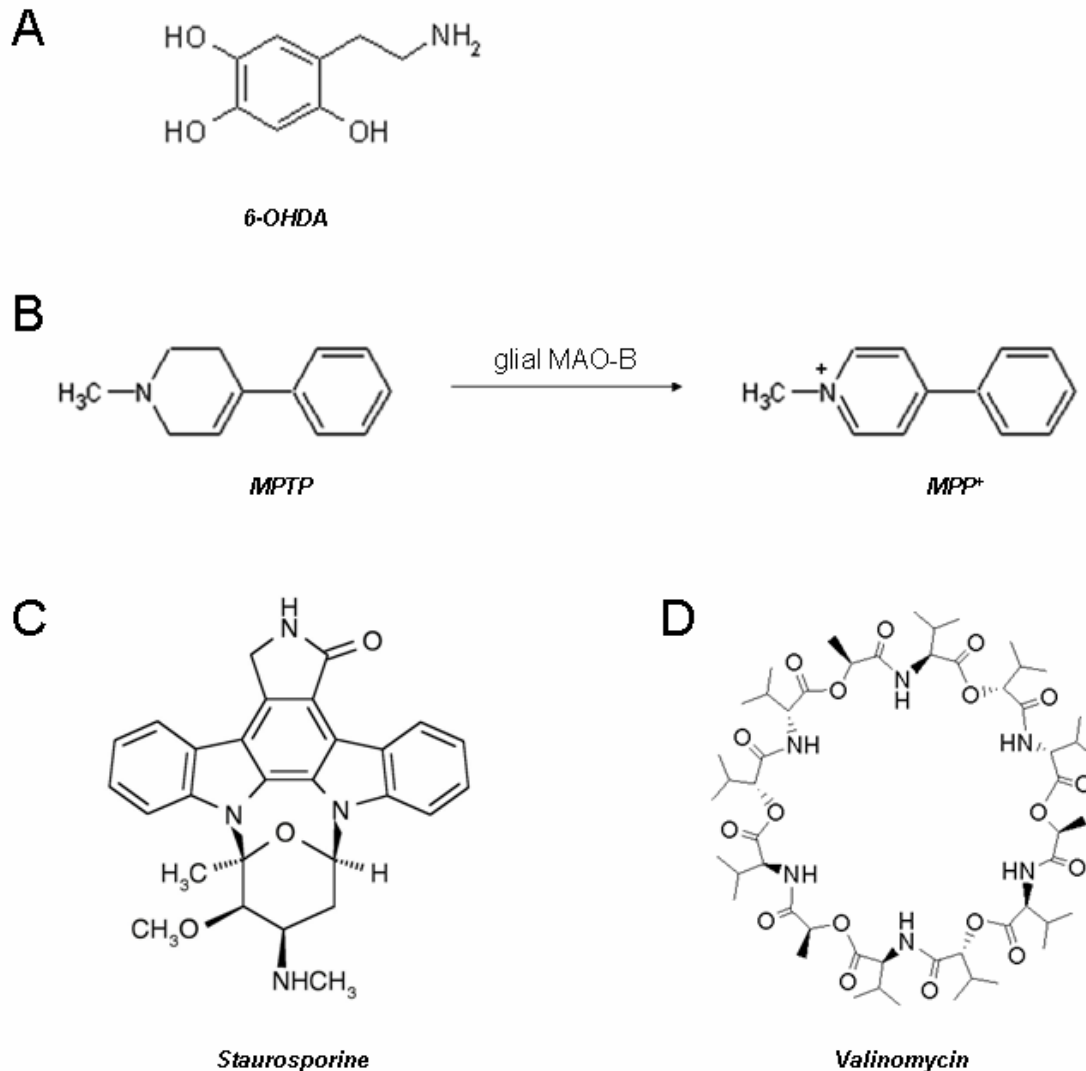


Figure 4. Applied stimuli (Source: Wikipedia.org, modified)

3.3.2.3 Staurosporine (STS)

Staurosporine (STS), isolated from the bacterium *Streptomyces staurosporeus* in 1977, possesses biological activities ranging from anti-fungal to anti-hypertensive (Rüegg and Burgess, 1989). The main feature of STS is the inhibition of a variety of protein kinases like protein kinase C (Tamaoki *et al.*, 1986). It is frequently used for its ability to induce cellular death via the mitochondrial apoptotic pathway, which includes the release of cytochrome c, caspase activation, intracellular ROS accumulation, and an increase in $[Ca^{2+}]_i$ (Krohn *et al.*,

1998; Prehn *et al.*, 1997; Kruman *et al.*, 1998). STS was used for setting up the flow cytometrical cell viability assay and as a positive control for increased ROS production. In those experiments, STS was administered at a concentration of 1 μM , prepared from a 1 mM stock solution in DMSO (so that the final DMSO concentration would not exceed 0.1%).

3.3.2.4 Valinomycin

Valinomycin is a cyclopeptide neutral ionophore synthesized by *Streptomyces fulvissimus*. This ionophore selectivity for K^+ renders biological membranes permeable to this cation and gives the compound the utility as an antibiotic (Cossarizza *et al.*, 1993; Pressman, 1976). In research Valinomycin is used to uncouple oxidative phosphorylation and disrupt the mitochondrial membrane potential ($\Delta\Psi_{\text{M}}$) (Cossarizza *et al.*, 1996; Sureda *et al.*, 1997). In this study Valinomycin was used in a concentration of 1 μM diluted from a 2 mM stock solution in ethanol as a positive control for $\Delta\Psi_{\text{M}}$ experiments.

3.3.3 Protection of PC12 cells

3.3.3.1 The JNK inhibitor SP600125

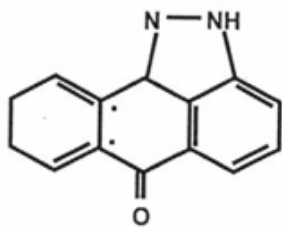
SP600125 (SP) is an anthrapyrazolone ATP-competitive inhibitor of JNK. Although it exerts a great specificity towards JNK, also other ERK and p38 kinases, the closest relative kinases, and the upstream kinases MKK4 and 7 can be targeted due to the similarity of the ATP binding site (Bogoyevitch *et al.*, 2004). SP was applied 30 min prior to stimulation with 6-OHDA. When 25 μM or 50 μM 6-OHDA were administered SP concentration was 2 μM , for this was found to be the minimal effective dose to inhibit the phosphorylation of the transcription factor c-Jun, the major target of JNK activity (Bennett *et al.*, 2001; Eminel *et al.*, 2004). Only at higher 6-OHDA concentrations (50 μM to 200 μM) SP600125 application was adjusted when indicated.

3.3.3.2 Methysticin

Methysticin is one of 6 major kavalactones yielded from *Piper methysticum* (kava-kava). Effects of kavalactones include mild sedation, improved cognitive performance and lift of spirits (Thompson *et al.*, 2004). Muscle relaxant, anaesthetic, anticonvulsive and anxiolytic effects are thought to result from direct interactions of methysticin with voltage-gated sodium channels (Magura *et al.*, 1997). Furthermore, methysticin reduces infarct size in mouse brains

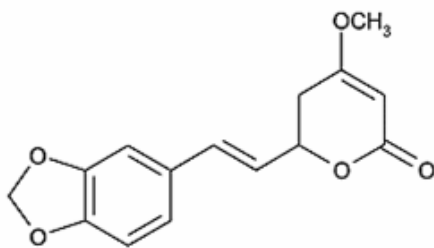
after ischemic insult by middle cerebral artery (MCA) occlusion in a comparable manner to memantine (Backhaus and Kriegstein, 1992). There are hints that methysticin could reduce oxidative stress, as it inhibits monoamine oxidase B (MAO-B), a source for oxygen radicals in the cytoplasm, and showed moderate radical scavenging abilities (Uebelhack *et al.*, 1998; Wu *et al.*, 2002). However, long-term kava use is associated with substantial alterations in liver enzymes and liver toxicity (Mathews *et al.*, 2005). In this study methysticin was used in a final concentration of 25 μ M, taken from a 25 mM stock solution in DMSO.

A



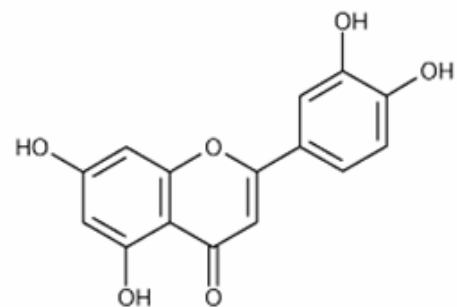
SP600125

B



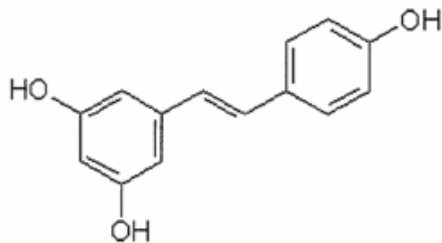
Methysticin

C



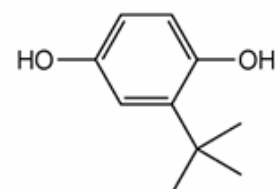
Luteolin

D



Resveratrol

E



tert-Butylhydroquinone

Figure 5. Protective agents (Source: Wikipedia.org, modified)

3.3.3.3 Luteolin

Luteolin, a 3',4',5,7-tetrahydroxyflavone, is usually found in a glycosylated form in *e.g.* celery, green pepper, and chamomile tea. Luteolin possesses high DNA protective effect in the presence of H₂O₂ (Romanova *et al.*, 2001), anti-inflammatory, antioxidant and phytoestrogen-like activities (Dall'Acqua and Innocenti, 2004). Luteolin is among the most potent and efficacious flavonoid inhibitors of lipopolysaccharide (LPS)-induced TNF- α and IL-6 production, as well as nitric oxide expression (Xagorari *et al.*, 2001). Its neuroprotective effects result from radical scavenging features and interaction with signaling pathways promoting cell survival (for review see Dajas *et al.*, 2003). Luteolin, in the final concentration of 5 μ M, prepared from a 5 mM stock solution in 100% ethanol, was used for assays in the PC12 cell model. This contributed to a study of our research group elucidating that neuroprotection by luteolin is mediated by the increased activity of the neuroprotective transcription factor Nrf-2 (Wruck *et al.*, 2007).

3.3.3.4 Resveratrol

Resveratrol (3,5,4'-trihydroxystilbene) belongs to the phytoalexins, antibacterial and anti-fungal chemicals produced by plants as a defense against infection by pathogens. The compound is primarily found in the skins of grapes, which has led to a vivid discussion about the contribution of resveratrol to health effects of red wine (Corder *et al.*, 2006). Indeed, there are many reports about beneficial health effects, such as anti-cancer, antiviral, neuroprotective, cardioprotective, anti-aging, anti-inflammatory and life-prolonging effects (for review see Pervaiz, 2003).

On cellular level, mechanisms of resveratrol actions include modulation of transcription factors, like NF- κ B, AP-1 (Jun/Fos) and Nrf-2, alteration of the expression and activity of cyclooxygenase (COX) enzymes, improvement of mitochondrial functions, antioxidant activities, inhibition of lipid oxidation, induction of cell death by release of pro-apoptotic mediators from mitochondria, increase in the expression of p53, inhibition of cyclin-dependent kinase (cdk), cell cycle arrest, inhibition of the JNK pathway (Pervaiz, 2003; Hsieh *et al.*, 1999; Manna *et al.*, 2000; Kutuk *et al.*, 2006; Leiro *et al.*, 2005; Plin *et al.*, 2005; Lagouge *et al.*, 2006; Wruck *et al.*, 2007). Resveratrol was applied in a final concentration of 5 μ M, prepared from a 5 mM stock solution in DMSO.

3.3.3.5 *tert*-Butylhydroquinone (*t*BHQ)

*t*BHQ is a highly effective antioxidant used to enhance storage life of goods and food. In research it is a standard compound to compare antioxidant efficacy. *t*BHQ was applied in a concentration of 5 μ M, prepared from a 25 mM stock solution in DMSO.

3.3.4 Trypan blue viability staining

Various manipulations of cells, including splitting, freezing and stimulations may provoke cell death. To determine the number of surviving cells in a given population, exclusion of the dye trypan blue was used. Healthy cells are able to exclude this dye for a certain time, but trypan blue will quickly diffuse into the cells which have lost their membrane integrity. The following protocol was used:

Protocol:

1. Cells were washed with PBS (37° C)
2. Cells were rinsed with 2 ml 0.5 M EDTA in PBS (37° C) and placed for 2 min in the incubator (37° C, 5% CO₂)
3. 5 ml of medium were added (37° C)
4. Cells were scraped off the cell culture plate and transferred into a 15 ml tube
5. Cells were centrifuged for 10 min (1000 x g, RT)
6. After centrifugation, the pellet was thoroughly resuspended in an appropriate amount of PBS
7. 20 μ l of the cell suspension were mixed with 20 μ l of trypan blue solution and transferred to a hemocytometer twin chamber. Living cells in the 16 squares of both chambers were counted, and the percentage of viable cells was determined.

3.3.5 Preparation of mitochondria

Mitochondria from PC12 cells were isolated adapting the method described by Kapirnich *et al.* (Kapirnich *et al.*, 2002). All steps were conducted at 4° C.

Protocol:

1. Cells plated on 20 cm cell culture plates were washed twice with PBS and harvested.
2. Centrifugation for 6 min (1000 x g, 4° C).

3. Pellets were resuspended in 4 ml of PBS and living cells were counted with trypan blue.
4. Cells were centrifuged again; pellets were resuspended in sucrose buffer (for 5×10^6 cells 100 μ l sucrose buffer) and transferred into 1.5 ml tubes. The cell solution was stored for 1 h on ice.
5. After 1 h cells were lysed by aspiration through a 27 gauge syringe (25 - 30 times).
6. Lysates were centrifuged for 5 min (750 x g, 4° C).
7. Pellets containing mainly nuclear proteins were washed, lysed in DLB-buffer and frozen at -80° C. Supernatants were collected into a sterile 1.5 ml tube and centrifuged for 15 min (10,000 x g, 4° C).
8. Supernatants containing the cytoplasmic proteins were transferred into a sterile 1.5 ml tube and SDS from a 10% stock solution was added to a final concentration of 1% SDS.
9. Pellets containing mitochondrial extracts were resuspended in sucrose buffer and centrifuged for 15 min (10,000 x g, 4° C). This washing step was repeated once more.
10. Mitochondrial pellets were lysed in DLB-buffer (*Tables 5*).
11. Cytoplasmic and mitochondrial extracts were boiled for 5 min at 95° C.
12. Mitochondrial extracts were sonicated twice for 5 sec and centrifuged (15 min, 13,000 x g, 4° C) to remove insoluble materials.
13. Cytoplasmic and mitochondrial extracts were stored at -80° C.

Table 4. Composition of sucrose buffer

Sucrose buffer	
HEPES	20 mM
KCl	10 mM
MgCl ₂	1.5 mM
EGTA	1 mM
EDTA	1 mM
Sucrose	250 mM
DTT	1 mM
PMSF	0.1 mM
Freshly prepared and kept at 4° C.	

Samples for the assessment of the changes of the cytosolic protein β -actin and the mitochondrially resident enzyme cytochrome c oxidase subunit IV (COX IV) were taken as follows: whole cell sample during step 3 (controls, C), resuspended mitochondrial suspension samples during washing step 9 (intermediate fractions, I1 and I2), and the final mitochondrial fraction (M).

3.3.6 Protein identification by Western blot

3.3.6.1 Denaturing protein extraction

Denatured protein extracts from mitochondria were prepared using a Tris-buffered sodium dodecyl sulfate (SDS) lysis buffer (denaturing lysis buffer).

1. The cell pellet collected in a 1.5 ml tube was resuspended in 50 - 300 μ l of lysis buffer (depending on the size of the pellet).
2. The cell solution was incubated for 5 min at 95° C in a heating block.
3. The samples were sonicated twice for 5 s to disrupt the cells by cresting vibrations which cause mechanical shearing of the cell wall.
4. Insoluble material was removed by centrifugation (15 min; 13,000 x g; 4° C).
5. The supernatant was transferred into a new 1.5 ml tube and stored at -80° C.

Table 5. Composition of denaturing lysis buffer.

Denaturing lysis buffer (DLB-buffer)	
Tris	10 mM
SDS	1%
Phosphatase inhibitor Cocktail II	1%

3.3.6.2 SDS-PAGE

Polyacrylamide gels were prepared by co-polymerization of acrylamide monomers with the cross-linker bis-acrylamide. The reaction was catalyzed by ammonium persulphate (APS) and initiated by N,N,N',N'-tetramethylethylenediamine (TEMED). For better resolution, a short stacking gel was set on top of the main resolving gel. Differences in composition between these two gels resulted in concentration of the protein samples into narrow bands in the

stacking gel and separation of the bands according to their size in the resolving gel (*Tables 6 and 7*). For preparation of the resolving gel different percentages of acrylamide were used, depending on the molecular weight of protein to be analyzed. 15% resolving gel was used to detect cytochrome c (cyt c), and cytochrome c oxidase subunit IV (COX IV), all other proteins were analyzed in a 12% resolving gel (*Tables 6 and 7*).

Table 6. Composition of solutions used in SDS-PAGE

Resolving buffer		Stacking buffer	
Tris, pH 8.8	1.5 M	Tris, pH 6.8	0.5 M
SDS	0.4%	SDS	0.4%
MgCl ₂	1.5 mM	Sucrose	250 mM
PMSF	0.1 mM	DTT	1 mM
Stored at 4° C		Stored at 4° C	
Acrylamide/bis-acrylamide solution		Electrophoresis buffer (10x)	
Acrylamide	30%	Tris, pH 8.3	0.25 M
Bis-acrylamide	0.8%	Glycine	1.92 M
		SDS	1%
Stored at 4° C in the dark		Stored at RT	
Sample buffer (5x)			
Tris, pH 6.8	312.5 mM		
SDS	10%		
2-Mercaptoethanol	10%		
Glycerol	50%		
Stored at 4° C			

3.3.6.3 Preparation of polyacrylamide gels

The MiniProtean II Vertical PAGE chamber and glass plated were set up. Resolving gel monomer solution combining all reagents containing TEMED and APS was prepared. The solution was carefully introduced to minimize possibility of air bubbles trapped within the

gel. When the appropriate resolving gel solution was added, the gel was over-layered with DDW to keep the gel surface even and allowed to polymerize for 10-30 min at RT. After polymerization, a distinct interface appeared between the separating gel and DDW which had to be removed. Subsequently, the stacking gel (*Table 7*) was prepared and pipetted over the polymerized resolving gel until the solution reached top of front plate. Immediately, a 10- or 15-well comb was inserted into gel plates until bottom of teeth reach top of front plate. It is important to be sure that bubbles were not trapped on the ends of teeth. The stacking gel was allowed to polymerize within 30 min at RT.

After the stacking gel had polymerized the comb was removed carefully and the gel plates were placed into the electrophoresis chamber. The chamber was filled with 1x electrophoresis buffer and the wells were cleaned from residual gel particles.

Table 7. Composition of separating gels for SDS-PAGE

Target protein size	< 30 kDa	30-60 kDa
Component	15% gel	12% gel
Acrylamide	6.7 ml	4 ml
4 x resolving buffer	2.3 ml	2.5 ml
Autoclaved DDW	2.3 ml	3.4 ml
TEMED	10 μ l	10 μ l
10% APS	100 μ l	100 μ l

Composition of the 3% stacking gel for SDS-PAGE

Component	Quantity
Acrylamide	0.6 ml
4 x stacking buffer	1.5 ml
Autoclaved DDW	3.9 ml
TEMED	6 μ l
10% APS	60 μ l

3.3.6.3 Preparation of protein samples

Protein samples, used for Western blot were diluted with autoclaved DDW in order to obtain 20 µg of total protein in a volume of 8 µl. 2 µl of 5x SDS sample buffer were added, and the samples were heated to 95° C for 5 min. Then the samples were loaded onto the gel. To estimate the molecular weights of bands detected by Western blotting, broad range prestained protein marker was used in the most left and/or most right lane.

3.3.6.4 Electrophoresis

The samples and the protein marker were carefully loaded into the cleaned wells and run through the stacking and resolving gels at a constant current of 30 mA. Usually, gels were run for 30 min after the tracking dye had passed the end of the gel. Finally, gels were removed from the gel plates, the stacking gel was discarded, and the resolving gel was used for Western blotting.

3.3.6.5 Immunoblotting

Table 8. Solutions for Western blotting experiments

TBS (10x)		TTBS	
Tris	200 mM	TBS (1x)	
NaCl	1.37 mM	Tween-20	1 ml/l
Stored at 4° C		Stored at 4° C	
Anode Buffer I		Anode Buffer II	
Tris	30 mM	Tris	300 mM
Methanol	20%	Methanol	20%
Stored at RT		Stored at RT	
Cathode Buffer			
Tris	300 mM		
Methanol	20%		
6-aminocaproic acid	10%		
Stored at RT			

MATERIALS AND METHODS

In Western blotting experiments proteins are transferred from a SDS-PAGE gel to a synthetic membrane, and blotted proteins are detected by specific antibodies. Prior to addition of antibodies, the membrane is coated with blocking solution (BS), *e.g.* 4% non-fat milk or 4% BSA in TTBS, to avoid non-specific binding to the membrane. The primary IgG (*e.g.* produced in mice) antibody recognizes the protein of interest while the secondary antibody recognizes the Fc region of the first antibody. This secondary antibody is coupled to an enzyme, *e.g.* a horseradish peroxidase (HRP), which converts a chemiluminescence substrate.

After the proteins were separated by SDS-PAGE, they were transferred to a polyvinylidene difluoride (PVDF) membrane by semi-dry blotting using an electroblotter. Three different transfer buffers were used (anode buffer I and II, cathode buffer). The PVDF membrane which was cut to the size of the gel (9 x 6 cm) was activated in 100% methanol for 3 min. Subsequently the membrane was rinsed in DDW for 2 min and equilibrated in anode buffer I until use. For each gel, 15 pieces of blotting paper were cut to the size of the gel (9 x 6 cm). 6 pieces of them were pre-soaked in anode buffer II and placed on a glass plate. Three pieces of blotting paper were pre-soaked in anode buffer I and placed over the anode buffer II-soaked filter paper. The equilibrated membrane was then placed over the filter paper and the gel was placed in close contact with membrane after pre-soaked in cathode buffer. The 'sandwich' was completed by stacking remaining 6 pieces of filter paper pre-soaked in cathode buffer. Finally, the blotting 'sandwich' was turned upside down and placed into the semi-dry transfer unit in which the lid is the cathode.

Proteins were transferred to the PVDF membrane using a constant current of 0.8 mA/cm² for 1 h (protein size 30-80 kDa) or 1.5 h (>80 kDa). After transferring the protein to the membrane, the membrane was washed for 20 min in 1x TTBS buffer and blocked with blocking solution for 60 min. Subsequently the membrane was incubated with the first antibody at 4° C overnight (see also *Table 9*). The next day, the primary antibody solution was discarded and the unbound antibodies were removed by washing the membranes once for 15 min and twice for 5 min each with TTBS. Usually the membrane was incubated with a dilution of 1:4000 goat-anti-rabbit secondary antibody or with a dilution of 1:3000 goat-anti-mouse secondary antibody for 30 min at RT. After discarding the secondary antibody solution, the membrane was washed once for 15 min and three times for 5 min each with TTBS.

Table 9. Primary and secondary antibodies for western blots

Antibody	Dilution and Buffer	Source	Manufacturer
COX IV	1:800 in 4% BS	rabbit	CST
Cytochrome c	1:5000 in 4% BS	mouse	BD
Grp75	1:5000 in TTBS	mouse	Stressgen
JNK1	1:1000 in TTBS	mouse	Pharmingen
JNK2	1:1000 in 4% BS	mouse	Santa Cruz
JNK3	1:1000 in TTBS	rabbit	Alexis
JIP-1	1:1000 in 4 % BS	rabbit	Santa Cruz
MKK4	1:500 in TTBS	rabbit	Santa Cruz
MKK7	1:1000 in 2% BS	rabbit	Santa Cruz
phospho-JNK	1:2500 in 4% BS	rabbit	Promega
phospho-MKK4	1:500 in TTBS	rabbit	Santa Cruz
total JNK	1:1000 in TTBS	rabbit	CST
β -actin	1:5000 in TTBS	mouse	Sigma

3.3.6.6 ECL-reaction

After the last washing step, the membrane was placed with the protein side up on a glass plate. For a 6 x 9 cm (standard sized) membrane, 1 ml of ECL Plus HRP substrate was prepared immediately prior to use by mixing 0.975 ml of ECL Plus Reagent A with 25 μ l of ECL Plus Reagent B. The membrane was carefully covered with the HRP substrate solution and incubated for 3 min. Subsequently, all the HRP substrate was allowed to drip off the membrane and the membrane was placed inside the plastic pocket of a film cassette. The chemiluminescence on the membranes was detected by exposing the membranes to Hyperfilm ECL films in a darkroom. Films were developed and fixed by a film processor.

3.3.6.7 Stripping of Western blot membranes

After Western blot and detection of the protein, the membrane can be used to detect an other protein. For stripping, the membrane was incubated with stripping solution (Tris 62.5 mM, SDS 2%, 2-Mercaptoethanol 100 mM) for 30 min at 50° C and 25 rpm in an incubator. After stripping, the membrane was washed twice for 10 min each with TTBS and blocked with blocking solution. Subsequently, the membrane was incubated with primary antibody.

3.3.6.8 Ponceau S staining of Western blot membranes

Ponceau S is the only staining method which is completely compatible with all procedures of immunological probing, because the stain is transient and can be washed away so that it does not interfere with subsequent detection of antigens. After the ECL reaction, membranes were washed twice with TTBS and then stained with Ponceau S for 20 min. The staining solution was re-used several times. Stained membranes were washed twice with DDW for 5 min each before air-drying.

3.3.7 Basic principles of flow cytometry

Flow cytometry is a sensitive and rapid method for the detection of single cells. The term derives from the measurement of single cells that are passed through a thin capillary in solution. In the flow chamber the suspension is hit by a laser beam, and cells/organelles that pass the beam lead to scattering of the laser light, which is detected at two different angles: the forward scatter (FSC) at low angle and the sideward scatter (SSC) at 90°. The intensity of the FSC signal is related to the size of the cell: large cells lead to a higher scattering than small cells. On the other hand the intensity of the SSC signal is related to the morphology of the cell: cells with high granularity exhibit higher sideward scatter than cells with little cellular structure. The intensities of FSC and SSC thus allow for identification of different cell populations and also for identification of intact cells, since apoptotic cells exhibit smaller size and higher granularity. Furthermore, cells can be stained with different fluorescent dyes that are excited by the laser light and emit fluorescent light which is also detected at 90°. The optical system contains different filters which allows for simultaneous detection of several different dyes in a single cell. *Figure 6* shows a schematic representation of the optical system in the Becton Dickinson FACSCalibur system.

The FACSCalibur system contains a 488 nm blue laser, photodetectors for FSC and SSC with 488 nm filters as well as photodetectors for three different fluorescence channels with filters of 530 nm (green), 585 nm (orange) and 650 nm (red). These different wavelengths are termed channels FL1, FL2 and FL3 respectively. A single cell can therefore be characterized by up to five signals from FSC, SSC and the three fluorescence channels. Although the detectors of the different fluorescence channels are equipped with filters specific for a certain wavelength range, most fluorescent dyes show a broad emission peak and therefore some light may be also detected in the adjacent fluorescence channels. This overlap of emission

spectra of different dyes has to be corrected by compensation if cells are simultaneously stained with several dyes. Compensation is the electronic subtraction of unwanted signal to remove the effects of spectral spillover.

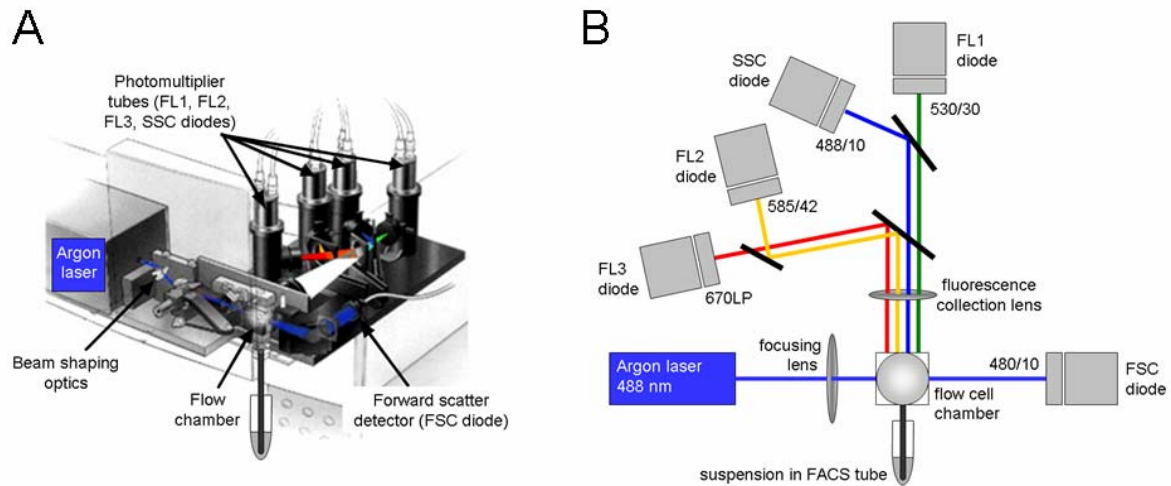


Figure 6. The Beckton Dickinson FACSCalibur system

The cell/organelle suspension is sucked into the flow chamber where fluorescent molecules in the solution are excited by a laser beam. Scattered light is detected in 180° (FSC) and 90° (SSC). Emitted fluorescence is split and narrowed to specific wavelength range and detected at 90° with photomultiplier tubes (FL diodes). (© Beckton Dickinson Inc., modified)

Abbreviations: FL1, FL2, FL3 (fluorescence channels 1, 2, 3), FSC (forward scatter), LP (long pass), SSC (side scatter).

3.3.7.1 Flow cytometrical data analysis

For quantification of ROS PC12 cells were stained with the ROS-sensitive dyes 2',7'-dichlorodihydrofluorescein-diacetate (H₂DCF-DA) and dihydrorhodamine 123 (DHR). For the characterization of the mitochondrial membrane potential ($\Delta\Psi_M$) samples were incubated with the dual-fluorescent probe JC-1, and for the detection of apoptotic and necrotic cells Annexin V-FITC and propidium iodide (PI) were used. All samples were analyzed by flow cytometry using Becton Dickinson FACSCalibur flow cytometer and Cell Quest Pro software. A minimum of 10,000 events were recorded per single measurement. Results represent a number of at least three independent experiments.

PC12 cells were gated according to size and morphology in the SSC vs. FSC density plot (*Figure 7A*), and only the gated events were evaluated for the intensities of fluorescent dyes.

Due to the small size of mitochondria, only a threshold was set to 60 in the FCS to rule out any events being counted below that.

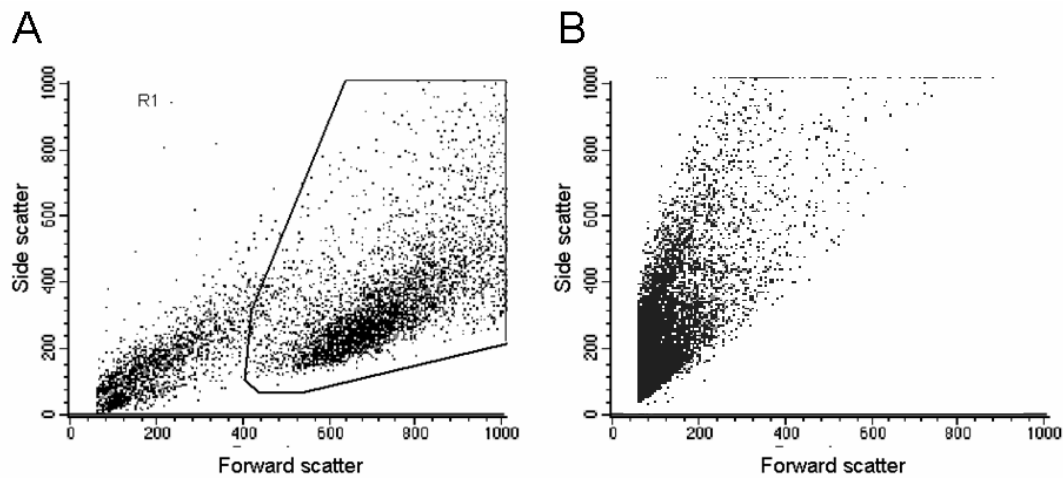


Figure 7. PC12 cells (A) and mitochondria (B) in the scatter plot.

3.3.7.2 Staining of PC12 cells with ROS-sensitive fluorescent dyes

In general, 1×10^6 /ml PC12 cells were incubated with ROS-sensitive dyes at 37°C in cell culture medium without phenol red, washed twice and resuspended for FACS analysis in FACS analysis medium (PBS containing 4.5 g/l glucose and 0.2% EDTA). Cells were analyzed immediately after staining and always kept on ice in the dark until measurement.

3.3.7.2.1 2',7'-Dichlorofluorescein (DCF)

2',7'-Dichloro-dihydrofluorescein-diacetate ($\text{H}_2\text{DCF-DA}$) is a widely used ROS-sensitive dye. The diacetate enables 2',7'-dichloro-dihydrofluorescein, also termed 2',7'-dichlorofluorescein (H_2DCF), to diffuse across the cell membrane where it is hydrolyzed by intracellular esterases to the non-fluorescent H_2DCF . Consequently, $\text{H}_2\text{DCF-DA}$ was administered to PC12 cells, and H_2DCF was given to samples of isolated mitochondria. In the cell H_2DCF is oxidized by various ROS to the highly fluorescent, 2-electron oxidation product, DCF (Bass *et al.*, 1983; Rothe and Valet, 1990; Hempel *et al.*, 1999). Mainly hydrogen peroxide in combination with enzymatic peroxidase activity seems to be responsible for H_2DCF oxidation (Walrand *et al.*, 2003). H_2DCF is a useful tool for monitoring cytosolic ROS levels, as well as ROS generated in the mitochondrial intermembrane space, and ROS that are released from mitochondria into the surrounding cytosol (Diaz *et al.*, 2003). The emission maximum of DCF is at 525 nm and can be detected in the FL1 channel.

After 20 min of H₂DCF-DA preloading, cells were washed twice with PBS and pellets were resuspended in FACS analysis medium. Analyzing PC12 cells, fluorescence was determined immediately for controls and stimulated samples. Results were reported as fluorescence intensity in percent of controls.

3.3.7.2.2 Dihydrorhodamine (DHR)

Dihydrorhodamine (DHR) is the non-fluorescent reduced form of rhodamine. Due to its lipophilicity it can easily diffuse across cell membranes. Inside the cell, it is oxidized by various ROS to the positively charged fluorescent rhodamine which is incorporated into mitochondria dependent on mitochondrial membrane potential (Johnson *et al.*, 1980). Although several ROS could be responsible for oxidation of DHR (Hempel *et al.*, 1999), it has been described to be most sensitive towards oxidation by hydrogen peroxide (Walrand *et al.*, 2003), especially in the presence of cytochrome c oxidase in mitochondria (Royall and Ischiropoulos, 1993). Thus it can be used as a marker for mitochondrial ROS production. The emission maximum of rhodamine is at 529 nm which is detected in channel FL1.

Table 10. Overview of the ROS-sensitive dyes, their properties and application

Dye	Ex (nm)	Em (nm)	FACS detection channel	Concentration	Incubation time at 37° C	Specificity
H ₂ DCF (DA)	504	525	FL1	10 µM	20 min	peroxides, cytosolic/whole-cell ROS, peroxynitrite
DHR	507	529	FL1	10 µM	30 min	peroxides, hydroxyl radical, mitochondrial ROS, peroxynitrite

3.3.7.3 Assessment of mitochondrial membrane potential with JC-1

The integrity of the inner mitochondrial membrane is determined by a specific potential gradient ($\Delta\Psi_M$) over this membrane. This can be correlated to the uptake of the cationic carbocyanine dye JC-1 (5,5',6,6'-tetrachloro-1,1',3,3'-tetraethylbenzimidazol-carbocyanine iodide) into the matrix (Reers *et al.*, 1991; Smiley *et al.*, 1991; Cossariza *et al.*, 1993). The mitochondrial membrane potential, across the inner membrane, determines the redistribution of this dye, which depends on the transmembrane electric field (negative inside of about 180 - 200 mV) and the concentration gradient of the dye.

The fluorophore JC-1 has the property that when excited at 485 nm (or in flow cytometry 488 nm by an Argon laser), the emission spectrum will be dependent on the concentration of the molecule. In dilute solutions of <300 nM it gives a green fluorescence at 527 nm, but raising the concentration over 1 mM leads to the appearance of a very strong red-orange fluorescence (at 590 nm, Invitrogen data sheet). This is due to the formation of aggregates of the dye, named J-aggregates. In a mitochondrial matrix, bounded by an inner membrane with a large $\Delta\Psi_M$, the dilute external concentration of the dye is concentrated to a level that enables the formation of J-aggregates.

JC-1 can be used as an indicator of mitochondrial potential in a variety of cell types, including PC12 cells (Dispersyn *et al.*, 1999; Nuydens *et al.*, 1999), as well as in isolated mitochondria (Cossariza *et al.*, 1996). JC-1 is more specific for mitochondrial versus plasma membrane potential, and more consistent in its response to depolarization, than other cationic dyes such as [DiOC₆ (3)] and rhodamine (Salvioli *et al.*, 1997). The ratio between red versus green fluorescence is often used as a measure to describe the $\Delta\Psi_M$ and integrity. In fact, measuring the red fluorescence alone is a superior way to represent $\Delta\Psi_M$, since the J-aggregates are specific for mitochondria whereas the monomers' distribution in the rest of the cell is heterogenous to its hydrophobic interaction (for review see Bernardi *et al.*, 1999).

PC12 cells and isolated mitochondria were subjected to the following protocol for determination of the $\Delta\Psi_M$ by the Becton Dickinson FACSCalibur flow cytometer (*Table 11*). This procedure is a fixed-point assay measuring the uptake of JC-1 with formation of the J-aggregates. It is also possible to follow the uptake with time using a kinetic program. The observed fluorescence of the solution rises to a plateau after 5 - 10 min.

Table 11. Protocol for the assessment of the mitochondrial membrane potential ($\Delta\Psi_M$)

PC12 cells	Mitochondria
1. PC12 cells were incubated in culture medium without phenol red and stimulated with 50 μ M 6-OHDA or 1 μ M valinomycin (positive control) for various time points	Mice brain mitochondria were isolated as described in section 3.3.13.
2. Cells were washed on the plate with PBS, and collected in PBS at a concentration of 10^6 cells/ml	A 50 μ l aliquot of the mitochondrial suspension was diluted in 1 ml PBS.
3. 10 μ M JC-1 was added, a concentration that had proven to be optimal regarding both fluorescence emission wavelengths (strong red and low green FI).	
4. Samples were incubated 20 min in the dark at RT.	
5. Samples were centrifuged briefly and pellets were resuspended in 1 ml PBS.	
6. PC12 cells were centrifuged briefly and pellets were resuspended in 1 ml FACS analysis medium	Mitochondria were centrifuged briefly and pellets were resuspended in MSH buffer. 10 μ M 6-OHDA or 1 μ M Valinomycin was added for the desired duration. Mitochondria were washed and resuspended in 1 ml FACS analysis medium
7. The flow cytometer was calibrated with a non-stained and a stained control.	
8. Fluorescence in FL1 and FL2 channels was measured for all samples applying voltages of 320 - 380 V for FL1 and FL2 each.	
9. For PC12 cells the FSC was set to E-1 (1.00), SSC to 350 V (1.00). Compensations were applied as follows: FL1-FL2 12%, FL2-FL1 28%	For isolated mitochondria the FSC was set to E-1 (7.00), SSC to 380 V (1.00). Compensations were applied as follows: FL1-FL2 20%, FL2-FL1 35%

3.3.7.4 Detection of apoptosis and necrosis in the flow cytometer

Apoptosis can be easily detected by staining with Annexin V and flow cytometrical analysis. Annexin V is a Ca^{2+} -dependent protein that binds to phospholipids, with a high affinity towards phosphatidylserine, normally located on the inside of the cell membrane of a living cell. During apoptosis phosphatidylserine is translocated to and presented on the outer cell surface. In this very early apoptotic stage, Annexin V coupled with FITC fluorophore (Ex.: 488 nm, Em.: 518 nm) can detect these cells. The cell membrane of necrotic cells becomes permeable for large molecules, making it possible for Annexin V to enter necrotic cells and stain them as well. To distinguish apoptotic from necrotic cells, propidium iodide (PI) fluorescence is measured from the same sample, a dye that only is detected in non-viable cells in flow cytometry. PI intercalates into the major groove of the DNA producing a highly fluorescent adduct. The dye can be excited by the FACS Argon laser (488 nm) and its fluorescence can be detected from 550 nm up to 670 nm. Despite the broad emission spectrum it still can be used in combination with other 488 nm-excited fluorophores like FITC, but this requires a proper compensation of the channels (Pigault *et al.*, 1994; Koopman *et al.*, 1994; Vermes *et al.*, 1995; van Engeland *et al.*, 1996).

In flow cytometrical analysis the dot plot of Annexin V-FITC and PI fluorescent events can be divided into four quadrants in the way that healthy cells, apoptotic cells and necrotic cells would be found in one specific quadrant. Living cells are Annexin V negative and PI negative (lower left quadrant, LL), apoptotic cells are Annexin V positive but PI negative (lower right quadrant, LR), and necrotic cells are both positive (upper right quadrant, UR) (*Figure 8*). The position where to set the quadrant was determined beforehand with healthy cells, saved and re-used in a set of three independent experiments. Events with strong PI but low Annexin V fluorescence could be cells that are necrotic and permeable for PI, but not yet for Annexin V. The Stats option in the Cell Quest program provided the exact percentages of each quadrant. The number of events in the lower left quadrant of the dot plot (healthy cells) was taken for each sample, and presented as bar charts, *i.e.* the change in viable cell number.

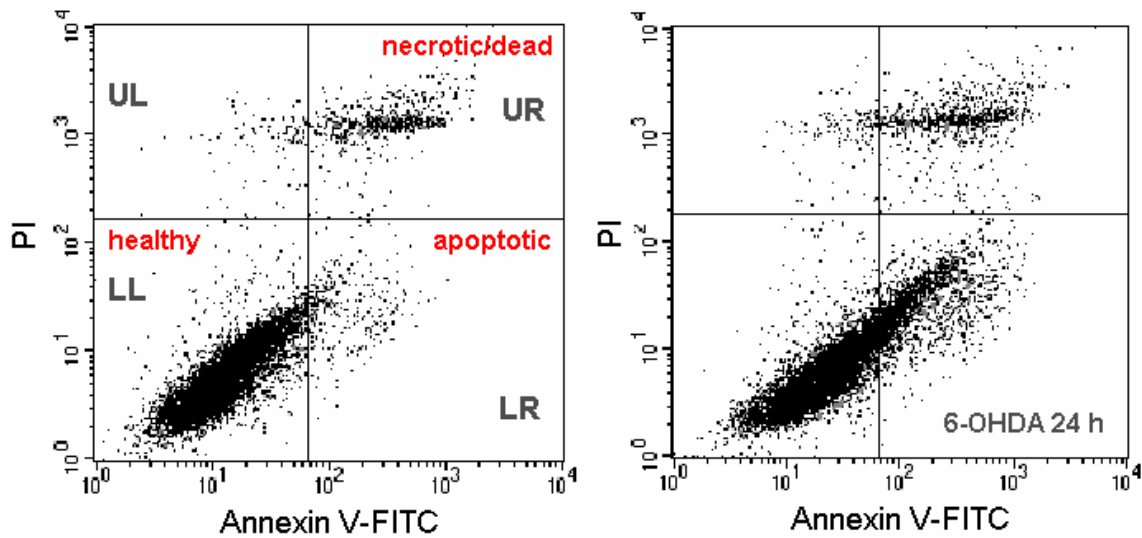


Figure 8. Quadrant setting for PC12 cell apoptosis and necrosis

In the preparation of Annexin V-FITC/PI fluorescence detection, PC12 cells were incubated with 50 μM 6-OHDA for 4, 8, 12, 16, and 24 h; and, in a second experiment, with 10, 25, 50, 100, and 200 μM 6-OHDA for 24 h. After that, cells were washed twice with cold PBS, centrifuged 5 min at 500 $\times g$ (4 $^{\circ}$ C) and resuspended in 1x binding buffer (1 part 10x binding buffer diluted in 9 parts DDW) at a concentration of 1×10^6 cells/ml. According to the manufacturer's protocol, 5 μl Annexin V-FITC (purchased solution, 50 $\mu\text{g}/\text{ml}$ in 50 mM Tris-HCl, pH 7.5, containing 100 mM NaCl, Sigma) and 5 μl PI (final concentration 2 $\mu\text{g}/\text{ml}$) were added to 490 μl of the cell suspension. Samples were incubated 15 min in the dark and gently vortexed from time to time and then analyzed with the flow cytometer.

Table 12. Settings for the detection of apoptosis and necrosis

FSC	E01	1.00	Lin
SSC	350	1.00	Lin
FL1	480	1.00	Log
FL2	500	1.00	Log
Threshold: FSC 20			
Compensation: FL2-FL1 (35%)			

Table 13. Buffers for the detection of apoptosis and necrosis

PI stock solution		10x Binding buffer	
PI	1 mg/ml	HEPES, pH 7.5	100 mM
KH ₂ PO ₄	10 mM	NaCl	1.4 M
NaCl	150 mM	CaCl ₂	25 mM
Stored at 4° C, protected from light		Sterile filtered. Stored at 4° C	

3.3.8 Experiments using the fluorescence microplate reader

The Fluoroskan Ascent[®] microplate reader was used to determine ROS generation in PC12 cells. In principle, emitting light from a quartz halogen lamp passes an excitation filter that selects only light from a certain wavelength. The sample in the multi-well plate is irradiated with this light, and the fluorescent dyes in the samples produce an emission spectrum at longer wavelengths which is detected in a 90° angle to reduce background signals from scattered light, also passing through a filter selected for the expected emission maximum (see *Figure 9*).

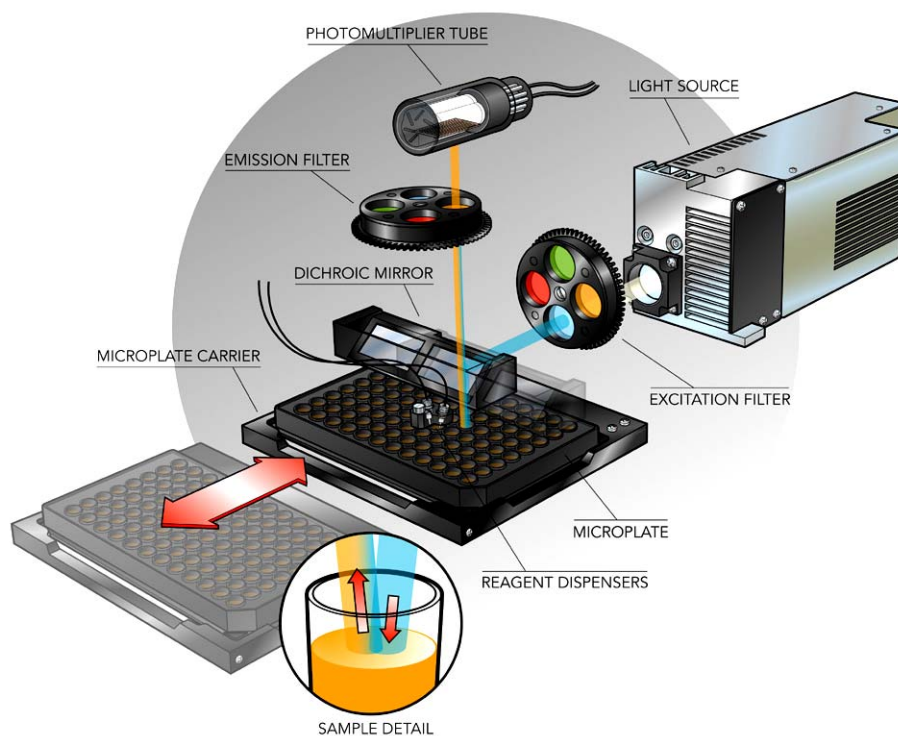


Figure 9. General measuring principle of fluorescence plate readers. (©BioTek Instruments Inc., Winooski, USA)

In this study isolated mitochondria and PC12 cells were tested for their ROS levels with the aid of DCF. Six aliquots of a suspension of isolated mitochondria were dispensed in six tubes (120 μ l in 1 ml MSH buffer per tube). Samples were preloaded with 10 μ M DCF for 60 min (4° C), and washed/centrifuged after this time. 6-OHDA was given 60 min (4° C) in various concentrations (10 μ M, 25 μ M, 50 μ M, 100 μ M and 200 μ M) and washed/centrifuged after this time. Each pellet was resuspended in 4 ml TBS and divided into 4 wells of a 24 well plate (24 well Nunc multidish). DHR fluorescence of controls and stimulated samples was measured immediately. Results were normalized to control protein levels and displayed as mean fluorescence intensity of four wells (in percent of control). A total number of three independent experiments were conducted.

To examine the effect of JNK inhibition on ROS generation following 6-OHDA, PC12 cells were preloaded with 10 μ M H₂DCF-DA for 30 min, and hereafter, washed once with TBS. Then 6-OHDA with or without the JNK inhibitor SP600125 was applied for 60 min. SP600125 was added according to the following scheme (Table 14).

Table 14. Treatment regimen to test the effect of JNK inhibition on ROS levels

6-OHDA	-	10 μ M	25 μ M	50 μ M	100 μ M	200 μ M
SP600125	2 μ M	2 μ M	2 μ M	2.5 μ M	3 μ M	4 μ M

Cells were washed once with prewarmed TBS, the pellets obtained after centrifugation were resuspended in 4 ml TBS for each sample and divided into four wells of a 24 well plate. DCF fluorescence was measured using the following filters (Ex: 485 nm, Em: 538 nm). A cell suspension aliquot from each sample was taken for cell count, fluorescence intensities were standardized to the number of control cells and results were normalized to control protein levels and displayed as percent of control.

Furthermore, the antioxidant effects of methysticin, luteolin, resveratrol and *tert*-butylhydroquinone (*t*BHQ) on 6-OHDA or MPP⁺-induced ROS elevation were investigated. PC12 cells were incubated with these antioxidants for 16 h, after that they were washed and preloaded with H₂DCF-DA (10 μ M) for 30 min, and stimulated with 50 μ M 6-OHDA or 100 μ M MPP⁺ for 60 min. Cells were washed once with prewarmed TBS, the pellets obtained after centrifugation were resuspended in 4 ml TBS for each sample and

divided into four wells of a 24 well plate. DCF fluorescence was measured using the following filters (Ex: 485 nm, Em: 538 nm). A cell suspension aliquot from each sample was taken for cell count, fluorescence intensities were standardized to the number of control cells and results were displayed as percent of control.

3.3.9 Experiments using the spectrofluorometer

In brief, the basic principle of fluorometry is that light from an excitation source passes through a filter or monochromator, and strikes the sample. A proportion of the incident light is absorbed by the sample. The fluorescent light is emitted in all directions. Some of this fluorescent light passes through a second filter or monochromator and reaches a detector, placed at 90° to the incident light beam to minimize the risk of transmitted or reflected incident light reaching the detector. Classical fluorometry was performed due to the advantage that fluorescence intensities of a sample could be monitored on-line. The instrument used was a monochromator, which allowed for the selection of single excitation and emission wavelengths. For experiments with the dual-fluorescent JC-1, the excitation wavelength was chosen to be 488 nm, the emission wavelengths were 530 nm and 590 nm.

100 µl PC12 cell suspension were added to 400 µl PBS, a suspension of isolated mitochondria was diluted 1:20 in 500 µl PBS. H₂DCF-DA (for cells) and H₂DCF (for mitochondria) was given at a concentration of 10 µM and incubated for 20 min. Samples were washed twice, transferred to a quartz cuvette and inserted into the appropriate slot in the fluorometer. When a linear baseline was gained (800 - 1400 sec), the excitation of the probe was terminated by closing the shutter, and 6-OHDA was pipetted carefully into the cuvette (50 µM for cells, 10 µM for isolated mitochondria; a total volume of 20 µl was added each). After the injection of the toxin the measurement was additionally paused for 30 sec to minimize fluorescence signal disturbances caused by turbulences in the solution. Then the shutter was opened and measurement continued until the new slope was linear. 1 µM valinomycin served as a control substance to disrupt the $\Delta\Psi_M$. JC-1 ratio of the emission wavelengths (590 nm/530 nm) was calculated and saved simultaneously, and was visualized after the experiment was completed.

3.3.10 Fluorescence microscopy

3.3.10.1 Principle of confocal laser scanning microscopy

An objective focuses an expanded light-beam originating from a laser source to a small spot on the sample, at the focal plane of the objective lens. Reflected light from the illuminated volume of the specimen is collected by the objective and reflected by a beamsplitter towards a pinhole arranged in front of the detector. In this case the pinhole is responsible for the confocal characteristics of the system. Information which does not originate from the focus level of the microscope objective, is faded out by this arrangement. In contrast, light from the focal plane is directed through a pinhole and registered by the detector (*Figure 10*). The advantage of out-fading information from above or below the focal plane enables the confocal microscope to perform depth-dependent measurements: optical tomography becomes possible. A genuine 3D-image can be processed by confocal scanning of sequential levels.

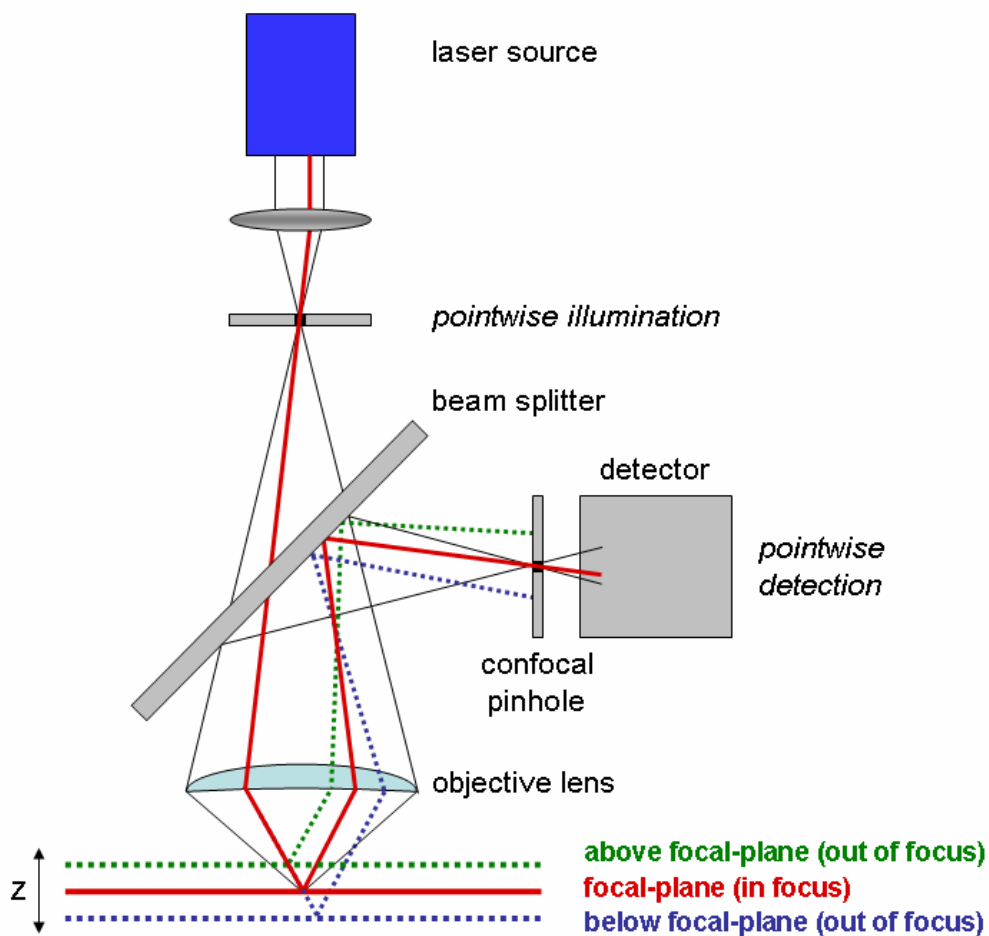


Figure 10. Principle of confocal laser scanning microscopy

3.3.10.2 Experimental setup

To investigate the subcellular distribution of mitochondria and JNK isoforms in PC12 cells by confocal microscopy, cells were grown on 2-well glass coverslips (Nunc) and stimulated with 50 μ M 6-OHDA for 4 h, the time point, when JNK had previously been identified to colocalize with mitochondria after 6-OHDA. Samples were subjected to the following protocol. As a first step, PC12 cells were incubated with MitoTracker[®] Red CM-H₂XRos (Molecular Probes; ex. 579 nm, em. 599 nm) at the concentration of 200 nM for 30 min.

Protocol:

1. Cells were washed with ice-cold PBS.
2. Cells were incubated with methanol at -20°C for 10 min.
3. Cells were washed with ice-cold PBS.
4. Cells were fixed with 2% para-formaldehyde in PBS, 30 min at RT.
5. Fixed cells were carefully washed twice with TBS.
6. Samples were blocked with a blocking solution of TBS/BSA/Glycine for 1 h at RT.
7. Primary antibodies of JNK1 or JNK2 (or cytochrome c in conventional fluorescence microscopy) were applied in a dilution of 1:100 in blocking solution.
8. Samples were incubated with primary antibody solution at 4° C over night, protected from light.
9. Fixed cells were washed with TTBS, 2 x 5 min.
10. Samples were washed with TBS, 3 x 10 min.
11. Secondary antibody (in all cases donkey anti-mouse FITC from Jackson ImmunoResearch Lab., West Grove, PA, USA) was applied in a dilution of 1:400 in TBS, and cells were incubated at 37° C for 1 h.
12. Samples were washed with TTBS, 2 x 5 min., and hence 10 min with TBS.
13. Hoechst 33258 dye was added 4 μ l per ml, and cells were incubated for 30 min at RT.
14. Samples were washed with TBS, 2 x 5 min.
15. Probes were mounted with SlowFade and sealed.

Confocal laser scanning analysis was carried out with a Zeiss LSM 510 laser scanning microscope (Carl Zeiss Jena, Jena, Germany). Triple staining pictures represent optical slices of 0.5 μ m. Original magnification was 400x.

PC12 cells were stained for cytochrome c using the same protocol, but the protein was detected by conventional fluorescence microscopy. The Leica DM L microscope was equipped with the following filter and reflector systems (cubes):

Table 15. Filter and reflector system of the Leica DM L microscope

Excitation filter (nm)	Suppression filter (nm)	Detected dye
BP 340 - 380	LP 425	Hoechst 33258
BP 450 – 490	LP 515	FITC
BP 515 – 560	LP 590	Mitotracker Red CM-H ₂ XRos

3.3.11 Breeding of mice

Genetic inactivation of JNK1, JNK2 and/or JNK3 in mice has been described in detail elsewhere (Yang *et al.*, 1997; Dong *et al.*, 1998; Kuan *et al.*, 1999). JNK knockout mice were backcrossed once with C57/BL6 wildtype mice. Thereafter, the heterozygous F1 offspring was crossed to obtain F2 homozygous JNK knockout mice and homozygous wildtype (WT) controls. This F2 generation was used as parent founders to breed the knockout and WT mice for animal experiments (F3). This breeding approach minimizes the genetic strain variability of knockout and control animals on the one hand, and on the other provides the large number of animals necessary for the different experiments according to international guidelines (Banbury Conference). All animal experiments have been performed according to the German and the Finnish law for protection of animals and the NIH guidelines for use and care of laboratory animals (approval by the Ministerium für Landwirtschaft und Naturschutz, Kiel, Germany).

3.3.12 Genetic characterization of JNK knock-out mice strains

JNK knock-out mice strains from the animal facility were checked regularly by PCR. Tail tissue pieces were immediately frozen in liquid nitrogen. In the laboratory surroundings, the tissue was thawed and trenched with scissors in a semisterile manner. The QIAamp DNA mini kit was used to conduct the following steps to isolate DNA:

Protocol:

1. To each sample 180 μ l ATL solution and 20 μ l Proteinase K were added, samples were vortexed, sealed and incubated at 55°C O/N; shaking at 1400 rpm.
2. Epp cups were centrifuged (13,000 rpm; 5 min).
3. Supernatant was mixed with 410 μ l AL buffer, transferred to a filter/collection tube and centrifuged at 6000 x g for 1 min.
4. Filtrate was discarded. Filter was combined with a new collection tube and DNA in the filter was washed with 500 μ l AW1 buffer by centrifugation (6000 x g for 1 min).
5. Filtrate was discarded. Filter was combined with a new collection tube and 500 μ l AW2 buffer was added. Tubes were centrifuged at 6000 x g for 3 min.
6. Filtrate was discarded. Filter unit was plugged in a sterile microcentrifuge tube.
7. 200 μ l AE buffer (70° C) was given to the samples. They were incubated for 3 min.
8. Samples were centrifuged (6000 x g; 1 min).
9. Step 7 and 8 were repeated without touching the filtrate.
10. 400 μ l filtrate containing DNA was obtained by centrifugation. Filter was discarded.

The concentration of DNA (in ng) was measured using 5 μ l sample solution in 1 ml ultrapure water by assessing the ratio of absorption in the photometer between 280 and 260 nm.

3.3.12.1 Polymerase chain reaction (PCR)

The PCR (polymerized chain reaction) comprise three steps. First, the target genetic material must be denatured, *i.e.* the strands of its helix must be unwound and separated by heating to 90-96° C. The second step is hybridization or annealing, in which the primers bind to their complementary bases on the single-stranded DNA. The preferred annealing temperature for a PCR depends directly on length and composition of the primers. The third step is DNA synthesis by a polymerase. Starting from the primer, the polymerase reads the template strand and matches it with complementary nucleotides. This results in two new helices in place of the first one, each composed of one of the original strands plus its newly assembled complementary strand. Frequent repeating of these cycles generates millions of DNA strand copies.

For PCR 100 ng/ μ l of DNA was used. PCR Master Mix was prepared freshly according to the protocol shown in *Table 17*. Values are for one sample, so upscaling was applied accordingly. JNK primer mixes were produced by combining the following primers obtained from MWG

Biotech/Pharmacia for detection of the complete double-band reaction (*Table 16*). After addition of PCR master mix, samples were placed in a thermocycler and PCR program was started.

PCR-Program

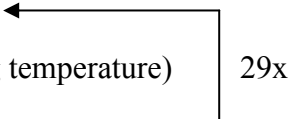
1. 94° C, 2 min
 2. 94° C, 30 min
 3. 56° C, 30 min (annealing temperature)
 4. 72° C, 1 min
 5. 4° C, ∞
- 

Table 16. Composition of the JNK primer mixes

Primer Mixes	
JNK 1	
MJ1B8 (100 μM)	20 μl
MJ1F8 (100 μM)	20 μl
PGKT1 (100 μM)	20 μl
Ultrapure water	73 μl
JNK 2	
MJ2B3 (100 μM)	20 μl
MJ2F5 (100 μM)	20 μl
PGKT1 (100 μM)	20 μl
Ultrapure water	30 μl
JNK 3	
MJ3B3 (100 μM)	20 μl
MJ3F3 (100 μM)	20 μl
PGKP1 (100 μM)	20 μl
Ultrapure water	73 μl

Table 17. Composition of the PCR Master Mix

PCR Master Mix	
10x PCR buffer	5 μ l
25 mM MgCl ₂	5 μ l
10 mM dNTP	1 μ l
Ultrapure water	34.5 μ l
DNA sample	1 μ l
Primer Mix JNK 1, 2, 3	3 μ l
Taq DNA Polymerase	0.5 μ l

3.3.12.2 Detection and analysis of the PCR reaction product

Table 18. Stock solutions required for agarose gel electrophoresis

10x TBE-Buffer		10x Loading Buffer	
Tris	9 M	Bromphenol blue	0.25%
Boric acid	9 M	Glycerol	30%
EDTA	0.2 M	TBE	1x
Stored at RT		Stored at 4° C	

The PCR product is a fragment of defined DNA lengths. A sample from these fragments is loaded with appropriate molecular-weight markers onto an agarose gel. 1% or 1.5% agarose gels were prepared with 1x Tris-buffer boric acid-EDTA. The 1x TBE (Tris-boric acid-EDTA) buffer was set up by diluting 10x TBE buffer with DDW. The required amount of agarose was dissolved in 1x TBE buffer by heating in a microwave oven. 5 μ l/100 ml of a 10 mg/ml ethidium bromide stock solution was added to warm agarose solution and mixed well. For agarose gel electrophoresis a horizontal gel system was used. The agarose solution with ethidium bromide was pipetted to this gel system and allowed to polymerize for 20-30 min. When the gel had polymerized, it was transferred to an electrophoresis chamber filled with 1x TBE buffer. 20 μ l DNA samples were mixed with 5 μ l 10x loading buffer in 1.5 ml tubes. At the same time 1 μ l DNA-ladder was mixed with 5 μ l 10x loading buffer and with 19 μ l TBE buffer, resulting in a total volume of 25 μ l. DNA-ladder and samples were

loaded into wells and the gel was run at 80 mV for approximately 60 min. Bands were visualized with 312 nm UV light.

3.3.13 Isolation of mitochondria from mice brain

Mice brain mitochondria were isolated according to the following optimized protocol (sources: Gogvadze *et al.*, 2003; Schild *et al.*, 1996; Zablocka *et al.*, 2003). All steps were performed on ice, with ice-cold solutions and pre-cooled tubes. Before the experiments, 3% and 6% Ficoll solutions were prepared from a 20% (w/v) Ficoll (Sigma) stock solution in Ficoll dilution buffer (see *Table 19*). For the isolation an overall time of 120 min was considered. Mitochondrial suspension could be used without any impairment for another 2-3 h when kept on ice.

Table 19. Composition of buffers for mitochondrial isolation

Isolation buffer (IB)		Ficoll dilution buffer	
Sucrose	320 mM	Mannitol	250 mM
EGTA	1 mM	Sucrose	60 mM
Tris-HCl pH 7.4	10 mM	EGTA	100 μ M
		Tris-HCl pH 7.5	10 mM
Respiration buffer (RB)		MSH buffer	
KCl	150 mM	Mannitol	210 mM
KH ₂ PO ₄	1 mM	Sucrose	70 mM
Tris	5 mM	HEPES	5 mM
Adjusted to pH 7.4 with HCl		Adjusted to pH 7.4 with KOH	

Protocol:

1. Five complete mice brains per group were collected in ice-cold PBS and dissected under the microscope removing blood vessels and fat. Tissue pieces weighed approx. 1 g.
2. Tissue pieces were washed 3x with ice-cold PBS and then homogenized in 10 ml ice-cold isolation buffer (IB) (10x tissue weight) in steps with a 2 ml all glass dounce tissue grinder.
3. Homogenized suspension was collected in a 15 ml Falcon tube and centrifuged at 2000 x g, 3 min (4° C).
4. The upper part of the solution with fatty acids floating and sticking to the tube walls was carefully taken away.
5. The remaining suspension was resuspended and transferred into a new tube and steps 3 and 4 were repeated once.
6. Supernatant was further processed in 2 ml tubes.
7. Samples were centrifuged at 13,000 x g, 10 min (4° C).
8. Supernatant (cytosol) was collected and frozen at -20° C. The pellets were resuspended each in 200 µl 3% Ficoll solution and layered onto 1 ml of ice-cold 6% Ficoll solution.
9. Tubes were centrifuged 20 min at 11,500 x g, 4° C.
10. The final pellet was resuspended in 100 - 200 µl MSH buffer depending on the size of the pellet, which yielded a protein concentration of 90-100 mg/ml (mitochondria). The true concentration was measured later by Bradford's colorimetric assay if necessary.

3.3.13.1 Determination of mitochondrial proteins

A defined volume (30 µl) of isolated mitochondrial suspension was taken and mixed with 300 µl denaturing lysis buffer (DLB, see *Table 5*). Samples were boiled for 5 min and immediately used for protein measurement or frozen for later use in Western blot analysis for assessment of the purity of the mitochondrial fraction. The exact mitochondrial concentrations were only necessary for fluorometric measurement with the cuvette/plate reader, for experiments in the flow cytometer, no protein measurement was needed since the instrument counts the same number of events in all samples.

Protein concentrations were determined using Dye Reagent, a variant of Bradford's colorimetric assay. To prepare working solution, the Dye Reagent stock solution was diluted 1:5 with DDW. To determine protein concentrations, bovine serum albumin (BSA) was used as protein standard. Serial dilutions of a 1.2 mg/ml BSA stock solution in autoclaved DDW (0.1 to 0.6 mg/ml) were performed. Samples were diluted 1:30 or 1:50 in autoclaved DDW. 20 µl of sample, standard and DDW (as blank) were pipetted into disposable plastic cuvettes. 1 ml of the working solution described above was added to each cuvette. All cuvettes were vortexed to start the reaction and incubated at RT for 10 min. The absorbance at 595 nm (A_{595}) was measured using a spectrophotometer. The protein concentrations were calculated based on a standard curve created from in-process standard concentrations of BSA.

3.3.13.2 Estimation of the quality of isolated mitochondria measuring the respiratory control ratio (RCR)

One of the keystones of the chemiosmotic theory of energy transduction is the impermeability of the inner mitochondrial membrane to protons. Oxidation of substrates results in extrusion of protons from the mitochondrial matrix to generate the mitochondrial membrane potential. High membrane potential suppresses further extrusion of protons and therefore inhibits respiration. Under resting conditions, the rate of respiration of mitochondria is quite low and determined by a passive leakage of protons into the mitochondrial intermembrane space.

Phosphorylation of ADP requires translocation of protons into the matrix by a mitochondrial ATP synthase. This results in a decrease of the membrane potential that stimulates respiration. Comparison of the respiration rates in the resting state and during phosphorylation of ADP is a useful measure of the efficiency of mitochondrial functioning. The most reliable and widely used criterion of the quality of a mitochondrial preparation is the respiratory control ratio (RCR). RCR is defined as the rate of respiration in the presence of ADP (phosphorylating respiration, state 3) divided by the rate obtained following the expenditure of ADP (state 4).

An oxygen monitor equipped with a Clark-type oxygen electrode (Oxygraph) was used and oxygen consumption by intact mitochondria was followed on screen with the supplied software. Mitochondrial samples were subjected to the following protocol:

Protocol:

1. The polarographic system was set up and calibrated to 100% oxygen saturation, delivering a 1 volt signal. Subsequent steps were performed at 25° C.
2. For testing the mitochondrial quality 2 ml of incubation buffer were placed into the sample chamber of the oxygen monitor and conditions were set to constant stirring. An aliquot of mitochondrial suspension (50 µl) was added to a final concentration of ~ 2 mg/ml.
3. After 30 sec 20 µl of 10 mM rotenone was added.
4. The stirring was stopped and the electrode was inserted into the sample chamber. All air was expelled through the slot in the plunger (slight twisting of the electrode helps to gather the bubbles at the slot) and the chart speed was set up (10 to 15 mm/min).
5. After 1 min stabilization observed by recorder trace 20 µl of 0.5 M sodium succinate was added, through the slot on electrode's body with a Hamilton syringe.
6. Mitochondria then started to consume oxygen. The slope of the curve showed the rate of respiration.
7. After stabilization of respiration (~ 2 min) 10 µl of 50 mM ADP was added. The rate of respiration than increased (state 3) with subsequent restoration of the initial rate of respiration (state 4) when all added ADP was phosphorylated.
8. 2 µl of 10 mM 2',4'-dinitrophenol (DNP) was added. DNP disrupts the mitochondrial potential that is the basis for oxygen consumption.
9. The rate of respiration was calculated from the recorder trace as the amount of oxygen consumed in 1 min assuming that at 25° C and normal atmospheric pressure the concentration of oxygen in the incubation buffer is 250 µM.
10. The RCR was calculated by dividing the state 3 respiration rate by the state 4 respiration rate.

Mitochondria with a respiratory control ratio above 3 were acceptable for use in experiments and were stable for the next four hours.

3.3.13.3 Purity of mitochondrial preparations

The purity of isolated mitochondria from mice brains was assessed by Western blot analysis of the obtained mitochondrial suspension. After lysis with DLB-buffer (see *Table 5*), electrophoresis and blotting, antibodies against the mitochondrial constitutional protein cytochrome c oxidase subunit IV (COX IV) and β -actin for the assessment of cytosolic contaminations were applied to the membranes.

3.3.14 Primary cells

Table 20. Solutions for primary cell culture

Hanks Solution		Dissection Solution	
Pulver media w/o Mg^{2+} and Ca^{2+}		Hanks solution	
NaHCO ₃	35 mg/ml	BSA	3 mg/ml
HEPES	10 mM	MgSO ₄	1.4 mg/ml
D-Glucose	6 mg/ml		
Gentamycin	5 μ g/ml		
Digestion Solution		Culture Media	
NaCl	8 mg/ml	MEM	
KCl	0.37 mg/ml	D-glucose	5mg/ml
Na ₂ HPO ₄	0.99 mg/ml	Transferrin	0.1 mg/ml
HEPES	5,95 mg/ml	Insulin	25 μ g/ml
NaHCO ₃	0.35 mg/ml	Glutamax	2 mM
		Gentamycin	5 μ g/ml
1st day Culture Media		2nd day Culture Media	
Culture media		Culture media	
FCS	10%	FCS	5%
		B 27 supplement	2%
		AraC	5 μ M

3.3.14.1 Coating of the plates

For providing attachment and growth of murine primary cells, 4-well plates and culture dishes (35 mm) had to be coated. Cover glasses or plastic cover slips were placed in 4-well plates in the laminar flow unit. Plastic culture dishes and 4-well plates were coated with poly-L-lysine, dissolved in ultrapure water (100 µg/ml). To coat the culture dishes or 4-well plates, the bottom of the slides was covered with a thin layer of poly-L-lysine, and placed in the incubator overnight. The next day, slides were washed two times with DDW. Subsequently, 1st day culture medium was added to the plates and placed in the incubator until use. Cover glasses used in this study were not sterile. So they were autoclaved before use and stored under sterile conditions.

3.3.14.2 Obtaining and cultivating primary murine neurons

All solutions were prepared in advance, adjusted to pH 7.4 and stored at 4° C. Hippocampal or cortical cultures were obtained from the newborn mice (up to 24 h postnatally). All the culturing procedure was performed on ice. Mice pups were decapitated and the brains were dissected under sterile conditions. Brains were transferred into petri-dishes which contained ice-cold dissection solution. Cortex and hippocampus were dissected and cleaned from blood vessels and meninges. Subsequently, they were transferred into different petri-dishes, cut into 1 mm³ pieces and finally transferred into 15 ml tubes. After washing 4 times with 3 ml dissection solution and treating with 5 ml Hanks solution, hippocampal and cortical slices were warmed for 1 min in digestion solution, mixed with trypsin 3.3 mg/ml, DNase 0.83 mg/ml, and treated with the same solution for 5 min at RT. The hippocampal and cortical slices were thereafter incubated in dissection solution with 0.6 mg/ml trypsin inhibitor to inhibit trypsin activity for 5 min and 3 min, respectively, and finally with fetal calf serum (200 µl/ml in dissection solution) for 10 min. Hippocampal and cortical slices were washed four times with dissection solution and homogenized in dissection solution, mixed with 0.4 mg/ml DNase, with three different diameter of fire polished Pasteur pipettes. Five ml of dissection solution was added and the cells were centrifuged (15 min; 800 x g; 4° C). To determine the number of surviving cells in cell suspension, cells were counted following trypan blue staining (see section 3.3.4). Subsequently, cells were plated on 4 well plates or 35 mm plastic culture dishes containing 1st day culture media (Culture Media, 10% horse serum). After two days half of the culture media was replaced with 3rd day media and every 2nd-3rd day half of the media was replaced with fresh culture medium.

This culturing procedure resulted in a mixed neuronal culture containing 70-80% neurons. The remaining cells were identified as astrocytes.

3.3.14.3 Treatment of primary cells

The JNK inhibitor SP600125 (2 μ M) was given to the both cultures immediately after the explantation and was applied with every change of culture medium.

3.3.14.4 Immunocytochemistry

Immunocytochemistry bases on the use of a primary antibody directed against the cellular target(s) and a secondary antibody which is directed against the primary antibody and labeled with an enzyme. The most commonly used enzymes are peroxidase and alkaline phosphatase. Peroxidase activity is most frequently detected using 3,3'-Diaminobenzidine (DAB) as the electron acceptor with hydrogen peroxide serving as the substrate. The reaction product forms a brown precipitate at the site of the enzyme activity. To enhance the signal, the secondary antibody is biotinylated and bound by avidin coupled to a complex containing the enzyme (avidin-biotin-complex coupled with a peroxidase for the substrate reaction, *i.e.* the ABC complex). Staining was performed using the following protocol.

Protocol:

1. Cells were incubated with pre-warmed para-formaldehyde (4% in PBS, 37° C) at RT for 30 min
2. The fixed cells were permeabilized with Triton X-100 (0.2% in PBS) at RT for 2 min
3. Cells were then blocked in 5% normal goat serum, diluted in PBS
4. Cells were washed in 1% normal goat serum, diluted in PBS, two times for 3 min each
5. Cells were incubated with primary antibody (overnight at 4° C)
6. Cells were washed in PBS, three times for 3 min each
7. Cells were, hence, incubated with secondary antibody for 1 h (37° C)
8. Cells were washed in PBS, three times for 3 min each
9. Cells were incubated with ABC complex for 1 h. (37° C). Two drops of reagent A of the Vectastain kit were added to 5 ml of PBS. After the addition of two drops of reagent B the solution was mixed immediately. The solution was ready to use after 30 min.
10. Cells were washed in PBS, two times for 3 min each.

11. DAB solution was applied until staining was optimal as determined by light microscopic examination (5-10 min at RT). One tablet of 3,3'-diaminobenzidine was dissolved in 5 ml DDW. Each Sigma Fast DAB tablet contains DAB (0.7 mg/ml), Urea Hydrogen Peroxide (0.2 mg/ml) and Tris buffer 0.06 M.
12. Cells were washed in DDW two times each for 5 min.
13. The stained cells were mounted and analyzed using a DMR microscope with a camera system and the software LeicaQwin program.

3.3.15 Statistical analysis

Data were analyzed using either GraphPad Prism or SPSS for Windows, version 14.0. Kruskal-Wallis test was performed to verify that results from 3 - 6 experiments had no significant differences before they were pooled to represent one joint control or treated group. Data were subjected to Student's *t*-test and one-way analysis of variance with repeated measures and post-hoc Bonferroni analysis. For data that were not normally distributed non-parametric statistical tests were run, consisting of Kruskal Wallis/Mann-Whitney *U*-test and post-hoc Bonferroni or Tukey's analysis.

P-value less than 0.05 was considered significant. All data are expressed as mean \pm standard deviation.

4. RESULTS

Table 21. Overview of all experiments.

Instrumental method	Parameters investigated in		
	PC12 cells	isolated mitochondria from PC12 (P) or mice brains (M)	hippocampal and cortical neurons
flow cytometry	<ul style="list-style-type: none"> → cell death → ROS detection → change in $\Delta\Psi_M$ 	<ul style="list-style-type: none"> → ROS detection (M) → change in $\Delta\Psi_M$ (M) 	
spectro-fluorometry	<ul style="list-style-type: none"> → change in $\Delta\Psi_M$ 	<ul style="list-style-type: none"> → change in $\Delta\Psi_M$ (M) 	
fluorescence plate reader	<ul style="list-style-type: none"> → ROS detection → antioxidant potential of drugs 	<ul style="list-style-type: none"> → ROS detection (M) 	
polarography		<ul style="list-style-type: none"> → oxygen consumption (M) 	
Western blot	<ul style="list-style-type: none"> → cytochrome c release 	<ul style="list-style-type: none"> → purity of mitochondria (M, P) → activation of mitochondrial JNK (P) → mitochondrial translocation (P) → inhibition of JNK translocation (P) → JNK upstream kinases (P) 	
fluorescence microscopy	<ul style="list-style-type: none"> → cytochrome c release → subcellular JNK pools → mitochondrial translocation of JNK 		<ul style="list-style-type: none"> → neurite length → effects of JNK inhibition

Abbreviations: JNK (c-Jun N-terminal kinases), $\Delta\Psi_m$ (mitochondrial membrane potential), ROS (reactive oxygen species)

4.1 Mechanisms of 6-hydroxydopamine mediated cell death

4.1.1 6-hydroxydopamine induces cell death in PC12 cells

6-hydroxydopamine was administered at the concentration of 50 μM to the rat pheocromocytoma cell line PC12. After 4 h (data not shown), 8, 12, 16 and 24 h cells were analyzed by flow cytometry for markers of cell death (Annexin V-FITC and propidium iodide) using the Becton Dickinson FACSCalibur flow cytometer. 6-OHDA stimulation lead to a significant cell loss of about $28\% \pm 6\%$ ($P < 0.001$) after 24 h (*Figure 11A*).

Furthermore, PC12 cells were treated for 24 h with 10, 25, 50, 100, or 200 μM 6-OHDA and apoptosis/necrosis was assessed by flow cytometry. 6-OHDA promoted death among PC12 cells in a dose-dependent fashion. At 10 μM concentration 6-OHDA did not show a significant decrease in the number of surviving cells, but cell death became evident at higher concentrations: 25 μM caused $23\% \pm 4\%$ loss of PC12 cells ($P < 0.001$), the use of 50 μM promoted a loss of $31\% \pm 7\%$ ($P < 0.001$), 100 μM and 200 μM showed a decrease by $49\% \pm 9\%$ and $51\% \pm 8\%$ ($P < 0.001$, each), respectively (*Figure 11B*). 6-OHDA induces cell death in PC12 cells in a time- and dose-dependent manner.

4.1.2 6-hydroxydopamine generates reactive oxygen species in PC12 cells

In order to elucidate the mechanism of 6-OHDA mediated cell death the role of oxygen radicals were investigated. ROS levels were assessed fluorometrically in the Fluoroskan Ascent[®] plate reader by 2',7'-dichlorofluorescein (DCF) fluorescence after administration of the redox-sensitive dye 2',7'-dichloro-dihydrofluorescein ($\text{H}_2\text{-DCF}$). The values were normalized according to the samples' protein contents and results were displayed as fluorescence intensity per mg protein in percent of control.

Incubation with 50 μM 6-OHDA was applied to investigate the time course of ROS production. Stimulation periods were 4, 8, 12, 16, or 24 h. DCF fluorescence was $37\% \pm 8\%$ higher than controls after 4 h ($P < 0.05$), the earliest time point chosen (*Figure 12A*). The minimal concentration to significantly generate ROS within 4 h was 25 μM (*Figure 12B*). Levels were elevated by $18\% \pm 3\%$ ($P < 0.05$).

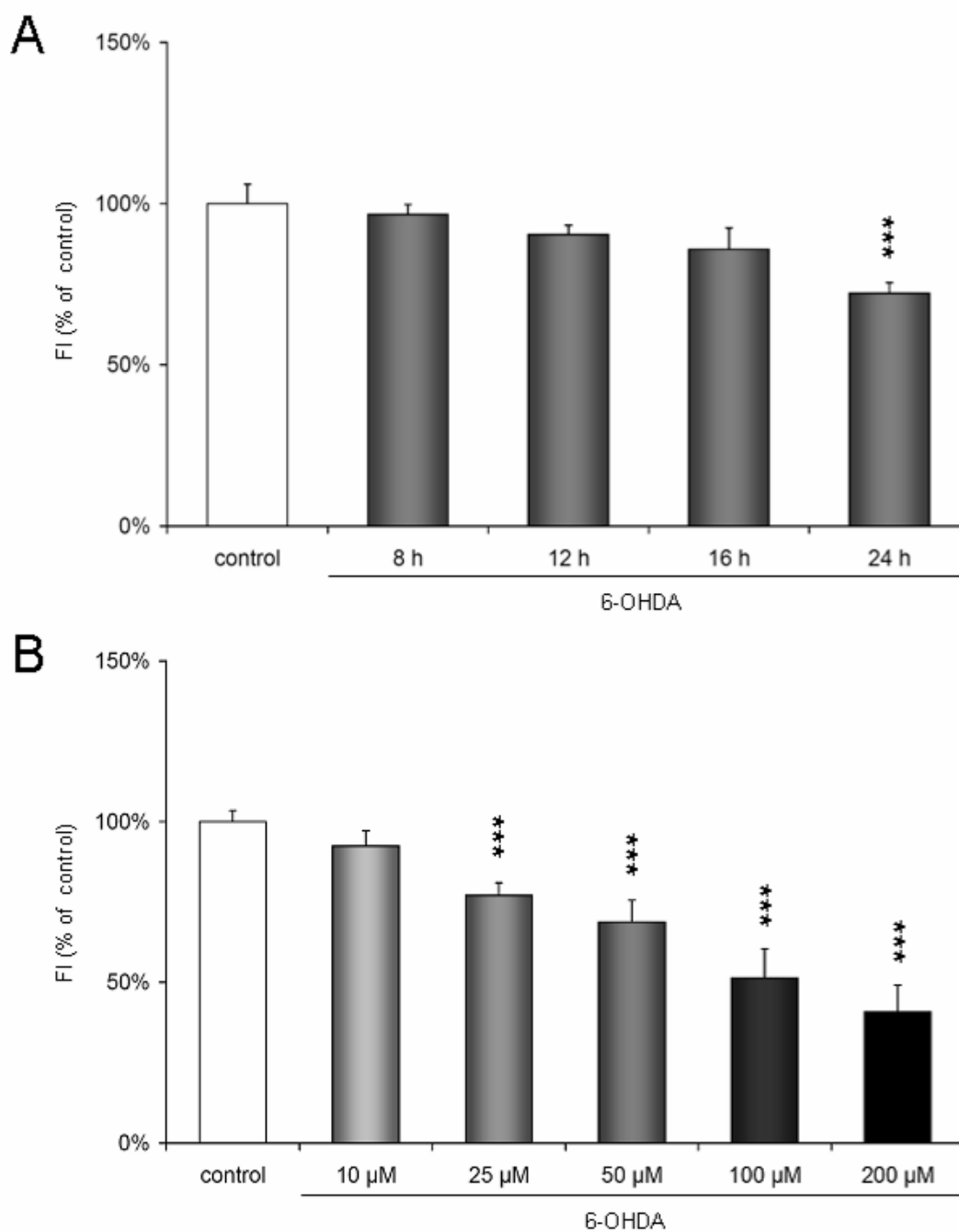


Figure 11. 6-hydroxydopamine and cell death

PC12 cell death was assessed using Annexin V-FITC/PI in the flow cytometer. From the original dot plots viable cells were identified, total number of surviving cells was counted and compared to controls. A) Time course of 6-OHDA mediated cell death at a concentration of 50 µM. There is a significant decrease in the number of viable PC12 cells after 24 h. B) Concentration-dependent decrease in viability 24 h after incubation with 6-OHDA. Vehicle-treated controls were used.

Abbreviations: 6-OHDA (6-hydroxydopamine), FI (fluorescence intensity), FITC (fluorescein-isothiocyanate), PI (propidium iodide).

*** $P < 0.001$

Statistical significances were calculated using *t*-test. Data are presented as mean ± standard deviation. N = 3.

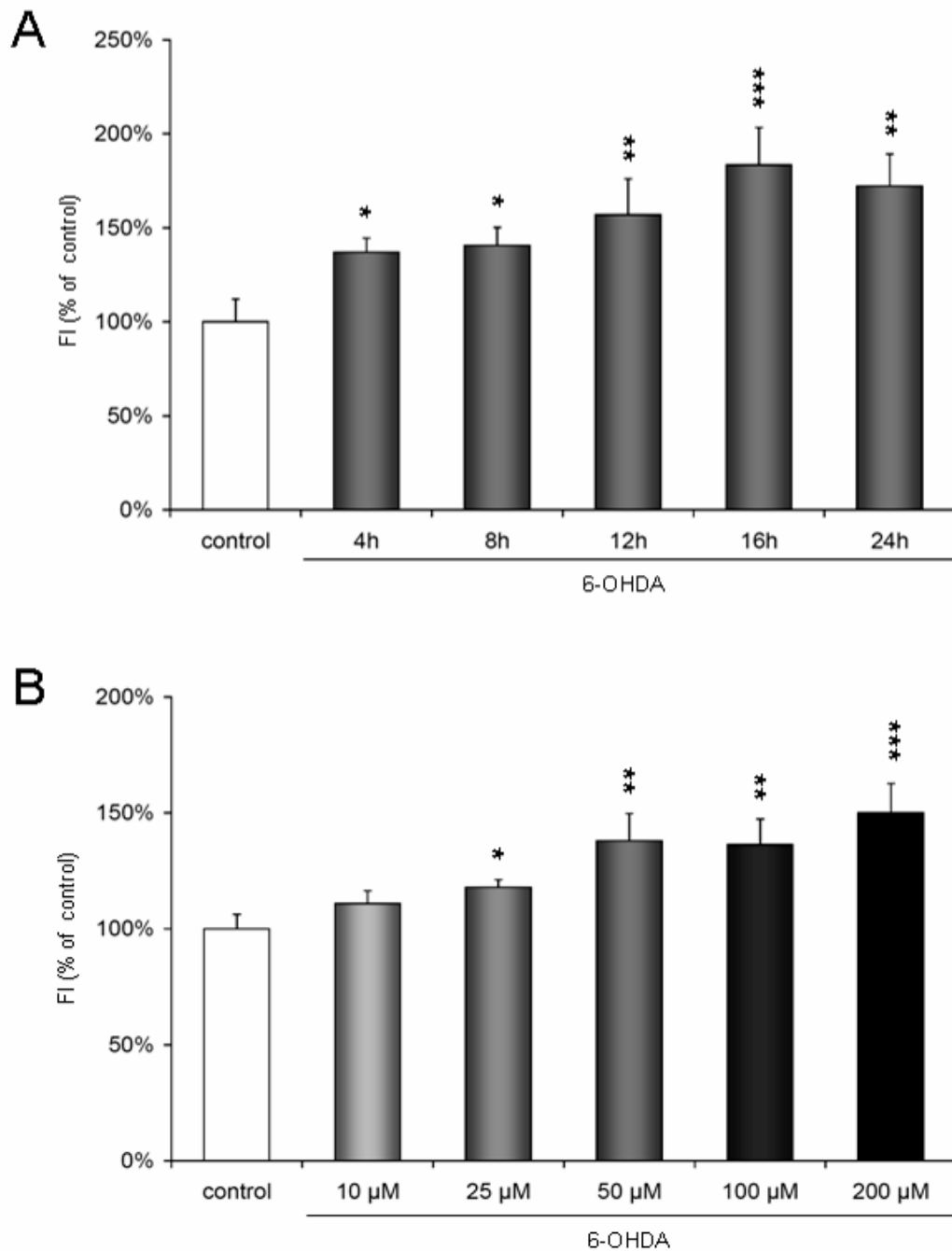


Figure 12. Reactive oxygen species levels after 6-OHDA

Reactive oxygen species (ROS) levels were measured fluorometrically in PC12 cells after 6-OHDA and incubation with H₂DCF. A) Time course of ROS production following 50 µM 6-OHDA shows an early increase in DCF fluorescence after 4 h. B) 50 µM 6-OHDA and higher concentrations induce ROS production in PC12 cells within 4 h of treatment. Vehicle-treated controls were used.

Abbreviations: 6-OHDA (6-hydroxydopamine), DCF (dichlorofluorescein), FI (fluorescence intensity), ROS (reactive oxygen species).

* $P < 0.05$; ** $P < 0.01$; *** $P < 0.001$

Statistical significances were calculated using *t*-test. Data are presented as mean \pm standard deviation. N = 6.

These findings raised the need to conduct additional experiments to assess early effects of ROS generation by 6-OHDA. 50 μ M 6-OHDA was administered for 15 min, 30 min, 1 h and 2 h and DCF fluorescence was measured from samples in the fluorescence plate reader and by flow cytometry. Both methods revealed that the very first significant increase in fluorescence intensity occurred after 60 min of stimulation (*Figure 13*). Staurosporine (STS) was used as a positive control for increased ROS production at a concentration of 1 μ M.

Given the profound changes of ROS levels in early stages of 6-OHDA intoxication, we were curious to assess the source of ROS in this model. H₂DCF is a useful tool for monitoring ROS generated in the cytosol or mitochondrial intermembrane space, and ROS that are released from mitochondria (Diaz *et al.*, 2003). Among the redox-sensitive fluorescent dyes dihydro-rhodamine (DHR) is most sensitive towards oxidation by hydrogen peroxide (Walrand *et al.*, 2003), especially in the presence of cytochrome c oxidase in mitochondria (Royall and Ischiropoulos, 1993). Thus, it can be used as a specific marker for the detection of mitochondrial ROS.

ROS levels as measured by DCF and DHR fluorescence in the flow cytometer after 60 min incubation with 6-OHDA were increased similarly in the dot plots (*Figure 14A*). Regions of interest (ROI) were drawn in the control dot plots in a manner that any higher fluorescence intensity for DCF or DHR would appear in this region and therefore become available for counting with the CellQuest program. After 60 min stimulation with 50 μ M 6-OHDA almost the whole cell populations appeared in the ROIs (R3 for DCF, R4 for DHR), shifting upwards due to higher fluorescence intensity in the samples. DCF fluorescence intensity increased from 4% \pm 3% to 90% \pm 3%, whereas DHR fluorescence increased from 8% \pm 2% in control cells to 81% \pm 2% after 6-OHDA. Based on the assumption that DHR is oxidized by a subpopulation of ROS that can be detected by DCF, a 90% overlap of mitochondrially generated ROS (as measured by DHR) and whole-cell DCF fluorescence was calculated (*Figures 14B and 14C*).

Oxidative stress is a very early event occurring within 60 min following the administration of 6-OHDA to PC12 cells. The source of ROS largely appears to be mitochondria.

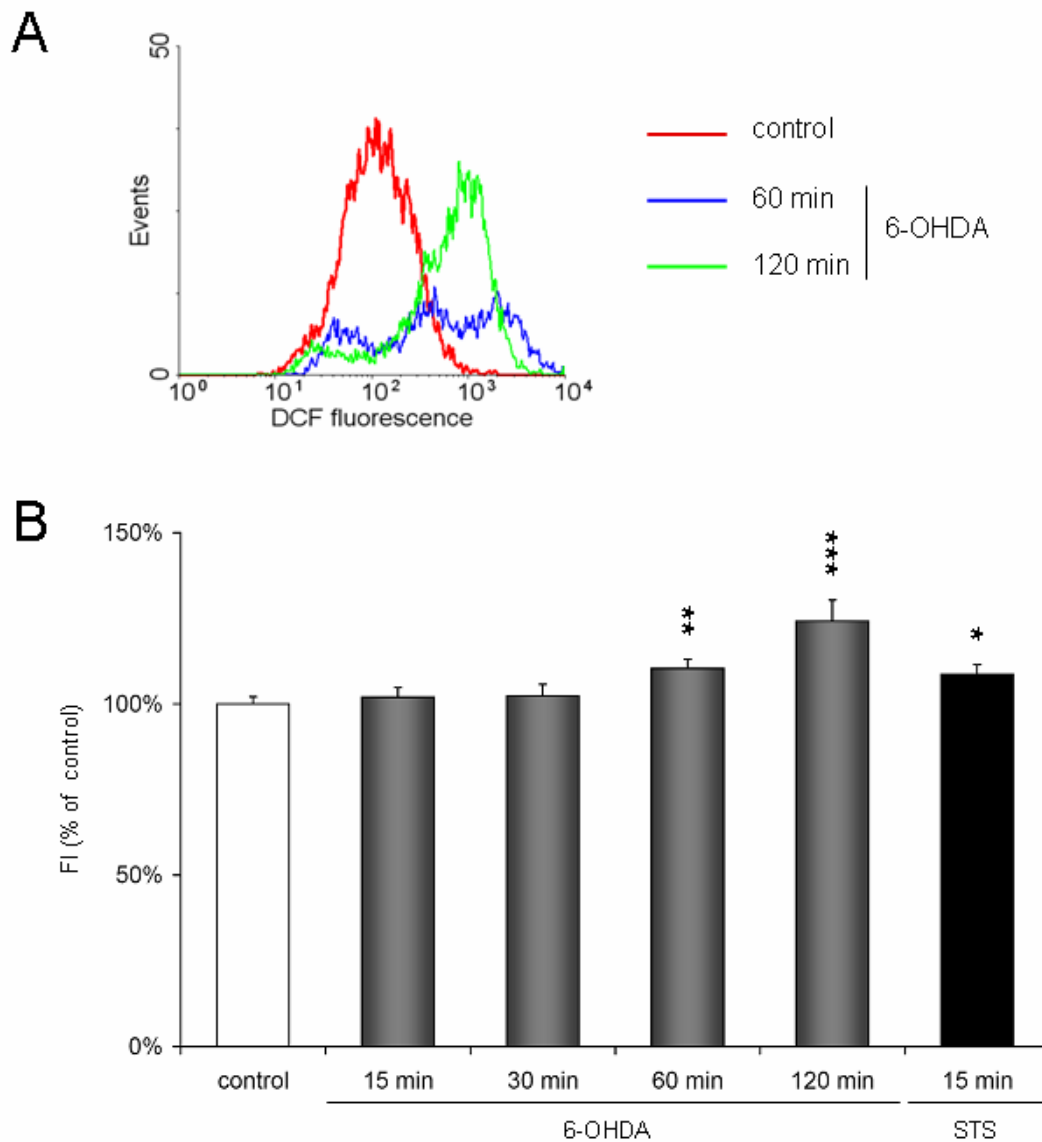


Figure 13. Reactive oxygen species at early time points

Reactive oxygen species (ROS) levels were measured by DCF fluorescence in PC12 cells after 6-OHDA. There was a critical increase when 6-OHDA was given for one hour. A) Histogram depicting ROS production in PC12 cells after 50 μ M 6-OHDA as measured by flow cytometry. B) Bar chart showing FI changes in percent of control in PC12 cells following 50 μ M 6-OHDA and 1 μ M staurosporine (STS), which served as a positive control. Vehicle-treated negative controls were used.

Abbreviations: 6-OHDA (6-hydroxydopamine), DCF (dichlorofluorescein), FI (fluorescence intensity), ROS (reactive oxygen species), STS (staurosporine)

* $P < 0.05$; ** $P < 0.01$; *** $P < 0.001$

Statistical significances were calculated using *t*-test. Data are presented as mean \pm standard deviation. N = 3.

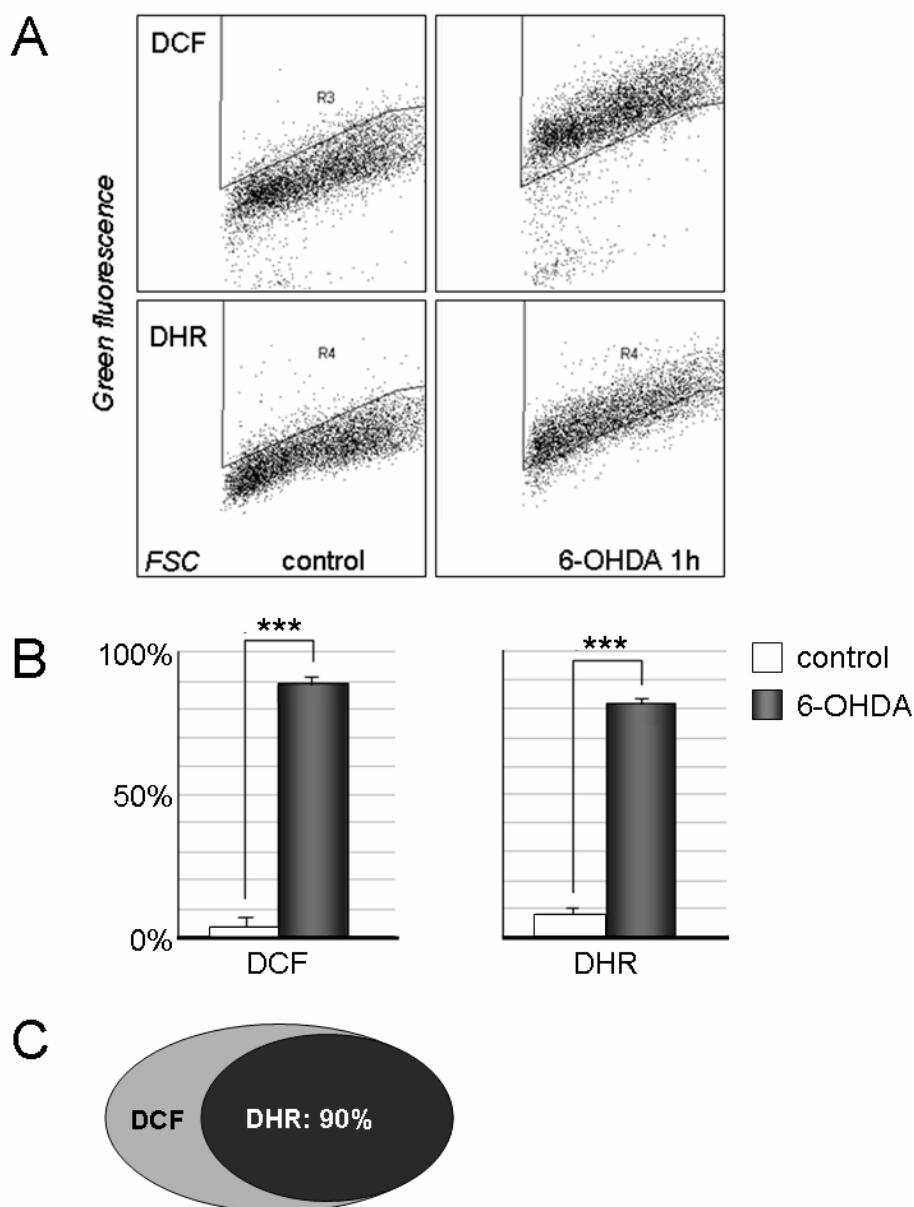


Figure 14. Sources of reactive oxygen species

Reactive oxygen species (ROS) levels were measured by DCF and DHR fluorescence intensity (FI) in PC12 cells after 1 h of incubation with 50 μ M 6-OHDA. A) Dot plots depicting control cell populations and PC12 cells after stimulation. B) Quantitative analysis of DCF and DHR fluorescence. Bar charts represent the number of events in the ROIs (R3 for DCF, R4 for DHR) for control cells (left columns) and 6-OHDA-treated samples (right columns). C) DHR FI values are 90% of the increase of DCF FI after 1 h 6-OHDA. Vehicle-treated controls were used.

Abbreviations: 6-OHDA (6-hydroxydopamine), DCF (dichlorofluorescein), DHR (dihydrorhodamine), FI (fluorescence intensity), ROS (reactive oxygen species).

*** $P < 0.001$

Statistical significances were calculated using *t*-test. Data are presented as mean \pm standard deviation. N = 3.

4.1.3 The mitochondrial membrane potential collapses after 6-hydroxydopamine treatment

ROS in mitochondria are originating from defects in the respiratory chain. Under healthy conditions there is a constant low-level ROS generation due to proton leakage. Following a disruption of the mitochondrial membrane potential, *i.e.* during apoptosis, ROS production increases exponentially. Therefore the question aroused if the marked elevation of ROS levels is due to the disruption of the mitochondrial membrane potential. The dual-fluorescent probe JC-1 is a tool to analyze the mitochondrial membrane potential ($\Delta\Psi_m$) in situ. Emission at 530 nm (green) derives from JC-1 monomers whereas aggregates emit fluorescence at 590 nm (red). Those aggregates form preferably in slightly acidic environment as it is found in the mitochondrial matrix due to the activity of the electron transport chain. Consequently, J-aggregates are regarded to be a sensor for mitochondrial respiration and mark an intact mitochondrial membrane potential (Reers *et al.*, 1991; Smiley *et al.*, 1991; Cossariza *et al.*, 1993). When the mitochondrial membrane potential gets disrupted, aggregates dissociate and the fluorescence intensity (FI) of monomers rises.

First, preliminary tests were performed to analyze how healthy PC12 cells react to different concentrations of JC-1, and which concentration to choose best. Concentrations of 0.1 μM , 1 μM , 5 μM , 10 μM and 50 μM JC-1 were applied to PC12 cells and the fluorescence intensities from the suspensions were measured fluorometrically in the cuvette. Fluorescence intensity of the aggregates at 590 nm was generally higher than compared to that of the monomers (530 nm). The emission in the red range was clearly dose-dependent (*Figure 15A*), whereas the fluorescence in the green range displayed the peculiarity that 5 μM and 10 μM JC-1 resulted in similar curves (*Figure 15B*). Conclusively, 10 μM JC-1 were chosen for further experiments, since this concentration provided the optimal aggregate/monomer ratio regarding healthy PC12 cells.

The next step was to analyze the stability of JC-1 fluorescence over the experimental time. The responsiveness of the model was verified using valinomycin as a positive control, an agent that acts as an ionophore and depolarizes the mitochondrial membrane potential. 1 μM was administered at the end of each 90 min session. As for the samples, untreated PC12 cells were selected, but also solvents that are contained in the stock solutions of 6-OHDA, valinomycin, and JC-1 itself (ascorbic acid, ethanol and DMSO) were checked. Finally, the importance of keeping the samples on ice during the experiment was evaluated. Dot plots

from flow cytometrical analysis were recorded and a region of interest (ROI) was selected to display events with high red and low green fluorescence, indicative for healthy cells. The change of the number of events in this ROI was analyzed.

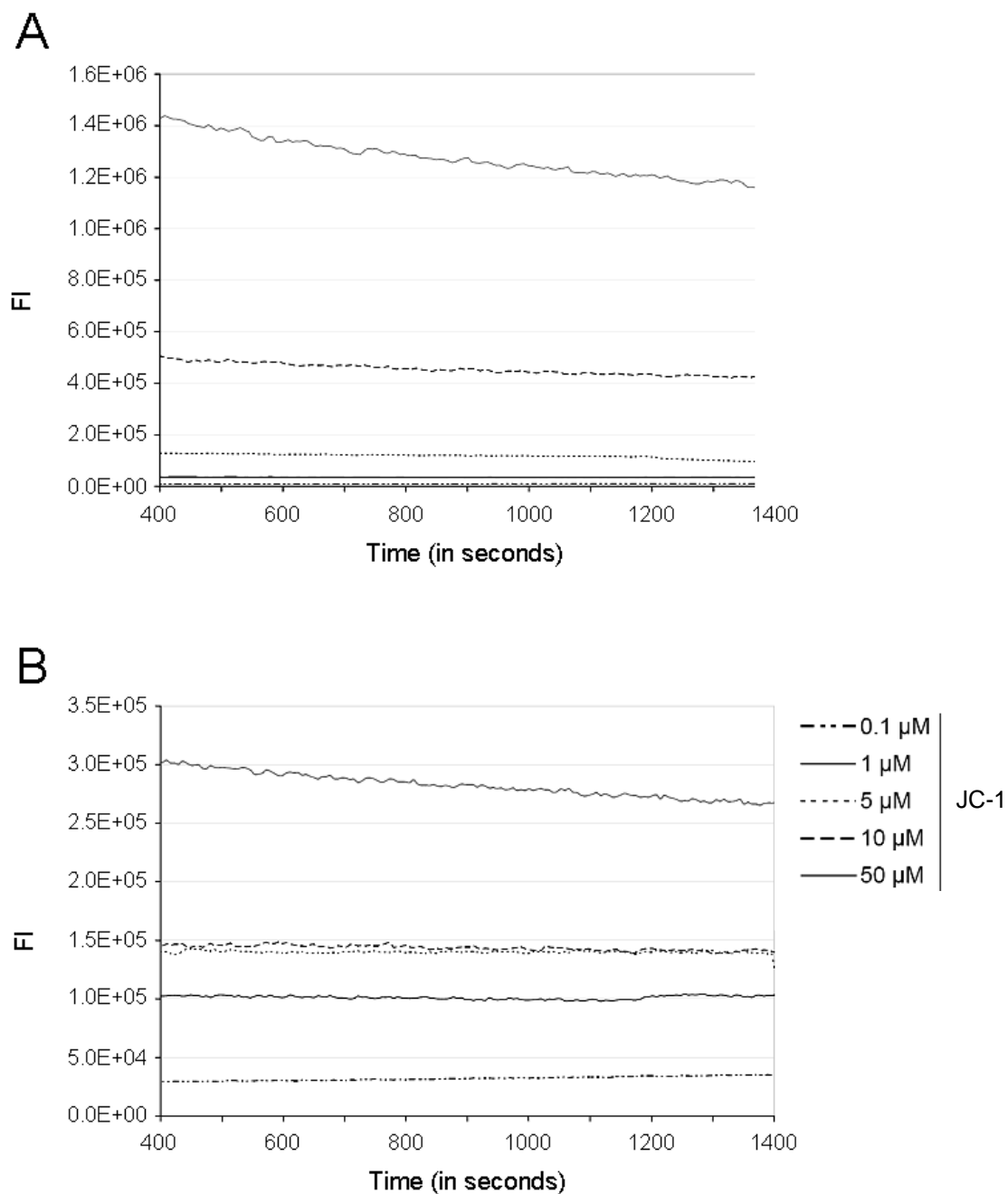


Figure 15. JC-1 dual fluorescence in healthy PC12 cells

Different concentrations of JC-1 and their fluorescence intensities (FI) in untreated PC12 cells followed for 1400 seconds. FI was measured fluorometrically in the cuvette by adding the dye to comparably concentrated cell suspensions. A) JC-1 emission at 590 nm (red). B) Fluorescence emission at 530 nm (green). 10 μM JC-1 provides the optimal ratio to describe $\Delta\Psi_m$ in healthy PC12 cells. Exemplary results (N=3) are displayed.

Abbreviations: FI (fluorescence intensity), $\Delta\Psi_m$ (mitochondrial membrane potential)

RESULTS

Untreated PC12 cells, as well as PC12 cells treated with ascorbic acid, ethanol or DMSO, maintained their $\Delta\Psi_M$ over a time course of 90 min (*Figure 16*). Untreated PC12 cells responded to 1 μ M valinomycin with a 72% decrease of red fluorescent events. Ascorbic acid, which was added to 6-OHDA stocks in a concentration of 0.02%, apparently attenuated depolarizing effects (62% decrease) under the same conditions as untreated cells, but the difference was not significant compared to untreated cells. J-aggregate FI decreased by 76% and 83% after addition of ethanol alone (used in JC-1 stocks at a concentration of 0.1%) and DMSO, respectively (final concentration 0.1%). The combination of all solvents in the analysis medium as applied to “control cells“ led to a similar decline (83%), despite the presence of ascorbic acid.

In all samples the FI of the 90 min time point is obviously lower than the previous values, therefore the assumption was made that the mitochondrial membrane could lose integrity after keeping PC12 in the vial for longer than 90 min. Handling the samples on ice could most likely prolong this time window, since the strongest and most consistent FI was found in this group. Still, cells were not handled on ice, because the response to valinomycin was weak (only 16% decrease of red fluorescence; $P < 0.001$) and could also affect the results from treatment with 6-OHDA (*Figure 16*). For further experiments samples were not kept on ice, since the responsiveness to the depolarizing agent valinomycin was obviously handicapped and could mask effects of 6-OHDA when applied.

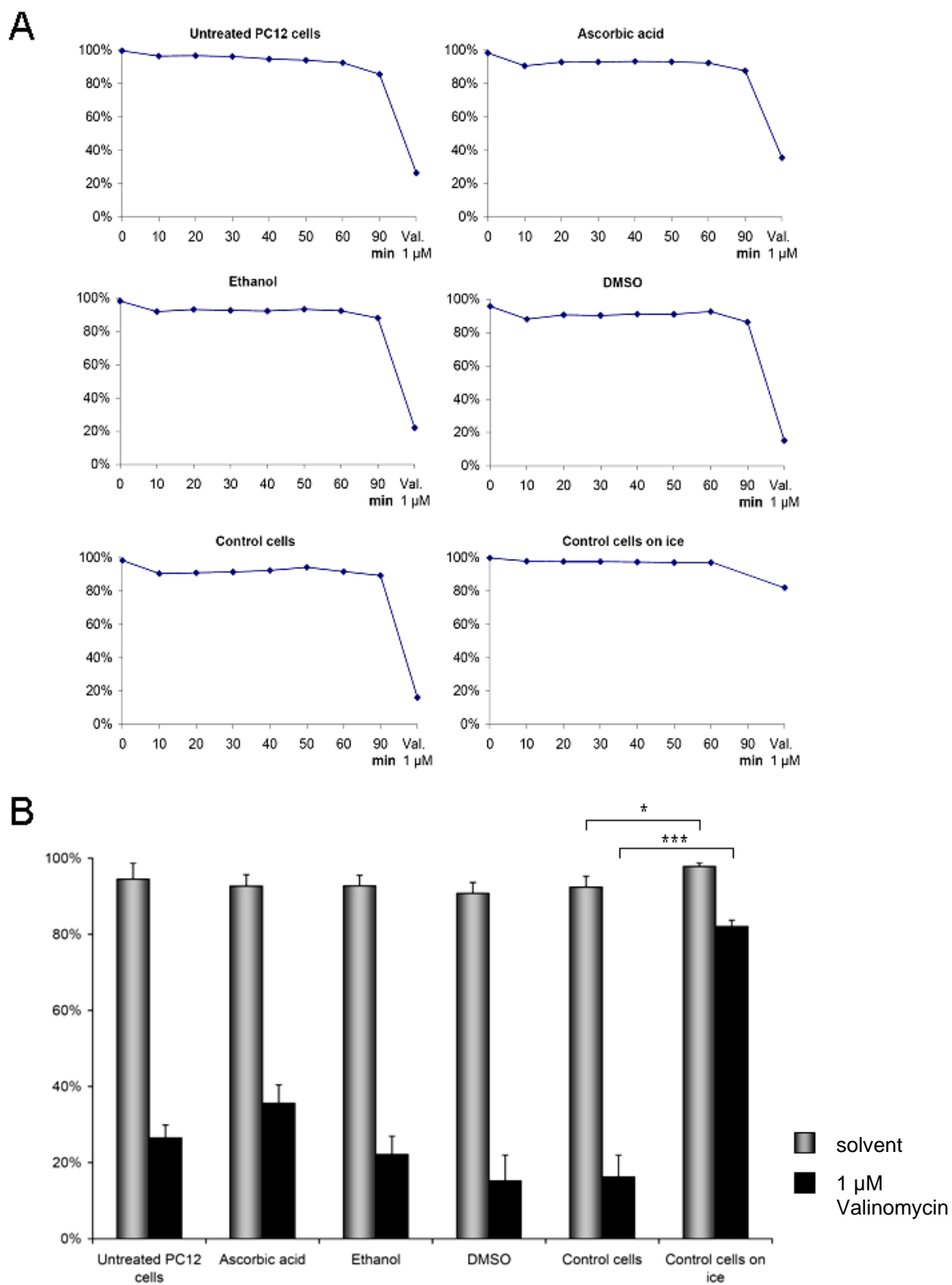


Figure 16. Stability of JC-1 fluorescence over the experimental time (see next page)

Figure 16. Stability of JC-1 fluorescence over the experimental time (see previous page)

Graphs show the number of events calculated from a region of interest (ROI) representing an intact mitochondrial membrane potential ($\Delta\Psi_M$). The intact $\Delta\Psi_m$ is demonstrated by low green and high red fluorescence intensity (FI) based on dot plots acquired by flow cytometry in percent of total number of events. A) Panel shows the change of events in the ROI after a follow-up time of 90 min and the response to 1 μM valinomycin after the observation period. The effect of different solvents on $\Delta\Psi_M$ was measured as well as stability over time with or without keeping the samples on ice meanwhile. B) Bars show the average mean of events in the ROI over the investigation period and the effect of 1 μM Valinomycin on $\Delta\Psi_M$.

Abbreviations: ROI (region of interest), $\Delta\Psi_m$ (mitochondrial membrane potential), FI (fluorescence intensity), DMSO (dimethylsulfoxide), Val. (valinomycin)

* $P < 0.05$; *** $P < 0.001$

Statistical significances were calculated using one-way ANOVA with post-hoc Bonferroni. Data are presented as mean \pm standard deviation. N = 3.

As a next step the effect of 6-OHDA at concentrations of 10 μM , 25 μM , 50 μM or 100 μM on $\Delta\Psi_M$ was investigated in PC12 cells at various incubation times (4, 8, 12, 16, or 24 h) and fluorescence of J-aggregates (emission at 590 nm) was assessed in the flow cytometer. Analysis was based on the number of events in a region of interest that contained the vast majority of events in healthy controls (upper left quadrant in the dot plot as brought in *Figure 17*).

A decrease in the red fluorescence counts specifically for a depolarization of the mitochondrial membrane (Bernardi *et al.*, 1999). After 8 h red fluorescence intensities (FI) of samples incubated with 25 μM , 50 μM and 100 μM 6-OHDA decreased substantially (*Figures 17 and 18*). 25 μM account for values of $80\% \pm 6\%$ of those of controls ($P < 0.05$), stimulation with 50 μM or 100 μM resulted in a decrease down to $65 \pm 10\%$ or $62\% \pm 6\%$, respectively ($P < 0.001$). Further duration of treatment resulted in continuously low levels of FI at 590 nm after 50 μM or 100 μM 6-OHDA ($61\% \pm 5\%$ or $47\% \pm 6\%$ of control levels; $P < 0.001$) (*Figure 18A*). Upon uncoupling the respiratory chain with 1 μM valinomycin the mitochondrial membrane became completely depolarized. The FI at 590 nm was 36% in average following treatment with these agents. Taking into account this range between controls and complete $\Delta\Psi_M$ disruption by valinomycin, 25 μM , 50 μM and 100 μM depolarized the mitochondrial membrane by $32\% \pm 9\%$, $55\% \pm 16\%$ and $59\% \pm 10\%$, respectively, after 8 h. At the 12 h time point, the decrease was $61\% \pm 7\%$ and $84\% \pm 9\%$ after 50 μM and 100 μM 6-OHDA, respectively.

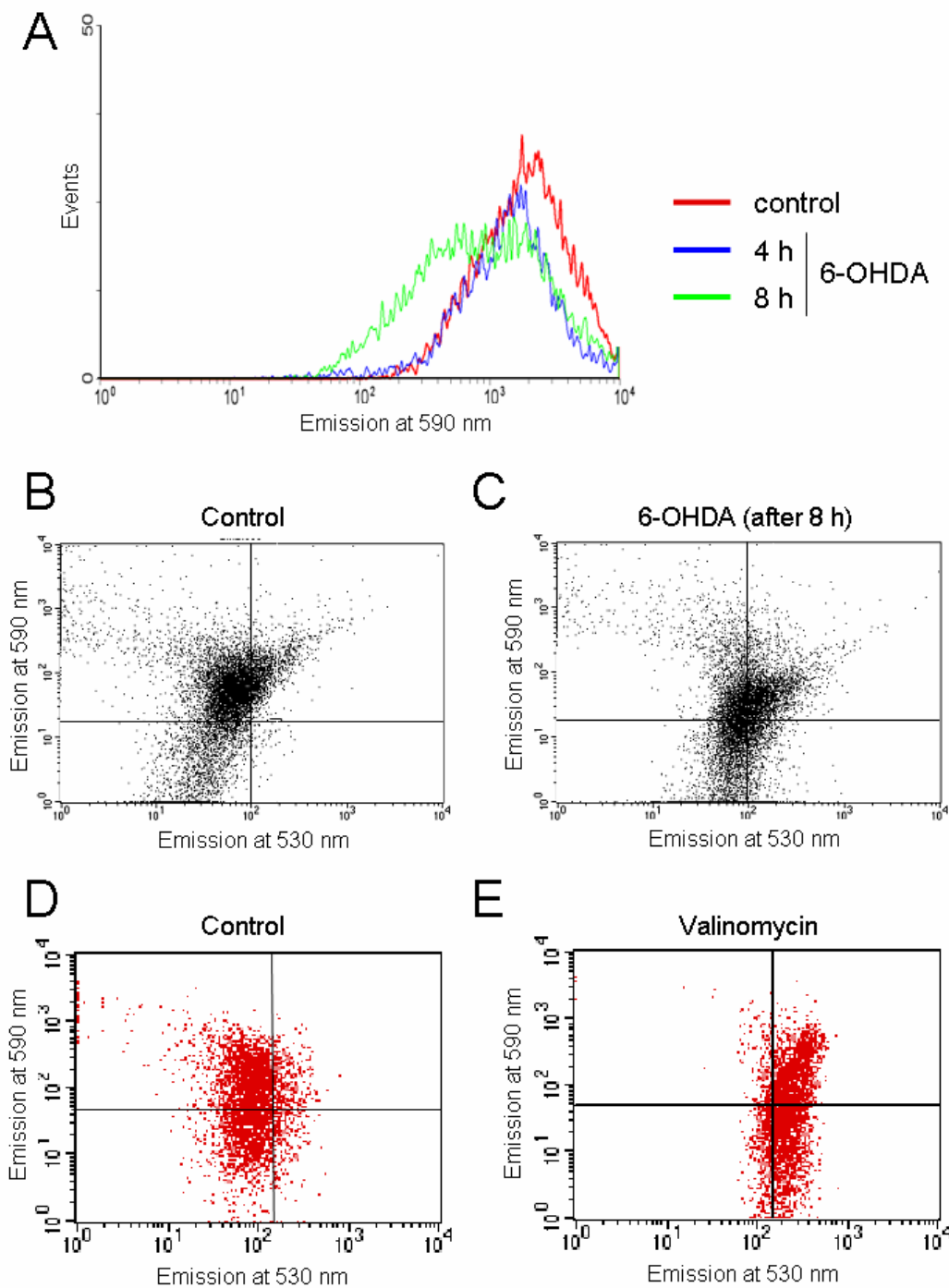


Figure 17. Time point of disruption of the mitochondrial membrane potential

Figure depicts exemplary results from 3-5 flow cytometrical analyses of PC12 cells following 50 μM of 6-OHDA. A) Graph presenting a time-dependent shift in the red fluorescence with a distinct decrease after 8 h. B) Dot plot analysis showing a control cell population with distinct intensities of red and green fluorescence. C) Dot plot analysis of PC12 cells treated with 50 μM 6-OHDA for 8 h. The cell population shifts to a segment of higher green and lower red fluorescence. D) and E) Valinomycin disrupts the $\Delta\Psi_m$. 1 μM served as a positive control depolarizing the mitochondrial membrane in PC12 cells as shown by the population shift to the lower right. Vehicle-treated controls were used.

Abbreviations: 6-OHDA (6-hydroxydopamine), $\Delta\Psi_m$ (mitochondrial membrane potential), FI (fluorescence intensity)

RESULTS

A different way to present data from JC-1 fluorescence is the determination of the ratio between red and green fluorescence. Although it has been found that only the decrease in red fluorescence is specific for the disruption of $\Delta\Psi_M$, this method is still widely used. Less red and stronger green fluorescence result in smaller ratios, indicating a disruption of $\Delta\Psi_M$. The number of events positive for JC-1 fluorescence at 590 nm (cells in the upper left quadrant) was divided by the number of events exhibiting high green fluorescence intensity (upper right and lower right quadrant). Ratios decreased over time following 6-OHDA in different concentrations, with, generally, the greatest decrease between 4 h and 8 h of incubation. 50 μM and 100 μM , however, exerted the lowest ratios (*Figure 18B*). Again, 1 μM valinomycin was applied to assess what values would represent a totally depolarized mitochondrial membrane. The JC-1 aggregate/monomer ratio acquired by this procedure was approx. 1.2. Thus, 10 μM 6-OHDA caused depolarization by 10% (4 h), 60% (8 h) and 54% (12 h); 25 μM yielded 29% (4 h) and 69% (8 h, $P < 0.05$; and 12 h); 50 μM showed a 33% (4 h), 91% (8 h, $P < 0.001$) and 95% (12 h, $P < 0.001$) decrease whereas 100 μM 6-OHDA resulted in a drop of 59% (4 h), 94% (8 h, $P < 0.001$) and 105% (12 h, $P < 0.001$) of $\Delta\Psi_M$ (*Figure 18B*).

Immediate effects following the administration of 6-OHDA were analyzed fluorometrically in a time-resolved manner. JC-1 red (excitation wavelength 488, emission wavelength 590) and green fluorescence (488:530) from a PC12 cell suspension in a cuvette, followed over a time period of 2000 seconds. At the indicated time, 50 μM 6-OHDA were pipetted into the solution, followed by a 30 seconds break before continuous measurement to reduce effects of turbulences. The FI in both emission wavelengths dropped, although changes in the green fluorescence were weak, and subsequently the red fluorescence decreased at a steeper slope than the base line. The ratio graph endorsed the immediate decline of $\Delta\Psi_M$ (*Figure 19*).

Following concentrations over 25 μM 6-OHDA PC12 cell mitochondria lose their integrity as shown by the disruption of $\Delta\Psi_M$ after 8 h. Not the time point but the initial concentration of the toxin seems to be the crossroads for milder $\Delta\Psi_M$ disturbance or heavy disruption of the electrochemical gradient.

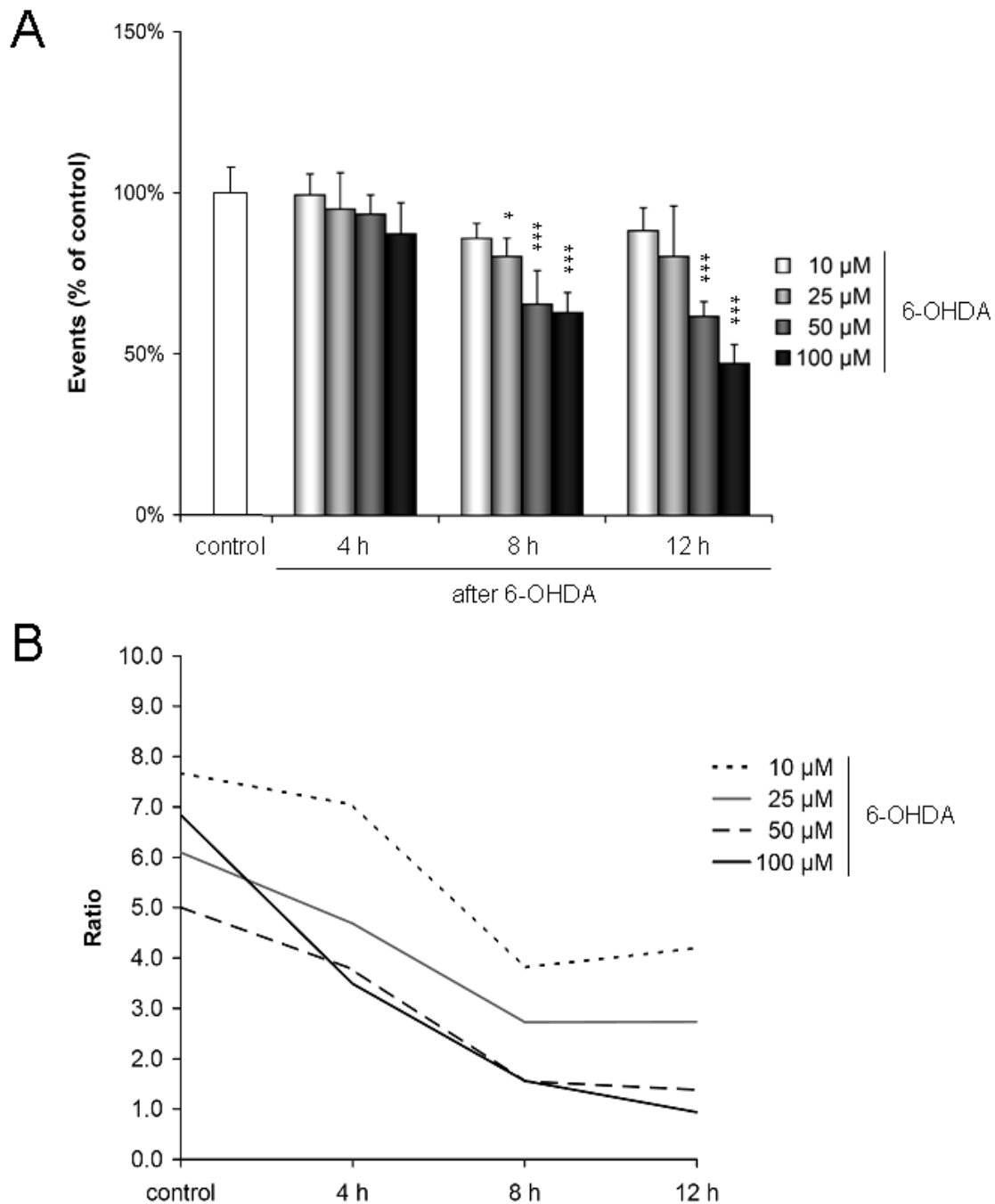


Figure 18. Mitochondrial membrane potential in PC12 cells following 6-OHDA

PC12 cells were incubated with 10 μM JC-1 and fluorescence intensity (FI) was measured by flow cytometry as described. A) 25 μM , 50 μM and 100 μM reduced the number of red fluorescent cells significantly after 8 h of incubation with 6-OHDA. B) Ratio of red/green fluorescence at the investigated time points. Vehicle-treated controls were used.

Abbreviations: 6-OHDA (6-hydroxydopamine), $\Delta\Psi_M$ (mitochondrial membrane potential), FI (fluorescence intensity)

* $P < 0.05$; *** $P < 0.001$

Statistical significances were calculated using one-way ANOVA with post-hoc Bonferroni. Data are presented as mean \pm standard deviation. N = 4.

RESULTS

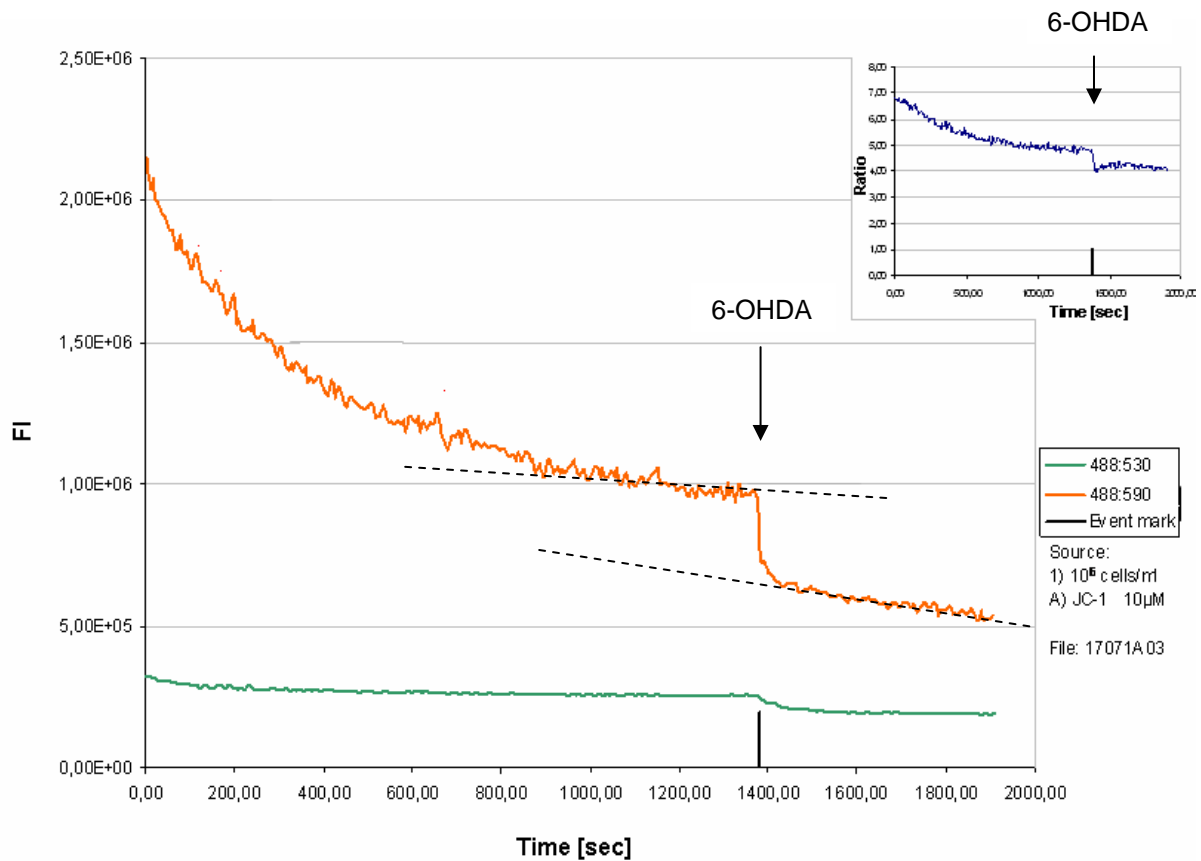


Figure 19. Immediate effect of 6-OHDA on $\Delta\Psi_M$ of PC12 cells

JC-1 red (excitation wavelength 488, emission wavelength 590) and green fluorescence (488:530) from a PC12 cell suspension (large graph) and their ratio (red vs. green; graph in the upper right corner), followed over a time period of 2000 seconds. JC-1 was used at a concentration of 10 μM . 50 μM 6-OHDA were given at the time point marked. The asymptote before 6-OHDA marks the base line, the second line's slope indicates an ongoing disturbance of $\Delta\Psi_M$ resulting from the administration of the toxin.

Abbreviations: 6-OHDA (6-hydroxydopamine), FI (fluorescence intensity), $\Delta\Psi_m$ (mitochondrial membrane potential)

4.1.4 6-OHDA induces cytochrome c release

JC-1 shows the impairment of the electron transport chain of mitochondria and $\Delta\Psi_M$ disruption which leads to formation of permeability transition pores, release of mitochondrial proteins and caspase activation leading to cell death (Cossariza *et al.*, 1993). The mitochondrial death pathway involves the release of cytochrome c into the cytosol. Under basal conditions cytochrome c is situated in the mitochondrial intermembrane space, mainly attached to the inner mitochondrial membrane, and is only found in the cytosol when the mitochondrial membrane integrity is lost. Substantial levels of cytochrome c were identified in cytosolic PC12 cells fractions after 8 h incubation with 25 μM 6-OHDA, as demonstrated by Western blot analysis (*Figure 20A*). Findings were confirmed using fluorescence microscopy of methanol/paraformaldehyde-fixed samples stained with anti-cytochrome c antibody and FITC-conjugated secondary antibody. In control cells cytochrome c staining is clustered (hint for localization in mitochondria), whereas 8 h after 25 μM 6-OHDA the distribution is changed to a completely diffuse pattern (cytochrome c in the cytosol) (*Figure 20B*).

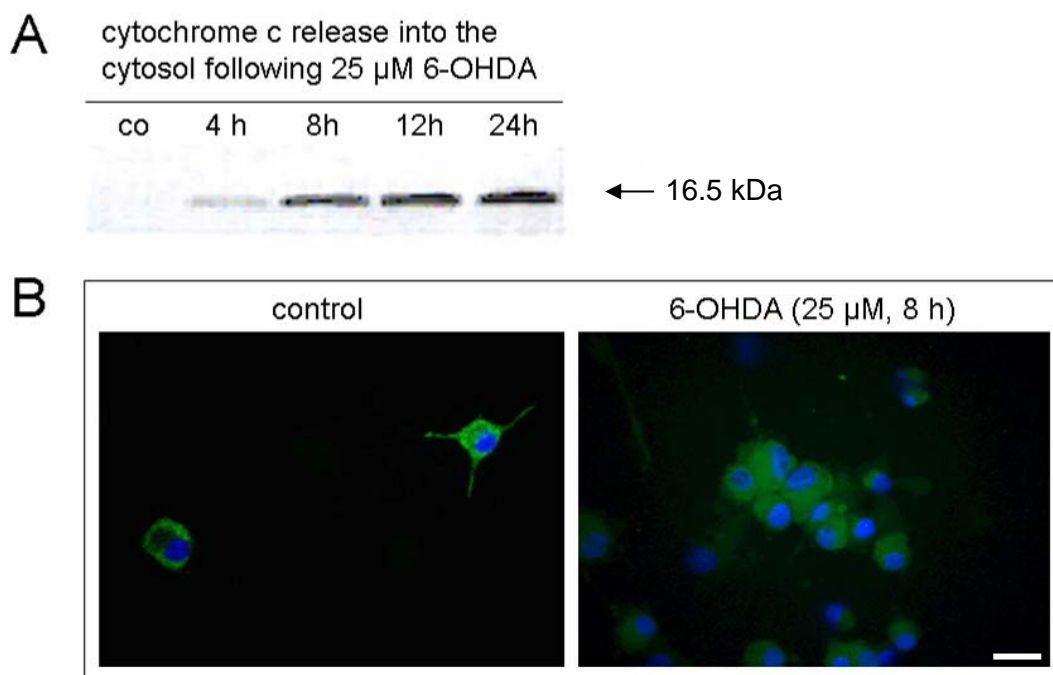


Figure 20. Cytochrome c release

Detection of cytochrome c release into the cytosol. Displayed are representative results ($n = 3$). A) In the Western blot substantial levels of cytochrome c were identified in the cytosolic fraction of PC12 cells after 8 h. B) Fluorescence microscopy of cells stained with anti-cytochrome c antibody combined with FITC-conjugated secondary antibody. Cytochrome c distribution changes from clusters (mitochondria) to a diffuse pattern (cytosol) after 8 h incubation with 25 μM 6-OHDA. Vehicle-treated controls were used. Scalebar represents 20 μm .

4.2 Responsiveness of isolated mitochondria to 6-hydroxydopamine

4.2.1 Analyses with isolated mitochondria

The next experiments addressed the question if isolated mitochondria responded to 6-OHDA in similar manner as cells. Isolated mice brain mitochondria were analyzed flow cytometrically. The production of reactive oxygen species (ROS) was determined using ROS-sensitive fluorescent dyes, and the integrity of the mitochondrial membrane was assessed by the dual-fluorescent dye JC-1. Additionally, the immediate effect of 6-OHDA on the mitochondrial membrane potential of a mitochondrial suspension in the cuvette was measured fluorometrically in a time-resolved manner.

4.2.2 Quality of isolated mitochondria

Subsequent to every isolation, a sample of mitochondria was studied for their functional integrity by assessing the RCR (*Figure 21*). Respiration on succinate (feeding complex II) in the presence of rotenone (inhibiting complex I) was established and ADP was added. State 4 respiration was calculated as the slope ($m = \Delta y / \Delta x$) of the asymptote, as it was done for state 3 respiration, after all ADP had been used up. In the example brought in *Figure 21*, the RCR was calculated as $0.5/0.16$ which resulted in 3.125. Mitochondria with a RCR above 3 were acceptable for use in experiments and were stable for the next 2 - 3 h.

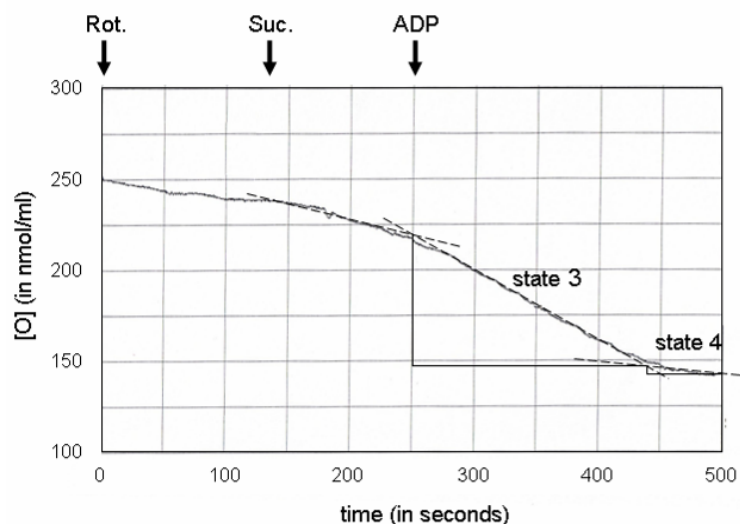


Figure 21. Assessment of mitochondrial functional integrity

Isolated mitochondria were analyzed for their functional integrity by measuring oxygen consumption with a Clark electrode. The slopes of state 3 and state 4 respiration are drawn. The RCR of this example was calculated as 3.125.

Abbreviations: ADP (adenosin-diphosphate), [O] (concentration of molecular oxygen in the sample), RCR (respiratory control ratio), Rot. (rotenone), Suc. (succinate).

4.2.3 Purity of mitochondrial fractions

Cytosolic and mitochondrial fractions obtained during the isolation procedure were subjected to Western blot analysis. Membranes were incubated with antibodies against the mitochondrial constitutional protein cytochrome c oxidase subunit IV (COX IV) and β -actin for the assessment of cytosolic contaminations. Usually, β -actin was present in low-level concentrations even in highly purified mitochondria (*Figure 22*). This can be explained by the tight connections between mitochondria and the cytoskeleton together with the nature of the isolation method.

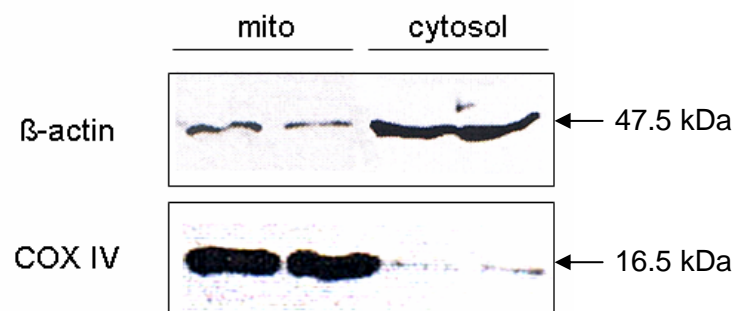


Figure 22. Purity of mitochondrial fraction obtained from mice brain

Representative Western blot detecting protein levels of β -actin (cytosolic marker) and cytochrome c oxidase subunit IV (COX IV; mitochondrial marker). The mitochondrial fraction (mito) shows high COX IV expression and little amounts of β -actin.

Abbreviations: COX IV (cytochrome c oxidase subunit IV), mito (mitochondrial fraction).

4.2.4 ROS levels in isolated mitochondria following 6-OHDA

Samples of isolated mitochondria were preloaded with 2',7'-dichloro-dihydrofluorescein (H₂DCF) and incubated with 6-OHDA. Concentrations of 10, 25, 50, or 100 μ M 6-OHDA were not sufficient to increase ROS levels in isolated mitochondria significantly when administered for 60 min, as measured in the Fluoroskan plate reader (*Figure 23*). Only at a very high concentration (200 μ M) a significant increase of DCF FI indicated higher ROS levels. DCF was sufficient as a marker of ROS in mitochondrial preparations since it can pass the outer mitochondrial membrane and therefore identify ROS generated in the mitochondrial intermembrane space. Secondly it would be oxidized by ROS diffusing from the matrix.

4.2.5 The mitochondrial membrane potential of isolated mitochondria following 6-OHDA

The mitochondrial membrane potential was measured with the aid of the dual-fluorescent redox sensitive probe JC-1. Emission at 530 nm (green) derives from the monomers whereas aggregates, which are formed in the slightly acidic milieu of the mitochondrial matrix, emit fluorescence at 590 nm (red). When the mitochondrial membrane potential gets disrupted, aggregates dissociate and the fluorescence intensity (FI) of monomers rises. Changes in $\Delta\Psi_M$ upon various concentrations of 6-OHDA treatment (10, 25, 50, and 100 μM) was measured by JC-1 fluorescence in the BD FACSCalibur flow cytometer. Administration of 50 μM 6-OHDA resulted in an increased FI of monomers (530 nm) while red FI (590 nm) decreased at the same time indicating a disruption of $\Delta\Psi_M$ (Figure 24A and B).

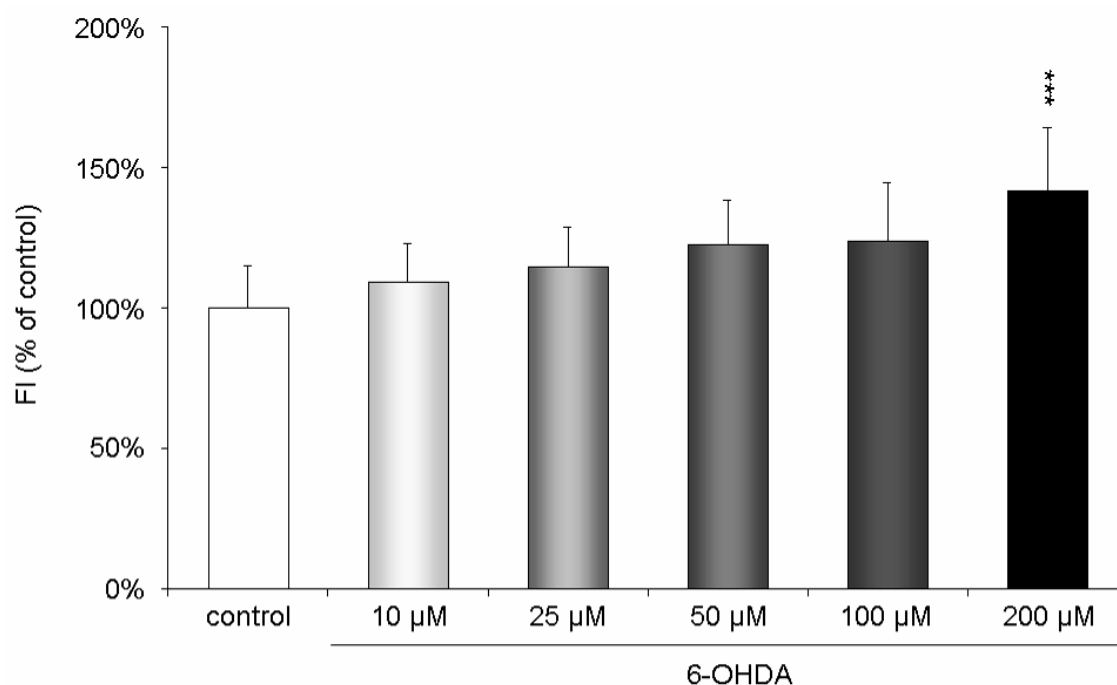


Figure 23. Measurement of reactive oxygen species in mitochondrial fractions

Reactive oxygen species (ROS) levels were measured by DCF fluorescence in 24 well plates in mitochondria isolated from mice brain. 200 μM 6-OHDA applied for 60 min elevated ROS levels significantly, altogether an increase in DCF fluorescence could be observed. Vehicle-treated controls were used.

Abbreviations: FI (fluorescence intensity), DCF (dichlorofluorescein), ROS (reactive oxygen species).

*** $P < 0.001$

Statistical significances were calculated using *t*-test. Data are presented as mean \pm standard deviation. N = 3.

Presenting the mitochondrial population in a dot plot (530 nm versus 590 nm) reveals an evident susceptibility of isolated mitochondria to 6-OHDA (30 min incubation), as shown by

the shift into the lower right quadrant (*Figure 24C and D*). Quantitative analysis of the number of events in the upper left quadrant (*Figure 24C and D*), representing the healthy mitochondrial population, was performed. The red fluorescence of J-aggregates decreased significantly (58% of control levels) after 30 min when 100 μM 6-OHDA were applied ($P < 0.05$). 40 min stimulation with 50 μM or 100 μM 6-OHDA disrupted $\Delta\Psi_{\text{M}}$ by 51% each ($P < 0.05$, and $P < 0.01$, respectively). After 50 min, FI at 590 nm decreased significantly at all concentrations. Incubation with 10 μM resulted in FI of 66% of control levels ($P < 0.05$), the other values were 60% following 25 μM ($P < 0.05$) and 41% following 50 μM or 100 μM ($P < 0.01$). 60 min stimulation with 10 μM 6-OHDA decreased $\Delta\Psi_{\text{M}}$ to 63% of control levels ($P < 0.05$), 25 μM led to 55% ($P < 0.05$), $\Delta\Psi_{\text{M}}$ decreased to 41% following 50 μM ($P < 0.01$) and 31% ($P < 0.001$) after treatment with 100 μM 6-OHDA (*Figure 25A*). Full depolarization of $\Delta\Psi_{\text{M}}$ with 1 μM valinomycin gave a ratio of approx. 0.9. The administration of 10 μM 6-OHDA caused, hence, a depolarization by 85% (50 min, $P < 0.05$) and 88% (60 min, $P < 0.05$). 25 μM resulted in a decrease of 90% (50 min, $P < 0.05$) and 95% (60 min, $P < 0.05$). 50 μM showed a 94% decline of $\Delta\Psi_{\text{M}}$ after 40 min ($P < 0.05$), and a drop of 102% (50 and 60 min, $P < 0.01$), whereas 100 μM 6-OHDA decreased $\Delta\Psi_{\text{M}}$ by 91% (30 min, $P < 0.05$), 99% (40 min, $P < 0.01$), 105% (50 min, $P < 0.01$) and 110% (60 min, $P < 0.001$) (*Figure 25B*).

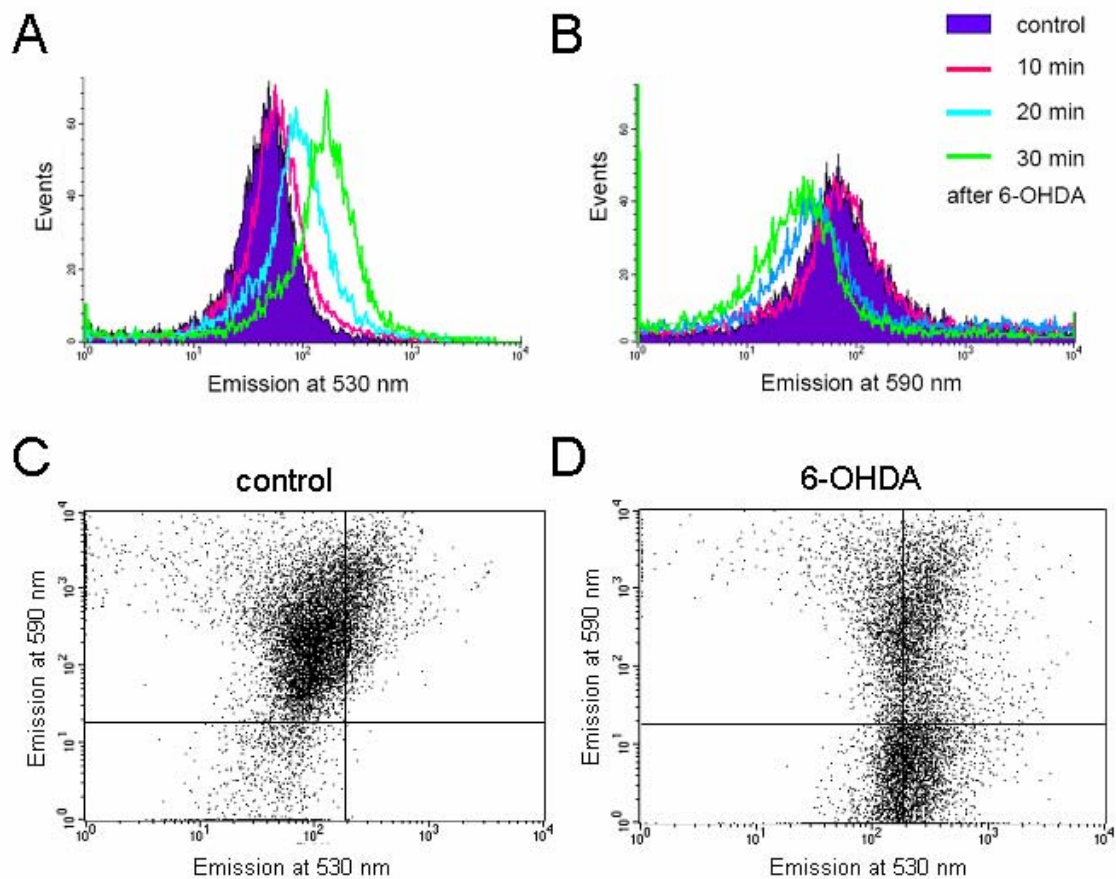


Figure 24. Isolated mitochondria and the mitochondrial membrane potential

Depicted are results from flow cytometrical analysis of $\Delta\Psi_M$ of isolated mice brain mitochondria. A) Curves show a time-dependent increase of mitochondria emitting green fluorescence (530 nm) after 50 μM 6-OHDA. B) Accordingly, there is a decrease in the red fluorescence upon longer incubation with 6-OHDA. C) Dot plot presents a representative example of a control mitochondrial population, with higher FI for the red than for the green emitting wavelength. A quadrant was set for later statistical analysis. D) After 100 μM 6-OHDA (30 min) the mitochondrial population shifts into the lower right quadrant, indicative for $\Delta\Psi_M$ disruption. Vehicle-treated controls were used.

Abbreviations: 6-OHDA (6-hydroxydopamine), FI (fluorescence intensity), $\Delta\Psi_M$ (mitochondrial membrane potential)

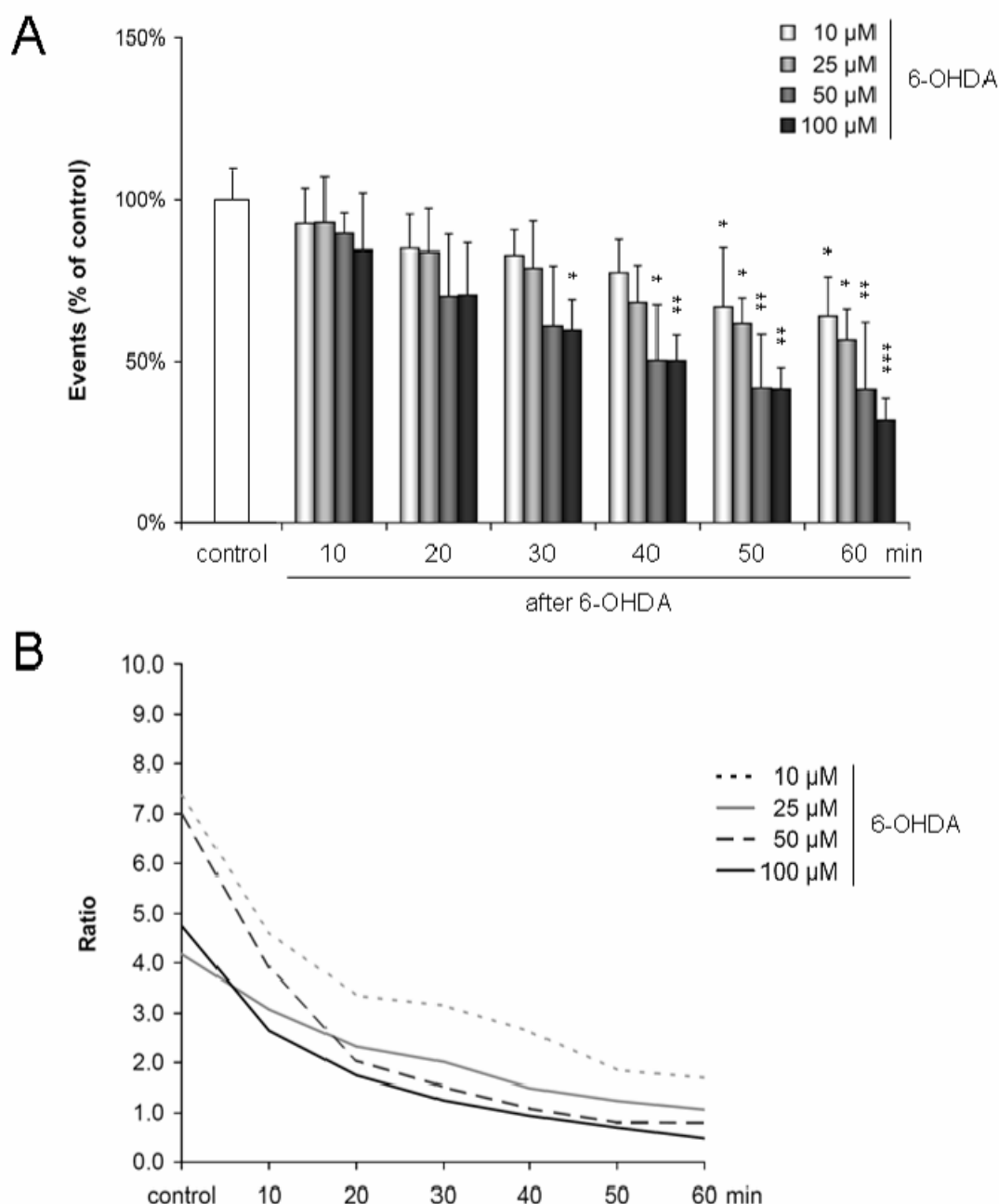


Figure 25. Mitochondrial membrane potential in isolated mitochondria following 6-hydroxydopamine

Isolated mitochondria were preloaded with 10 μM JC-1, then stimulated with 6-OHDA, and fluorescence intensity (FI) was measured by flow cytometry. Analysis is based on the number of events in a region of interest that was set to contain the vast majority of events in healthy controls (upper left quadrant in the dot plot as depicted in *Figure 19C*). A) Effects of various concentrations of 6-OHDA on $\Delta\Psi_{\text{M}}$ of isolated mitochondria. B) Ratio of red/green fluorescence at the investigated time points. Vehicle-treated controls were used.

Abbreviations: 6-OHDA (6-hydroxydopamine), $\Delta\Psi_{\text{M}}$ (mitochondrial membrane potential), FI (fluorescence intensity)

* $P < 0.05$, ** $P < 0.01$, *** $P < 0.001$

Statistical significances were calculated using one-way ANOVA with post-hoc Bonferroni. Data are presented as mean \pm standard deviation. N = 4.

RESULTS

Suspensions of isolated brain mitochondria were diluted 1:20 and subjected to fluorometrical analysis in a time-resolved manner to discover immediate changes in $\Delta\Psi_M$ following 6-OHDA. JC-1 red (ex. 488, em. 590) and green fluorescence (ex. 488, em. 530) were followed over a time period of 1600 sec. Before the addition of 6-OHDA isolated mitochondria were administered rotenone (10 μM) and succinate (0.5 mM), rotenone inhibiting complex I while succinate being the substrate to feed complex II of the respiratory chain. After achieving stable conditions, 10 μM 6-OHDA was pipetted into the solution, followed by a 30 seconds break before continuous measurement to reduce effects of turbulences. The result was an immediate decrease of mainly the red signal, and the ratio of red to green fluorescence (*Figure 26*), indicating a loss of mitochondrial membrane integrity.

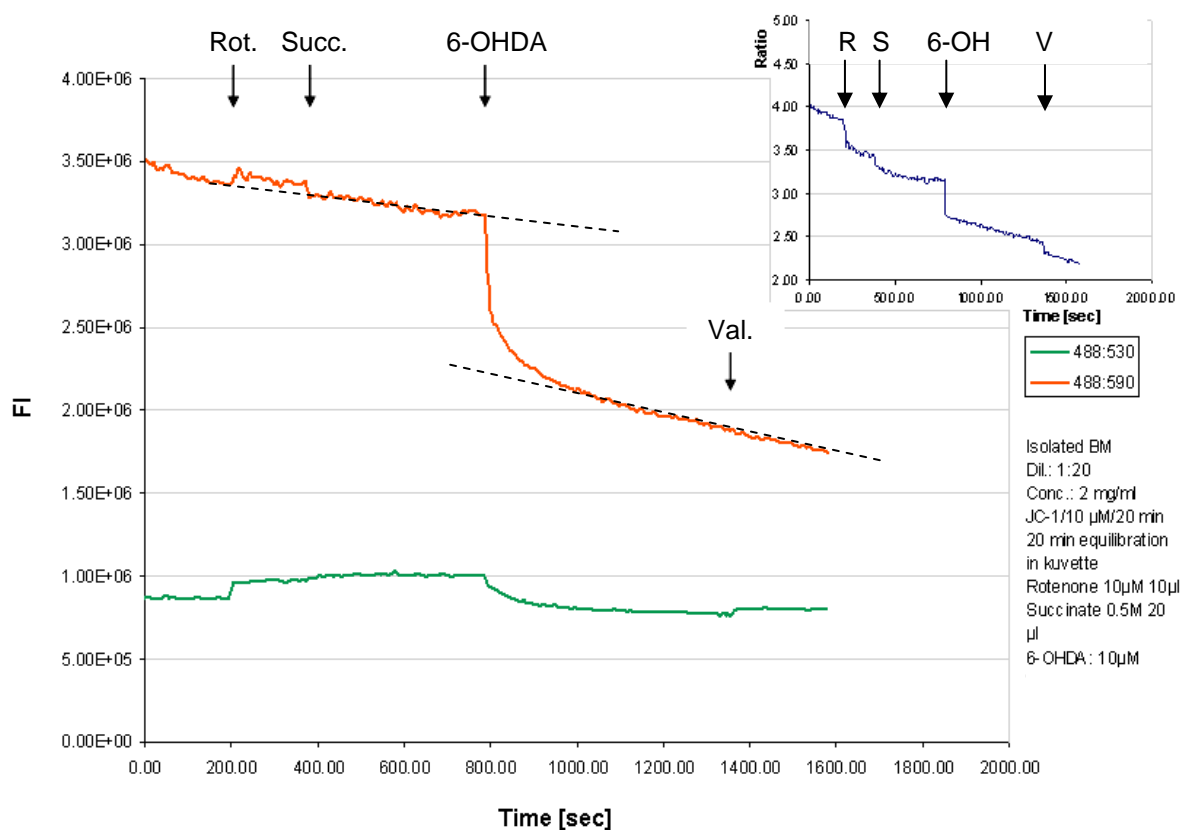


Figure 26. Immediate effect of 6-OHDA on isolated mitochondria

The representative graph shows JC-1 red (ex. 488, em. 590) and green fluorescence (ex. 488, em. 530) from a suspension of isolated mitochondria, followed fluorometrically over a time period of 1600 seconds. Before the addition of 6-OHDA isolated mitochondria were administered rotenone (10 μM) and succinate (0.5 mM). At the indicated time, 10 μM 6-OHDA was pipetted into the solution. The graph in the upper right corner depicts changes in the ratio of red to green fluorescence over the duration of the experiment. Administration of 1 μM Valinomycin resulted in a further drop of the ratio.

Abbreviations: 6-OH (6-OHDA), BM (brain mitochondria), FI (fluorescence intensity), Rot./R (rotenone), Succ./S (succinate), Val./V (valinomycin)

4.3 The mitochondrial death pathway and c-Jun N-terminal kinase signaling

c-Jun N-terminal kinases (JNK) are central mediators in stress-signaling pathways and play a role in the mitochondrial death pathway. Kharbanda *et al.* found that JNK translocated to mitochondria in various cell lines following ionizing radiation (Kharbanda *et al.*, 2000). We hypothesized that 6-OHDA treatment could provoke JNK translocation to mitochondria as well.

4.3.1 Purification of PC12 cell mitochondrial fractions

At first, an isolation method to obtain mitochondrial fractions from PC12 cells was established. The purity of these fractions was analyzed by Western blot detection of mitochondrial and cytosolic markers (*Figure 27*). Lysed PC12 cells (C), intermediate samples from the isolation procedure (I1, I2; see materials and methods, section 3.3.5) and the final mitochondrial fraction were stained with antibodies against the mitochondrial resident protein cytochrome c oxygenase subunit IV (COX IV) and β -actin, to determine cytosolic contaminations of the fractions. It was revealed that the first mitochondrial fraction obtained during the isolation procedure (I1) was already rich in mitochondrial COX IV protein, and contained rather low levels of β -actin, but the washing step reduced cytosolic contamination further (I2). The final mitochondrial fraction (M) was almost cleared from β -actin, and was enriched in mitochondrial COX IV protein.

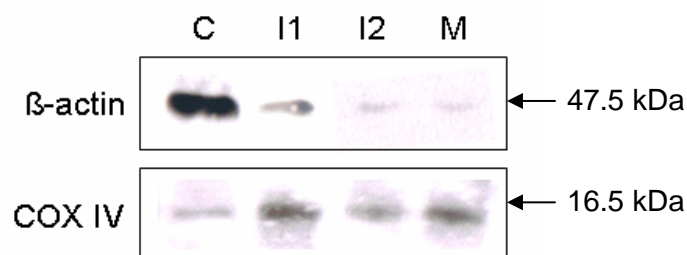


Figure 27. Isolation and purification of mitochondria from PC12 cells

Western blot analysis of representative intermediate samples from the isolation procedure to obtain mitochondrial fractions from PC12 cells. Expression of cytosolic β -actin and mitochondrial cytochrome c oxidase subunit IV (COX IV) was determined for samples taken before the incubation in sucrose buffer (controls, C), two samples from in between the centrifugation steps (I1 and I2), and one taken from the final mitochondrial suspension (M).

Abbreviations: C (controls), COX IV (cytochrome c oxidase subunit IV), I1, I2, M (see legend text).

4.3.2 Activation of the mitochondrial pool of JNK following 6-OHDA

Mitochondrial fractions from PC12 cells were analyzed by Western blot for their total JNK and *phospho-* (active) JNK content after incubation with 25 μ M 6-OHDA for various durations (4, 8, 12, 16, 24, and 48 h) (*Figure 28*). Total-JNK protein content is virtually unchanged regardless of the stimulation. Under basal conditions, hardly any phosphorylated JNK could be detected in mitochondrial fractions. *Phospho-JNK* expression is upregulated within 4 h and levels remain high up to 24 h after 6-OHDA addition (*Figure 28*).

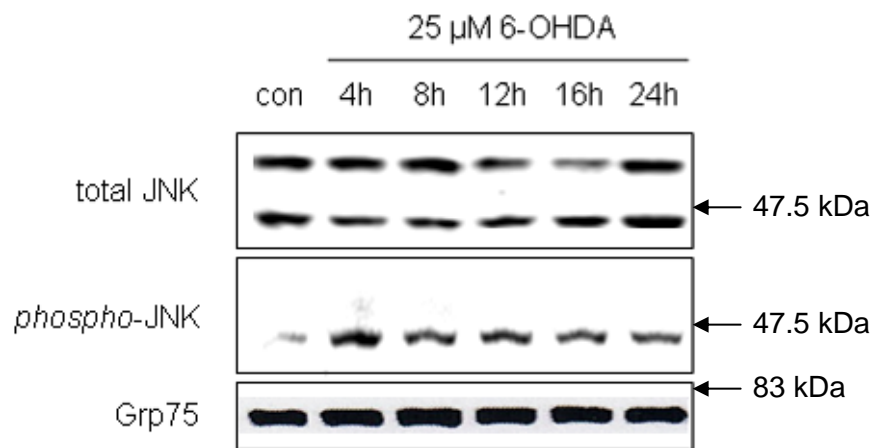


Figure 28. Activation of JNK in mitochondrial fractions

Representative results of Western blot analysis of total- and (active) phospho-JNK levels in mitochondrial fractions of unstimulated PC12 cells and following incubation with 25 μ M 6-OHDA for 4, 8, 12, 16, 24 and 48 h. Grp75 is a residential protein in the mitochondrial matrix. Vehicle-treated cells served as controls.

Abbreviations: 6-OHDA (6-hydroxydopamine), con (unstimulated control), JNK (c-Jun N-terminal kinase)

4.3.3 Translocation of c-Jun N-terminal kinase isoform 2 (JNK2) to mitochondria

Detection of JNK isoforms 1 and 2 in Western blots of mitochondrial preparations revealed differential patterns. The pool of JNK1 at the mitochondria did not change after addition of 25 μ M 6-OHDA. In contrast, JNK2 levels in basal conditions were low and increased upon stimulation in mitochondrial fractions within 4 h (*Figure 29A*). The JNK inhibitor SP600125 was able to prevent JNK2 translocation as compared to stimulated cells at the four hour time point, but had no effect on the presence of JNK1 at the mitochondria (*Figure 29B*).

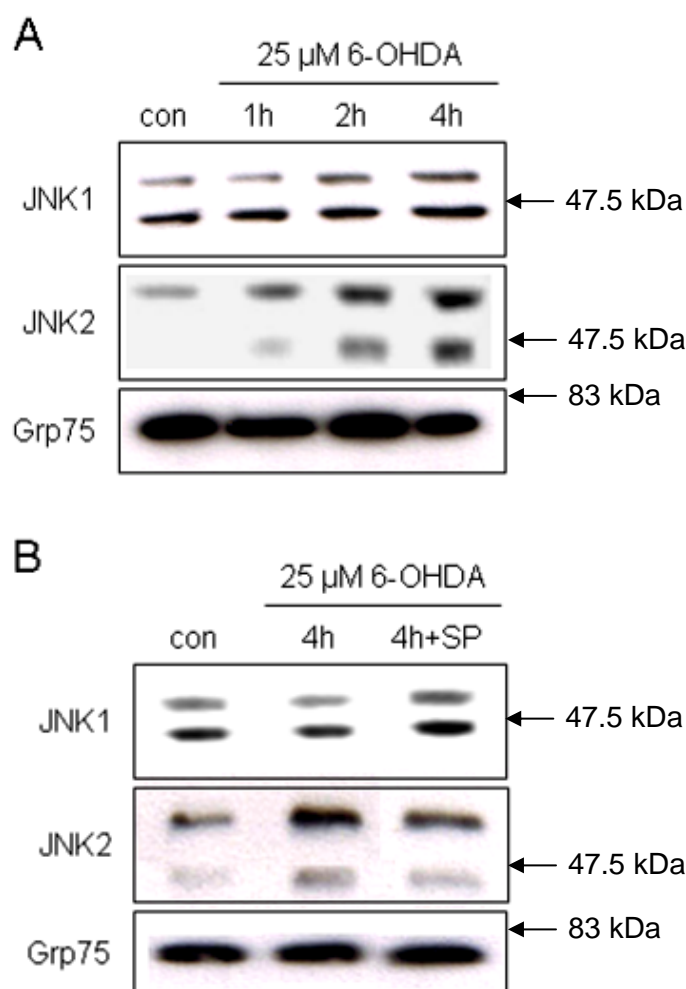


Figure 29. JNK1 and JNK2 expression in mitochondrial fractions

Representative results of Western blot analysis of mitochondrial fractions from PC12 cells. Grp75 is a residential protein in the mitochondrial matrix. A) JNK1 and JNK2 expression in mitochondrial fractions of unstimulated controls and following 1 h, 2 h, and 4 h incubation with 25 μ M 6-OHDA. B) JNK1 and JNK2 expression in mitochondrial fractions of unstimulated controls, and after 4 h stimulation with 25 μ M 6-OHDA, with or without the JNK inhibitor SP600125 (SP). Vehicle-treated controls were used.

Abbreviations: 6-OHDA (6-hydroxydopamine), con (unstimulated control), SP (SP600125), JNK (c-Jun N-terminal kinase)

To support these findings, confocal microscopy was performed with samples of PC12 cells stained with mitotracker red, anti-JNK primary antibodies plus FITC-conjugated secondary antibodies and Hoechst 33258 for visualization of nuclei. JNK1 distribution in controls showed some overlay with mitochondria in the merged picture, but generally JNK1 was found throughout the cytosol, and particularly in the nucleus. Treatment with 50 μ M 6-OHDA did not change the pattern apart from slightly more clustering and a minor increase of JNK1 in the nucleus (*Figure 30*).

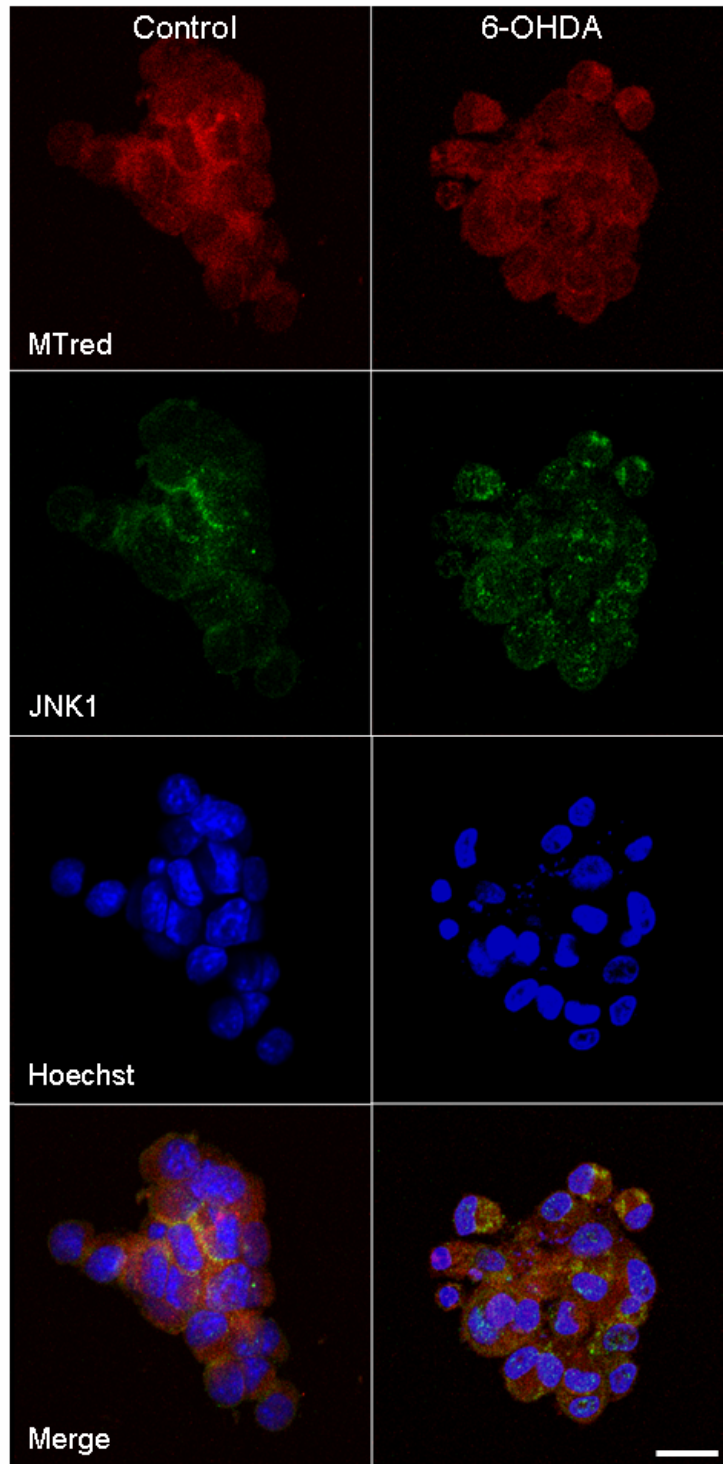


Figure 30. JNK1 distribution in PC12 as measured by confocal microscopy

In preparation for confocal microscopy, nuclei were stained with the DNA dye Hoechst 33258, mitochondria were localized by mitotracker red (MTred) and JNK1 was visualized with anti-JNK1 primary antibody plus FITC-conjugated secondary antibody. JNK1 expression in control cells was mainly cytosolic, with some hints for basal expression in mitochondria and nuclei. Following 6-OHDA (50 μ M, 4 h), a slight increase of JNK1 levels in the nucleus could be detected in the merged picture. Scalebar represents 20 μ M.

Abbreviations: 6-OHDA (6-hydroxydopamine), JNK (c-Jun N-terminal kinase), MTred (mitotracker red), FITC (fluorescein-isothiocyanate)

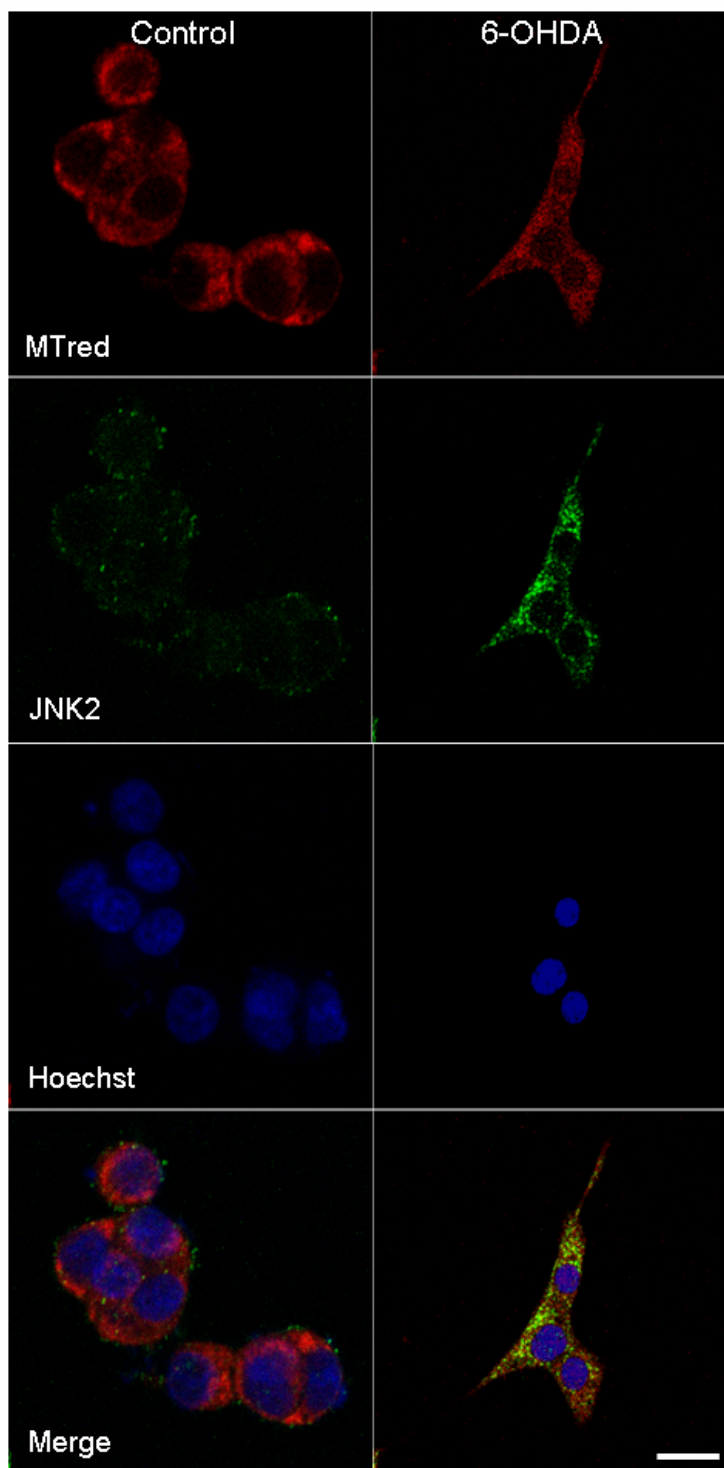


Figure 31. JNK2 distribution in PC12 as measured by confocal microscopy

In preparation for confocal microscopy, nuclei were stained with Hoechst 33258, mitochondria were localized by mitotracker red (MTred) and JNK2 was visualized with anti-JNK2 primary antibody plus FITC-conjugated secondary antibody. JNK2 expression in control cells was low and appeared to be cytosolic. Following 6-OHDA (50 μ M, 4 h), JNK2 was found to be clustered and co-localized with mitochondria, as brought in the merged picture. Scalebar represents 10 μ M (for control) and 20 μ M (for 6-OHDA), respectively.

Abbreviations: 6-OHDA (6-hydroxydopamine), JNK (c-Jun N-terminal kinase), MTred (mitotracker red), FITC (fluorescein-isothiocyanate)

RESULTS

JNK2 expression was weaker in controls as compared to JNK1 levels and displayed no co-localization with mitochondria (*Figure 31*). Stimulation with 50 μ M 6-OHDA resulted in bright clusters of JNK2 at the same spots as mitochondria were stained confirming near proximity/co-localization of both (*Figure 31*). Levels in the nucleus were a bit higher than in controls, but not as high as JNK1 levels were under the same conditions.

4.3.4 Upstream kinases and JNK scaffolds in mitochondrial fractions

The upstream kinases for JNK comprise MKK4 and MKK7. To differentiate their contribution to the translocation of JNK2 to mitochondria, the expression of these MAPKKs was analyzed by Western blot. MKK4 was present in mitochondrial preparations from PC12 cells, and levels did not change following 25 μ M 6-OHDA. Nonetheless, the pool of MKK4 was activated by addition of an active phosphate 2 - 4 h after 6-OHDA stimulation (*Figure 32A*). Administration of SP600125 attenuated the presence of MKK4 in mitochondrial fractions compared to 4 h treatment with 6-OHDA alone (*Figure 32B*). MKK7 was not found in mitochondrial fractions at all, control experiments confirmed MKK7 expression in the cytosol (*Figure 32C*). The JNK scaffold JIP was present at mitochondria, but expression levels remained unchanged following stimulation with 6-OHDA (*Figure 32D*).

Taken together, 6-OHDA induced the translocation of MKK4 and the JNK isoform 2 to mitochondria, as well as the activation of these kinases within 4 h. Subsequently, 6-OHDA treatment resulted in the release of cytochrome c from the mitochondrial intermembrane space into the cytosol, which is a key event in apoptotic processes.

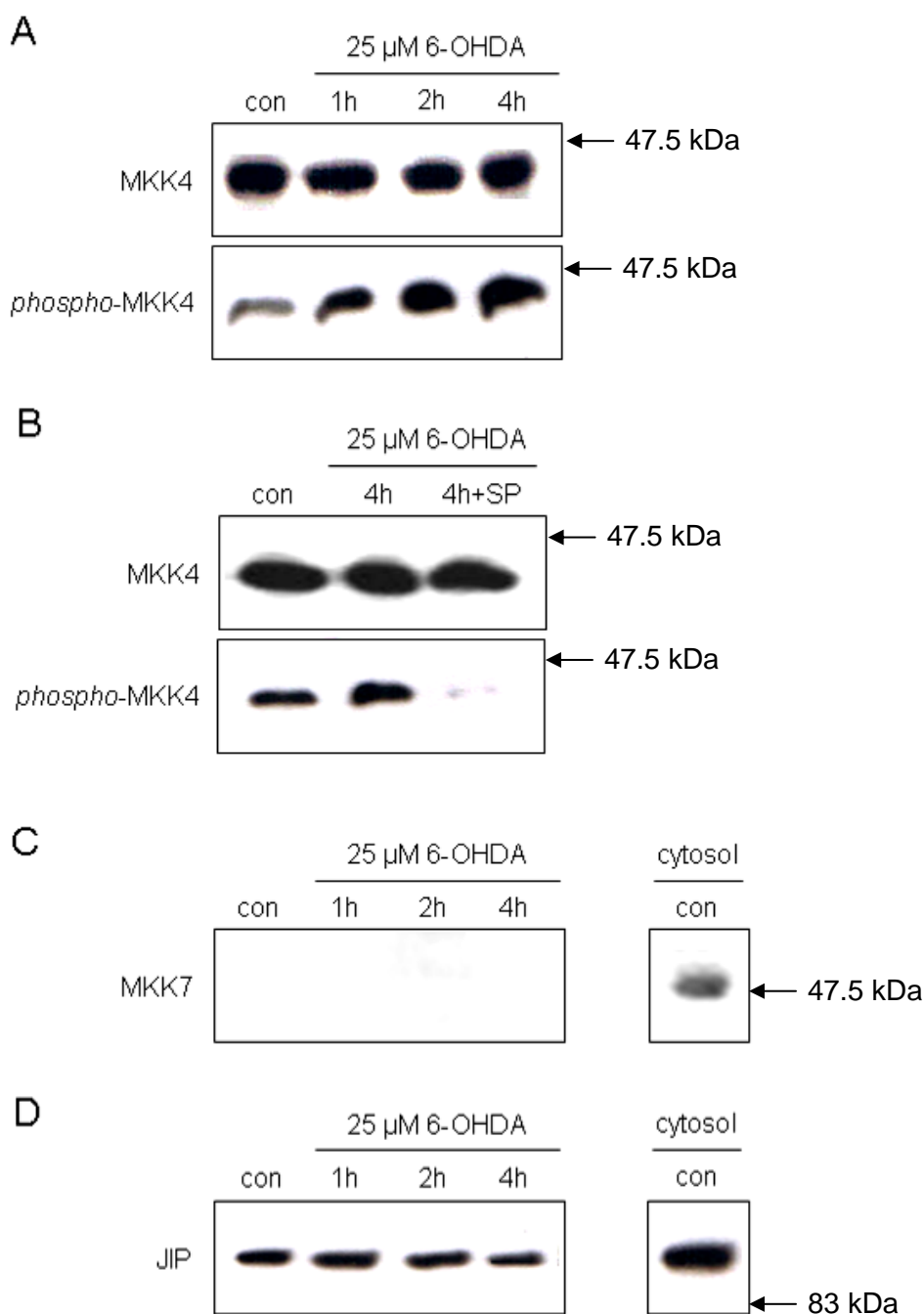


Figure 32. Upstream kinases and scaffolds in mitochondrial fractions

Representative results of Western blot analysis. A) MKK4 was found in mitochondrial preparations from PC12 cells, its levels did not change following 25 μ M 6-OHDA up to 4 h. However, 6-OHDA activated mitochondrial MKK4 between 2 h and 4 h. B) Expression of *phospho*-MKK4, but not MKK4, was reduced below control levels by SP600125. C) MKK7 was not detected in mitochondrial, but in cytosolic fractions. D) The JNK scaffold JIP was present at mitochondria, but 6-OHDA showed no effect on protein levels. Vehicle-treated controls were used.

Abbreviations: 6-OHDA (6-hydroxydopamine), con (unstimulated control), JIP (JNK interacting protein), JNK (c-Jun N-terminal kinase), MKK4/7 (mitogen activated protein kinase 4/7), SP (SP600125)

4.4 Inhibition of JNK and ROS production

4.4.1 JNK inhibition does not prevent from oxidative stress

Does the inhibition of JNK also affect ROS levels that are elevated after treatment with 6-OHDA? The JNK inhibitor SP600125, which prevents JNK2 from translocation to mitochondria, was applied, and DCF fluorescence was measured in the Fluoroskan plate reader. Higher concentrations of SP inhibitor were used for higher concentrations of 6-OHDA (2 μ M SP in controls, and for 10 μ M and 25 μ M 6-OHDA, 2.5 μ M SP for 50 μ M 6-OHDA, and 3 μ M and 4 μ M SP for 100 μ M and 200 μ M 6-OHDA, respectively). Still, SP600125 could not prevent ROS production (*Figure 33*).

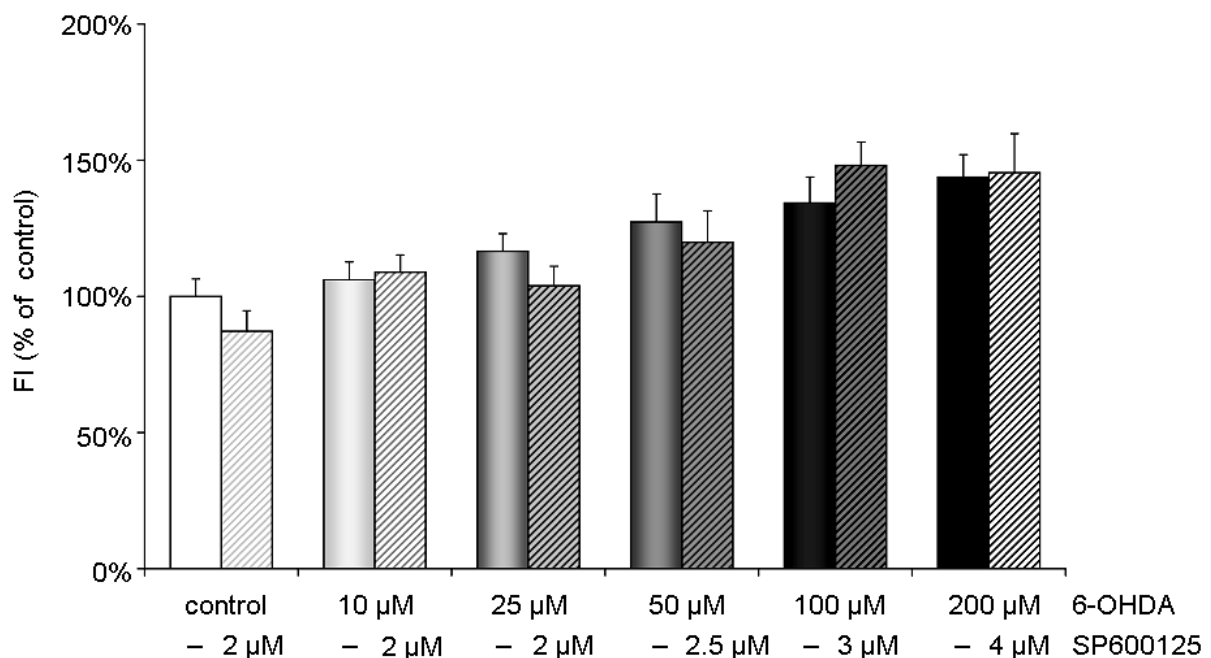


Figure 33. Effect of JNK inhibition on the production of reactive oxygen species

Data was obtained from PC12 cells incubated with H₂DCF to assess the amount of reactive oxygen species (ROS) with and without the addition of 6-OHDA for 4 h. ROS production could not be attenuated by the JNK inhibitor SP600125 at any 6-OHDA concentration. Vehicle-treated controls were used.

Abbreviations: 6-OHDA (6-hydroxydopamine), FI (fluorescence intensity), H₂DCF (2',7'-dichloro-dihydrofluorescein), JNK (c-Jun N-terminal kinase), ROS (reactive oxygen species)

Statistical significances were calculated using one-way ANOVA with post-hoc Bonferroni. Data are presented as mean \pm standard deviation. N = 3.

4.4.2 Antioxidant mediated neuroprotection against ROS generation

The kavalactone methysticin, the flavon luteolin, and the phytoalexin resveratrol, as well as *tert*-butylhydroquinone (*t*BHQ) were tested for their ability to protect against 6-OHDA- or MPP⁺ (1-methyl-4-phenylpyridinium ion)-induced ROS production. 16 h preincubation with the protectors was followed by 1 h stimulation; 6-OHDA was used in a concentration of 50 μ M, MPP⁺ was applied at 100 μ M. Results were correlated to controls. Application of only the protectors did not change DCF fluorescence compared to controls (data not shown). Administration of 50 μ M 6-OHDA resulted in a 36% \pm 8% ($P < 0.01$), 100 μ M MPP⁺ in a 22% \pm 6% increase of ROS levels ($P < 0.05$).

Higher ROS production following 6-OHDA could be significantly prevented by the preincubation with all investigated antioxidants (*Figure 29A*). In detail, 25 μ M methysticin almost completely prevented an increase of ROS (105% \pm 8% of control levels; $P < 0.01$), preloading with 5 μ M luteolin (111% \pm 9%; $P < 0.05$), 5 μ M resveratrol (110% \pm 6%; $P < 0.05$), and 5 μ M *t*BHQ (109% \pm 11%; $P < 0.05$) attenuated ROS elevation effectively as well (*Figure 29A*).

MPP⁺ served as a second model substance to induce oxidative stress in Parkinson's disease. MPP⁺ was administered at a concentration that resulted in a comparable increase of ROS production as contrasted to 6-OHDA treatment. Statistical analysis revealed that ROS levels following 100 μ M MPP⁺ or 50 μ M 6-OHDA did not differ significantly. Again, methysticin (97% \pm 7%; $P < 0.05$), luteolin (95% \pm 9%; $P < 0.05$) and *t*BHQ (96% \pm 9%; $P < 0.05$) prevented ROS generation following the application of the toxin. However, resveratrol was not effective against MPP⁺-induced ROS production.

Comparing the generation of ROS in our model, 6-OHDA takes the lead over MPP⁺ despite the lower concentration. Antioxidants could effectively prevent the oxidative stress response to the toxins, with one exception. Resveratrol failed to inhibit ROS production after MPP⁺.

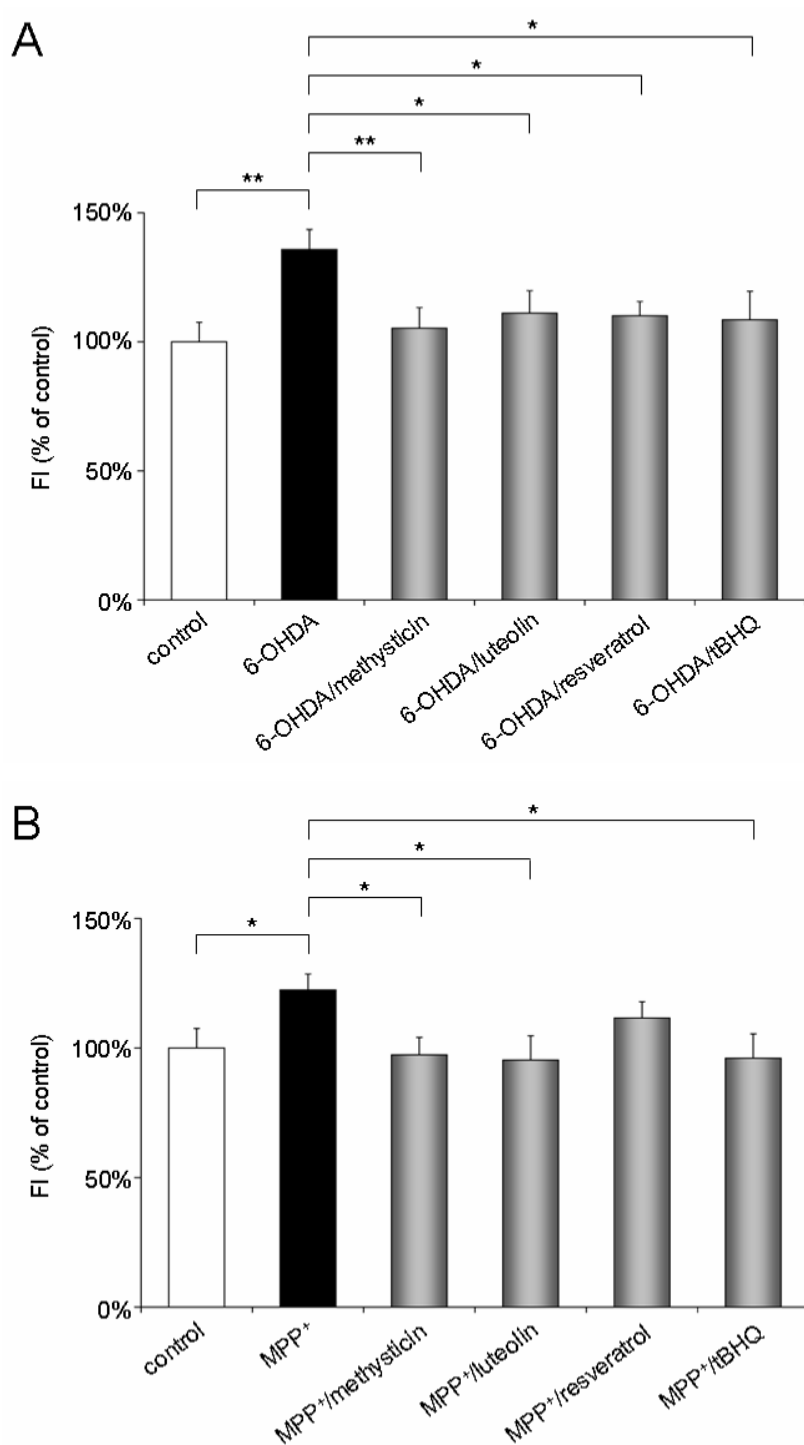


Figure 34. Antioxidant mediated protection against reactive oxygen species

The effect of 25 μ M methysticin, 5 μ M luteolin, 5 μ M resveratrol, and 5 μ M *tert*-butylhydroquinone (*t*BHQ) on ROS levels following stimulation with 6-OHDA (A) or MPP⁺ (B). Data are presented as the percentage of DCF FI of vehicle-treated controls, as measured in the fluorescence plate reader.

Abbreviations: 6-OHDA (6-hydroxydopamine), DCF (2',7'-dichlorofluorescein), FI (fluorescence intensity), MPP⁺ (1-methyl-4-phenylpyridinium ion), ROS (reactive oxygen species), *t*BHQ (*tert*-butylhydroquinone)

Statistical significances were calculated using one-way ANOVA with post-hoc Tukey's analysis. Data are presented as mean \pm standard deviation. N = 4.

4.5 Involvement of c-Jun N-terminal kinase isoforms in neurite outgrowth

Besides their apoptotic functions, JNKs are essential for the formation and elongation of neurites (Waetzig and Herdegen, 2003, Gelderblom *et al.*, 2004). To investigate this effect mouse hippocampi were obtained and separate primary cell cultures were set up and maintained for up to 6 days. JNK1, JNK2 and JNK3 knock-out (ko) animals and corresponding wild type (wt) mice were used. To verify the genetic background, mouse parents and pups were subjected to DNA analysis as described above (materials and methods, section 3.3.12). *Figure 35* shows exemplary PCR results (*Figure 35*).

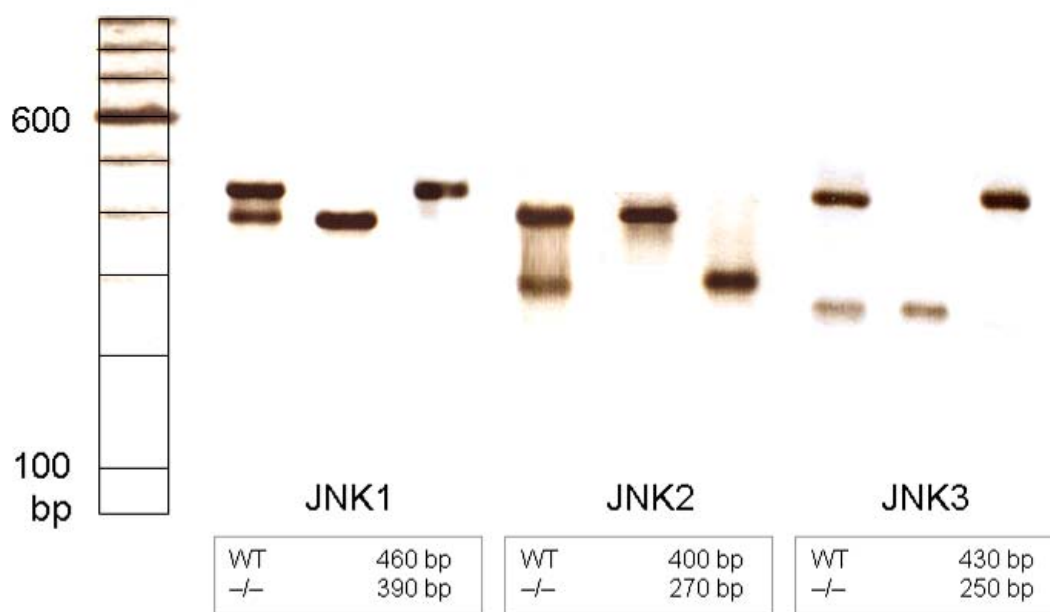


Figure 35. Genetic background of mice

Exemplary PCR results illustrating the interpretation of mice tissue samples. Double bands correspond to a heterozygous gene pair, whereas a single upper band denotes homozygous wild type JNK, the lower one consists of two truncated gene copies from knock-out mice.

Abbreviations: bp (base pairs), JNK (c-Jun N-terminal kinase), WT (wild type)

Wt animals were pooled since they displayed no significant differences between their groups. One set of Wt samples was exposed to 2 μ M of the JNK inhibitor SP600125 immediately after the explantation. At days 2 and 6 *in vitro*, cultures were fixed and stained with an antibody against the neurite marker MAP-2 and neurite lengths were measured. Obtained values were classified into four groups (lengths of 0 - 39 μ m, 40 - 79 μ m, 80 - 119 μ m, and >120 μ m). The results are brought in *Figure 36*.

RESULTS

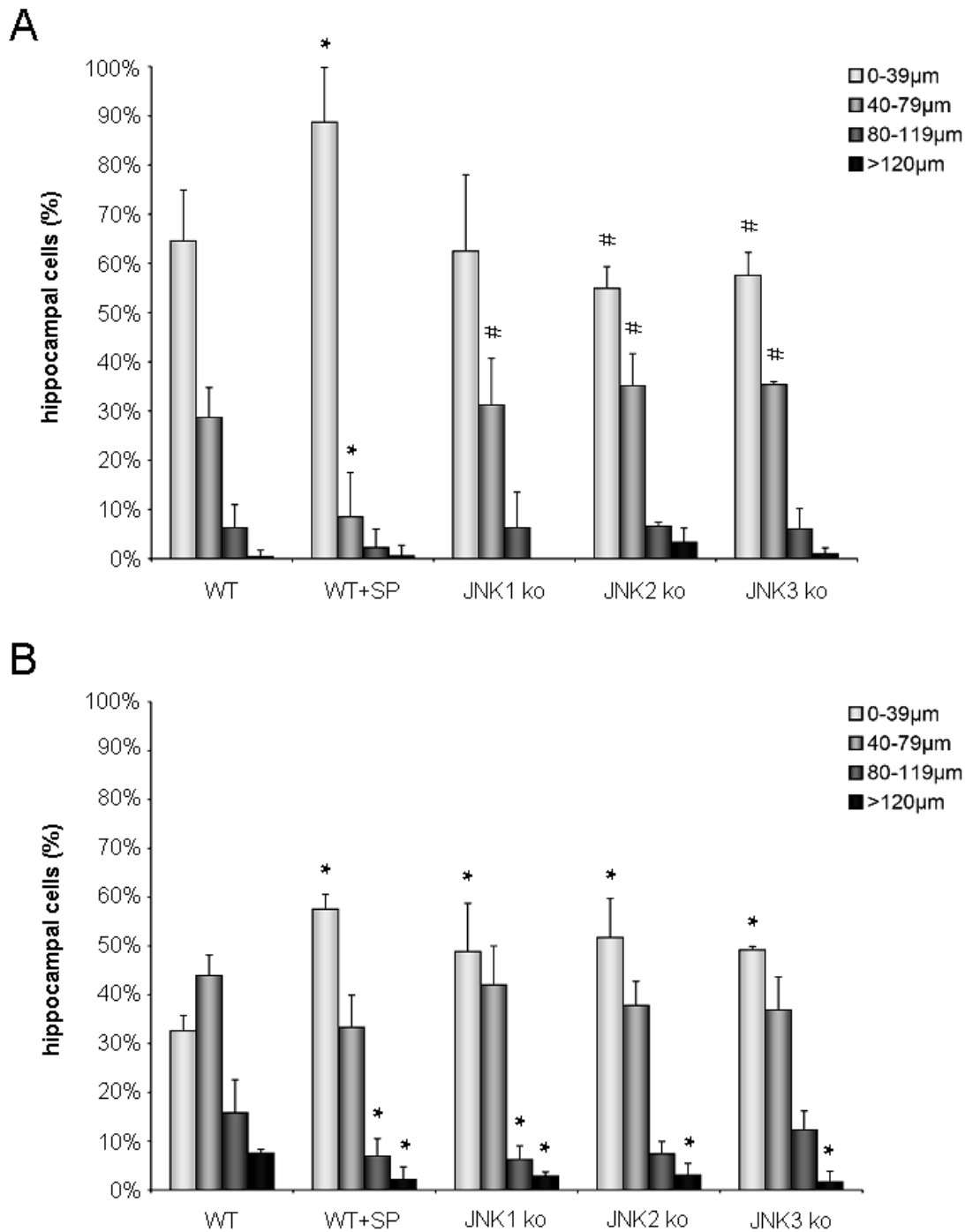


Figure 36. Effects of JNK isoforms and JNK inhibition on neurite elongation

The effect of total JNK inhibition by SP600125 (SP) and knock-out (ko) of specific JNK isoforms on neurite outgrowth of primary mice hippocampal neurons was analyzed compared to a joint group of their corresponding wild types (WT). Cells were grown for 48 h (A) or 6 d (B), and then stained with the neurite marker MAP-2. Neurite lengths were classified into four groups. SP600125 was applied immediately after the explantation.

Abbreviations: JNK (c-Jun N-terminal kinase), ko (knock-out), MAP-2 (microtubule associated protein-2), SP (SP600125), WT (wildtype).

* $P < 0.05$ (compared to corresponding WT group), # $P < 0.05$ (compared to WT+SP)

Statistical significances were calculated using Kruskal-Wallis and Mann-Whitney U test. Data are presented as mean \pm standard deviation. N = 3 (minimum).

After 2 d, wt controls were composed of $65\% \pm 10\%$ neurites shorter than $40\ \mu\text{m}$, $29\% \pm 6\%$ neurites of $40 - 79\ \mu\text{m}$ length, $6\% \pm 5\%$ neurites of $80 - 119\ \mu\text{m}$ length, and almost none longer than $120\ \mu\text{m}$, yet. Inhibition of *total*-JNK, as achieved by SP600125, lead to a further increase within the largest group ($<40\ \mu\text{m}$; $89\% \pm 11\%$, $P < 0.05$), accompanied by the decline in groups of longer neurites ($40 - 89\ \mu\text{m}$; $9\% \pm 9\%$, $P < 0.05$). In this early stage, none of the cultures from isoform-specific knock-out mice displayed differences as compared to controls, only the simultaneous inhibition of all isoforms had an effect (*Figure 36A*).

When cultivated for 6 d in total, wt hippocampal neurons comprised $33\% \pm 3\%$ neurites shorter than $40\ \mu\text{m}$, $44\% \pm 4\%$ neurites of $40 - 79\ \mu\text{m}$ length, $16\% \pm 7\%$ neurites of $80 - 119\ \mu\text{m}$ length, and $8\% \pm 1\%$ longer than $120\ \mu\text{m}$. The SP inhibitor substantially attenuated neurite elongation as demonstrated by less numbers of neurites longer than $80\ \mu\text{m}$ and $120\ \mu\text{m}$ ($7\% \pm 4\%$, $P < 0.05$ and $2\% \pm 3\%$, $P < 0.05$, respectively) and an increase in the group with shortest neurites ($58\% \pm 3\%$, $P < 0.05$). This time, each JNK isoform specific knock-out alone resulted in a similar pattern as that of total JNK inhibition (as statistical analysis revealed no differences between these groups). However, regarding the class of $0 - 39\ \mu\text{m}$ neurites, none of the knock-outs could level with the value acquired by SP incubation ($58\% \pm 3\%$ (SP) versus $49\% \pm 10\%$ (JNK1), $52\% \pm 8\%$ (JNK2) or $49\% \pm 1\%$ (JNK3)). Additionally, JNK2 and JNK3 ko cells did not show a significant decrease in the numbers of neurites between $80\ \mu\text{m}$ and $120\ \mu\text{m}$ compared to controls, as it was the case for total JNK inhibition and elimination of the isoform 1 (*Figure 36B*).

Taken together, JNKs are needed for neurite outgrowth *in vitro*. Hippocampal neurons in culture do not depend on a single JNK isoform for their neurite elongation, although JNK1 shows a slightly greater influence. However, the attenuation of neurite outgrowth by total JNK inhibition is much more prominent.

5. DISCUSSION

In the present thesis we sought to investigate the pathological events mediated by the toxin 6-hydroxydopamine (6-OHDA), a model substance to induce PD-like symptoms *in vivo* and *in vitro*. We assessed when and to what extent PC12 cells die following the administration of 6-OHDA. We analyzed the redox status over 24 h, measuring reactive oxygen species (ROS) by rather compartment-specific fluorescent dyes, and checked the integrity of the mitochondrial membrane potential ($\Delta\Psi_M$). Mitochondria are the most relevant sites of ROS generation, especially when $\Delta\Psi_M$ is disrupted. The loss of mitochondrial integrity leads to release of certain pro-apoptotic proteins into the cytosol, and cell death signaling via caspases reaches a point of no return. We therefore also measured the levels of cytochrome c, which is an important constituent of the mitochondrial respiratory chain, but induces cell death when in contact with the cytosol by forming the apoptosis protease activating factor-1 (APAF-1). Filling the gap between oxidative stress and mitochondria-mediated cellular death, we investigated the role of c-Jun N-terminal stress kinases (JNK). There are numerous reports addressing a role to JNK-induced release of pro-apoptotic factors from mitochondria (see below). Thus, we looked at the isoform-specific expression of JNK in isolated PC12 cell mitochondria, but also in the nucleus where JNK is supposed activate a variety of transcription-factors, including AP-1 and c-Jun. Results from this thesis demonstrate a role of JNK isoform 2 (JNK2) in the vicinity of mitochondria. The inhibition of JNK protected PC12 from events following downstream of/after JNK activation, however, it did not exert any effect on 6-OHDA-induced ROS. Instead, four antioxidants (methysticin, luteolin, resveratrol and *tert*-butylhydroquinone (*t*BHQ)).

5.1 6-OHDA-induced cell death

Previous studies showed that 6-OHDA induces apoptosis in various model organisms. Among these were hemiparkinsonian rats, with injection to the median forebrain (He *et al.*, 2000), the striatum (Mladenovic *et al.*, 2004), and the substantia nigra (Jeon *et al.*, 1999), as well as different cell types, including the rat pheocromocytoma PC12 cells (Walkinshaw and Waters, 1994; Blum *et al.*, 1997; Ochu *et al.*, 1998; Takai *et al.*, 1998; Hanrott *et al.*, 2006), the human neuroblastoma SH-SY5Y cell line (von Coelln *et al.*, 2001; Jordan *et al.*, 2004), the dopaminergic (DA) cell line MN9D, a fusion of ventral mesencephalic and neuroblastoma cells of human origin (Choi *et al.*, 1999; Oh *et al.*, 1998), and primary DA neurons from rats

and mice (Han *et al.*, 2003; Lotharius *et al.*, 1999). DNA fragmentation and chromatin condensation, caspase activation, p53- and bax expression, PARP cleavage and the release of cytochrome c from mitochondria were taken as evidence for apoptotic processes in these models. In contrast to the low molar range (10-50 μM), doses of 100 μM 6-OHDA and more result in distinct features of necrotic cell death, e.g. loss of membrane integrity (Ochu *et al.*, 1998). The discrete signaling cascades of the apoptotic machinery remain the targets for pharmacists to stop PD in patients.

In the present thesis, 6-OHDA concentrations ranged from 10 μM to 200 μM . PC12 cell death was assessed by fluorescence of the apoptotic marker Annexin V and propidium iodide (PI), a marker for necrosis, in the flow cytometer. Following our protocol (see section 3.3.7.4), it was not possible to point out a specific dividing rule at what concentration necrosis, as measured by PI, would occur. In all 6-OHDA samples a small proportion of PI fluorescent events, though with an increasing tendency towards higher concentrations, was detectable (data not shown).

We propose that a loss of membrane integrity, which is necessary for PI to be detected in the flow cytometer, is an integral part of 6-OHDA mediated toxic events. Only few studies have analyzed direct effects of 6-OHDA to the cell membrane. Berretta *et al.* found that 6-OHDA rapidly damages the cell membrane, with special regard to distal dendrites of SNpc neurons. Blockade of the dopamine transporter (DAT) did not prevent membrane disturbances (Berretta *et al.*, 2005). However, the specificity of 6-OHDA towards dopaminergic cells via the uptake by the DAT is controversial. Due to the similarity to dopamine there is no doubt that 6-OHDA can be taken up by the DAT. On the other hand, there are several studies pointing out that 6-OHDA toxicity cannot be prevented by inhibition of the uptake (Abad *et al.*, 1995; Blum *et al.*, 2000; Hanrott *et al.*, 2006), and that 6-OHDA mediated cell death is not restricted to DA neurons (Blum *et al.*, 2000; Dodel *et al.*, 1999; Lotharius *et al.*, 1999; Seitz *et al.*, 2000). Additionally, the administration of catalase, an enzyme of molecular weight so large that it cannot enter the cell under normal circumstances, strongly protects against the toxin (Abad *et al.*, 1995; Yamada *et al.*, 1997; Hanrott *et al.*, 2006).

In our cell model, incubation with 50 μM 6-OHDA leads to a significant loss of viability after 24 h ($72\% \pm 6\%$ of vehicle-treated controls). Comparisons with other published data of 6-OHDA toxicity in cell models can only be drawn with caution as to the concentration and

the cell loss. Many studies analyze other apoptotic markers than Annexin V/PI (*e.g.* tyrosine hydroxylase↓, TUNEL, MTT assay, trypan blue staining, etc.), and different apoptotic markers give different results (Kylarová *et al.*, 2002). 6-OHDA is an agent that is susceptible to autoxidation, so it is very important to know how it was applied and stored. Unfortunately, this information is often unsatisfactory. Additionally, many researchers tend to use 100 μM 6-OHDA or even more. The effect of the toxin depends also very much on the cell type due to their different origins, culture conditions and expression patterns. There are even differences between younger and older cells in culture from the same cell line, and between controls and cells transfected with a vehicle. However, 6-OHDA-induced cell death has been analyzed by Annexin V/PI staining in the flow cytometer by three research groups, Salinas *et al.* found 12% Annexin V-positive PC12 cells after 6 h of 40 μM 6-OHDA (Salinas *et al.*, 2003), Ebert *et al.* analyzed MN9D cells and saw 35% apoptotic neurons four hours after 100 μM 6-OHDA (Ebert *et al.*, 2005), and Guo *et al.* made a very thorough time-line and concentration analysis of 6-OHDA in SH-SY5Y cells, with $81\% \pm 8\%$ surviving following 50 μM 6-OHDA for 24 h (Guo *et al.*, 2005). The results of time- and concentration-dependency of cell death induced by 6-OHDA in this thesis are generally in line with results obtained by Guo *et al.*, despite the fact that they investigated another cell line. Other data from PC12 cells (mainly MTT viability assays) that show 6-OHDA toxicity in a concentration-dependent and time-resolved manner are congruent with our findings (Hanrott *et al.*, 2006; Saito *et al.*, 2007).

5.2 6-OHDA toxicity to mitochondria

From the variety of apoptotic pathways, our data provides evidence that mitochondria are a target of 6-OHDA toxicity. The release of mitochondrial cytochrome c into the cytosol is the key event of the intrinsic pathway (Liu *et al.*, 1996; Kantrow and Piantadosi, 1997; Kluck *et al.*, 1997). Thereafter, this has been named the “point of no return” in the apoptotic process, since cytochrome c is a constituent of the apoptosome that activates caspases (Li *et al.*, 1997; Zou *et al.*, 1999; Kroemer and Reed, 2000). However, cyt c is abundant in the mitochondrial intermembrane space (Forman and Azzi, 1997), and there is no evidence, that the pool of cyt c, which resides in the cristae as a participant in the respiratory chain, is released in early apoptosis (Waterhouse *et al.*, 2001). It seems that this pool requires more drastic remodelling of the mitochondrial structure, which eventually occurs in the course of mitochondrial damage, leading to the loss of $\Delta\Psi_M$ (Scorrano *et al.*, 2002). We investigated the mitochondrial

membrane potential in our model, and found that 6-OHDA induced a clear decline after 8 h, which is coinciding with the release of cytochrome c into the cytosol (25 μ M). Low concentrations of 6-OHDA (10 μ M) did not have an effect, $\Delta\Psi_M$ dropped at the 8 hour time point but then was stabilized following medium doses (25 μ M, 50 μ M), whereas high level 6-OHDA incubation led to a consecutive decline over the investigation period. These results can be explained by studies that describe the mitochondria as a checkpoint, that is able to compensate and intensify death signals, dependent on the strength and duration of the insult (Nicholls and Budd, 2000).

In isolated mice brain mitochondria 6-OHDA even promotes a faster and more profound disruption of $\Delta\Psi_M$. Possible reasons for these findings could be that cytosolic 6-OHDA- and ROS-detoxifying enzymes are missing in the mitochondrial fractions, or that 6-OHDA/ROS exert direct membrane-disturbing activities which now fully target to mitochondrial membranes alone, and not to the cell membrane as proposed by early PI accumulation (see above) or to vesicular membranes. Not only is the cytosol equipped with strong antioxidant enzymes and radical scavengers compared to the mitochondrial matrix or the intermembrane space, but mitochondria are naturally more exposed to oxygen radicals. Particularly isolated mitochondria in a non-optimal environment are more vulnerable. However, the results underline the strong toxicity of 6-OHDA to mitochondria.

In experiments to analyze its effects on $\Delta\Psi_M$ in a continuous manner, 6-OHDA was administered to PC12 cells and isolated mice brain mitochondria. Surprisingly, we observed an immediate $\Delta\Psi_M$ lowering effect. Generally, 6-OHDA has been shown to impair $\Delta\Psi_M$ in preparations of isolated rat brain mitochondria (Lee *et al.*, 2002). In that study, safranin O was used as a, however, there are no studies that used the dye JC-1 in the fluorometer to analyze isolated mice brain mitochondria after 6-OHDA incubation. Our results from isolated mitochondria are not in contrast to studies using the flow cytometer, since the time points are not overlapping. Furthermore, in the experiments with isolated mitochondria in the spectrofluorometer, complex I is passed by inhibition by rotenone and providing complex II with the natural substrate succinate. So one could speculate that this immediate disruption is due to an inhibition of complex II, III or IV of the respiratory chain, an oxidative attack to the mitochondrial membrane followed by ROS scavenging, or a direct interaction of 6-OHDA with the red fluorescent J-aggregates in the mitochondrial matrix, resulting in the transient dissociation to green monomers. However, the acidic properties of 6-OHDA are in contrast to

this theory, because J-aggregates form in the presence of protons (Cossariza *et al.*, 1996). We hypothesize, that an intracellularly produced, unknown metabolite or peroxide from autoxidation/metabolism processes targets complex I, or 6-OHDA/ROS oxidize essential proteins of the mitochondrial membrane leading to the decrease of $\Delta\Psi_M$.

5.3 Profound and early oxidative stress in PC12 cells, but not isolated mitochondria following 6-OHDA

Oxidative stress has been documented throughout the years of research in PD (Götz *et al.*, 1990; Jenner, 2003). From the model toxins investigated, 6-OHDA exerts the highest impact of oxidative stress, whereas other toxins that target the respiratory chain (*e.g.* MPP⁺) show less oxidative burden (Choi *et al.*, 1999). In agreement with this, our results show that MPP⁺ could only increase ROS levels when administered in a concentration twice as high as compared with 6-OHDA. The latter induces ROS production in virtually all models, *in vivo* (Perumal *et al.*, 1989; Kumar *et al.*, 1995) as well as *in vitro* (Decker *et al.*, 1993; Abad *et al.*, 1995; Choi *et al.*, 1999; Lotharius *et al.*, 1999; Hanrott *et al.*, 2006). Also, the recent descriptions of a genetic predisposition leading to higher susceptibility of PD patients towards oxidative stress has strengthened the importance of ROS in the development of the disease (Zimprich *et al.*, 2004).

ROS production induced by 6-OHDA originates from the following three main sources: (I) ROS generation by autoxidation, (II) H₂O₂ generation after deamination by monoamine oxidase (MAO), and/or (III) direct inhibition of the mitochondrial respiratory chain (for review see Blum *et al.*, 2001a).

This study demonstrates that ROS cannot be generated by 6-OHDA concentrations lower than 200 μ M in isolated mice brain mitochondria. The uncoupling properties of 6-OHDA cannot play a role here because they have been described to come into play primarily in very high concentrations of 6-OHDA (Brand, 2000; Thakar and Hassan, 1988). However, the relevance of ROS generation following 6-OHDA is not of question (see above). Our results show that in whole PC12 cells oxidative stress is an early and dominant mediator of 6-OHDA toxicity. A lot of studies have used high concentrations of 6-OHDA in their systems (*e.g.* 100 - 200 μ M). Here we show that doses of 50 μ M, 100 μ M and 200 μ M are comparable after an incubation

of 4 h regarding the elevation of ROS levels. The observation of ROS production over time revealed a great increase within the first 2 h, which was followed by a second boost between 8 and 16 h of treatment. A very much similar pattern has been described by Choi *et al.* in MN9D cells using 100 μ M 6-OHDA (Choi *et al.*, 1999).

The major intracellular source of ROS are mitochondria. We were interested where the first ROS are generated in our model. In comparison between mitochondrial and cytosolic ROS-sensitive dyes our data point to a major contribution of mitochondrially originated ROS during the early boost. The specificity of ROS-sensitive dyes, however, is still a matter of debate, so the argument of mitochondrial ROS generation might require additional proof. In fact, a number of studies have demonstrated that 6-OHDA does not induce toxicity either by direct mitochondrial inhibition or by enzymatic deamination by MAO, but via an extracellular mechanism (Blum *et al.*, 2000; Hanrott *et al.*, 2006; Soto-Otero *et al.*, 2000). Inhibitors of dopamine and noradrenaline transporters failed to prevent PC12 cells from ROS generation, cytochrome c release and cell death (Hanrott *et al.*, 2006; Saito *et al.*, 2007).

But also extracellular H₂O₂ generation by autoxidation alone cannot explain the mechanism of 6-OHDA toxicity, since hydrogen peroxide degradation by catalase does not result in full protection (Saito *et al.*, 2007). When adding 6-OHDA to our preparations of isolated mitochondria, the autoxidation process, which is still likely to occur, does not induce ROS from mitochondria. Among the autoxidation products are H₂O₂ and cyclization products (semi-quinones, quinones, aminochromes, melanin). From all known dopamine analogues 6-OHDA is most susceptible to autoxidation (Izumi *et al.*, 2005). Autoxidation of 100 μ M 6-OHDA occurs rapidly, the toxin is completely oxidized within 3.5 h when given to PC12 cells (Blum *et al.*, 2000). In the human disease, however, 6-OHDA is a very rare metabolite of dopamine, addressing a high impact of oxidative stress to dopamine autoxidation itself. Nevertheless, autoxidation products of dopamine and also 6-OHDA play a major role in PD cell models (Arriagada *et al.*, 2004; Asanuma *et al.*, 2004). High toxin concentrations administered to isolated mitochondria do result in ROS production also in our system. We hypothesize that sufficiently high concentrations can induce ROS generation, low level 6-OHDA incubation may be intensified by cell membrane or cytosolic compounds, which are lost in mitochondrial homogenates. Dopamine (DA) and DA analogues-toxifying enzymes COX-2 (Tyurina *et al.*, 2006), tyrosine hydroxylase (Arriagada *et al.*, 2004) and cytochrome P450 (Bernhardt *et al.*, 1996) have been addressed a role in PD pathology. To date, the

intermediate products *p*-quinone and the highly reactive leucoaminochrome radical from the metabolic pathway target cellular vital functions, and pose a high oxidative threat to essential proteins (Watanabe and Forman, 2003). A facilitated conversion to the end-product melanin could thereby provide some protection, though melanin complexes iron that in turn can increase the oxidative burden (Izumi *et al.*, 2005).

Our findings lead to the conclusion that (I) 6-OHDA toxicity cannot only be dependent on autoxidation, as suggested also by Saito *et al.* (Saito *et al.*, 2007), (II) MAO activity in the outer mitochondrial membrane may only be relevant in ROS production following higher 6-OHDA concentrations (Hanrott *et al.*, 2006; Soto-Otero *et al.*, 2000), and (III) there is also no evidence for a direct effect of 6-OHDA on the respiratory chain in concentrations less than 200 μ M (conflicting data on the relevance of complex I inhibition from Glinka *et al.*, 1996 and Storch *et al.*, 2000). An explanation could be that a metabolite of 6-OHDA is responsible for targeting complex I, that would be generated intracellularly and not extracellularly. During our studies with the toxin, we have seen that PC12 cells do not undergo apoptosis if 6-OHDA is administered in its oxidized form (data not shown; see also Pedrosa *et al.*, 2002), and reports point out, that H₂O₂ alone does not fully represent 6-OHDA-induced pathological events (Saito *et al.*, 2007).

5.4 6-OHDA-induced JNK2 activation and translocation to mitochondria

Toxic features of 6-OHDA involve the activation of c-Jun N-terminal kinases in a variety of cell types, including the dopaminergic MN9D cell line (Choi *et al.*, 1999), and SHSY-5Y cells (Ha *et al.*, 2003). The inhibition of JNK is protective against caspase activation and apoptosis induced by cytotoxic agents in Jurkat cells (Krilleke *et al.*, 2003), rat intestinal (Bhattacharya *et al.*, 2003) and human colon cancer cells (Xiao and Liu, 2003). Furthermore, JNK are strong activators of mitochondrial stress and the release of mitochondrial apoptogenic proteins (Bhattacharya *et al.*, 2003; Blum *et al.*, 2001a; Krilleke *et al.*, 2003; Okuno *et al.*, 2004; Tournier *et al.*, 2000; for review see Waetzig and Herdegen, 2005). The relevance of JNK inhibition for PD has been demonstrated for various *in vitro* and *in vivo* models of the disease (for reviews see Wang *et al.*, 2004; Kuan and Burke, 2005; Borsello and Forloni, 2007). However, inhibitors like SP600125 that target the common activation site of all JNK isoforms have failed in early clinical studies (Waldmeier *et al.*, 2006).

Nonetheless, isoform-specific inhibition, small peptide drugs that bind outside the ATP-docking site, or upstream kinase inhibition may still provide breakthrough potential in pharmacological intervention of apoptotic processes (Barr *et al.*, 2002; Kuan and Burke, 2005).

6-OHDA-induced activation of JNK in PC12 mitochondria was first described by our group (Eminel *et al.*, 2004). PC12 cells are a cell line of peripheral origin, so only JNK1 and 2 are expressed (Butterfield *et al.*, 1999; Mielke *et al.*, 2000). Since the JNK isoform specific antibodies on the market allow only for differentiation between JNK1 and JNK2/3 (Coffey *et al.*, 2002), this model allows us to detect specific changes of JNK1 and 2. Several studies have proposed that JNK effects on mitochondria would need JNK in close vicinity to this organelle, before Kharbanda *et al.* actually found JNK present and increasing in mitochondrial fractions following ionizing radiation (Kharbanda *et al.*, 2000). We were interested if JNK would also be detectable in isolated mitochondria from PC12 cells, if this pool of JNK was reflected by a specific isoform, and if JNK isoform levels reacted substantially and specifically to 6-OHDA treatment.

Under basal conditions, JNK are found in mitochondrial preparations. Our results attribute this pool to consist mainly of JNK1. Mitochondria-associated JNK was strongly activated in response to 6-OHDA within 4 h and continued to be active up to 24 h. This activation was accompanied by a translocation of JNK2 into the nucleus and to the mitochondria. Since the expression of phosphorylated JNK cannot be determined in an isoform-specific way, we conclude by the timely overlap of simultaneous activation and JNK2 increase in mitochondrial fractions, that JNK2 is the isoform that is mainly phosphorylated and is responsible for further signal transduction in this organelle. Transfection of PC12 cells with a dominant-negative mutant JNK2 (dnJNK2) produced an altered gene product, that acted antagonistically to the wild-type allele, and reduced the pool of phosphorylated JNK in the nucleus after stimulation with 6-OHDA and strongly reduced the 6-OHDA-induced translocation of endogenous JNK2 to the nucleus while dnJNK1 had not such effect (data from our group, Eminel *et al.*, 2004). Similarly, JNK inhibitor SP600125 attenuated the translocation of JNK2, but not JNK1 into the nucleus following 6-OHDA treatment (Eminel *et al.*, 2004). The translocation of JNK2 to the mitochondria supports the notion that the assembly of a selective JNK2 signalosome propagates the mitochondrial pathology. A central role of JNK2, but not JNK1, for cellular degeneration was seen in fibroblasts where JNK2

mediates tumor necrosis factor- α -induced cell death (Dietrich *et al.*, 2004). Similarly, JNK2/3 have been addressed an impact for neuronal stress in primary cerebellar granule neurons (Coffee *et al.*, 2002). Recently, it was shown that in various cell types including fibroblasts, erythroblasts and hepatocytes, JNK2 deficiency leads to increased cellular proliferation (Sabapathy and Wagner, 2004). Importantly, SP600125, which prevents the stress-induced alterations in the membrane potential (Sanna *et al.*, 2002), blocks the mitochondrial translocation of JNK2, but not JNK1. This finding suggests that intracellular distribution of JNK2 depends on its activation and, by a positive feedback mechanism, on activated upstream kinases (Holtz *et al.*, 2003). So altogether, our findings suggest that JNK2 is the active JNK isoform which mediates the neurodegenerative effects of 6-OHDA *in vitro*.

5.5 Intracellular JNK pools

The presence of JNK1 did not change in mitochondria, but was amplified in cytosol and nucleus upon the administration of 50 μ M 6-OHDA. JNK2 levels remained low in cytosol and nucleus. Cell stress signaling, *e.g.* by JNK, results in death and differentiation (as discussed below). Therefore, specific actions should be mediated by individual isoforms in specific parts of the cell. The intracellular localization may be the ultimately critical factor. For example, JNK1 is an important mediator of insulin resistance associated with obesity (Hirosumi *et al.*, 2002; Kaneto *et al.*, 2004), but it is also indispensable for the intact cytoarchitecture of the brain (Chang *et al.*, 2003). JNK2 is recruited by apoptotic stimuli (Coffee *et al.*, 2002; Dietrich *et al.*, 2004), but it is also important for the coordinated differentiation of, for example, activated immune cells (Jaeschke *et al.*, 2004), and for brain development (Kuan *et al.*, 1999). JNK3, in particular, is considered to be a potent effector of neuronal death (Yang *et al.*, 1997; Hunot *et al.*, 2004; Brecht *et al.*, 2005). However, as proof-of-principle of the context-specific functions of JNK variants, a splice variant of JNK3 mediates neurite outgrowth in addition to stress-induced apoptosis in PC12 cells (Waetzig and Herdegen, 2003).

5.6 Upstream and downstream effectors of JNK signaling at the mitochondria

The specific mitochondrial translocation of JNK2, but not JNK1, raises the question which signaling pathways control the JNK translocation to and/or the JNK activation at the mitochondria. In leukaemia cells, the phosphorylation of JNK is a prerequisite for translocation which is supported by the absence of JNK2 in the mitochondria (Ito *et al.*, 2001). In our model, MKK4 and JIP-1 are localized at the mitochondria, whereas MKK7 was not detectable in the mitochondrial fraction. This points to a specific JNK pathway in mitochondrial pathology. MKK4 was previously found in mitochondrial fractions from cardiomyocytes (Okuno *et al.*, 2004), whereas the presence of JIP-1 and the absence of MKK7 are novel observations. The absence of MKK7 in mitochondrial preparations is also comprehensible when considering findings, that the MKK7/JNK pathway is responsible for neuritogenesis and neurite regrowth after injury (Hidding *et al.*, 2005; Coffee *et al.*, 2000). The scaffold protein JIP-1 forms complexes with JNKs and selected members of the upstream phosphorylating kinases (Dickens *et al.*, 1997; Whitmarsh *et al.*, 1998). It is not a counter-argument against a translocation of the MKK4-JNK2-JIP complex to mitochondria that JIP levels do not obviously change in mitochondrial fractions, but are kept in balance. In fact, JIPs have been found to direct JNK and their upstream kinases to different compartments of the cell by associating with microtubules (Goldstein, 2001; Verhey *et al.*, 2001). We believe that JNK2 activation in the cytosol, and/or effects on anchor proteins would target the signalosome to the mitochondria.

Our data sets the release of cytochrome c downstream of JNK activation and translocation of JNK2 to mitochondria, since this event can be inhibited by SP600125. What may be the connection between JNK and cytochrome c release? The proapoptotic Bax resides in the cytosol due to the binding to an isoform of the 14-3-3 anchor protein (Nomura *et al.*, 2003). Upon phosphorylation of this cytosolic anchor by phospho-JNK the complex dissociates and Bax translocates to the mitochondria where it forms channels that would allow cytochrome c to leave the intermembrane space and establish the apoptosome leading to cell death (Tsuruta *et al.*, 2004; Nomura *et al.*, 2003; Putcha *et al.*, 1999). The JNK inhibitor SP600125 prevented bax translocation to mitochondria (Tsuruta *et al.*, 2004). Before that study, there were already publications showing that JNK regulates Bax translocation via the phosphorylation of Bim after trophic factor withdrawal (Lei and Davis, 2003; Putcha *et al.*, 2003). In contrast to these

DISCUSSION

results, Tsuruta *et al.* saw no effect of either SP600125 or the overexpression of a constitutively active JNK on the activation of Bim (Tsuruta *et al.*, 2004). Following 6-OHDA our group also saw no increase in bim mRNA levels, but the inhibition of JNK by dnJNK2 reduced bim expression (Eminel *et al.*, 2004). These results can not ultimately determine the role of Bim in 6-OHDA-induced, JNK-mediated cell death. However, bax is strongly activated by the administration of 6-OHDA to PC12 cells (Blum *et al.*, 1997), and bax pores could lead to the release of cytochrome c, that we found subsequently to JNK activation and translocation.

JNK activity also targets the group of anti-apoptotic bcl-2 family members, Bcl-2 and Bcl-XL. These proteins locate in mitochondrial, nuclear and ER membranes (Blagosklonny, 2001). Their main function is to prevent the assembly of bax proteins and the formation of a pore, thereby protecting mitochondria from mitochondrial membrane disruption and release of apoptogenic factors (Gross *et al.*, 1998; Nomura *et al.*, 1999; Yang *et al.*, 1995). JNK phosphorylation of Bcl-2 and Bcl-XL leads to a decrease in the levels of Bax heterodimers with Bcl-2 or Bcl-XL, and promotes the formation of potentially toxic bax homodimers, which form bax pores channeling *e.g.* cytochrome c into the cytosol (Kharbanda *et al.*, 2000). Cyt c levels became elevated following 6-OHDA treatment in our model way after the activation of JNK and translocation of JNK2 to mitochondria. So rather the inhibition of mitochondrially residing anti-apoptotic Bcl-2 and Bcl-XL than the cytosolic activation of Bax serves as an explanation of JNK2 apoptotic functions in mitochondrial preparations of PC12 cells.

What happens upstream of JNK2 activation and translocation to the mitochondria? Our data provides evidence that from the two upstream kinases of JNK (Ip and Davis, 1998) only MKK4 is involved. The activation of MKK4 is controlled by MEKK1/4, the mixed-lineage kinases (MLK) 2/3 and apoptosis signal-regulating kinase 1 (ASK1) (for review see Schlesinger *et al.*, 1998; Chang and Karin, 2003). Very recently, Chen *et al.* described the protective effects of adenoviral transfer of dominant-negative constructs from the dual-leucine zipper kinase (DLK) of the MEKK family after 6-OHDA lesions in mice (Chen *et al.*, 2008). The role of MLK3 has been investigated in mice and rats treated with 6-OHDA, however, results are conflicting (Chen *et al.*, 2008; Pan *et al.*, 2007). ASK1 is a strong regulator of MKKs and JNKs. Ouyang *et al.* found that inhibition of ASK1 activity by siRNA or by overexpression of a kinase-dead mutant protected SHSY-5Y cells from 2 h incubation of 100 μ M 6-OHDA (Ouyang *et al.*, 2006). The authors also showed that ROS scavenging

reduces phosphorylation of ASK1. This sheds new light on the mechanism of JNK activation by ROS (Crossthwaite *et al.*, 2002; Ouyang *et al.*, 2006).

5.7 Time course of pathological events mediated by 6-OHDA

Our studies aimed at giving an overview of events in one model, that occur due to the treatment with 6-OHDA and may shed more light on the mechanism by which the toxin mediates these actions. We used mainly 25 μM or 50 μM 6-OHDA, which is lower than the concentration used in most other studies, while investigating the following parameters: cell death, ROS production, disturbances of the mitochondrial membrane potential, cytochrome c release, JNK activation and localization.

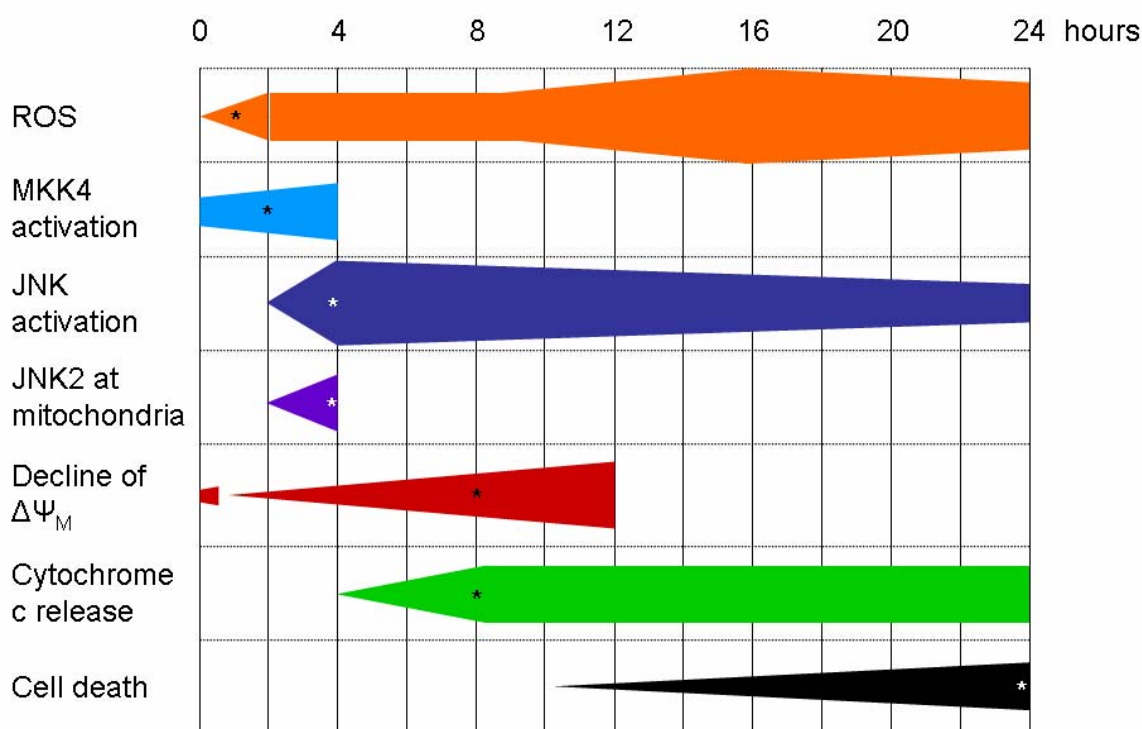


Figure 37. Time course of events in 6-OHDA mediated cell death

Time course depicting the parameters analyzed in this study following the administration of 6-OHDA. ROS production is increased first, then the upstream kinase MKK4 appears activated at mitochondria, followed by phosphorylated JNK, and an increase of JNK2 in mitochondrial preparations. Sub-sequently, the mitochondrial membrane potential is disrupted, and cytochrome c is released. Cell death occurs at around 24 h, after ROS have peaked. The * denotes the first significant change compared to vehicle-treated controls.

Abbreviations: $\Delta\Psi_M$ (mitochondrial membrane potential), JNK (c-Jun N-terminal kinase), MKK4 (mitogen-activated protein kinase kinase 4), ROS (reactive oxygen species).

DISCUSSION

Our results demonstrate a profound and early increase of reactive oxygen species (60 min), ROS levels stabilize between 4 and 8 hours, then a second significant increase can be observed over a period of 8 hours (*Figure 37*).

The source for ROS generated within 60 min appears to be mitochondrial. So the mitochondrial pathology is already ongoing, when the upstream kinase MKK4 and JNK are activated (within 4 hours), and levels of the JNK isoform 2 increase in mitochondrial fractions by the same time. We can only speculate here, how ROS activate MKK4 and JNKs, *e.g.* via ASK1 (Ouyang *et al.*, 2006). The activation, translocation to mitochondria and the pore formation of bax, mediated by JNK and ROS (Okuno *et al.*, 2004; Putcha *et al.*, 2003; Tsuruta *et al.*, 2004), serves as an explanation to the subsequent release of cytochrome c (supposedly through bax pores). This is accompanied by a disruption of the mitochondrial membrane potential when incubated with 6-OHDA for 8 hours. At the 16 hour time point ROS peak; in the following 8 hours PC12 cells start to die, by about 30% (data from 50 μ M 6-OHDA treatment).

5.8 JNK inhibition and protection from oxidative stress

JNK inhibition is protective against PC12 neuronal death (Fujita *et al.*, 2006; Ito *et al.*, 2006; Marques *et al.*, 2003) and is regarded as a therapeutic strategy in PD (Kuan and Burke, 2005), as well as against the release of cytochrome c from mitochondria, as shown by us and other groups (Eminel *et al.*, 2004; Guan *et al.*, 2006; Krilleke *et al.*, 2003). Furthermore, we could demonstrate that SP600125 inhibited also the activation of the JNK upstream kinase MKK4 plus the translocation of JNK2 to mitochondria. However, JNK inhibition did at no concentration prevent from 6-OHDA-induced ROS elevation in 4 hours. Since SP600125 does not exert any antioxidant features itself, this shows distinctly that ROS are upstream of JNK activation and translocation to mitochondria. The JNK inhibitor is not able to target JNK isoform-specifically, so we need to accept that the protective effects could be counteracted by suppression of physiological features of JNK, as JNK inhibition also dramatically impairs neurite outgrowth of hippocampal neurons (as discussed below).

Therefore, we tested the kavalactone methysticin, the flavon luteolin and the phytoalexin resveratrol, as well as *tert*-butylhydroquinone (*t*BHQ), which has been already shown to

protect SHSY-5Y cells against 6-OHDA-induced ROS production, JNK activation and cell death (Hara *et al.*, 2003). Additionally to radical scavenging properties the authors described the activation of the antioxidant response element (ARE), that regulates the expression of enzymes relevant in the cellular defense system. Just recently, our group also discovered that luteolin activates protective genes via the Nrf-2-ARE pathway (Wruck *et al.*, 2007). The results of this thesis show that preincubation with all four protectors prevented the rise of ROS induced by 50 μ M 6-OHDA. Even though the antioxidants were not present anymore when the toxin was given (due to washing steps) and the samples were analyzed, they were protective against oxidative stress. We propose a similar lasting effect on cellular defense mechanisms, provided by the preincubation with these compounds, as our group could already demonstrate for luteolin (Wruck *et al.*, 2007). In comparison, incubation of PC12 cells with methysticin, luteolin and *t*BHQ protects from ROS generation induced by the neurotoxicant MPP⁺ (100 μ M). Resveratrol does not confer any protection from MPP⁺-induced ROS. However, despite using double the concentration the increase in ROS production after MPP⁺ is little (ca. 20% vs. 40% of 6-OHDA). It has been noted before that oxidative stress is a less relevant part of the toxin's mechanism to induce dopaminergic cell death (Choi *et al.*, 1999; Fall *et al.*, 1999; Wadia *et al.*, 1998). Following MPP⁺ and the precubation with all protectors, their ROS levels did not differ significantly from controls. We conclude that the precubation with methysticin, luteolin, resveratrol and *t*BHQ confers increased cellular protection against oxidative stress induced by 6-OHDA. Furthermore, our results, based on our experimental setup, suggest that it is not only a scavenging effect, but possibly also other pathways such as the activation of the transcription factor Nrf-2 and consequent upregulation of cytoprotective gene products (*e.g.* glutathion synthetase).

5.9 JNK in neuronal death and survival

Therapeutic JNK inhibition may come along with side effects, since up to date, also physiological functions of JNK can not clearly be distinguished from pathological features (for review see Waetzig and Herdegen, 2005). Our investigations addressed the question to which extent JNK stresskinases are involved also in neurite outgrowth, the main morphological feature of neuronal differentiation and repair in the rodent brain.

DISCUSSION

We dissected murine neonatal brains, obtained and cultivated hippocampal neurons, which express all JNK isoforms including JNK3. Inhibition of JNK activity by SP600125 dramatically attenuates the formation of longer neurites after 48 h and 6 d *in vitro*. Primary cell cultures from JNK1 ko, JNK2 ko and JNK3 ko mice revealed that all three JNK isoforms contribute to neurite outgrowth. The JNK1 ko provided the most pronounced impairment and this corresponds to its role during development and for maintenance of the neuronal cytoskeleton (Chang *et al.* 2003; Björkblom *et al.* 2005). Our group has shown in PC12 cells (which are devoid of JNK3) that JNK2, but not JNK1, triggers neurite regrowth following injury (Waetzig and Herdegen, 2005). The analysis of the role of JNK3 for regrowth was complicated by the finding that the absence of JNK3 handicapped the success of keeping these cells in culture. The question remains whether JNK3 deficiency only affects neurite outgrowth and/or primary cell growth and adhesion. In any case, the sensitivity of hippocampal neurons for JNK3 deficiency correlates with the findings that a truncated JNK3 mutant with loss of the activation domain is not compatible with the survival of PC12 cells; importantly, this truncated JNK3 mutation provokes severe neurological symptoms in humans (Shoichet *et al.* 2006). These observations confirm that besides JNK3, JNK2 is involved in physiological and regenerative responses. Total JNK inhibition by SP600125 leaves only about 10% of longer neurites ($> 40 \mu\text{m}$) after 2 days, which is in contrast to controls and knock-out of an individual isoform at that stage (ca. 40% neurites $> 40 \mu\text{m}$). After 6 d in culture, JNK isoforms do not seem to be able to compensate for the lack of one of them anymore. All knock-outs have shorter neurite length as compared with controls. The results of this study account for a profound involvement of JNK in neuronal sprouting with no regards to a specific isoform.

Our microscopical analyses reveal a substantially large pool of JNK1 in the nucleus of control PC12 cells. The intensity of the FITC-marked isoform increases slightly upon stimulation with 6-OHDA, and there was also an increase of JNK2 in the nucleus. The activity of JNK in the nucleus is connected with the pro-apoptotic actions of JNK (Björkblom *et al.*, 2005), and inhibition of JNK activity by SP600125 was reported to increase neurite outgrowth in embryonic cerebellar neurons (Coffey *et al.* 2000). However, JNK activity is the major trigger of neurite outgrowth and regrowth even dominating the role of ERK (Kuan *et al.*, 1999; Sabapathy *et al.*, 1999). And the transcription factor c-Jun, which is mainly but not only activated by JNK in the nucleus, is imperative for the regeneration of axons *in vivo* (Raivich

et al. 2004) and can be linked to outgrowth of axons, dendrites and neurites (Besirli *et al.* 2005; Herdegen *et al.* 1998; Lindwall and Kanje, 2005).

How can JNK signaling selectively activate either neuronal (apoptotic death) or regrowth/regeneration? This dichotomy can not be attributed to individual JNK isoforms, but might be inherent in one JNK isoform (for review see Waetzig and Herdegen, 2005). We conclude that in the highly plastic hippocampal neurons, all JNKs participate in neuritogenesis. In consequence, the search for the side-effect free inhibitor of 'the apoptotic' JNK isoform appears yet to be an illusion which requests different therapeutic strategies against the neurodegenerative impact of JNK (Waetzig and Herdegen, 2005).

5.10 Technical considerations

5.10.1 The PC12 cell model

The rat pheochromocytoma cell line PC12 is widely used to study neurodegeneration and neuronal differentiation *in vitro* (Shafer *et al.*, 1991). Upon stimulation with nerve growth factor (NGF) PC12 cells elongate their processes and display a neuronal phenotype (Greene and Tischler, 1976). In this study we used undifferentiated PC12 cells, because their enzymatic composition and channel expression has been found to be higher in regard to dopamine metabolism (Shafer *et al.*, 1991), more reliable (Woodgate *et al.*, 1999) and experiments with these cells more reproducible. Of note, undifferentiated PC12 cells are more susceptible to toxic stimuli, while NGF is protective to the cells (Salinas *et al.*, 2003; Woodgate *et al.*, 1999).

5.10.2 Preparation of isolated mitochondria

The protocols for the preparation of isolated mitochondria from PC12 cells and mice brains were optimized independently to minimize cytosolic contaminations. Usually, β -actin was present in low-level concentrations even in highly purified mitochondria. This can be explained by the tight connections between mitochondria and the cytoskeleton together with the nature of the isolation method. We consider low-level contamination of mitochondrial preparations with the abundant β -actin inevitable against the background of possible functional damage to the organelle, if the isolation procedure increases with time. However, expression levels of JNK found in mitochondria are higher than could be explained by

DISCUSSION

cytosolic origin, and higher than comparable β -actin expression from the same sample, so that we are certain, that JNK either anchors in the outer mitochondrial membrane, or enters the intermembrane space.

6. REFERENCES

- Abad F, Maroto R, López MG, Sánchez-García P, García AG (1995). Pharmacological protection against the cytotoxicity induced by 6-hydroxydopamine and H₂O₂ in chromaffin cells. *European Journal of Pharmacology*. May 26;293(1):55-64.
- Adler V, Yin Z, Fuchs SY, Benezra M, Rosario L, Tew KD, Pincus MR, Sardana M, Henderson CJ, Wolf CR, Davis RJ, Ronai Z (1999). Regulation of JNK signaling by GSTp. *Annual Reviews of Pharmacology and Toxicology*. 39:67-101.
- Allen RG, Tresini M (2000). Oxidative stress and gene regulation. *Free Radicals in Biology and Medicine*. Feb 1;28(3):463-99.
- Andreyev AY, Fahy B, Fiskum G (1998). Cytochrome c release from brain mitochondria is independent of the mitochondrial permeability transition. *FEBS Letters*. Nov 20;439(3):373-6.
- Aoki H, Kang PM, Hampe J, Yoshimura K, Noma T, Matsuzaki M, Izumo S (2002). Direct activation of mitochondrial apoptosis machinery by c-Jun N-terminal kinase in adult cardiac myocytes. *Journal of Biological Chemistry*. Mar 22;277(12):10244-50.
- Arai H, Schmidt ML, Lee VM, Hurtig HI, Greenberg BD, Adler CH, Trojanowski JQ (1992). Epitope analysis of senile plaque components in the hippocampus of patients with Parkinson's disease. *Neurology*. Jul;42(7):1315-22.
- Arriagada C, Paris I, Sanchez de las Matas MJ, Martinez-Alvarado P, Cardenas S, Castañeda P, Graumann R, Perez-Pastene C, Olea-Azar C, Couve E, Herrero MT, Caviedes P, Segura-Aguilar J (2004). On the neurotoxicity mechanism of leucoaminochrome o-semiquinone radical derived from dopamine oxidation: mitochondria damage, necrosis, and hydroxyl radical formation. *Neurobiological Disorders*. Jul;16(2):468-77.
- Asanuma M, Miyazaki I, Diaz-Corrales FJ, Ogawa N (2004). Quinone formation as dopaminergic neuron-specific oxidative stress in the pathogenesis of sporadic Parkinson's disease and neurotoxin-induced parkinsonism. *Acta Medica Okayama*. Oct;58(5):221-33.
- Backhauss C, Krieglstein J (1992). Extract of kava (*Piper methysticum*) and its methysticin constituents protect brain tissue against ischemic damage in rodents. *European Journal of Pharmacology*. May 14;215(2-3):265-9.
- Ballard PA, Tetrad JW, Langston JW (1985). Permanent human parkinsonism due to 1-methyl-4-phenyl-1,2,3,6-tetrahydropyridine (MPTP): seven cases. *Neurology*. Jul;35(7):949-56.
- Barr RK, Bogoyevitch MA (2001). The c-Jun N-terminal protein kinase family of mitogen-activated protein kinases (JNK MAPKs). *International Journal of Biochemistry and Cell Biology*. Nov;33(11):1047-63.
- Barr RK, Kendrick TS, Bogoyevitch MA (2002). Identification of the critical features of a small peptide inhibitor of JNK activity. *Journal of Biological Chemistry*. Mar 29;277(13):10987-97.

REFERENCES

- Bass DA, Parce JW, Dechatelet LR, Szejda P, Seeds MC, Thomas M (1983). Flow cytometric studies of oxidative product formation by neutrophils: a graded response to membrane stimulation. *Journal of Immunology*. Apr;130(4):1910-7.
- Beal MF (1995). Aging, energy, and oxidative stress in neurodegenerative diseases. *Annals of Neurology*. Sep;38(3):357-66.
- Behrens MM, Strasser U, Koh JY, Gwag BJ, Choi DW (1999). Prevention of neuronal apoptosis by phorbol ester-induced activation of protein kinase C: blockade of p38 mitogen-activated protein kinase. *Neuroscience*. 94(3):917-27.
- Beilina, A., Van Der Brug, M., Ahmad, R., Kesavapany, S., Miller, D.W., Petsko, G.A. and Cookson, M.R. (2005). Mutations in PTEN-induced putative kinase 1 associated with recessive parkinsonism have differential effects on protein stability. *The Proceedings of the National Academy of Sciences*. 102, 5703–5708.
- Benamira M, Johnson K, Chaudhary A, Bruner K, Tibbetts C, Marnett LJ (1995). Induction of mutations by replication of malondialdehyde-modified M13 DNA in Escherichia coli: determination of the extent of DNA modification, genetic requirements for mutagenesis, and types of mutations induced. *Carcinogenesis*. Jan;16(1):93-9.
- Bennett BL, Sasaki DT, Murray BW, O'Leary EC, Sakata ST, Xu W, Leisten JC, Motiwala A, Pierce S, Satoh Y, Bhagwat SS, Manning AM, Anderson DW (2001). SP600125, an anthrapyrazolone inhibitor of Jun N-terminal kinase. *The Proceedings of the National Academy of Sciences*. Nov 20;98(24):13681-6.
- Bernardi P, Azzone GF (1981). Cytochrome c as an electron shuttle between the outer and inner mitochondrial membranes. *Journal of Biological Chemistry*. Jul 25;256(14):7187-92.
- Bernardi P, Colonna R, Costantini P, Eriksson O, Fontaine E, Ichas F, Massari S, Nicolli A, Petronilli V, Scorrano L (1998). The mitochondrial permeability transition. *Biofactors*. 8(3-4): 273-81.
- Bernardi P, Scorrano L, Colonna R, Petronilli V, Di Lisa F (1999). Mitochondria and cell death. Mechanistic aspects and methodological issues. *European Journal of Biochemistry*. Sep;264(3):687-701.
- Bernhardt R (1996). Cytochrome P450: Structure, function, and generation of reactive oxygen species. *Reviews of Physiology, Biochemistry and Pharmacology*. 127: 137–221.
- Berretta N, Freestone PS, Guatteo E, de Castro D, Geracitano R, Bernardi G, Mercuri NB, Lipski J. (2005). Acute effects of 6-hydroxydopamine on dopaminergic neurons of the rat substantia nigra pars compacta *in vitro*. *Neurotoxicology*. Oct;26(5):869-81.
- Besirli CG, Wagner EF, Johnson EM Jr (2005). The limited role of NH2-terminal c-Jun phosphorylation in neuronal apoptosis: identification of the nuclear pore complex as a potential target of the JNK pathway. *Journal of Cellular Biology*. Aug 1;170(3):401-11.
- Betarbet R, Sherer TB, MacKenzie G, Garcia-Osuna M, Panov AV, Greenamyre JT (2000). Chronic systemic pesticide exposure reproduces features of Parkinson's disease. *Nature Neuroscience*. Dec;3(12):1301-6.

- Bhattacharya S, Ray RM, Viar MJ, Johnson LR (2003). Polyamines are required for activation of c-Jun NH₂-terminal kinase and apoptosis in response to TNF- α in IEC-6 cells. *American Journal of Physiology – Gastrointestinal and Liver Physiology*. Nov;285(5): G980-91.
- Björkblom B, Östman N, Hongisto V, Komarovski V, Filén JJ, Nyman TA, Kallunki T, Courtney MJ, Coffey ET (2005). Constitutively active cytoplasmic c-Jun N-terminal kinase 1 is a dominant regulator of dendritic architecture: role of microtubule-associated protein 2 as an effector. *Journal of Neuroscience*. Jul 6;25(27):6350-61.
- Blagosklonny MV (2001). Unwinding the loop of Bcl-2 phosphorylation. *Leukemia*. Jun;15(6):869-74.
- Blatt NB, Glick GD (2001). Signaling pathways and effector mechanisms pre-programmed cell death. *Bioorganic and Medical Chemistry*. Jun;9(6):1371-84.
- Blum D, Torch S, Lambeng N, Nissou M, Benabid AL, Sadoul R, Verna JM (2001 a). Molecular pathways involved in the neurotoxicity of 6-OHDA, dopamine and MPTP: contribution to the apoptotic theory in Parkinson's disease. *Progress in Neurobiology*. 65(2):135-72.
- Blum D, Torch S, Nissou MF, Benabid AL, Verna JM (2000). Extracellular toxicity of 6-hydroxydopamine on PC12 cells. *Neuroscience Letters*. Apr 14;283(3):193-6.
- Blum D, Torch S, Nissou MF, Verna JM (2001 b). 6-hydroxydopamine-induced nuclear factor-kappa B activation in PC12 cells. *Biochemical Pharmacology*. Aug 15;62(4):473-81.
- Blum D, Wu Y, Nissou MF, Arnaud S, Alim-Louis-Benabid, Verna JM (1997). p53 and Bax activation in 6-hydroxydopamine-induced apoptosis in PC12 cells. *Brain Research*. Mar 14; 751(1):139-42.
- Bogoyevitch MA, Boehm I, Oakley A, Ketterman AJ, Barr RK (2004). Targeting the JNK MAPK cascade for inhibition: basic science and therapeutic potential. *Biochimica et Biophysica Acta*. Mar 11;1697(1-2):89-101.
- Bonni A, Brunet A, West AE, Datta SR, Takasu MA, Greenberg ME (1999). Cell survival promoted by the Ras-MAPK signaling pathway by transcription-dependent and -independent mechanisms. *Science*. Nov 12;286(5443):1358-62.
- Borsello T, Forloni G (2007). JNK signalling: a possible target to prevent neurodegeneration. *Current Pharmaceutical Design*. 13(18):1875-86. Review.
- Bostantjopoulou S, Kyriazis G, Katsarou Z, Kiosseoglou G, Kazis A, Mentenopoulos G (1997). Superoxide dismutase activity in early and advanced Parkinson's disease. *Functional Neurology*. Mar-Apr;12(2):63-8.
- Boveris A, Cadenas E, Stoppani AO (1976). Role of ubiquinone in the mitochondrial generation of hydrogen peroxide. *Biochemical Journal*. May 15;156(2):435-44.
- Boveris A, Chance B (1973). The mitochondrial generation of hydrogen peroxide. General properties and effect of hyperbaric oxygen. *Biochemical Journal*. Jul;134(3):707-16.

REFERENCES

- Boveris A, Oshino N, Chance B (1972). The cellular production of hydrogen peroxide. *Biochemical Journal*. Jul;128(3):617-30.
- Bozyczko-Coyne D, Saporito MS, Hudkins RL (2002). Targeting the JNK pathway for therapeutic benefit in CNS disease. *Current Drug Targets - CNS Neurological Disorders*. Feb;1(1):31-49.
- Brand MD (2000). Uncoupling to survive? The role of mitochondrial inefficiency in ageing. *Experiments in Gerontology*. 35: 811-20.
- Brecht S, Kirchhof R, Chromik A, Willesen M, Nicolaus T, Raivich G, Wessig J, Waetzig V, Goetz M, Claussen M, Pearse D, Kuan CY, Vaudano E, Behrens A, Wagner E, Flavell RA, Davis RJ, Herdegen T (2005). Specific pathophysiological functions of JNK isoforms in the brain. *European Journal of Neuroscience*. Jan;21(2):363-77.
- Buschmann T, Potapova O, Bar-Shira A, Ivanov VN, Fuchs SY, Henderson S, Fried VA, Minamoto T, Alarcon-Vargas D, Pincus MR, Gaarde WA, Holbrook NJ, Shiloh Y, Ronai Z (2001). Jun NH2-terminal kinase phosphorylation of p53 on Thr-81 is important for p53 stabilization and transcriptional activities in response to stress. *Molecular and Cellular Biology*. Apr;21(8):2743-54.
- Butterfield L, Zentrich E, Beekman A, Heasley LE (1999). Stress- and cell type-dependent regulation of transfected c-Jun N-terminal kinase and mitogen-activated protein kinase isoforms. *Biochemical Journal*. Mar 15;338 (Pt 3):681-6.
- Carboni L, Carletti R, Tacconi S, Corti C, Ferraguti F (1998). Differential expression of SAPK isoforms in the rat brain. An in situ hybridisation study in the adult rat brain and during post-natal development. *Brain Research Molecular Brain Research*. Sep 18;60(1):57-68.
- Carboni L, Tacconi S, Carletti R, Bettini E, Ferraguti F (1997). Localization of the messenger RNA for the c-Jun NH2-terminal kinase in the adult and developing rat brain: an in situ hybridization study. *Neuroscience*. Sep;80(1):147-60.
- Cha GH, Kim S, Park J, Lee E, Kim M, Lee SB, Kim JM, Chung J, Cho KS (2005). Parkin negatively regulates JNK pathway in the dopaminergic neurons of *Drosophila*. *The Proceedings of the National Academy of Sciences*. Jul 19;102(29):10345-50.
- Chae HZ, Kim HJ, Kang SW, Rhee SG (1999). Characterization of three isoforms of mammalian peroxiredoxin that reduce peroxides in the presence of thioredoxin. *Diabetes Research and Clinical Practice*. Sep;45(2-3):101-12.
- Chang HY, Nishitoh H, Yang X, Ichijo H, Baltimore D (2003). Activation of apoptosis signal-regulating kinase 1 (ASK1) by the adapter protein Daxx. *Science*. Sep 18;281(5384):1860-3.
- Chang L, Jones Y, Ellisman MH, Goldstein LS, Karin M (2003). JNK1 is required for maintenance of neuronal microtubules and controls phosphorylation of microtubule-associated proteins. *Developmental Cell*. Apr;4(4):521-33.
- Chang L, Karin M (2001). Mammalian MAP kinase signalling cascades. *Nature*. Mar 1; 410(6824):37-40.

- Chauhan D, Li G, Hideshima T, Podar K, Mitsiades C, Mitsiades N, Munshi N, Kharbanda S, Anderson KC (2003). JNK-dependent release of mitochondrial protein, Smac, during apoptosis in multiple myeloma (MM) cells. *Journal of Biological Chemistry*. May 16; 278(20):17593-6.
- Chen J, Tang XQ, Zhi JL, Cui Y, Yu HM, Tang EH, Sun SN, Feng JQ, Chen PX (2006). Curcumin protects PC12 cells against 1-methyl-4-phenylpyridinium ion-induced apoptosis by bcl-2-mitochondria-ROS-iNOS pathway. *Apoptosis*. Jun;11(6):943-53.
- Chen X, Rzhetskaya M, Kareva T, Bland R, During MJ, Tank AW, Kholodilov N, Burke RE (2008). Antiapoptotic and trophic effects of dominant-negative forms of dual leucine zipper kinase in dopamine neurons of the substantia nigra *in vivo*. *Journal of Neuroscience*. Jan 16; 28(3):672-80.
- Chen XL, Kunsch C (2004). Induction of cytoprotective genes through Nrf2/antioxidant response element pathway: a new therapeutic approach for the treatment of inflammatory diseases. *Current Pharmaceutical Design*. 10(8):879-91.
- Chinopoulos C, Adam-Vizi V (2001). Mitochondria deficient in complex I activity are depolarized by hydrogen peroxide in nerve terminals: relevance to Parkinson's disease. *Journal of Neurochemistry*. Jan;76(1):302-6.
- Choi WS, Yoon SY, Oh TH, Choi EJ, O'Malley KL, Oh YJ (1999). Two distinct mechanisms are involved in 6-hydroxydopamine- and MPP⁺-induced dopaminergic neuronal cell death: role of caspases, ROS, and JNK. *Journal of Neuroscience Research*. Jul 1;57(1):86-94.
- Chow CW, Rincón M, Cavanagh J, Dickens M, Davis RJ (1997). Nuclear accumulation of NFAT4 opposed by the JNK signal transduction pathway. *Science*. Nov 28;278(5343): 1638-41.
- Coffey ET, Hongisto V, Dickens M, Davis RJ, Courtney MJ (2000). Dual roles for c-Jun N-terminal kinase in developmental and stress responses in cerebellar granule neurons. *Journal of Neuroscience*. Oct 15;20(20):7602-13.
- Coffey ET, Smiciene G, Hongisto V, Cao J, Brecht S, Herdegen T, Courtney MJ (2002). C-Jun N-terminal protein kinase (JNK) 2/3 is specifically activated by stress, mediating c-Jun activation, in the presence of constitutive JNK1 activity in cerebellar neurons. *Journal of Neuroscience*. Jun 1;22(11):4335-45.
- Cohen G, Heikkila RE (1974). The generation of hydrogen peroxide, superoxide radical, and hydroxyl radical by 6-hydroxydopamine, dialuric acid, and related cytotoxic agents. *Journal of Biological Chemistry*. Apr 25;249(8):2447-52.
- Collins TJ, Berridge MJ, Lipp P, Bootman MD (2002). Mitochondria are morphologically and functionally heterogeneous within cells. *EMBO Journal*. Apr 2;21(7):1616-27.
- Cooper AJ, Kristal BS (1997). Multiple roles of glutathione in the central nervous system. *Biological Chemistry*. Aug;378(8):793-802. Review.

REFERENCES

- Corder EH, Mellick GD (2006). Parkinson's disease in relation to pesticide exposure and nuclear encoded mitochondrial complex I gene variants. *Journal of Biomedicine and Biotechnology*. 2006(3):27601.
- Cossarizza A, Baccarani-Contri M, Kalashnikova G, Franceschi C (1993). A new method for the cytofluorimetric analysis of mitochondrial membrane potential using the J-aggregate forming lipophilic cation 5,5',6,6'-tetrachloro-1,1',3,3'-tetraethylbenzimidazolcarbocyanine iodide (JC-1). *Biochemical and Biophysical Research Communication*. Nov 30;197(1):40-5.
- Cossarizza A, Ceccarelli D, Masini A (1996). Functional heterogeneity of an isolated mitochondrial population revealed by cytofluorometric analysis at the single organelle level. *Experimental Cell Research*. Jan 10;222(1):84-94.
- Crompton M (1999). The mitochondrial permeability transition pore and its role in cell death. *Biochemical Journal*. Jul 15;341 (Pt 2):233-49. Review.
- Crossthwaite AJ, Hasan S, Williams RJ (2002). Hydrogen peroxide-mediated phosphorylation of ERK1/2, Akt/PKB and JNK in cortical neurones: dependence on Ca(2+) and PI3-kinase. *Journal of Neurochemistry*. Jan;80(1):24-35.
- Dajas F, Rivera F, Blasina F, Arredondo F, Echeverry C, Lafon L, Morquio A, Heizen H (2003). Cell culture protection and *in vivo* neuroprotective capacity of flavonoids. *Neurotoxicological Research*. 5(6):425-32.
- Dall'Acqua S, Innocenti G (2004). Antioxidant compounds from *Chaerophyllum hirsutum* extracts. *Fitoterapia*. Sep;75(6):592-5.
- Dalton TP, Shertzer HG, Puga A (1999). Regulation of gene expression by reactive oxygen. *Annual Reviews of Pharmacology & Toxicology*. 39:67-101. Review.
- D'Amato RJ, Lipman ZP, Snyder SH (1986). Selectivity of the parkinsonian neurotoxin MPTP: toxic metabolite MPP⁺ binds to neuromelanin. *Science*. Feb 28;231(4741):987-9.
- Damier P, Hirsch EC, Zhang P, Agid Y, Javoy-Agid F (1993). Glutathione peroxidase, glial cells and Parkinson's disease. *Neuroscience*. Jan;52(1):1-6.
- Daugas E, Susin SA, Zamzami N, Ferri KF, Irinopoulou T, Larochette N, Prévost MC, Leber B, Andrews D, Penninger J, Kroemer G (2000). Mitochondrio-nuclear translocation of AIF in apoptosis and necrosis. *FASEB Journal*. Apr;14(5):729-39.
- Denisov IG, Grinkova YV, McLean MA, Sligar SG (2007). The one-electron autoxidation of human cytochrome P450 3A4. *Journal Biological Chemistry*. Sep 14;282(37):26865-73.
- Dérjard B, Hibi M, Wu IH, Barrett T, Su B, Deng T, Karin M, Davis RJ (1994). JNK active protein kinase stimulated by UV light and Ha-Ras that binds and phosphorylates the c-Jun activation domain. *Cell*. Mar 25;76(6):1025-37.
- Desagher S, Martinou JC (2000). Mitochondria as the central control point of apoptosis. *Trends in Cellular Biology*. Sep;10(9):369-77.

- Deumens R, Blokland A, Prickaerts J (2002). Modeling Parkinson's disease in rats: an evaluation of 6-OHDA lesions of the nigrostriatal pathway. *Experimental Neurology*. Jun;175(2):303-17.
- Dexter DT, Carter CJ, Wells FR, Javoy-Agid F, Agid Y, Lees A, Jenner P, Marsden CD (1989). Basal lipid peroxidation in substantia nigra is increased in Parkinson's disease. *Journal of Neurochemistry*. Feb;52(2):381-9.
- Diaz G, Liu S, Isola R, Diana A, Falchi AM (2003). Mitochondrial localization of reactive oxygen species by dihydrofluorescein probes. *Histochemistry and Cell Biology*. Oct;120(4):319-25.
- Dickens M, Rogers JS, Cavanagh J, Raitano A, Xia Z, Halpern JR, Greenberg ME, Sawyers CL, Davis RJ (1997). A cytoplasmic inhibitor of the JNK signal transduction pathway. *Science*. Aug 1;277(5326):693-6.
- Dietrich N, Thastrup J, Holmberg C, Gyrð-Hansen M, Fehrenbacher N, Lademann U, Lerdrup M, Herdegen T, Jäättelä M, Kallunki T (2004). JNK2 mediates TNF-induced cell death in mouse embryonic fibroblasts via regulation of both caspase and cathepsin protease pathways. *Cell Death & Differentiation*. Mar;11(3):301-13.
- Dispersyn G, Nuydens R, Connors R, Borgers M, Geerts H (1999). Bcl-2 protects against FCCP-induced apoptosis and mitochondrial membrane potential depolarization in PC12 cells. *Biochimica et Biophysica Acta*. Aug 5;1428(2-3):357-71.
- Dodel RC, Du Y, Bales KR, Ling Z, Carvey PM, Paul SM (1999). Caspase-3-like proteases and 6-hydroxydopamine induced neuronal cell death. *Brain Research Molecular Brain Research*. Jan 22;64(1):141-8.
- Dong C, Yang DD, Wysk M, Whitmarsh AJ, Davis RJ, Flavell RA (1998). Defective T cell differentiation in the absence of Jnk1. *Science*. Dec 11;282(5396):2092-5.
- Donovan N, Becker EB, Konishi Y, Bonni A (2002). JNK phosphorylation and activation of BAD couples the stress-activated signaling pathway to the cell death machinery. *Journal of Biological Chemistry*. Oct 25;277(43):40944-9.
- Dringen R (2000). Glutathione metabolism and oxidative stress in neurodegeneration *European Journal of Biochemistry*. Aug;267(16):4903.
- Ebert AD, Chen F, He X, Cryns VL, Bohn MC (2005). A tetracycline-regulated adenovirus encoding dominant-negative caspase-9 is regulated in rat brain and protects against neurotoxin-induced cell death *in vitro*, but not *in vivo*. *Experiments in Neurology*. Feb;191 Suppl 1:S80-94.
- Eckl PM, Ortner A, Esterbauer H (1993). Genotoxic properties of 4-hydroxyalkenals and analogous aldehydes. *Mutational Research*. Dec;290(2):183-92.
- Eguchi Y, Shimizu S, Tsujimoto Y (1997). Intracellular ATP levels determine cell death fate by apoptosis or necrosis. *Cancer Research*. May 15;57(10):1835-40.

REFERENCES

- Eminel S, Klettner A, Roemer L, Herdegen T, Waetzig V (2004). JNK2 translocates to the mitochondria and mediates cytochrome c release in PC12 cells in response to 6-hydroxydopamine. *Journal of Biological Chemistry*. Dec 31;279(53):55385-92
- Fall CP, Bennett JP Jr (1999). Characterization and time course of MPP⁺-induced apoptosis in human SH-SY5Y neuroblastoma cells. *Journal of Neuroscience Research*. Mar 1;55(5): 620-8.
- Farrer M, Chan P, Chen R, Tan L, Lincoln S, Hernandez D, Forno L, Gwinn-Hardy K, Petrucelli L, Hussey J, Singleton A, Tanner C, Hardy J, Langston JW (2001). Lewy bodies and parkinsonism in families with parkin mutations. *Annals in Neurology*. Sep;50(3):293-300.
- Ferrari R, Guardigli G, Mele D, Percoco GF, Ceconi C, Curello S (2004). Oxidative stress during myocardial ischaemia and heart failure. *Current Pharmaceutical Design*. 10(14): 1699-711.
- Finkel T (1998). Oxygen radicals and signaling. *Current Opinions in Cell Biology*. Apr;10(2): 248-53.
- Forman HJ, Azzi A (1997). On the virtual existence of superoxide anions in mitochondria: thoughts regarding its role in pathophysiology. *FASEB Journal*. Apr;11(5):374-5.
- Forno LS (1986). Lewy bodies. *New England Journal of Medicine*. Jan 9;314(2):122.
- Fujita H, Ogino T, Kobuchi H, Fujiwara T, Yano H, Akiyama J, Utsumi K, Sasaki J (2006). Cell-permeable cAMP analog suppresses 6-hydroxydopamine-induced apoptosis in PC12 cells through the activation of the Akt pathway. *Brain Research*. Oct 3;1113(1):10-23.
- Gelderblom M, Eminel S, Herdegen T, Waetzig V (2004). c-Jun N-terminal kinases (JNKs) and the cytoskeleton--functions beyond neurodegeneration. *International Journal of Developmental Neuroscience*. Nov;22(7):559-64.
- Glinka Y, Tipton KF, Youdim MB (1996). Nature of inhibition of mitochondrial respiratory complex I by 6-Hydroxydopamine. *Journal of Neurochemistry*. May;66(5):2004-10.
- Gluck MR, Youngster SK, Ramsay RR, Singer TP, Nicklas WJ (1994). Studies on the characterization of the inhibitory mechanism of 4'-alkylated 1-methyl-4-phenylpyridinium and phenylpyridine analogues in mitochondria and electron transport particles. *Journal of Neurochemistry*. Aug;63(2):655-61.
- Goedert M, Hasegawa M, Jakes R, Lawler S, Cuenda A, Cohen P (1997). Phosphorylation of microtubule-associated protein tau by stress-activated protein kinases. *FEBS Letters*. Jun 2; 409(1):57-62.
- Gogvadze V, Orrenius S, Zhivotovsky B, Juan S (2003). Analysis of Mitochondrial Dysfunction During Cell Death, from Current Protocols in Cell Biology. Bonifacino JC, Dasso M, Harford JB, Lippincott-Schwartz J, Yamada KM (eds.), *John Wiley & Sons, Inc.*
- Golbe LI (1991). Young-onset Parkinson's disease: a clinical review. *Neurology*. Feb;41(2(Part 1)):168-73.

- Goldstein LS (2001). Molecular motors: from one motor many tails to one motor many tales. *Trends in Cell Biology*. Dec;11(12):477-82. Review.
- Goon D, Saxena M, Awasthi YC, Ross D (1993). Activity of mouse liver glutathione S-transferases toward trans,trans-muconaldehyde and trans-4-hydroxy-2-nonenal. *Toxicological Applications in Pharmacology*. Apr;119(2):175-80.
- Götz ME, Freyberger A, Riederer P (1990). Oxidative stress: a role in the pathogenesis of Parkinson's disease. *Journal of Neural Transmission Supplement*. 29:241-9.
- Gray MW, Burger G, Lang BF (1999). Mitochondrial evolution. *Science*. Mar 5;283(5407):1476-81.
- Green DR, Reed JC (1998). Mitochondria and apoptosis. *Science*. Aug 28;281(5381):1309-12.
- Greenamyre JT, MacKenzie G, Peng TI, Stephans SE (1999). Mitochondrial dysfunction in Parkinson's disease. *Biochemical Society Symposium*. 66:85-97.
- Greene LA, Tischler AS (1976). Establishment of a noradrenergic clonal line of rat adrenal pheochromocytoma cells which respond to nerve growth factor. *The Proceedings of the National Academy of Sciences*. Jul;73(7):2424-8.
- Gross A, Jockel J, Wei MC, Korsmeyer SJ (1998). Enforced dimerization of BAX results in its translocation, mitochondrial dysfunction and apoptosis. *EMBO Journal*. Jul 15;17(14):3878-85.
- Gross A, Yin XM, Wang K, Wei MC, Jockel J, Milliman C, Erdjument-Bromage H, Tempst P, Korsmeyer SJ (1999). Caspase cleaved BID targets mitochondria and is required for cytochrome c release, while BCL-X_L prevents this release but not tumor necrosis factor-R1/Fas death. *Journal of Biological Chemistry*. Jan 8;274(2):1156-63.
- Grünblatt E, Mandel S, Youdim MB (2000). MPTP and 6-hydroxydopamine-induced neurodegeneration as models for Parkinson's disease: neuroprotective strategies. *Journal of Neurology*. Apr;247 Suppl 2:II95-102.
- Guan QH, Pei DS, Liu XM, Wang XT, Xu TL, Zhang GY (2006). Neuroprotection against ischemic brain injury by SP600125 via suppressing the extrinsic and intrinsic pathways of apoptosis. *Brain Research*. May 30;1092(1):36-46.
- Guo S, Bezdard E, Zhao B (2005). Protective effect of green tea polyphenols on the SH-SY5Y cells against 6-OHDA induced apoptosis through ROS-NO pathway. *Free Radicals in Biology and Medicine*. Sep 1;39(5):682-95.
- Gupta S, Campbell D, Dérijard B, Davis RJ (1995). Transcription factor ATF2 regulation by the JNK signal transduction pathway. *Science*. Jan 20;267(5196):389-93.
- Ha KS, Kim KM, Kwon YG, Bai SK, Nam WD, Yoo YM, Kim PK, Chung HT, Billiar TR, Kim YM (2003). Nitric oxide prevents 6-hydroxydopamine-induced apoptosis in PC12 cells through cGMP-dependent PI3 kinase/Akt activation. *FASEB Journal*. Jun;17(9):1036-47.

REFERENCES

- Halestrap AP, Kerr PM, Javadov S, Woodfield KY (1998). Elucidating the molecular mechanism of the permeability transition pore and its role in reperfusion injury of the heart. *Biochimica et Biophysica Acta*. Aug 10;1366(1-2):79-94.
- Han BS, Hong HS, Choi WS, Markelonis GJ, Oh TH, Oh YJ (2003). Caspase-dependent and -independent cell death pathways in primary cultures of mesencephalic dopaminergic neurons after neurotoxin treatment. *Journal of Neuroscience*. Jun 15;23(12):5069-78.
- Hanneken A, Lin FF, Johnson J, Maher P (2006). Flavonoids protect human retinal pigment epithelial cells from oxidative-stress-induced death. *Investigative Ophthalmology and Visual Sciences*. Jul;47(7):3164-77.
- Hanrott K, Gudmunsen L, O'Neill MJ, Wonnacott S (2006). 6-hydroxydopamine-induced apoptosis is mediated via extracellular auto-oxidation and caspase 3-dependent activation of protein kinase Cdelta. *Journal of Biological Chemistry*. Mar 3;281(9):5373-82.
- Hantraye P, Brouillet E, Ferrante R, Palfi S, Dolan R, Matthews RT, Beal MF (1996). Inhibition of neuronal nitric oxide synthase prevents MPTP-induced parkinsonism in baboons. *Nature Medicine*. Sep;2(9):1017-21.
- Hara H, Ohta M, Ohta K, Kuno S, Adachi T (2003). Apomorphine attenuates 6-hydroxydopamine-induced apoptotic cell death in SH-SY5Y cells. *Redox Report*. 8(4):193-7.
- Hardy J, Cai H, Cookson MR, Gwinn-Hardy K, Singleton A (2006). Genetics of Parkinson's disease and parkinsonism. *Annals of Neurology*. Oct;60(4):389-98.
- Hartley DP, Ruth JA, Petersen DR (1995). The hepatocellular metabolism of 4-hydroxynonenal by alcohol dehydrogenase, aldehyde dehydrogenase, and glutathione S-transferase. *Archives of Biochemistry and Biophysics*. Jan 10;316(1):197-205.
- Hatai T, Matsuzawa A, Inoshita S, Mochida Y, Kuroda T, Sakamaki K, Kuida K, Yonehara S, Ichijo H, Takeda K (2000). Execution of apoptosis signal-regulating kinase 1 (ASK1)-induced apoptosis by the mitochondria-dependent caspase activation. *Journal of Biological Chemistry*. Aug 25;275(34):26576-81.
- Hayakawa T, Sugimoto Y, Chen Z, Fujii Y, Kamei C (1999). Effects of anti-Parkinsonian drugs on neurobehavioural changes induced by bilateral 6-hydroxydopamine lesions in rats. *Clinical and Experimental Pharmacology and Physiology*. May-Jun;26(5-6):421-5.
- He Y, Lee T, Leong SK (2000). 6-Hydroxydopamine induced apoptosis of dopaminergic cells in the rat substantia nigra. *Brain Research*. Mar 6;858(1):163-6.
- Heikkila RE, Manzino L, Cabbat FS, Duvoisin RC (1984). Protection against the dopaminergic neurotoxicity of 1-methyl-4-phenyl-1,2,5,6-tetrahydropyridine by monoamine oxidase inhibitors. *Nature*. Oct 4-10;311(5985):467-9.
- Hempel SL, Buettner GR, O'Malley YQ, Wessels DA, Flaherty DM (1999). Dihydrofluorescein diacetate is superior for detecting intracellular oxidants: comparison with 2',7'-dichlorodihydrofluorescein diacetate, 5 (and 6)-carboxy-2',7'-dichlorodihydrofluorescein

- diacetate, and dihydrorhodamine 123. *Free Radicals in Biology and Medicine*. Jul;27(1-2): 146-59.
- Herdegen T, Claret FX, Kallunki T, Martin-Villalba A, Winter C, Hunter T, Karin M (1998). Lasting N-terminal phosphorylation of c-Jun and activation of c-Jun N-terminal kinases after neuronal injury. *Journal of Neuroscience*. Jul 15;18(14):5124-35.
- Hibi M, Lin A, Smeal T, Minden A, Karin M (1993). Identification of an oncoprotein- and UV-responsive protein kinase that binds and potentiates the c-Jun activation domain. *Genes & Development*. Nov;7(11):2135-48.
- Hidding U, Mielke K, Waetzig V, Brecht S, Hanisch U, Behrens A, Wagner E, Herdegen T (2002). The c-Jun N-terminal kinases in cerebral microglia: immunological functions in the brain. *Biochemical Pharmacology*. Sep;64(5-6):781-8.
- Hirosumi J, Tuncman G, Chang L, Görgün CZ, Uysal KT, Maeda K, Karin M, Hotamisligil GS (2002). A central role for JNK in obesity and insulin resistance. *Nature*. Nov 21; 420(6913):333-6.
- Hirsch EC, Hunot S, Damier P, Faucheux B (1998). Glial cells and inflammation in Parkinson's disease: a role in neurodegeneration? *Annals of Neurology*. Sep;44(3 Suppl 1): S115-20. Review.
- Holtz WA, O'Malley KL (2003). Parkinsonian mimetics induce aspects of unfolded protein response in death of dopaminergic neurons. *Journal of Biological Chemistry*. May 23; 278(21):19367-77.
- Hsieh, T. C., Juan, G., Darzynkiewicz, Z., and Wu, J. M. (1999). Resveratrol increases nitric oxide synthase, induces accumulation of p53 and p21 (WAF1/CIP1), and suppresses cultured bovine pulmonary artery endothelial cell proliferation by perturbing progression through S and G2. *Cancer Research*. 59, 2596–2601.
- Hughes AJ, Daniel SE, Kilford L, Lees AJ (1992). Accuracy of clinical diagnosis of idiopathic Parkinson's disease: a clinicopathological study of 100 cases. *Journal of Neurology, Neurosurgery, and Psychiatry*. 55:181–184.
- Hughes AJ, Daniel SE, Lees AJ (2001). Improved accuracy of clinical diagnosis of Lewy body Parkinson's disease. *Neurology*. 57:1497–1499.
- Hunot S, Brugg B, Ricard D, Michel PP, Muriel MP, Ruberg M, Faucheux BA, Agid Y, Hirsch EC (1997). Nuclear translocation of NF-kappaB is increased in dopaminergic neurons of patients with parkinson disease. *The Proceedings of the National Academy of Sciences*. Jul 8;94(14):7531-6.
- Hunot S, Vila M, Teismann P, Davis RJ, Hirsch EC, Przedborski S, Rakic P, Flavell RA (2004). JNK-mediated induction of cyclooxygenase 2 is required for neurodegeneration in a mouse model of Parkinson's disease. *The Proceedings of the National Academy of Sciences*. Jan 13;101(2):665-70.

REFERENCES

- Ichas F, Mazat JP (1998). From calcium signaling to cell death: two conformations for the mitochondrial permeability transition pore. Switching from low- to high-conductance state. *Biochimica et Biophysica Acta*. Aug 10;1366(1-2):33-50.
- Ichijo H, Nishida E, Irie K, ten Dijke P, Saitoh M, Moriguchi T, Takagi M, Matsumoto K, Miyazono K, Gotoh Y (1997). Induction of apoptosis by ASK1, a mammalian MAPKKK that activates SAPK/JNK and p38 signaling pathways. *Science*. Jan 3;275(5296):90-4.
- Ikebe S, Tanaka M, Ozawa T (1995). Point mutations of mitochondrial genome in Parkinson's disease. *Brain Research Molecular Brain Research*. Feb;28(2):281-95.
- Ip YT, Davis RJ (1998). Signal transduction by the c-Jun N-terminal kinase (JNK)--from inflammation to development. *Current Opinions in Cell Biology*. Apr;10(2):205-19. Review.
- Ito Y, Mishra NC, Yoshida K, Kharbanda S, Saxena S, Kufe D (2001). Mitochondrial targeting of JNK/SAPK in the phorbol ester response of myeloid leukemia cells. *Cell Death and Differentiation*. Aug;8(8):794-800.
- Ito Y, Oh-Hashi K, Kiuchi K, Hirata Y (2006). p44/42 MAP kinase and c-Jun N-terminal kinase contribute to the up-regulation of caspase-3 in manganese-induced apoptosis in PC12 cells. *Brain Research*. Jul 12;1099(1):1-7
- Izumi Y, Sawada H, Yamamoto N, Kume T, Katsuki H, Shimohama S, Akaike A (2005). Iron accelerates the conversion of dopamine-oxidized intermediates into melanin and provides protection in SH-SY5Y cells. *Journal of Neuroscience Research*. Oct 1;82(1):126-37.
- Jaeschke A, Czech MP, Davis RJ (2004). An essential role of the JIP1 scaffold protein for JNK activation in adipose tissue. *Genes & Development*. Aug 15;18(16):1976-80.
- Javitch JA, D'Amato RJ, Strittmatter SM, Snyder SH (1985). Parkinsonism-inducing neurotoxin, N-methyl-4-phenyl-1,2,3,6-tetrahydropyridine: uptake of the metabolite N-methyl-4-phenylpyridine by dopamine neurons explains selective toxicity. *The Proceedings of the National Academy of Sciences*. Apr;82(7):2173-7.
- Jenner P (2003). Oxidative stress in Parkinson's disease. *Annals of Neurology*. 53 Suppl 3: S26-36; discussion S36-8. Review.
- Jenner P, Olanow CW (1998). Understanding cell death in Parkinson's disease. *Annals of Neurology*. Sep;44(3 Suppl 1):S72-84. Review.
- Jenner P, Olanow CW (2006). The pathogenesis of cell death in Parkinson's disease. *Neurology*. May 23;66(10 Suppl 4):S24-36.
- Jeon BS, Jackson-Lewis V, Burke RE (1995). 6-Hydroxydopamine lesion of the rat substantia nigra: time course and morphology of cell death. *Neurodegeneration*. Jun;4(2):131-7.
- Jeon BS, Kholodilov NG, Oo TF, Kim SY, Tomaselli KJ, Srinivasan A, Stefanis L, Burke RE (1999). Activation of caspase-3 in developmental models of programmed cell death in neurons of the substantia nigra. *Journal of Neurochemistry*. Jul;73(1):322-33.

- Johnson LV, Walsh ML, Chen LB (1980). Localization of mitochondria in living cells with rhodamine 123. *The Proceedings of the National Academy of Sciences*. Feb;77(2):990-4.
- Jordán J, Galindo MF, Tornero D, González-García C, Ceña V (2004). Bcl-xL blocks mitochondrial multiple conductance channel activation and inhibits 6-OHDA-induced death in SH-SY5Y cells. *Journal of Neurochemistry*. Apr;89(1):124-33.
- Kallunki T, Su B, Tsigelny I, Sluss HK, Dérijard B, Moore G, Davis R, Karin M (1994). JNK2 contains a specificity-determining region responsible for efficient c-Jun binding and phosphorylation. *Genes & Development*. Dec 15;8(24):2996-3007.
- Kamata H, Hirata H (1999). Redox regulation of cellular signalling. *Cell Signaling*. Jan;11(1):1-14. Review.
- Kaneto H, Nakatani Y, Miyatsuka T, Kawamori D, Matsuoka TA, Matsuhisa M, Kajimoto Y, Ichijo H, Yamasaki Y, Hori M (2004). Possible novel therapy for diabetes with cell-permeable JNK-inhibitory peptide. *Nature Medicine*. Oct;10(10):1128-32.
- Kang D, Miyako K, Kuribayashi F, Hasegawa E, Mitsumoto A, Nagano T, Takeshige K (1997). Changes of energy metabolism induced by 1-methyl-4-phenylpyridinium (MPP⁺)-related compounds in rat pheochromocytoma PC12 cells. *Archives of Biochemistry and Biophysics*. 337 (1): 75-80.
- Kang DC, Motwani M, Fisher PB (1998). Role of the transcription factor AP-1 in melanoma differentiation. *International Journal of Oncology*. Dec;13(6):1117-26. Review.
- Kantrow SP, Piantadosi CA (1997). Release of cytochrome c from liver mitochondria during permeability transition. *Biochemical and Biophysical Research Communication*. Mar 27; 232(3):669-71.
- Kapsa RM, Jean-Francois MJ, Lertrit P, Weng S, Siregar N, Ojaimi J, Donnan G, Masters C, Byrne E (1996). Mitochondrial DNA polymorphism in substantia nigra. *Journal of Neurology in Science*. Dec;144(1-2):204-11.
- Karpinich NO, Tafani M, Rothman RJ, Russo MA, Farber JL (2002). The course of etoposide-induced apoptosis from damage to DNA and p53 activation to mitochondrial release of cytochrome c. *Journal of Biological Chemistry*. May 10;277(19):16547-52.
- Keller JN, Mattson MP (1998). Roles of lipid peroxidation in modulation of cellular signaling pathways, cell dysfunction, and death in the nervous system. *Reviews in the Neurosciences*. 9(2):105-16. Review.
- Kharbanda S, Saxena S, Yoshida K, Pandey P, Kaneki M, Wang Q, Cheng K, Chen YN, Campbell A, Sudha T, Yuan ZM, Narula J, Weichselbaum R, Nalin C, Kufe D (2000). Translocation of SAPK/JNK to mitochondria and interaction with Bcl-x(L) in response to DNA damage. *Journal of Biological Chemistry*. Jan 7;275(1):322-7.
- Kim RH, Smith PD, Aleyasin H, et al. Hypersensitivity of DJ-1-deficient mice to 1-methyl-4-phenyl-1,2,3,6-tetrahydropyridine (MPTP) and oxidative stress. *The Proceedings of the National Academy of Sciences*. 102:5215–5220.

REFERENCES

- Kitamura Y, Kosaka T, Kakimura JI, Matsuoka Y, Kohno Y, Nomura Y, Taniguchi T (1998). Protective effects of the antiparkinsonian drugs talipexole and pramipexole against 1-methyl-4-phenylpyridinium-induced apoptotic death in human neuroblastoma SH-SY5Y cells. *Molecular Pharmacology*. Dec;54(6):1046-54.
- Klivenyi, P., Siwek, D., Gardian, G., Yang, L., Starkov, A., Cleren, C., Ferrante, R.J., Kowall, N.W., Abeliovich, A. and Beal, M.F. (2006) Mice lacking alpha-synuclein are resistant to mitochondrial toxins. *Neurobiological Disorders*., 21, 541–548.
- Kluck RM, Bossy-Wetzel E, Green DR, Newmeyer DD (1997). The release of cytochrome c from mitochondria: a primary site for Bcl-2 regulation of apoptosis. *Science*. Feb 21; 275(5303):1132-6.
- Koopman G, Taher TE, Mazzucchelli I, Keehnen RM, van der Voort R, Manten-Horst E, Ricevuti G, Pals ST, Das PK (1998). CD44 isoforms, including the CD44 V3 variant, are expressed on endothelium, suggesting a role for CD44 in the immobilization of growth factors and the regulation of the local immune response. *Biochemical and Biophysical Research Communication*. Apr 7;245(1):172-6.
- Kowaltowski AJ, Netto LE, Vercesi AE (1998). The thiol-specific antioxidant enzyme prevents mitochondrial permeability transition. Evidence for the participation of reactive oxygen species in this mechanism. *Journal of Biological Chemistry*. May 22;273(21): 12766-9.
- Krilleke D, Ucur E, Pulte D, Schulze-Osthoff K, Debatin KM, Herr I (2003). Inhibition of JNK signaling diminishes early but not late cellular stress-induced apoptosis. *International Journal of Cancer*. Nov 20;107(4):520-7.
- Kroemer G, Dallaporta B, Resche-Rigon M (1998). The mitochondrial death/life regulator in apoptosis and necrosis. *Annual Reviews in Physiology*. 60:619-42. Review.
- Kroemer G, Reed JC (2000). Mitochondrial control of cell death. *Nature Medicine*. May;6(5):513-9. Review.
- Krohn AJ, Preis E, Prehn JH (1998). Staurosporine-induced apoptosis of cultured rat hippocampal neurons involves caspase-1-like proteases as upstream initiators and increased production of superoxide as a main downstream effector. *Journal of Neuroscience*. Oct 15; 18(20):8186-97.
- Kruman I, Guo Q, Mattson MP (1998). Calcium and reactive oxygen species mediate staurosporine-induced mitochondrial dysfunction and apoptosis in PC12 cells. *Journal of Neuroscience Research*. Feb 1;51(3):293-308.
- Kuan CY, Burke RE (2005). Targeting the JNK signaling pathway for stroke and Parkinson's diseases therapy. *Current Drug Targets - CNS Neurological Disorders*. 4:63–7.
- Kuan, C. Y., D. D. Yang, D. R. Samanta Roy, R. J. Davis, P. Rakic, and R. A. Flavell (1999). The Jnk1 and Jnk2 protein kinases are required for regional specific apoptosis during early brain development. *Neuron*. 22:667–676.

- Kumar R, Agarwal AK, Seth PK (1995). Free radical-generated neurotoxicity of 6-hydroxydopamine. *Journal of Neurochemistry*. Apr;64(4):1703-7. Erratum in: *Journal of Neurochemistry*. 1995 Oct;65(4):1906.
- Kutuk O, Poli G, Basaga H (2006). Resveratrol protects against 4-hydroxynonenal-induced apoptosis by blocking JNK and c-JUN/AP-1 signaling. *Toxicological Sciences*. Mar;90(1):120-32.
- Kylarová D, Procházková J, Mad'arová J, Bartos J, Lichnovský V (2002). Comparison of the TUNEL, lamin B and annexin V methods for the detection of apoptosis by flow cytometry. *Acta Histochemistry*. 104(4):367-70.
- Kyriakis JM, Avruch J (2001). Mammalian mitogen-activated protein kinase signal transduction pathways activated by stress and inflammation. *Physiological Reviews*. Apr;81(2):807-69. Review.
- Kyriakis JM, Banerjee P, Nikolakaki E, Dai T, Rubie EA, Ahmad MF, Avruch J, Woodgett JR (1994). The stress-activated protein kinase subfamily of c-Jun kinases. *Nature*. May 12; 369(6476):156-60.
- La Fauci G, Lahiri DK, Salton SR, Robakis NK (1989). Characterization of the 5'-end region and the first two exons of the beta-protein precursor gene. *Biochemical and Biophysical Research Communication*. Feb 28;159(1):297-304.
- Lagouge M, Argmann C, Gerhart-Hines Z, Meziane H, Lerin C, Daussin F, Messadeq N, Milne J, Lambert P, Elliott P, Geny B, Laakso M, Puigserver P, Auwerx J (2006). Resveratrol improves mitochondrial function and protects against metabolic disease by activating SIRT1 and PGC-1alpha. *Cell*. Dec 15;127(6):1109-22.
- Langston JW, Ballard P, Tetrud JW, Irwin I (1983). Chronic Parkinsonism in humans due to a product of meperidine-analog synthesis. *Science*. Feb 25;219(4587):979-80.
- Langston JW, Ballard PA Jr (1983). Parkinson's disease in a chemist working with 1-methyl-4-phenyl-1,2,5,6-tetrahydropyridine. *New England Journal of Medicine*. Aug 4;309(5):310.
- Langston JW, Irwin I, Langston EB, Forno LS (1984 a). 1-Methyl-4-phenylpyridinium ion (MPP⁺): identification of a metabolite of MPTP, a toxin selective to the substantia nigra. *Neuroscience Letters*. 1984 Jul 13;48(1):87-92.
- Langston JW, Langston EB, Irwin I (1984 b). MPTP-induced parkinsonism in human and non-human primates - clinical and experimental aspects. *Acta Neurologica Scandinavica Supplement*. 100:49-54.
- Langston JW, Sastry S, Chan P, Forno LS, Bolin LM, Di Monte DA (1998). Novel alpha-synuclein-immunoreactive proteins in brain samples from the Contursi kindred, Parkinson's, and Alzheimer's disease. *Experimental Neurology*. Dec;154(2):684-90.
- Lee CS, Han JH, Jang YY, Song JH, Han ES (2002). Differential effect of catecholamines and MPP(+) on membrane permeability in brain mitochondria and cell viability in PC12 cells. *Neurochemistry International*. Apr;40(4):361-9.

REFERENCES

- Lee JM, Shih AY, Murphy TH, Johnson JA (2003). NF-E2-related factor-2 mediates neuroprotection against mitochondrial complex I inhibitors and increased concentrations of intracellular calcium in primary cortical neurons. *Journal of Biological Chemistry*. Sep 26; 278(39):37948-56.
- Lei K, Davis RJ (2003). JNK phosphorylation of Bim-related members of the Bcl2 family induces Bax-dependent apoptosis. *The Proceedings of the National Academy of Sciences*. Mar 4;100(5):2432-7.
- Lei K, Nimnual A, Zong WX, Kennedy NJ, Flavell RA, Thompson CB, Bar-Sagi D, Davis RJ (2002). The Bax subfamily of Bcl2-related proteins is essential for apoptotic signal transduction by c-Jun NH(2)-terminal kinase. *Molecular and Cellular Biology*. Jul;22(13):4929-42.
- Leiro J, Arranz JA, Fraiz N, Sanmartín ML, Quezada E, Orallo F (2005). Effect of cis-resveratrol on genes involved in nuclear factor kappa B signaling. *International Immunopharmacology*. Feb;5(2):393-406.
- Leist M, Jäättelä M (2001). Four deaths and a funeral: from caspases to alternative mechanisms. *Nature Reviews of Molecular and Cellular Biology*. Aug;2(8):589-98. Review.
- Leist M, Single B, Castoldi AF, Kühnle S, Nicotera P (1997). Intracellular adenosine triphosphate (ATP) concentration: a switch in the decision between apoptosis and necrosis. *Journal of Experimental Medicine*. Apr 21;185(8):1481-6.
- Lenaz G (2001). The mitochondrial production of reactive oxygen species: mechanisms and implications in human pathology. *IUBMB Life*. Sep-Nov;52(3-5):159-64. Review.
- Le-Niculescu H, Bonfoco E, Kasuya Y, Claret FX, Green DR, Karin M (1999). Withdrawal of survival factors results in activation of the JNK pathway in neuronal cells leading to Fas ligand induction and cell death. *Molecular and Cellular Biology*. Jan;19(1):751-63.
- Leutenecker, A.L., Salih, M.A., Ibanez, P., Mukhtar, M.M., Lesage, S., Arabi, A., Lohmann, E., Durr, A., Ahmed, A.E. and Brice, A. (2006) Juvenile-onset Parkinsonism as a result of the first mutation in the adenosine triphosphate orientation domain of PINK1. *Archives of Neurology*. 63, 1257–1261.
- Li C, Beal MF (2005). Leucine-rich repeat kinase 2: a new player with a familiar theme for Parkinson's disease pathogenesis. *The Proceedings of the National Academy of Sciences*. Nov 15;102(46):16535-6.
- Li P, Nijhawan D, Budihardjo I, Srinivasula SM, Ahmad M, Alnemri ES, Wang X (1997). Cytochrome c and dATP-dependent formation of Apaf-1/caspase-9 complex initiates an apoptotic protease cascade. *Cell*. Nov 14;91(4):479-89.
- Lindwall C, Kanje M (2005). The role of p-c-Jun in survival and outgrowth of developing sensory neurons. *Neuroreport*. Oct 17;16(15):1655-9.

- Liu R, Li B, Flanagan SW, Oberley LW, Gozal D, Qiu M (2002). Increased mitochondrial antioxidative activity or decreased oxygen free radical propagation prevent mutant SOD1-mediated motor neuron cell death and increase amyotrophic lateral sclerosis-like transgenic mouse survival. *Journal of Neurochemistry*. Feb;80(3):488-500.
- Liu X, Kim CN, Yang J, Jemmerson R, Wang X (1996). Induction of apoptotic program in cell-free extracts: requirement for dATP and cytochrome c. *Cell*. Jul 12;86(1):147-57.
- Lockshin RA, Zakeri Z (2004). Apoptosis, autophagy, and more. *The International Journal of Biochemistry and Cell Biology*. Dec;36(12):2405-19. Review.
- Logrosino G (2005). The role of early life environmental risk factors in Parkinson disease: what is the evidence? *Environmental health perspectives*. Sep;113(9):1234-8. Review.
- Loschen G, Azzi A. (1975). On the formation of hydrogen peroxide and oxygen radicals in heart mitochondria. *Recent advances in studies on cardiac structure and metabolism*. 7:3-12.
- Loschen G, Chance B (1971). Rapid kinetic studies of the light emitting protein aequorin. *Nature: New biology*. Oct 27;233(43):273-4.
- Lotharius J, Dugan LL, O'Malley KL (1999). Distinct mechanisms underlie neurotoxin-mediated cell death in cultured dopaminergic neurons. *Journal of Neuroscience*. Feb 15; 19(4):1284-93.
- Lu C, Chan SL, Fu W, Mattson MP (2002). The lipid peroxidation product 4-hydroxynonenal facilitates opening of voltage-dependent Ca²⁺ channels in neurons by increasing protein tyrosine phosphorylation. *Journal of Biological Chemistry*. Jul 5;277(27):24368-75.
- Magura EI, Kopanitsa MV, Gleitz J, Peters T, Krishtal OA (1997). Kava extract ingredients, (+)-methysticin and (+/-)-kavain inhibit voltage-operated Na(+)-channels in rat CA1 hippocampal neurons. *Neuroscience*. Nov;81(2):345-51. Erratum in: *Neuroscience* 1998. May;84(1):323.
- Makino N, Mochizuki Y, Bannai S, Sugita Y (1994). Kinetic studies on the removal of extracellular hydrogen peroxide by cultured fibroblasts. *Journal of Biological Chemistry*. Jan 14;269(2):1020-5.
- Manna, S. K., Mukhopadhyay, A., and Aggarwal, B. B. (2000). Resveratrol suppresses TNF-induced activation of nuclear transcription factors NF-kappa B, activator protein-1, and apoptosis: potential role of reactive oxygen intermediates and lipid peroxidation. *Journal of Immunology*. 164, 6509–6519.
- Manning-Bog AB, McCormack AL, Li J, Uversky VN, Fink AL, Di Monte DA (2002). The herbicide paraquat causes up-regulation and aggregation of alpha-synuclein in mice: paraquat and alpha-synuclein. *Journal of Biological Chemistry*. Jan 18;277(3):1641-4.
- Markey SP, Johannessen JN, Chiueh CC, Burns RS, Herkenham MA (1984). Intraneuronal generation of a pyridinium metabolite may cause drug-induced parkinsonism. *Nature*. Oct 4-10;311(5985):464-7.

REFERENCES

- Marklund SL, Westman NG, Lundgren E, Roos G (1982). Copper- and zinc-containing superoxide dismutase, manganese-containing superoxide dismutase, catalase, and glutathione peroxidase in normal and neoplastic human cell lines and normal human tissues. *Cancer Research*. May;42(5):1955-61.
- Maroney AC, Glicksman MA, Basma AN, Walton KM, Knight E Jr, Murphy CA, Bartlett BA, Finn JP, Angeles T, Matsuda Y, Neff NT, Dionne CA (1998). Motoneuron apoptosis is blocked by CEP-1347 (KT 7515), a novel inhibitor of the JNK signaling pathway. *Journal of Neuroscience*. Jan 1;18(1):104-11.
- Marques CA, Keil U, Bonert A, Steiner B, Haass C, Muller WE, Eckert A (2003). Neurotoxic mechanisms caused by the Alzheimer's disease-linked Swedish amyloid precursor protein mutation: oxidative stress, caspases, and the JNK pathway. *Journal of Biological Chemistry*. Jul 25;278(30):28294-302.
- Mathews JM, Etheridge AS, Valentine JL, Black SR, Coleman DP, Patel P, So J, Burka LT (2005). Pharmacokinetics and disposition of the kavalactone kawain: interaction with kava extract and kavalactones *in vivo* and *in vitro*. *Drug metabolism and disposition: the biological fate of chemicals*. Oct;33(10):1555-63.
- McCord JM (1985). Oxygen-derived free radicals in postischemic tissue injury. *New England Journal of Medicine*. Jan 17;312(3):159-63. Review.
- McCormack AL, Thiruchelvam M, Manning-Bog AB, Thiffault C, Langston JW, Cory-Slechta DA, Di Monte DA (2002). Environmental risk factors and Parkinson's disease: selective degeneration of nigral dopaminergic neurons caused by the herbicide paraquat. *Neurobiological Disorders*. Jul;10(2):119-27.
- McMahon M, Itoh K, Yamamoto M, Chanas SA, Henderson CJ, McLellan LI, Wolf CR, Cavin C, Hayes JD (2001). The Cap'n'Collar basic leucine zipper transcription factor Nrf2 (NF-E2 p45-related factor 2) controls both constitutive and inducible expression of intestinal detoxification and glutathione biosynthetic enzymes. *Cancer Research*. Apr 15;61(8):3299-307.
- Meco G, Bonifati V, Vanacore N, Fabrizio E (1994). Parkinsonism after chronic exposure to the fungicide maneb (manganese ethylene-bis-dithiocarbamate). *Scandinavian Journal of Work, Environment & Health*. Aug;20(4):301-5.
- Mielke K, Damm A, Yang DD, Herdegen T (2000). Selective expression of JNK isoforms and stress-specific JNK activity in different neural cell lines. *Brain Research Molecular Brain Research*. Jan 10;75(1):128-37.
- Miller DW, Ahmad R, Hague S et al. (2003). L166P mutant DJ-1, causative for recessive Parkinson's disease, is degraded through the ubiquitin-proteasome system. *Journal of Biological Chemistry*. 278: 36588–36595.
- Mizuno Y, Ohta S, Tanaka M, Takamiya S, Suzuki K, Sato T, Oya H, Ozawa T, Kagawa Y (1989). Deficiencies in complex I subunits of the respiratory chain in Parkinson's disease. *Biochemical and Biophysical Research Communication*. Sep 29;163(3):1450-5.

- Mladenović A, Perović M, Raicević N, Kanazir S, Rakić L, Ruzdijić S (2004). 6-Hydroxydopamine increases the level of TNF α and bax mRNA in the striatum and induces apoptosis of dopaminergic neurons in hemiparkinsonian rats. *Brain Research*. Jan 23;996(2):237-45.
- Mochizuki H, Goto K, Mori H, Mizuno Y (1996). Histochemical detection of apoptosis in Parkinson's disease. *Journal of Neurological Sciences*. May;137(2):120-3.
- Münch G, Thome J, Foley P, Schinzel R, Riederer P (1997). Advanced glycation endproducts in ageing and Alzheimer's disease. *Brain Research Brain Research Reviews*. Feb;23(1-2): 134-43. Review.
- Nicholls DG, Budd SL (2000). Mitochondria and neuronal survival. *Physiology Reviews*. Jan;80(1):315-60. Review.
- Nomura M, Shimizu S, Ito T, Narita M, Matsuda H, Tsujimoto Y (1999). Apoptotic cytosol facilitates Bax translocation to mitochondria that involves cytosolic factor regulated by Bcl-2. *Cancer Research*. 1999 Nov 1;59(21):5542-8.
- Nomura M, Shimizu S, Sugiyama T, Narita M, Ito T, Matsuda H, Tsujimoto Y (2003). 14-3-3 interacts directly with and negatively regulates pro-apoptotic Bax. *Journal of Biological Chemistry*. Jan 17;278(3):2058-65.
- Nuydens R, Novalbos J, Dispersyn G, Weber C, Borgers M, Geerts H (1999). A rapid method for the evaluation of compounds with mitochondria-protective properties. *Journal of Neuroscience Methods*. Oct 15;92(1-2):153-9.
- Ochu EE, Rothwell NJ, Waters CM (1998). Caspases mediate 6-hydroxydopamine-induced apoptosis but not necrosis in PC12 cells. *Journal of Neurochemistry*. Jun;70(6):2637-40.
- Oh JH, Choi WS, Kim JE, Seo JW, O'Malley KL, Oh YJ (1998). Overexpression of HA-Bax but not Bcl-2 or Bcl-X_L attenuates 6-hydroxydopamine-induced neuronal apoptosis. *Experiments in Neurology*. Nov;154(1):193-8.
- Okado-Matsumoto A, Fridovich I (2001). Subcellular distribution of superoxide dismutases (SOD) in rat liver: Cu,Zn-SOD in mitochondria. *Journal of Biological Chemistry*. Oct 19; 276(42):38388-93.
- Okuno S, Saito A, Hayashi T, Chan PH (2004). The c-Jun N-terminal protein kinase signaling pathway mediates Bax activation and subsequent neuronal apoptosis through interaction with Bim after transient focal cerebral ischemia. *Journal of Neuroscience*. Sep 8;24(36):7879-87.
- Ouyang M, Shen X (2006). Critical role of ASK1 in the 6-hydroxydopamine-induced apoptosis in human neuroblastoma SH-SY5Y cells. *Journal of Neurochemistry*. Apr;97(1):234-44.
- Pan J, Wang G, Yang HQ, Hong Z, Xiao Q, Ren RJ, Zhou HY, Bai L, Chen SD (2007). K252a prevents nigral dopaminergic cell death induced by 6-hydroxydopamine through inhibition of both mixed-lineage kinase 3/c-Jun NH2-terminal kinase 3 (JNK3) and apoptosis-inducing kinase 1/JNK3 signaling pathways. *Molecular Pharmacology*. Dec;72(6):1607-18.

REFERENCES

- Park J, Kim SY, Cha GH (2005). *Drosophila* DJ-1 mutants show oxidative stress-sensitive locomotive dysfunction. *Gene*. 361:133–139.
- Park JA, Lee KY, Oh YJ, Kim KW, Lee SK (1997). Activation of caspase-3 protease via a Bcl-2-insensitive pathway during the process of ginsenoside Rh2-induced apoptosis. *Cancer Letters*. Dec 16;121(1):73-81.
- Park SH, Choi WS, Yoon SY, Ahn YS, Oh YJ (2004). Activation of NF-kappaB is involved in 6-hydroxydopamine-but not MPP⁺-induced dopaminergic neuronal cell death: its potential role as a survival determinant. *Biochemical and Biophysical Research Communication*. Sep 24;322(3):727-33.
- Parker WD Jr, Boyson SJ, Parks JK (1989). Abnormalities of the electron transport chain in idiopathic Parkinson's disease. *Annals in Neurology*. Dec;26(6):719-23.
- Parkinson J (1817). An essay on the shaking palsy. *Sherwood, Neely and Jones*. London.
- Paul A, Wilson S, Belham CM, Robinson CJ, Scott PH, Gould GW, Plevin R (1997). Stress-activated protein kinases: activation, regulation and function. *Cell Signaling*. Sep;9(6):403-10.
- Pearson LL, Castle BE, Kehry MR (2001). CD40-mediated signaling in monocytic cells: up-regulation of tumor necrosis factor receptor-associated factor mRNAs and activation of mitogen-activated protein kinase signaling pathways. *International Immunology*. Mar;13(3):273-83.
- Pedrosa R, Soares-da-Silva P (2002). Oxidative and non-oxidative mechanisms of neuronal cell death and apoptosis by L-3,4-dihydroxyphenylalanine (L-DOPA) and dopamine. *British Journal of Pharmacology*. Dec;137(8):1305-13.
- Penaloza C, Lin L, Lockshin RA, Zakeri Z (2006). Cell death in development: shaping the embryo. *Histochemistry and cell biology*. Aug;126(2):149-58.
- Perumal AS, Tordzro WK, Katz M, Jackson-Lewis V, Cooper TB, Fahn S, Cadet JL (1989). Regional effects of 6-hydroxydopamine (6-OHDA) on free radical scavengers in rat brain. *Brain Research*. Dec 11;504(1):139-41.
- Pervaiz S (2003). Resveratrol: from grapevines to mammalian biology. *FASEB Journal*. Nov;17(14):1975-85. Review.
- Pigault C, Follenius-Wund A, Schmutz M, Freyssinet JM, Brisson A (1994). Formation of two-dimensional arrays of annexin V on phosphatidylserine-containing liposomes. *Journal of Molecular Biology*. Feb 11;236(1):199-208.
- Plin C, Tillement JP, Berdeaux A, Morin D (2005). Resveratrol protects against cold ischemia-warm reoxygenation-induced damages to mitochondria and cells in rat liver. *European Journal of Pharmacology*. Dec 28;528(1-3):162-8.
- Poli G, Leonarduzzi G, Biasi F, Chiarotto E (2004). Oxidative stress and cell signalling. *Current Medicinal Chemistry*. May;11(9):1163-82. Review.

- Polster BM, Fiskum G (2004). Mitochondrial mechanisms of neural cell apoptosis. *Journal of Neurochemistry*. Sep;90(6):1281-9. Review.
- Polymeropoulos MH, Higgins JJ, Golbe LI, Johnson WG, Ide SE, Di Iorio G, Sanges G, Stenroos ES, Pho LT, Schaffer AA, Lazzarini AM, Nussbaum RL, Duvoisin RC (1996). Mapping of a gene for Parkinson's disease to chromosome 4q21-q23. *Science*. Nov 15; 274(5290):1197-9.
- Prehn JH, Jordán J, Ghadge GD, Preis E, Galindo MF, Roos RP, Krieglstein J, Miller RJ (1997). Ca^{2+} and reactive oxygen species in staurosporine-induced neuronal apoptosis. *Journal of Neurochemistry*. Apr;68(4):1679-85.
- Pressman BC (1976). Biological applications of ionophores. *Annual Reviews of Biochemistry*. 45:501-30.
- Przedborski S, Jackson-Lewis V, Yokoyama R, Shibata T, Dawson VL, Dawson TM (1996). Role of neuronal nitric oxide in 1-methyl-4-phenyl-1,2,3,6-tetrahydropyridine (MPTP)-induced dopaminergic neurotoxicity. *The Proceedings of the National Academy of Sciences*. May 14;93(10):4565-71.
- Przedborski S, Kostic V, Jackson-Lewis V, Naini AB, Simonetti S, Fahn S, Carlson E, Epstein CJ, Cadet JL (1992). Transgenic mice with increased Cu/Zn-superoxide dismutase activity are resistant to N-methyl-4-phenyl-1,2,3,6-tetrahydropyridine-induced neurotoxicity. *Journal of Neuroscience*. May;12(5):1658-67.
- Putcha GV, Deshmukh M, Johnson EM Jr (1999). BAX translocation is a critical event in neuronal apoptosis: regulation by neuroprotectants, BCL-2, and caspases. *Journal of Neuroscience*. Sep 1;19(17):7476-85.
- Putcha GV, Le S, Frank S, Besirli CG, Clark K, Chu B, Alix S, Youle RJ, LaMarche A, Maroney AC, Johnson EM Jr (2003). JNK-mediated BIM phosphorylation potentiates BAX-dependent apoptosis. *Neuron*. Jun 19;38(6):899-914.
- Raivich G, Bohatschek M, Da Costa C, Iwata O, Galiano M, Hristova M, Nateri AS, Makwana M, Riera-Sans L, Wolfer DP, Lipp HP, Aguzzi A, Wagner EF, Behrens A (2004). The AP-1 transcription factor c-Jun is required for efficient axonal regeneration. *Neuron*. Jul 8;43(1):57-67.
- Ramsay RR, Youngster SK, Nicklas WJ, McKeown KA, Jin YZ, Heikkila RE, Singer TP (1989). Structural dependence of the inhibition of mitochondrial respiration and of NADH oxidase by 1-methyl-4-phenylpyridinium (MPP⁺) analogs and their energized accumulation by mitochondria. *The Proceedings of the National Academy of Sciences*. Dec;86(23):9168-72.
- Rang HP, Dale M, Ritter JM, Moore P (2003). Pharmacology. 5th revised edition. *Churchill Livingstone*; 20 Mar 2003.
- Reers M, Smith TW, Chen LB (1991). J-aggregate formation of a carbocyanine as a quantitative fluorescent indicator of membrane potential. *Biochemistry*. May 7;30(18):4480-6.

REFERENCES

- Rehm M, Düsselmann H, Prehn JH (2003). Real-time single cell analysis of Smac/DIABLO release during apoptosis. *Journal of Cellular Biology*. Sep 15;162(6):1031-43.
- Richter C, Schweizer M, Cossarizza A, Franceschi C (1996). Control of apoptosis by the cellular ATP level. *FEBS Letters*. Jan 8;378(2):107-10. Review.
- Romanová D, Vachálková A, Cipák L, Ovesná Z, Rauko P (2001). Study of antioxidant effect of apigenin, luteolin and quercetin by DNA protective method. *Neoplasma*. 2001;48(2):104-7.
- Ross GW, Abbott RD, Petrovitch H, White LR, Tanner CM (2000). Relationship between caffeine intake and parkinson disease. *JAMA: the journal of the American Medical Association*. Sep 20;284(11):1378-9.
- Rothe G, Valet G (1990). Flow cytometric analysis of respiratory burst activity in phagocytes with hydroethidine and 2',7'-dichlorofluorescein. *Journal of Leukocyte Biology*. May;47(5):440-8.
- Royall JA, Ischiropoulos H (1993). Evaluation of 2',7'-dichlorofluorescein and dihydrorhodamine 123 as fluorescent probes for intracellular H₂O₂ in cultured endothelial cells. *Archives of Biochemistry and Biophysics*. May;302(2):348-55.
- Rüegg UT, Burgess GM. (1989) Staurosporine, K-252 and UCN-01: potent but nonspecific inhibitors of protein kinases. *Trends in Pharmacological Science*. 29: 253-257.
- Sabapathy K, Jochum W, Hochedlinger K, Chang L, Karin M, Wagner EF (1999). Defective neural tube morphogenesis and altered apoptosis in the absence of both JNK1 and JNK2. *Mechanisms of Development*. Dec;89(1-2):115-24.
- Sabapathy K, Wagner EF (2004). JNK2: a negative regulator of cellular proliferation. *Cell Cycle*. Dec;3(12):1520-3.
- Saito Y, Nishio K, Ogawa Y, Kinumi T, Yoshida Y, Masuo Y, Niki E (2007). Molecular mechanisms of 6-hydroxydopamine-induced cytotoxicity in PC12 cells: involvement of hydrogen peroxide-dependent and -independent action. *Free Radicals in Biology and Medicine*. Mar 1;42(5):675-85.
- Salinas M, Diaz R, Abraham NG, Ruiz de Galarreta CM, Cuadrado A (2003). Nerve growth factor induces anti-apoptotic heme oxygenase-1 in rat pheochromocytoma PC12 cells. *Journal of Biological Chemistry*. Apr 18;278(16):13898-904.
- Salvioli S, Ardizzoni A, Franceschi C, Cossarizza A (1997). JC-1, but not DiOC₆(3) or rhodamine 123, is a reliable fluorescent probe to assess delta psi changes in intact cells: implications for studies on mitochondrial functionality during apoptosis. *FEBS Letters*. Jul 7;411(1):77-82.
- Saner A, Thoenen H (1971). Model experiments on the molecular mechanism of action of 6-hydroxydopamine. *Molecular Pharmacology*. Mar;7(2):147-54.

- Sanna MG, da Silva Correia J, Ducrey O, Lee J, Nomoto K, Schrantz N, Deveraux QL, Ulevitch RJ (2002). IAP suppression of apoptosis involves distinct mechanisms: the TAK1/JNK1 signaling cascade and caspase inhibition. *Molecular and Cellular Biology*. Mar;22(6):1754-66.
- Saporito MS, Brown EM, Miller MS, Carswell S (1999). CEP-1347/KT-7515, an inhibitor of c-jun N-terminal kinase activation, attenuates the 1-methyl-4-phenyl tetrahydropyridine-mediated loss of nigrostriatal dopaminergic neurons *in vivo*. *The Journal of Pharmacology and Experimental Therapeutics*. Feb;288(2):421-7.
- Saporito MS, Thomas BA, Scott RW (2000). MPTP activates c-Jun NH(2)-terminal kinase (JNK) and its upstream regulatory kinase MKK4 in nigrostriatal neurons *in vivo*. *Journal of Neurochemistry*. Sep;75(3):1200-8.
- Sawada H, Shimohama S, Tamura Y, Kawamura T, Akaike A, Kimura J (1996). Methylphenylpyridium ion (MPP⁺) enhances glutamate-induced cytotoxicity against dopaminergic neurons in cultured rat mesencephalon. *Journal of Neuroscience Research*. Jan 1;43(1):55-62.
- Scarlett JL, Murphy MP (1997). Release of apoptogenic proteins from the mitochondrial intermembrane space during the mitochondrial permeability transition. *FEBS Letters*. Dec 1; 418(3):282-6.
- Schapira AH (1994). Evidence for mitochondrial dysfunction in Parkinson's disease--a critical appraisal. *Movement Disorders*. Mar;9(2):125-38. Review.
- Schapira AH (2008). Mitochondria in the aetiology and pathogenesis of Parkinson's disease. *Lancet Neurology*. Jan;7(1):97-109. Review.
- Schapira AH, Cooper JM, Dexter D, Clark JB, Jenner P, Marsden CD (1990). Mitochondrial complex I deficiency in Parkinson's disease. *Journal of Neurochemistry*. Mar;54(3):823-7.
- Schild L, Westphal S, Scheithauer S, Holfeld M, Augustin W, Sabel BA (1996). Isolation of functionally intact pig retina mitochondria. *Acta Ophthalmologica Scandinavica*. Aug;74(4):354-7.
- Schlesinger TK, Fanger GR, Yujiri T, Johnson GL (1998). The TAO of MEKK. *Frontiers in Biosciences*. Nov 15;3:D1181-6. Review.
- Schlingensiepen KH, Wollnik F, Kunst M, Schlingensiepen R, Herdegen T, Brysch W (1994). The role of Jun transcription factor expression and phosphorylation in neuronal differentiation, neuronal cell death, and plastic adaptations *in vivo*. *Cellular and Molecular Neurobiology*. Oct;14(5):487-505.
- Schroeter H, Boyd CS, Ahmed R, Spencer JP, Duncan RF, Rice-Evans C, Cadenas E (2003). c-Jun N-terminal kinase (JNK)-mediated modulation of brain mitochondria function: new target proteins for JNK signalling in mitochondrion-dependent apoptosis. *Biochemical Journal*. Jun 1;372(Pt 2):359-69.

REFERENCES

- Scorrano L, Ashiya M, Buttle K, Weiler S, Oakes SA, Mannella CA, Korsmeyer SJ (2002). A distinct pathway remodels mitochondrial cristae and mobilizes cytochrome c during apoptosis. *Developmental Cell*. 2002 Jan;2(1):55-67.
- Seitz G, Stegmann HB, Jäger HH, Schlude HM, Wolburg H, Roginsky VA, Niethammer D, Bruchelt G (2000). Neuroblastoma cells expressing the noradrenaline transporter are destroyed more selectively by 6-fluorodopamine than by 6-hydroxydopamine. *Journal of Neurochemistry*. Aug;75(2):511-20.
- Sen CK, Packer L (1996). Antioxidant and redox regulation of gene transcription. *FASEB Journal*. May;10(7):709-20. Review.
- Shafer TJ, Atchison WD (1991). Transmitter, ion channel and receptor properties of pheochromocytoma (PC12) cells: a model for neurotoxicological studies. *Neurotoxicology*. Fall;12(3):473-92. Review.
- Sherer TB, Betarbet R, Stout AK, Lund S, Baptista M, Panov AV, Cookson MR, Greenamyre JT (2002). An *in vitro* model of Parkinson's disease: linking mitochondrial impairment to altered alpha-synuclein metabolism and oxidative damage. *Journal of Neuroscience*. Aug 15;22(16):7006-15.
- Sherer TB, Betarbet R, Testa CM, Seo BB, Richardson JR, Kim JH, Miller GW, Yagi T, Matsuno-Yagi A, Greenamyre JT (2003). Mechanism of toxicity in rotenone models of Parkinson's disease. *Journal of Neuroscience*. Nov 26;23(34):10756-64.
- Shimizu S, Narita M, Tsujimoto Y (1999). Bcl-2 family proteins regulate the release of apoptogenic cytochrome c by the mitochondrial channel VDAC. *Nature*. Jun 3;399(6735):483-7. Erratum in: *Nature* 2000 Oct 12;407(6805):767.
- Shoffner JM, Watts RL, Juncos JL, Torroni A, Wallace DC (1991). Mitochondrial oxidative phosphorylation defects in Parkinson's disease. *Annals of Neurology*. Sep;30(3):332-9.
- Shoichet SA, Duprez L, Hagens O, Waetzig V, Menzel C, Herdegen T, Schweiger S, Dan B, Vamos E, Ropers HH, Kalscheuer VM (2006). Truncation of the CNS-expressed JNK3 in a patient with a severe developmental epileptic encephalopathy. *Human Genetics*. Jan;118(5):559-67.
- Siems WG, Hapner SJ, van Kuijk FJ (1996). 4-hydroxynonenal inhibits Na(+)-K(+)-ATPase. *Free Radicals in Biology and Medicine*. 20(2):215-23.
- Sies H (1991). Role of reactive oxygen species in biological processes. *Klinische Wochenschrift*. Dec 15;69(21-23):965-8. Review.
- Singleton AB (2005). Altered alpha-synuclein homeostasis causing Parkinson's disease: the potential roles of dardarin. *Trends in Neuroscience*. Aug;28(8):416-21. Review.
- Sipos I, Tretter L, Adam-Vizi V (2003). The production of reactive oxygen species in intact isolated nerve terminals is independent of the mitochondrial membrane potential. *Neurochemical Research*. Oct;28(10):1575-81.

- Skulachev VP (1998). Cytochrome c in the apoptotic and antioxidant cascades. *FEBS Letters*. Feb 27;423(3):275-80. Review.
- Slivka A, Cohen G (1985). Hydroxyl radical attack on dopamine. *Journal of Biological Chemistry*. Dec 15;260(29):15466-72.
- Sluss HK, Barrett T, Dérijard B, Davis RJ (1994). Signal transduction by tumor necrosis factor mediated by JNK protein kinases. *Molecular and Cellular Biology*. Dec;14(12): 8376-84.
- Smiley ST, Reers M, Mottola-Hartshorn C, Lin M, Chen A, Smith TW, Steele GD Jr, Chen LB (1991). Intracellular heterogeneity in mitochondrial membrane potentials revealed by a J-aggregate-forming lipophilic cation JC-1. *The Proceedings of the National Academy of Sciences*. May 1;88(9):3671-5.
- Snyder SH, D'Amato RJ (1985). Predicting Parkinson's disease. *Nature*. Sep 19-25; 317(6034):198-9.
- Song DD, Shults CW, Sisk A, Rockenstein E, Masliah E (2004). Enhanced substantia nigra mitochondrial pathology in human alpha-synuclein transgenic mice after treatment with MPTP. *Experiments in Neurology*. Apr;186(2):158-72.
- Song, D.D., Shults, C.W., Sisk, A., Rockenstein, E. and Masliah, E. (2004). Enhanced substantia nigra mitochondrial pathology in human alpha-synuclein transgenic mice after treatment with MPTP. *Experiments in Neurology*, 186, 158–172.
- Soto-Otero R, Méndez-Alvarez E, Hermida-Ameijeiras A, Muñoz-Patiño AM, Labandeira-Garcia JL (2000). Autoxidation and neurotoxicity of 6-hydroxydopamine in the presence of some antioxidants: potential implication in relation to the pathogenesis of Parkinson's disease. *Journal of Neurochemistry*. Apr;74(4):1605-12.
- Spencer JP, Kuhnle GG, Williams RJ, Rice-Evans C (2003). Intracellular metabolism and bioactivity of quercetin and its *in vivo* metabolites. *Biochemical Journal*. May 15;372 (Pt 1):173-81.
- Stadtman ER (2004). Cyclic oxidation and reduction of methionine residues of proteins in antioxidant defense and cellular regulation. *Archives of Biochemistry and Biophysics*. Mar 1; 423(1):2-5. Review.
- Standen CL, Brownlees J, Grierson AJ, Kesavapany S, Lau KF, McLoughlin DM, Miller CC (2001). Phosphorylation of thr(668) in the cytoplasmic domain of the Alzheimer's disease amyloid precursor protein by stress-activated protein kinase 1b (Jun N-terminal kinase-3). *Journal of Neurochemistry*. Jan;76(1):316-20.
- Storch A, Kaftan A, Burkhardt K, Schwarz J (2000). 6-Hydroxydopamine toxicity towards human SH-SY5Y dopaminergic neuroblastoma cells: independent of mitochondrial energy metabolism. *Journal of Neural Transmission*. 107(3):281-93.
- Sun Y, Oberley LW (1996). Redox regulation of transcriptional activators. *Free Radicals in Biology and Medicine*. 21(3):335-48. Review.

REFERENCES

- Sureda FX, Escubedo E, Gabriel C, Comas J, Camarasa J, Camins A (1997). Mitochondrial membrane potential measurement in rat cerebellar neurons by flow cytometry. *Cytometry*. May 1;28(1):74-80.
- Susin SA, Lorenzo HK, Zamzami N, Marzo I, Brenner C, Larochette N, Prévost MC, Alzari PM, Kroemer G (1999). Mitochondrial release of caspase-2 and -9 during the apoptotic process. *Journal of Experimental Medicine*. Jan 18;189(2):381-94.
- Susin SA, Zamzami N, Kroemer G (1998). Mitochondria as regulators of apoptosis: doubt no more. *Biochimica et Biophysica Acta*. Aug 10;1366(1-2):151-65. Review.
- Takai N, Nakanishi H, Tanabe K, Nishioku T, Sugiyama T, Fujiwara M, Yamamoto K (1998). Involvement of caspase-like proteinases in apoptosis of neuronal PC12 cells and primary cultured microglia induced by 6-hydroxydopamine. *Journal of Neuroscience Research*. Oct 15;54(2):214-22.
- Takizawa S, Matsushima K, Shinohara Y, Ogawa S, Komatsu N, Utsunomiya H, Watanabe K (1994). Immunohistochemical localization of glutathione peroxidase in infarcted human brain. *Journal of the Neurological Sciences*. Mar;122(1):66-73.
- Tamaoki T, Nomoto H, Takahashi I, Kato Y, Morimoto M, Tomita F (1986). Staurosporine, a potent inhibitor of phospholipid/Ca⁺⁺dependent protein kinase. *Biochemical and Biophysical Research Communication*. Mar 13;135(2):397-402.
- Tanner CM, Ottman R, Goldman SM, Ellenberg J, Chan P, Mayeux R, Langston JW (1999). Parkinson disease in twins: an etiologic study. *JAMA: the journal of the American Medical Association*. Jan 27;281(4):341-6.
- Tatton NA, Maclean-Fraser A, Tatton WG, Perl DP, Olanow CW (1998). A fluorescent double-labeling method to detect and confirm apoptotic nuclei in Parkinson's disease. *Annals of Neurology*. Sep;44(3 Suppl 1):S142-8. Review.
- Thakar JH, Hassan MN (1988). Effects of 6-hydroxydopamine on oxidative phosphorylation of mitochondria from rat striatum, cortex, and liver. *Canadian Journal of Physiology and Pharmacology*. Apr;66(4):376-9.
- Thiruchelvam M, Brockel BJ, Richfield EK, Baggs RB, Cory-Slechta DA (2000). Potentiated and preferential effects of combined paraquat and maneb on nigrostriatal dopamine systems: environmental risk factors for Parkinson's disease? *Brain Research*. Aug 11;873(2):225-34.
- Thomas B, Beal MF (2007). Parkinson's disease. *Human Molecular Genetics*. Oct 15;16 Spec No. 2:R183-94. Review.
- Thompson R, Ruch W, Hasenöhrl RU. (2004). Enhanced cognitive performance and cheerful mood by standardized extracts of *Piper methysticum* (Kava-kava). *Human Psychopharmacology*. 19 (4): 243-250.
- Tipton KF, Singer TP (1993). Advances in our understanding of the mechanisms of the neurotoxicity of MPTP and related compounds. *Journal of Neurochemistry*. Oct;61(4): 1191-206.

- Torres M (2003). Mitogen-activated protein kinase pathways in redox signaling. *Frontiers in Biosciences*. Jan 1;8:d369-91. Review.
- Tournier C, Hess P, Yang DD, Xu J, Turner TK, Nimnual A, Bar-Sagi D, Jones SN, Flavell RA, Davis RJ (2000). Requirement of JNK for stress-induced activation of the cytochrome c-mediated death pathway. *Science*. May 5;288(5467):870-4.
- Trejo J, Massamiri T, Deng T, Dewji NN, Bayney RM, Brown JH (1994). A direct role for protein kinase C and the transcription factor Jun/AP-1 in the regulation of the Alzheimer's beta-amyloid precursor protein gene. *Journal of Biological Chemistry*. Aug 26;269(34):21682-90.
- Tretiakoff C (1919). Contribution à l'étude de l'anatomie pathologique du locus niger de Soemmering avec quelques deductions relatives à la pathogenie des troubles du tonus musculaire et de la maladie du Parkinson. These de Paris.
- Troy CM, Rabacchi SA, Xu Z, Maroney AC, Connors TJ, Shelanski ML, Greene LA (2001). beta-Amyloid-induced neuronal apoptosis requires c-Jun N-terminal kinase activation. *Journal of Neurochemistry*. Apr;77(1):157-64.
- Tsuruta F, Sunayama J, Mori Y, Hattori S, Shimizu S, Tsujimoto Y, Yoshioka K, Masuyama N, Gotoh Y (2004). JNK promotes Bax translocation to mitochondria through phosphorylation of 14-3-3 proteins. *EMBO Journal*. Apr 21;23(8):1889-99.
- Turrens JF, Boveris A (1980). Generation of superoxide anion by the NADH dehydrogenase of bovine heart mitochondria. *Biochemical Journal*. Nov 1;191(2):421-7.
- Tyurina YY, Kapralov AA, Jiang J, Borisenko GG, Potapovich AI, Sorokin A, Kochanek PM, Graham SH, Schor NF, Kagan VE (2006). Oxidation and cytotoxicity of 6-OHDA are mediated by reactive intermediates of COX-2 overexpressed in PC12 cells. *Brain Research*. Jun 6;1093(1):71-82.
- Uebelhack R, Franke L, Schewe HJ (1998). Inhibition of platelet MAO-B by kava pyrone-enriched extract from Piper methysticum Forster (kava-kava). *Pharmacopsychiatry*. Sep;31(5):187-92.
- Ueda S, Masutani H, Nakamura H, Tanaka T, Ueno M, Yodoi J (2002). Redox control of cell death. *Antioxidants & Redox Signaling*. Jun;4(3):405-14. Review.
- Ungerstedt U. (1971). Adipsia and aphagia after 6-hydroxydopamine induced degeneration of the nigro-striatal dopamine system. *Acta Physiologica Scandinavica Supplement*. 367:95-122.
- Valente, E.M., Abou-Sleiman, P.M., Caputo, V., Muqit, M.M., Harvey, K., Gispert, S., Ali, Z., Del Turco, D., Bentivoglio, A.R., Healy, D.G. et al. (2004) Hereditary early-onset Parkinson's disease caused by mutations in PINK1. *Science*, 304, 1158–1160.
- van Engeland M, Ramaekers FC, Schutte B, Reutelingsperger CP (1996). A novel assay to measure loss of plasma membrane asymmetry during apoptosis of adherent cells in culture. *Cytometry*. Jun 1;24(2):131-9.

REFERENCES

- Venugopal R, Jaiswal AK (1998). Nrf2 and Nrf1 in association with Jun proteins regulate antioxidant response element-mediated expression and coordinated induction of genes encoding detoxifying enzymes. *Oncogene*. Dec 17;17(24):3145-56.
- Verhagen AM, Ekert PG, Pakusch M, Silke J, Connolly LM, Reid GE, Moritz RL, Simpson RJ, Vaux DL (2000). Identification of DIABLO, a mammalian protein that promotes apoptosis by binding to and antagonizing IAP proteins. *Cell*. Jul 7;102(1):43-53.
- Verhey KJ, Meyer D, Deehan R, Blenis J, Schnapp BJ, Rapoport TA, Margolis B (2001). Cargo of kinesin identified as JIP scaffolding proteins and associated signaling molecules. *Journal of Cellular Biology*. Mar 5;152(5):959-70.
- Vermes I, Haanen C, Steffens-Nakken H, Reutelingsperger C (1995). A novel assay for apoptosis. Flow cytometric detection of phosphatidylserine expression on early apoptotic cells using fluorescein labelled Annexin V. *Journal of Immunological Methods*. Jul 17;184(1):39-51.
- Vitorica J, Machado A, Satrústegui J (1984). Age-dependent variations in peroxide-utilizing enzymes from rat brain mitochondria and cytoplasm. *Journal of Neurochemistry*. Feb;42(2):351-6.
- von Coelln R, Kügler S, Bähr M, Weller M, Dichgans J, Schulz JB (2001). Rescue from death but not from functional impairment: caspase inhibition protects dopaminergic cells against 6-hydroxydopamine-induced apoptosis but not against the loss of their terminals. *Journal of Neurochemistry*. Apr;77(1):263-73.
- Votyakova TV, Reynolds IJ (2001). DeltaPsi(m)-Dependent and -independent production of reactive oxygen species by rat brain mitochondria. *Journal of Neurochemistry*. Oct;79(2):266-77.
- Wadia JS, Chalmers-Redman RM, Ju WJ, Carlile GW, Phillips JL, Fraser AD, Tatton WG (1998). Mitochondrial membrane potential and nuclear changes in apoptosis caused by serum and nerve growth factor withdrawal: time course and modification by (-)-deprenyl. *Journal of Neuroscience*. Feb 1;18(3):932-47.
- Waetzig V, Herdegen T (2003). The concerted signaling of ERK1/2 and JNKs is essential for PC12 cell neurogenesis and converges at the level of target proteins. *Molecular and Cellular Neuroscience*. Sep;24(1):238-49.
- Waetzig V, Herdegen T (2004). Neurodegenerative and physiological actions of c-Jun N-terminal kinases in the mammalian brain. *Neuroscience Letters*. May 6;361(1-3):64-7. Review.
- Waetzig V, Herdegen T (2005). Context-specific inhibition of JNKs: overcoming the dilemma of protection and damage. *Trends in Pharmacological Sciences*. Sep;26(9):455-61. Review.
- Waldmeier P, Bozyczko-Coyne D, Williams M, Vaught JL (2006). Recent clinical failures in Parkinson's disease with apoptosis inhibitors underline the need for a paradigm shift in drug discovery for neurodegenerative diseases. *Biochemical Pharmacology*. Nov 15;72(10):1197-206.

- Walkinshaw G, Waters CM (1994). Neurotoxin-induced cell death in neuronal PC12 cells is mediated by induction of apoptosis. *Neuroscience*. Dec;63(4):975-87.
- Walrand S, Valeix S, Rodriguez C, Ligot P, Chassagne J, Vasson MP (2003). Flow cytometry study of polymorphonuclear neutrophil oxidative burst: a comparison of three fluorescent probes. *Clinica Chimica Acta*. May;331(1-2):103-10.
- Wang W, Shi L, Xie Y, Ma C, Li W, Su X, Huang S, Chen R, Zhu Z, Mao Z, Han Y, Li M (2004). SP600125, a new JNK inhibitor, protects dopaminergic neurons in the MPTP model of Parkinson's disease. *Neuroscience Research*, Feb;48(2):195-202.
- Watanabe N, Forman HJ (2003). Autoxidation of extracellular hydroquinones is a causative event for the cytotoxicity of menadione and DMNQ in A549-S cells. *Archives of Biochemistry and Biophysics*. Mar 1;411(1):145-57.
- Waterhouse NJ, Goldstein JC, von Ahsen O, Schuler M, Newmeyer DD, Green DR (2001). Cytochrome c maintains mitochondrial transmembrane potential and ATP generation after outer mitochondrial membrane permeabilization during the apoptotic process. *Journal of Cellular Biology*. Apr 16;153(2):319-28.
- Whitmarsh AJ, Cavanagh J, Tournier C, Yasuda J, Davis RJ (1998). A mammalian scaffold complex that selectively mediates MAP kinase activation. *Science*. Sep 11;281(5383):1671-4.
- Wilhelm D, Bender K, Knebel A, Angel P (1997). The level of intracellular glutathione is a key regulator for the induction of stress-activated signal transduction pathways including Jun N-terminal protein kinases and p38 kinase by alkylating agents. *Molecular and Cellular Biology*. Aug;17(8):4792-800.
- Winterbourn CC, Metodiewa D (1994). The reaction of superoxide with reduced glutathione. *Archives of Biochemistry and Biophysics*. Nov 1;314(2):284-90.
- Woodgate A, MacGibbon G, Walton M, Dragunow M (1999). The toxicity of 6-hydroxydopamine on PC12 and P19 cells. *Brain Research Molecular Brain Research*. May 21;69(1):84-92.
- Wruck CJ, Claussen M, Fuhrmann G, Römer L, Schulz A, Pufe T, Waetzig V, Peipp M, Herdegen T, Götz ME (2007). Luteolin protects rat PC12 and C6 cells against MPP⁺ induced toxicity via an ERK dependent Keap1-Nrf2-ARE pathway. *Journal of Neural Transmission Supplement*. (72):57-67.
- Wu D, Yu L, Nair MG, DeWitt DL, Ramsewak RS (2002). Cyclooxygenase enzyme inhibitory compounds with antioxidant activities from Piper methysticum (kava kava) roots. *Phytomedicine*. Jan;9(1):41-7.
- Wu Y, Blum D, Nissou MF, Benabid AL, Verna JM (1996). Unlike MPP⁺, apoptosis induced by 6-OHDA in PC12 cells is independent of mitochondrial inhibition. *Neuroscience Letters*. Dec 27;221(1):69-71.

REFERENCES

- Xagorari A, Papapetropoulos A, Mauromatis A, Economou M, Fotsis T, Roussos C (2001). Luteolin inhibits an endotoxin-stimulated phosphorylation cascade and proinflammatory cytokine production in macrophages. *The Journal of Pharmacology and Experimental Therapeutics*. Jan;296(1):181-7.
- Xia Z, Dickens M, Raingeaud J, Davis RJ, Greenberg ME (1995). Opposing effects of ERK and JNK-p38 MAP kinases on apoptosis. *Science*. Nov 24;270(5240):1326-31.
- Xiao J, Liu Y (2003). Differential roles of ERK and JNK in early and late stages of neurogenesis: a study in a novel PC12 model system. *Journal of Neurochemistry*. Sep;86(6):1516-23.
- Xu C, Yuan X, Pan Z, Shen G, Kim JH, Yu S, Khor TO, Li W, Ma J, Kong AN (2006). Mechanism of action of isothiocyanates: the induction of ARE-regulated genes is associated with activation of ERK and JNK and the phosphorylation and nuclear translocation of Nrf2. *Molecular Cancer Therapeutics*. Aug;5(8):1918-26.
- Xu X, Raber J, Yang D, Su B, Mucke L (1997). Dynamic regulation of c-Jun N-terminal kinase activity in mouse brain by environmental stimuli. *The Proceedings of the National Academy of Sciences*. Nov 11;94(23):12655-60.
- Yamada K, Umegaki H, Maezawa I, Iguchi A, Kameyama T, Nabeshima T (1997). Possible involvement of catalase in the protective effect of interleukin-6 against 6-hydroxydopamine toxicity in PC12 cells. *Brain Research Bulletin*. 43(6):573-7.
- Yang DD, Kuan CY, Whitmarsh AJ, Rincón M, Zheng TS, Davis RJ, Rakic P, Flavell RA (1997). Absence of excitotoxicity-induced apoptosis in the hippocampus of mice lacking the *Jnk3* gene. *Nature*. Oct 23;389(6653):865-70.
- Yang E, Zha J, Jockel J, Boise LH, Thompson CB, Korsmeyer SJ (1995). Bad, a heterodimeric partner for Bcl-x_L and Bcl-2, displaces Bax and promotes cell death. *Cell*. 1995 Jan 27;80(2):285-91.
- Yang LY, Ko WC, Lin CM, Lin JW, Wu JC, Lin CJ, Cheng HH, Shih CM (2005). Antioxidant N-acetylcysteine blocks nerve growth factor-induced H₂O₂/ERK signaling in PC12 cells. *Annals of the New York Academy of Sciences*. May;1042:325-37.
- Yang SH, Whitmarsh AJ, Davis RJ, Sharrocks AD (1998). Differential targeting of MAP kinases to the ETS-domain transcription factor Elk-1. *EMBO Journal*. Mar 16;17(6):1740-9.
- Youdim MB (1990). Monoamine oxidase (MAO)-A but not MAO-B inhibitors potentiate tyramine-induced catecholamine release from PC12 cells. *Journal of Neurochemistry*. Feb;54(2):411-4.
- Younes-Mhenni S, Frih-Ayed M, Kerkeni A, Bost M, Chazot G (2007). Peripheral blood markers of oxidative stress in Parkinson's disease. *European Neurology*. 58(2):78-83.
- Yousefi S, Conus S, Simon HU (2003). Cross-talk between death and survival pathways. *Cell Death & Differentiation*. Aug;10(8):861-3. Review.

- Zablocka B, Dluzniewska J, Zajac H, Domańska-Janik K (2003). Opposite reaction of ERK and JNK in ischemia vulnerable and resistant regions of hippocampus: involvement of mitochondria. *Brain Research Molecular Brain Research*. Feb 20;110(2):245-52. Erratum in: *Brain Research Molecular Brain Research*. 2003 May 12;113(1-2):143.
- Zamzami N, Hirsch T, Dallaporta B, Petit PX, Kroemer G (1997). Mitochondrial implication in accidental and programmed cell death: apoptosis and necrosis. *Journal of Bioenergetics and Biomembranes*. Apr;29(2):185-93. Review.
- Zamzami N, Marzo I, Susin SA, Brenner C, Larochette N, Marchetti P, Reed J, Kofler R, Kroemer G (1998). The thiol crosslinking agent diamide overcomes the apoptosis-inhibitory effect of Bcl-2 by enforcing mitochondrial permeability transition. *Oncogene*. Feb 26; 16(8):1055-63.
- Zamzami N, Susin SA, Marchetti P, Hirsch T, Gómez-Monterrey I, Castedo M, Kroemer G (1996). Mitochondrial control of nuclear apoptosis. *Journal of Experimental Medicine*. Apr 1; 183(4):1533-44.
- Zhang SP, Prozialeck WC, Weiss B (1990). Differential inhibition of calcium-dependent and calmodulin-dependent enzymes by drug-calmodulin adducts. *Molecular Pharmacology*. Nov;38(5):698-704.
- Zimmermann KC, Bonzon C, Green DR (2001). The machinery of programmed cell death. *Pharmacology & Therapeutics*. Oct;92(1):57-70. Review.
- Zimprich A, Biskup S, Leitner P, Lichtner P, Farrer M, Lincoln S, Kachergus J, Hulihan M, Uitti RJ, Calne DB, Stoessl AJ, Pfeiffer RF, Patenge N, Carbajal IC, Vieregge P, Asmus F, Müller-Myhsok B, Dickson DW, Meitinger T, Strom TM, Wszolek ZK, Gasser T (2004). Mutations in LRRK2 cause autosomal-dominant parkinsonism with pleomorphic pathology. *Neuron*. Nov 18;44(4):601-7.
- Zong WX, Lindsten T, Ross AJ, MacGregor GR, Thompson CB (2001). BH3-only proteins that bind pro-survival Bcl-2 family members fail to induce apoptosis in the absence of Bax and Bak. *Genes & Development*. Jun 15;15(12):1481-6.
- Zou H, Li Y, Liu X, Wang X (1999). An APAF-1 cytochrome c multimeric complex is a functional apoptosome that activates procaspase-9. *Journal of Biological Chemistry*. Apr 23; 274(17):11549-56.

7. ABBREVIATIONS

$\Delta\Psi_M$	delta psi, mitochondrial membrane potential
6-OHDA	6-hydroxydopamine
ABC	avidin-biotin-complex
AP-1	activator protein-1
APS	ammonium persulphate
AraC	Cytosine arabinoside (arabinofuranosylcytosine)
ASK1	apoptosis signal-regulating kinase-1
ATF-2	activating transcription factor-2
ATP	adenosine triphosphate
Bcl-2	B cell lymphoma-2
Bax	Bcl Associated X Protein
Bad	BAD, Bcl-2/Bcl-XL-antagonist, causing cell death
Bid	BH3 interacting death domain agonist
Bim	Bcl-2 Interacting Mediator of Cell Death
bp	base pairs
BSA	bovine serum albumin (albumin fraction V)
cAMP	cyclic adenosine monophosphate
caspase	cysteine aspartate-specific protease
cDNA	complementary DNA
c-Fos	v-fos FBJ murine osteosarcoma viral oncogene homologue
c-Jun	v-Jun avian sarcoma virus 17 oncogene homologue
$[Ca^{2+}]_i$	intracellular calcium concentration
CNS	central nervous system
COX	cyclo-oxygenase
Cu/Zn-SOD	copper zinc-SOD
Cyt c	cytochrome c
DA	dopamine
DAT	dopamine transporter
DAB	diamino-benzidine
DCF	2',7'-dichlorofluorescein
DDC	DOPA decarboxylase
DDW	double-distilled water
DHR	dihydrorhodamine

DIABLO	direct IAP binding protein with low pI
DLB	denaturing lysis buffer
DMSO	dimethylsulfoxide
dn	dominant negative
DNA	deoxyribonucleic acid
DNase	deoxyribonuclease
dNTP	2'-deoxynucleoside-5'-triphosphate
DOPA	3,4-Dihydroxyphenylalanin
DTT	dithiothreitol
ECL	enhanced chemiluminescence
EDTA	ethylenediaminetetraacetic acid
EGTA	Ethylene-bis(oxyethylenitrilo)tetraacetic acid
EGF	epidermal growth factor
Elk-1	Ets-like gene-1
em.	emission wavelength
ERK	extracellular signal-regulated kinase
ex.	excitation wavelength
FCS	fetal calf serum
FI	fluorescence intensity
Fig.	figure
FITC	Fluorescein-isothiocyanat
x g	relative centrifugal force (RCF)
H ₂ DCF	2',7'-dichloro-dihydrofluorescein
HEPES	N-2-Hydroxyethylpiperazine-N'-2-ethanesulfonic acid
HRP	horseradish peroxidase
HS	Horse serum
IC ₅₀	inhibitory concentration 50% (concentration leading to 50% inhibition)
IgG	immunoglobulin G
IL	interleukin
IMM	inner mitochondrial membrane
IMS	mitochondrial intermembrane space
IR	immunoreactivity
IU	international unit(s)
JIP	c-Jun N-terminal kinase-interacting protein
JNK	c-Jun N-terminal kinase

ABBREVIATIONS

kb	kilobase
kDa	Kilodalton
K_M	Michaelis-Menten constant
k.o.	knock-out
LB	Luria-Bertani medium
LDH	Lactate dehydrogenase
MAP	mitogen-activated protein
MAPK	mitogen-activated protein kinase
MAPKK	MAP2K, MEK, MKK, mitogen-activated protein kinase kinase
MAP3K	MAPKKK, MEKK, mitogen-activated protein kinase kinase kinase
MCA	middle cerebral artery
MEK	mitogen-activated protein / extracellular signal-regulated kinase kinase
MEKK	mitogen-activated protein / extracellular signal-regulated kinase kinase kinase
MFB	medial forebrain bundle
MKK	mitogen-activated protein kinase kinase
MLK	mixed-lineage kinase
Mn-SOD	manganese SOD
MPP ⁺	1-methyl-4-phenyl-1,2,3,6-tetrahydropyridinium ion
MPTP	1-methyl-4-phenyl-1,2,3,6-tetrahydropyridine
mPTP	mitochondrial permeability transition pore
mRNA	messenger RNA
MTred	mitotracker red
N	number of independent experiments per experimental series
NFAT	nuclear factor of activated T cells
NGF	nerve growth factor
N-terminal	amino-terminal
<i>P</i>	probability
<i>p. a.</i>	<i>pro analysis</i>
PAGE	polyacrylamide gel electrophoresis
PARP	poly(ADP-ribose) polymerase
PBS	phosphate-buffered saline
PBST	PBS containing Triton X-100
PCR	polymerase chain reaction
PD	Parkinson's disease
pH	<i>potentia hydrogenii</i> (hydrogen ion concentration)

PKC	protein kinase C
PMSF	phenyl-methyl sulfonyl fluoride
PVDF	polyvinylidene difluoride
RNA	ribonucleic acid
RNAse	ribonuclease
ROI	region of interest
ROS	reactive oxygen species
rpm	rotations per minute (centrifuge parameter)
RPMI-1640	Roswell Park Memorial Institute culture medium 1640
RT	room temperature (ca. 20°C)
SAPK	stress-activated protein kinase
SDS	sodium dodecyl sulfate
SDS-PAGE	sodium dodecyl sulfate polyacrylamide gel electrophoresis
SEK	JNK kinase
Smac	second mitochondria-derived activator of caspase
SNpc	<i>Substantia Nigra pars compacta</i>
SOD	superoxide dismutase
SP600125	anthra(1,9-cd)pyrazol-6(2H)-one
STS	staurosporine
Taq	<i>Thermus aquaticus</i>
TBE	Tris-boric acid-EDTA buffer
TBS	Tris-buffered saline
TBST	TBS with Tween-20
TEMED	N,N,N',N'-tetramethylethylenediamine
T _M	melting / annealing temperature of primers
TNF-alpha	tumour necrosis factor-alpha
Tris	tris-(hydroxymethyl)-aminomethane
Trx	thioredoxin
w/o	without
w/v	weight per volume

8. DANKSAGUNG/*ACKNOWLEDGEMENTS*

Ich möchte mich herzlich bedanken bei

I wish to express my gratitude towards

Meinem Doktorvater Prof. Dr. Thomas Herdegen für seine große Unterstützung bei der Durchführung dieser Arbeit, für sein Vertrauen in mich und für seine motivierende und inspirierende Art innerhalb und außerhalb der Forschung.

Meinem Betreuer Prof. Dr. Eric Beitz für die Korrektur meiner Dissertation, für wertvolle Ratschläge und die freundliche und unkomplizierte Übernahme meiner Betreuung.

PD Dr. Mario Götz für die freundschaftliche und fruchtbare Zusammenarbeit, und seine fachliche Beratung.

Desweiteren aus der Pharmakologie in Kiel all meinen Kollegen und Kolleginnen, im Besonderen der besten Bürokollegin Sevgi Eminel, Zhao Yi, Elke Schröder und Inga Wohlers für die immer sehr gute Zusammenarbeit; Vicki und Annika für ihre wertvolle Hilfe und ihren Rat, sowie Tom, Matze und Katja aus der Nephrologie für ideelle Unterstützung.

Prof. Dr. Jari Koistinaho and his group in Kuopio, Finland, for the possibility to learn and to conduct my experiments in his lab.

Meinen Freunden, die mir immer zur Seite gestanden haben, im Besonderen Robert und Lucy, Yun-Bon und Christian.

My friends from around the world, in particular Otto and Terhi, my cat mother Veera, Joana, Kiran, Juliane and Eva.

Conni, Fiffi, Meike und Malin für Eure Unterstützung.

Christine, for your endurance and your faith.

9. LEBENS LAUF/*CURRICULUM VITAE*

Persönliche Daten

Name: Lutz Römer
 Geburtsdatum: 21.12.1976
 Geburtsort: Marl
 Staatsangehörigkeit: deutsch

Schul Ausbildung

1987 – 1989 Städtisches Gymnasium Haltern, Haltern
 1989 – 1996 Clemens-Brentano-Gymnasium, Dülmen
 1996 Allgemeine Hochschulreife

Ersatzdienst

1996 – 1997 Betreuung behinderter Kinder, Regenbogen e.V., Dülmen

Studium und Praktisches Jahr

WS 1997 – SS 2002 Studium der Pharmazie an der Christian-Albrechts-Universität zu Kiel
 Juni 2002 – Dez. 2002 Pharmaziepraktikum in der Anker-Apotheke in Kiel
 Jan. 2003 – Aug. 2003 Pharmaziepraktikum im Institut für Pharmakologie, UK-SH (Universitätsklinikum Schleswig-Holstein), Campus Kiel
 20. August 2003 Erteilung der Approbation

Promotion und Weiterbildung

Sept. 2003 – Feb. 2008 Wissenschaftlicher Mitarbeiter am Institut für Pharmakologie, UK-SH, Campus Kiel. Anfertigung einer Dissertation unter Leitung von Prof. Dr. Thomas Herdegen. Forschungsaufenthalt in Kuopio, Finnland (Prof. Dr. Jari Koistinaho, März 2006 bis Juni 2007).
 seit Juli 2003 Weiterbildung zum Fachapotheker für Arzneimittelinformation, Betreuung Prof. Dr. Walter Raasch, Institut für Pharmakologie, UK-SH, Campus Lübeck

Publikationen

Eminel S, Roemer L, Waetzig V, Herdegen T (2008). c-Jun N-terminal kinases trigger both degeneration and neurite outgrowth in primary hippocampal and cortical neurons. *Journal of Neurochemistry*. Feb;104(4):957-69.

Wruck CJ, Claussen M, Fuhrmann G, Römer L, Schulz A, Pufe T, Waetzig V, Peipp M, Herdegen T, Goetz ME (2007). Flavonoid mediated neuroprotection requires activation of the transcription factor nuclear factor E2-related factor 2 (Nrf-2). *Journal of Neural Transmission Supplement*.(72):57-67.

Wessig J, Brecht S, Claussen M, Roemer L, Goetz M, Bigini P, Schutze S, Herdegen T. (2005). Tumor necrosis factor-alpha receptor 1 (p55) knockout only transiently decreases the activation of c-Jun and does not affect the survival of axotomized dopaminergic nigral neurons. *European Journal of Neuroscience*. Jul;22(1):267-72.

Erminel S, Klettner A, Roemer L, Herdegen T, Waetzig V (2004). JNK2 translocates to the mitochondria and mediates cytochrome c release in PC12 cells in response to 6-hydroxydopamine. *Journal of Biological Chemistry*. Dec 31;279(53):55385-92.

Tagungsbeiträge

Roemer L, Goldsteins G, Koistinaho J. Generation of reactive oxygen species and mitochondrial impairment following 6-hydroxydopamine. Oral presentation and abstract. Graduate School of Molecular Medicine – Winter School 2007. Vuokatti, Finland, 2007.

Eminel S, Roemer L, Klettner A, Herdegen T. JNK2 translocates to mitochondria and mediates cytochrome c release following 6-hydroxydopamine. Abstract and poster presentation. 30th Göttingen Neurobiology Conference. 2005.

10. ERKLÄRUNG ZU §10 ABS. 2 NR. 2 DER PROMOTIONSORDNUNG

Der Inhalt dieser Abhandlung wurde, abgesehen von der Beratung durch meinen Betreuer, selbstständig von mir erarbeitet und in dieser Form zusammengestellt. Die Arbeit hat an keiner anderen Stelle im Rahmen eines Prüfungsverfahrens vorgelegen.

Kiel, im März 2008

Lutz Römer

11. SUMMARY

Parkinson's disease (PD) is a progressive neurodegenerative disorder of less defined etiology and limited treatment options. An important role in the development of the disease has been addressed to oxidative stress, mitochondrial impairment and stress kinase signaling. The c-Jun N-terminal kinases (JNK) belong to a subgroup of the mitogen-activated protein kinases/stresskinases. Together with their upstream kinases and downstream effectors JNK compose the JNK signaling pathway. We used PC12 cells from rat pheochromocytoma, a model for catecholaminergic cells, together with the addition of 6-hydroxydopamine (6-OHDA), which is a well-established model toxin to induce PD-like symptoms *in vivo* and *in vitro*.

The results of this thesis demonstrate that production of reactive oxygen species (ROS) is increased shortly after administration of 6-OHDA (60 min). These ROS appear to derive from mitochondria, which are the greatest intracellular source of ROS if a leakage of protons occurs; we could also detect an immediate effect of 6-OHDA (or its metabolism products) on the mitochondrial membrane potential.

Furthermore, we discovered that a single JNK isoform (JNK2) translocates to mitochondria after stimulus. The signalosome was present at the mitochondria within 4 h, and it consisted of presumably activated JNK2, the upstream activator MKK4 and the scaffold protein for both, JIP. 6-OHDA also lead to a release of cytochrome c from the mitochondrial intermembrane space into the cytosol starting 8 h following 6-OHDA. This indicates disturbances of the outer mitochondrial membrane, formation of pores, and the cytosolic activation of caspases, which finally lead to cell death after 24 h.

JNK inhibition prevents various features of JNK pathology such as activation, translocation to the mitochondria, cytochrome c release and cell death, but not from ROS generation. PC12 cells could only be protected from this early event, upstream of JNK, by preincubation of plant-derived antioxidants, that also increase cellular defense mechanisms.

Our data confirm that JNK exhibit dual involvement in cell death and survival, as inhibition of JNK attenuates neuritogenesis of primary hippocampal neurons severely, regardless of the isoform. Therefore, the perspective of therapeutic JNK inhibition has to be reconsidered.

12. ZUSAMMENFASSUNG

Der Morbus Parkinson ist eine progressiv-degenerative Erkrankung des Gehirns mit derzeit limitierten Behandlungsoptionen, dessen Aetiologie noch nicht eindeutig beschrieben werden konnte. Eine wichtige Rolle in der Krankheitsentstehung spielen oxidativer Stress, Beeinträchtigung der Mitochondrienfunktion und intrazelluläre Signalkaskaden vermittelt von Stresskinasen. Die c-Jun N-terminalen Kinasen (JNK) gehören zu einer Untergruppe dieser Mitogen-aktivierten Proteinkinase/Stresskinasen. JNK bilden zusammen mit ihren Upstream-Kinasen und Downstream-Zielstrukturen den JNK Signalweg. Wir wählten die permanente Zelllinie PC12 aus dem Rattenphäochromocytom, ein Modell einer zentralen catecholaminergen Zelllinie, und behandelten diese mit 6-Hydroxydopamin (6-OHDA), ein Toxin, welches zur Darstellung von Parkinson-ähnlichen Symptomen *in vivo* und *in vitro* eingesetzt wird.

Die Ergebnisse dieser Arbeit zeigen, daß 6-OHDA die Produktion reaktiver Sauerstoffspezies (ROS) innerhalb kurzer Zeit stark erhöht (60 min). Die ROS wurden in Mitochondrien gebildet, der größten Quelle für Sauerstoffradikale, sofern das Membranpotential nicht stabil ist und Protonen in der intermembranären Zwischenraum gelangen können. Wir beobachteten ferner einen sofortigen Effekt von 6-OHDA (oder dessen Metabolisationsprodukten) auf das mitochondriale Membranpotential.

Desweiteren fanden wir heraus, daß eine einzige JNK Isoform (JNK2) nach Gabe des Stimulus 6-OHDA zu den Mitochondrien transloziert. Das gesamte Signalosom aus aktiviertem JNK2, der Upstream-Kinase MKK4, welche verantwortlich für die Aktivierung von JNK ist, und dem Scaffold-Protein JIP findet sich an den Mitochondrien innerhalb von 4 Stunden nach Stimulus. Außerdem führte die Zugabe von 6-OHDA zu einer Freisetzung von Cytochrom C aus den Mitochondrien ins Zytosol, beginnend nach etwa 8 Stunden. Dies deutet klar auf eine eingeschränkte Funktion der äußeren Mitochondrienmembran, der Bildung von Poren und der Aktivierung von Caspasen im Zytosol hin. Nach 24 Stunden beobachteten wir dann einen deutlichen Zelltod *in vitro* im Anschluß an die Freisetzung von Cytochrom C.

JNK Inhibierung bewahrt die Zelle vor verschiedenen apoptotischen Effekten der beschriebenen Pathologie, wie der JNK-Aktivierung, der Translokation zu den

ZUSAMMENFASSUNG

Mitochondrien, Cytochrom-C-Freisetzung und vor Zelltod, jedoch nicht vor oxidativem Stress. PC12 Zellen konnten davor nur geschützt werden, wenn vor der Toxingabe mit einem pflanzlichen Antioxidans (Methysticin, Luteolin, Resveratrol; und *tert*-Butylhydroquinon) behandelt wurde, ein Hinweis, daß ROS upstream von JNK sind.

Unsere Ergebnisse bestätigen, daß JNKs eine Rolle sowohl im neuronalen Zelltod, als auch dem Überleben spielen, da wir mit der Inhibierung von JNK die Neuritogenese von primären hippokampalen Neuronen stark beeinträchtigen, unabhängig von der Isoform. Aus diesem Grunde muß die JNK-Inhibition mit SP600125 als potentieller Therapieansatz beim Morbus Parkinson überdacht werden.